AMIDYL RADICAL-MEDIATED POLYOLEFIN C–H FUNCTIONALIZATION

Jill Williamson Alty

A dissertation submitted to the faculty of The University of North Carolina at Chapel Hill in partial fulfillment of the requirements for the degree of Doctor of Philosophy in the Department of Chemistry.

Chapel Hill
2021

Approved by:

Frank Leibfarth

Erik Alexanian

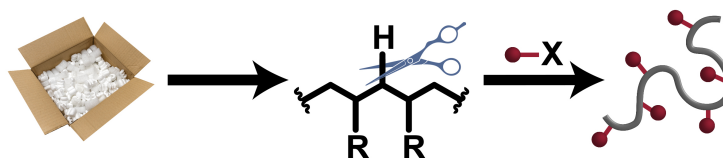Aleksandr Zhukhovitskiy

Abigail Knight

Jillian Dempsey

ABSTRACT

Jill Williamson Alty: Amidyl Radical-Mediated Polyolefin C–H Functionalization
(Under the direction of Frank Leibfarth and Erik Alexanian)

CHAPTER I. *Modern Strategies for the C–H Functionalization of Commodity Polymers*

Polyolefins, polyaromatics, polyesters, and polyethers comprise 63% of plastics worldwide. Their utility in modern society has enabled advancements but consequently has also led to rapid plastic accumulation. Using these waste materials as reactants, recent developments in the field of C–H functionalization as a post-polymerization modification technique of the commodity polymers are discussed.


CHAPTER II. *Regioselective Polyolefin C–H Xanthylation via Blue Light Irradiation with a Xanthylamide Reagent*
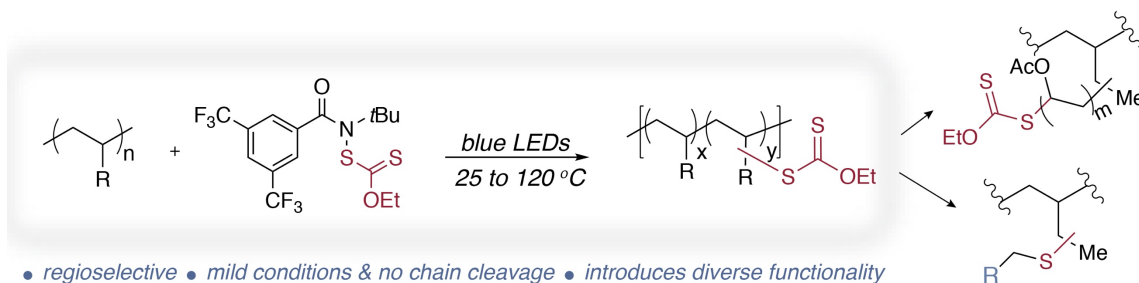
• *regioselective* • *mild conditions & no chain cleavage* • *introduces diverse functionality*

Xanthylation of atactic poly(butene) was possible via the use of a *N*-xanthylamide reagent. The method was regioselective, chemoselective, and modular to establish this as a platform methodology for the functionalization of polyolefins using blue light irradiation.

CHAPTER III. *Thermal Polyolefin C–H Functionalization via an Amidyl Radical: Mechanistic Studies and Application in Reactive Extrusion*

isotactic polypropylene

xanthylated polypropylene
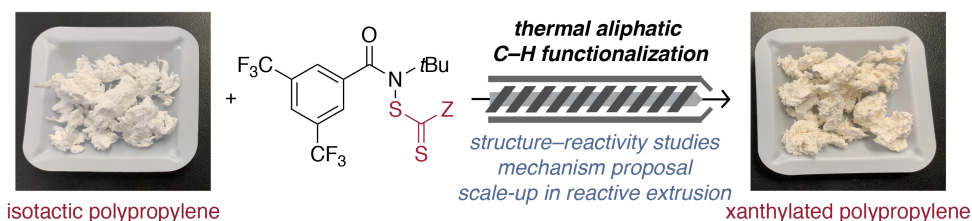
Hyperbranched polyethylene was thermally xanthylated, trithiocarbonylated, and dithiocarbamylated via an amidyl radical intermediate. The mechanism of C–H functionalization was deduced through kinetic and crossover experiments. The method was translated to semicrystalline polymers and ultimately to reacting within a twin-screw extruder, yielding 10 grams of xanthylated isotactic polypropylene.

CHAPTER IV. *A General Strategy for the Diversification of Aliphatic C–H Bonds via Radical Chain Transfer*
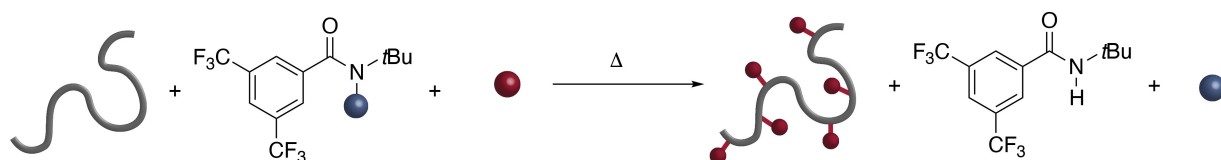
In this work, we report an approach to aliphatic C–H diversification via radical chain transfer featuring an easily prepared *O*–alkenylhydroxamate reagent, which upon mild heating facilitates a variety of valuable aliphatic C–H functionalizations. This method enabled the functionalization of a range of polyolefins via challenging and previously undeveloped C–H transformations. The simplicity and generality of this strategy constitute an ideal approach for the diversification of unactivated, aliphatic C–H bonds.

To my family, for their unconditional love and support throughout my degree.

ACKNOWLEDGEMENTS

First and foremost, I would like to thank my advisor, Frank Leibfarth, for his support and guidance over the past five years. With his mentorship, I have grown from a naïve, recipe-follower into a thoughtful chemist capable of creatively designing new and necessary projects. Through my next phase as a chemist, I will carry with me a sense of pride in myself and community in others, byproducts of the mentorship of Frank and my co-advisor, Erik Alexanian. I also want to thank Erik for always being open to new ideas and pushing our science to the next level. I would like to thank Abby Knight and Alex Zhukhovitskiy for their contributions to my time at UNC and for serving on my committee. A special thanks to Jillian Dempsey for serving on my committee and being an advocate for women in STEM, mentoring me through the Clare Boothe Luce fellowship.

I am appreciative of the friends who have become family within the Leibfarth and Alexanian groups. Your friendship and support made graduate school a formative and fun experience, especially the original members of the Leibfarth group: Sally Lewis, Marcus Reis, Travis Varner, and Dr. Aaron Teator. Thank you to past and present group members whom I have collaborated with on projects: Irene Manning, Rob Johnson, Nick Taylor, Victoria Barber, Eliza Neidhart, Will Czaplyski, Christina Na, Carla Staton, Matt Tierney, Tim Fazekas, and Austin Miller. I was fortunate enough to work with each of you at different points during my graduate school career, and I have learned a tremendous amount from each of our

collaborations. Additionally, I am grateful to the Dingemans group for the use of their instrumentation and to William Daniel for his assistance.

There is no way I would be finishing this degree without the profound influence of The College of William & Mary. The mentorship of my undergraduate advisor, Dr. Jonathan Scheerer, has extended beyond the Virginia state line through my time in graduate school. Tribe-members-turned-Tarheels, thank you to my classmates who helped establish a community in Chapel Hill rooted in the William & Mary welcoming spirit: Kaila Margrey, Will Czaplyski, Kelsey Miller, Hannah Shenouda, Jacob Robins, Eric Roos, Michelle Townsend, and Bob Wiley. The W&M chemistry department also brought my husband into my life along with my best friends Heidi Crockett, Amanda VanInwegen, and Hannah Smith.

My parents, Wendy and Neil Williamson, have been unwavering in their love and support through my journey as a scientist, fervently learning all they can to comprehend my chemistry. My brother, Mark Williamson, always brought me laughter when the end wasn't in sight. My parents-in-law, Lisa and Greg Alty, showed me tremendous inspiration whether through stories of how Lisa persevered through her degree or how their love story survived 4 years of long distance. It was really my husband, Isaac Alty, who convinced me I could get a Ph.D. in chemistry and has pushed me every day to grow into a deeper thinker. Departing my UNC, I finally feel like I have the confidence in my abilities as a chemist that Isaac always believed I had inside of me.

TABLE OF CONTENTS

LIST OF FIGURES

LIST OF TABLES

LIST OF ABBREVIATIONS AND SYMBOLS

^{13}C NMR	Carbon-13 nuclear magnetic resonance
^{1}H NMR	Proton magnetic resonance
Ac	Acetyl
Ar	Aromatic ring
AIBN	Azobisisobutyronitrile
BDE	Bond dissociation energy
BLED	Blue light emitting diode
BPO	Benzoyl peroxide
Đ	Dispersity
DCB	1,2-dichlorobenzene
DCP	Dicumyl peroxide
DEPT	Distortionless enhancement by polarization transfer
DLP	Dilauroyl peroxide
DSC	Differential scan calorimetry
DTBP	Di-tert-butyl peroxide
EtOAc	Ethyl acetate
GC	Gas chromatography
GPC	Gel permeation chromatography
HBPE	Hyperbranched polyethylene
HDPE	High density polyethylene
Hex	Hexyl

*i*PP	Isotactic polypropylene
IR	Infrared
k	General symbol for rate constant
LLDPE	Linear low density polyethylene
LDPE	Low density polyethylene
M	Molar or mol L^{-1}
M_n	Number-average molecular weight
M_w	Weight-average molecular weight
m/z	Mass per charge
MeCN	Acetonitrile
MS	Mass spectrometry
MWD	Molecular weight distribution
NMR	Nuclear magnetic resonance
PDA	Photodiode array
PE	Polyethylene
PEG	Polyethylene glycol
PP	Polypropylene
PEE	Poly(ethylethylene)
PEP	Poly(ethylene-alt-propylene)
PET	Polyethylene Terephlate
PhCl	Chlorobenzene
PhH	Benzene
$PhCF_3$	Trifluorotoluene

PhMe	Toluene
PPM	Post-polymerization modification
PS	Polystyrene
RAFT	Reversible addition–fragmentation chain transfer
T	Temperature
*t*Bu	*tert*-Butyl
TCB	1,3,5-Trichlorobenzene
T_g	Glass transition temperature
TGA	Thermal gravimetric analysis
Ts	*p*-Toluenesulfonyl
UV-Vis	Ultraviolet-visible absorption spectroscopy

CHAPTER I.

UPCYCLING COMMODITY POLYOLEFINS VIA C–H FUNCTIONALIZATION
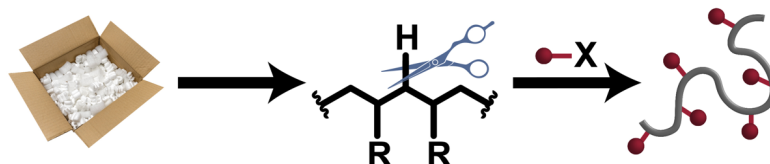
I-A. UPCYCLING OF PLASTIC WASTE

Plastics are the largest synthetic consumer product in the world with an annual production that reached 359 million metric tons in 2018.[1] Plastics are the material-of-choice for many diverse applications ranging from packaging, construction materials, electronics, biomedical devices, to energy storage. Their ubiquity is due to their light weight, low cost, easy processability, and diverse properties. Despite these considerable advantages, the end-of-life management of plastic waste has not advanced at a rate proportionate to their production. The resulting accumulation of nonbiodegradable plastic waste represents a Faustian bargain where environmental consideration is sacrificed. Developing strategies to reduce, reuse, and recycle plastic waste is therefore a pressing scientific and societal challenge.

Upon disposal, plastics are either landfilled, incinerated, or recycled. Landfilling and incineration are most plastics' fates, but both further contribute to the pollution of our planet. While incineration partially recovers the thermal energy stored in plastic waste in the short-term, it does not create economic value or mitigate resource depletion of the materials in the long-term.[2,3] Moreover, incineration leads to the release of carbon dioxide and other harmful gasses that further contribute to climate change. Large scale recycling strategies to repurpose

plastics have been implemented over the past 30 years, but even today only 32% of the collected plastic from municipal solid waste in Europe[1] and 9% in the United States[4] is recycled. The majority of these recycled plastics are mechanically recombined into materials of a diminished quality and utility. Additives and contaminants found in plastic waste streams, such as attached moisture and dirt, missorted polymers, multilayer products, or dyes, lead to significant deterioration of properties during and after reprocessing, decreasing the polymer's economic value. Therefore, mechanical recycling of post-consumer plastics too often leads to *downcycled* materials of lower quality.

The challenges inherent to recycling arise from the technical-grade products that result from these processes being more expensive or more energy intensive than homologues synthesized from petroleum, making broader uptake and implementation unfavorable. An alternative approach is to consider plastic waste as a chemical feedstock, thus positioning it at the beginning of the value chain instead of at its end. Under such a framework, post-consumer plastic waste becomes a low-cost and abundant starting material for the synthesis of materials or molecules. But, finding solutions for transforming post-consumer plastics into materials with an added economic value remains elusive with complex interrelated chemical, economic and environmental challenges to overcome. To address this opportunity, innovative concepts are emerging which transform plastic waste streams into value-added markets, a process known as *upcycling*, that can be raised into new circular economies.

Polymer-to-polymer upcycling directly transforms discarded plastics into a compositionally distinct polymer that is more economically valuable than the parent material. Furthermore, the use of some plastic waste to design next-generation materials could also reduce our current reliance on petrochemical resources to produce these plastics, thus

improving the sustainability of their production. Polymer functionalization, a post-polymerization modification, is a common industrial approach to differentiate the properties of virgin plastics. Compared to chemical recycling, polymer functionalization is an attractive approach for vinyl polymers, which comprise 78% of global plastic materials[5], due to the high enthalpic barrier for their depolymerization. Thus, we challenged ourselves to meet this need by employing modern organic chemistry methods to functionalize vinyl polymers in a polymer-to-polymer upcycling approach through post-polymerization modification.

I-B. C–H FUNCTIONALIZATION OF COMMODITY POLYMERS AS A POST-POLYMERIZATION MODIFICATION

The following has been adapted from a Review I contributed to on the topic of C–H functionalization of commodity polymers: J. B. Williamson, S. E. Lewis, R. R. Johnson III, I. M. Manning, F. A. Leibfarth. *Angew. Chem. Int. Ed.* **2019,** *58*, 8654.[6]

The post-polymerization modification of commodity polymers holds significant potential to increase the value of these pervasive materials, uncover entirely new material properties, and introduce a viable path to upcycling post-consumer plastic waste. Major challenges remain in order to develop practical and chemoselective approaches that transform commodity polymers into high-value materials. Commodity polymers are useful in part due to their chemical stability. Current process-driven commercial approaches to polymer modification rely on harsh conditions, non-selective reagents, and re-optimization for each new desired property. A molecular-level approach to modify recalcitrant commodity substrates will require polymer chemists to rethink their strategies for post-polymerization modification, seeing C–H bonds as potential points of diversification rather than unreactive functionality.

Modern advances in organic and medicinal chemistry have resulted in powerful methods for the C–H functionalization of complex small molecules.[7–10] Translating concepts from late-stage pharmaceutical diversification to polymer science requires the consideration of parameters unique to macromolecular structure and final material properties. For example, properties such as adhesion or surface

Functionalization of custom-made polymers

▸ Generates complex & functional materials
▸ Requires custom-made polymer precursor
▸ Supplanting current materials with designer polymers, even if they are superior, is challenging.

C–H functionalization of commodity polymers

▸ Leverages high-volume, low-cost polymer production
▸ Interfaces with established industrial infrastructure
▸ Potential to increase the value of commodity materials, discover new properties, & upcycle plastic waste

Figure 1.1 C–H functionalization has the potential to uncover added value from polymers produced at a commodity scale.

tension can be drastically altered with the addition of only a small amount of functionality; therefore, yield is many times not the primary consideration for polymer C–H functionalization.[11,12]

Conversely, polymer functionalization is generally less tolerant to side reactions associated with functionalization than in small molecule chemistry, since multiple functional groups on the same polymer chain cannot be purified from one another. This requirement for exquisite chemoselectivity is especially paramount if the C–H functionalization causes even small amounts of elimination or coupling side-reactions, which results in polymer chain-scission or crosslinking, respectively.[13] These deleterious reaction pathways significantly alter the molecular weight distribution of the sample and play an outsized role in determining final material properties.

Considering the unique challenges posed by polymer C–H functionalization combined with the significant potential of this approach, we define here aspirational criteria for a polymer C–H functionalization method. These transformations should:

1. Include minimal chemical operations and occurs under mild reaction conditions.

2. Not significantly change the degree of polymerization or molecular weight distribution.

3. Alter chemical structure by taking advantage of the innate functionality on the polymer.

4. Result in a significant change in material properties.

In addition to these guidelines, ideally polymer C–H functionalization is general to a polymer class, is a one-pot transformation, and provides the ability to predictively tune the density of functionalization.

I-C. METAL-CATALYZED POLYOLEFIN C–H FUNCTIONALIZATIONS

Polyolefins constitute nearly 55% of the world's plastic production.[5] Despite their omnipresence, these hydrocarbons are limited by their inability to interface with polar additives, fillers, or other materials, making them inadequate for high-performance engineering applications.[14] If functionality could be imparted onto these materials without compromising the desirable properties of the parent material, new and unusual properties could be obtained that are not typically associated with polyolefins.[14–16]

Efforts towards functionalized polyolefins have typically focused on either the copolymerization of an α-olefin with a polar monomer or post-polymerization modification.[15] Copolymerization has been a long-standing challenge in the field of polymer chemistry, but the high oxophilicity of early transition-metal catalysts leads to catalyst poisoning by strongly π-donating Lewis bases and hinders their utility.[16] Late-transition metal catalysts, which are generally more tolerant to polar functionality, have shown promise.[14,17,18] Although significant

effort has been devoted to this research area, state-of-the-art phosphine sulfonate (and related) palladium complexes synthesize low molecular weights with moderate functional group incorporation and lack sufficient catalytic activities necessary for translation.[19–22]

Post-polymerization modification of polyolefins transforms these high-volume and low-cost commodity polymers into value-added materials. The foundational challenge of this approach is the need to selectively functionalize unactivated C–H bonds. This compelling modern problem has led to a number of contemporary approaches for the selective C–H functionalization of polyolefins.[15] Advances in catalyst and reagent design have enabled the development of metal-catalyzed methods that display exquisite chemo- and regio-selectivity on complex natural products and pharmaceuticals.[8,9,23] The importance of functionalized polyolefins have inspired a number of efforts to translate the methods developed on small molecules to polymer substrates. For example, following comprehensive studies of iridium pincer complexes,[24] Goldman, Coates, and coworkers employed these privileged catalysts for the direct dehydrogenation of polyolefins (Figure 1.2A). Poly(1-hexene) (PHex) and polyethylene (PE) were regioselectively dehydrogenated to generate terminal olefins, with reaction efficiency reaching 18 mol% and 4.4 mol%, respectively.[25–28] In the case of PHex, the terminal olefin was found to re-engage the catalyst and isomerize to generate internal olefins along the polymer side chain. The functionalization approach resulted in value-added polyolefins with no observable change in the MWD of the polymer. Guan and Huang report a tandem catalytic dehydrogenation and cross-metathesis for highly efficient degradation of polyethylenes under mild conditions.[29] Reacting a mixture of PEs and low molecular weight alkanes, alkenes are generated throughout both substrates during the dehydrogenation and,

6

upon cross-metathesis, useful liquid fuels and waxes are generated, even from complex mixtures such as post-consumer plastic waste.

The direct oxidation of C–H sites in polyolefins has been pursued to impart polar alcohol or carbonyl groups. Boaen and Hillmyer employed a bioinspired manganese porphyrin catalyst to functionalize branched polyolefins using Oxone® as the terminal oxidant (Figure 1.2B).[30] The manganese complex installed hydroxyl groups at tertiary carbon sites along the polymer backbone, as well as oxidized secondary carbons to carbonyls. Using amorphous

A. Dehydrogenation
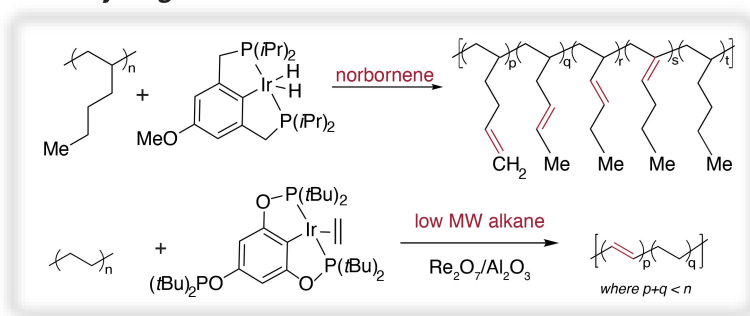
B. Oxyfunctionalization
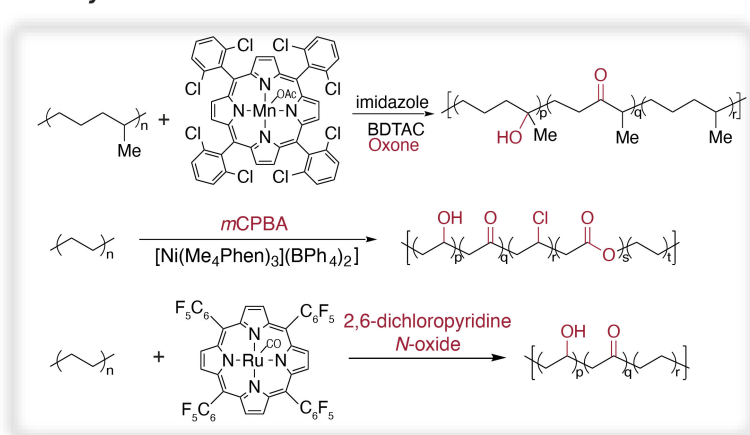
C. Esterification
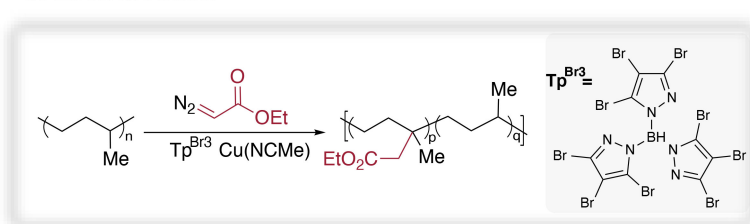
D. Borylation
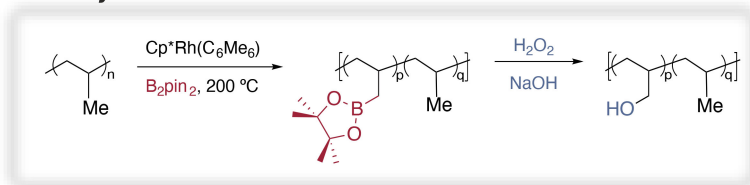
Figure 1.2 Metal-catalyzed routes toward functionalized polyolefins.

poly(ethylene-alt-propylene) (PEP) with a molecular weight of 5.0 kg/mol as a model polyolefin, 7 mol% hydroxyl groups were installed without significant changes to the MWD of the material. PEP with a molecular weight of 50 kg/mol required long reaction times to

achieve 1.6 mol % functionalization, which the authors attributed to the difficulty of the polymer in accessing sterically encumbered catalyst active site. More recently, Hartwig and coworkers reported a Ni-catalyzed C–H oxidation to install a mixture of hydroxyl, ketone, and chloride functionality onto commercial PE substrates. The mild conditions and use of an abundant transition metal catalyst are notable compared to previous work. This method was able to install up to 5 mol% of the desired hydroxyl functionality, but unintentional chlorination, formylation, and esterification occurred coincidently.[31] Further exploration of this work enabled the Hartwig work to chemoselectively oxidize PEs, adorning the polymer chain with only hydroxyl and carbonyl groups.[32] They report the C–H oxidation of PEs via a polyfluorinated ruthenium porphyrin catalyst in the presence of pyridine *N*-oxide achieves 4 mol% oxidation, imbuing the polymer with new adhesive and paintability properties (Figure 1.2B).

Metal-catalyzed C–H insertion has proven to be a successful approach for polyolefin functionalization. Pérez and coworkers reported the copper-catalyzed generation of carbenes from ethyl diazoacetate (EDA) to achieve the addition of up to 13 mol% ester groups onto various polyolefins (Figure 1.2C).[33] The reaction was conducted at room temperature and resulted in tertiary regioselectivity for poly(2-butene) and secondary regioselectivity for poly(ethylene-1-octene). This switch in selectivity was attributed to the substantial increase of methylene sites in poly(ethylene-1-octene) compared to poly(2-butene).[34]

Building upon the regiospecific C–H borylation of linear alkanes,[35,36] Hartwig and Hillmyer pioneered a rhodium-catalyzed functionalization strategy to borylate the primary carbons of branched polyolefins in the polymer melt (Figure 1.2D). The method was demonstrated on a number of commercially important and challenging substrates, including

isotactic polypropylene (*i*PP) and linear low density PE.[37–39] Importantly, the approach did not significantly influence the molecular weight, MWD, or tacticity of the polymer substrates. The pinacolborane functionality was quantitatively converted to an alcohol through peroxide oxidation, achieving up to 19.2 mol% functionalization of linear low-density polyethylene and up to 1.5 mol% functionalization of *i*PP.[38,39] The hydroxylated polymers were shown to be effective as initiators for ring-opening polymerization of caprolactone, as a site to install initiators for ATRP,[40] and as a versatile intermediate for the introduction of aldehyde or amino moieties.[38]

I-D. METAL-FREE POLYOLEFIN C–H FUNCTIONALIZATIONS

While transition metal-catalyzed polyolefin functionalization has shown great promise, trace metal in the final polymer can catalyze oxidative degradation processes.[41] Furthermore, the use of precious metals or the challenging synthesis of designer ligands is difficult to implement on a commodity scale. For these reasons, a metal-free method to impart versatile functionality onto polyolefins remains an important pursuit.

Conventional metal free polyolefin modification methods rely on hydrogen atom transfer (HAT) chemistry initiated by the thermally-induced homolysis of organic peroxides.[13] HAT is the concerted exchange of a proton and an electron.[42] In the example of polyolefin functionalization, HAT involves the homolysis of a C–H bond to reveal a carbon-centered radical on the polymer backbone. Typically, a highly reactive alkoxy radical is generated from the thermal decomposition of a peroxide that subsequently abstracts a hydrogen atom from the polyolefin. The relatively high bond dissociation free energy (BDFE) of C–H bonds (96–101 kcal/mol) and moderate BDFE of organic peroxides typically utilized in these processes (84–89 kcal/mol) leads to a reactivity mismatch.[43] For branched polyolefins, these conditions

predominantly lead to HAT of the weakest (*i.e.* tertiary) C–H bond (Figure 1.3). The resulting tertiary radical commonly undergoes β-scission, chain transfer, chain coupling, and other uncontrollable free radical addition reactions faster than radical trapping. Consequently, the thermal and mechanical properties of the parent material are significantly degraded.

The current commercial route for polyolefin functionalization is the peroxide-initiated grafting of maleic anhydride (MAH) from the polyolefin backbone (Figure 1.3).[44] This yields a maleic anhydride-functionalized polyolefin, while concomitant β-scission results in polymer chain scission and compromises the molecular weight of the final material. For example, peroxide-initiated polypropylene functionalization results in the degree of functionalization being inversely proportional to the molecular weight of
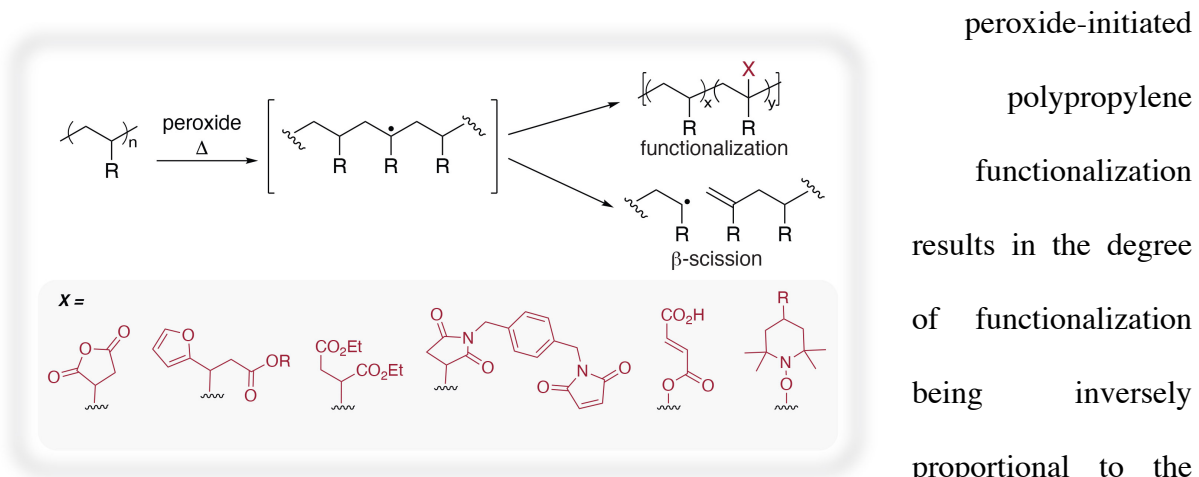
Figure 1.3 Routes towards functionalized polyolefins upon HAT by the thermally initiated homolysis of a peroxide.

the final material.[44,45] Other functionalization approaches have sought to add alternative radical traps to study their impact on polyolefin functionalization, including nitroxide free radicals[46–49] and α,β-unsaturated esters[50–53]. In a creative solution to the challenge of β-scission, Moore and coworkers employed a non-symmetric peroxo-species that, upon homolysis, provided both a radical for C–H abstraction and a radical for C–H functionalization.[54] The process of homolysis, hydrogen atom abstraction, and radical trapping were proposed to occur inside a "melt-cage" before Fickian diffusion can separate the radical species. The "melt-cage"

approach requires stoichiometric radical initiator, but was shown to significantly decrease polymer chain scission during reactive extrusion compared to typical methods of MAH functionalization.[54]

Crosslinked polyolefins are valuable materials and used commercially in hot-water piping and medical devices.[55,56] Peroxide-induced radical generation in the absence of a radical trap generates crosslinked polyolefins through chain coupling, but the ultimate gel content and properties of these materials is limited due to coincident chain-scission.[57] The addition of a di-functional radical trap such as the *bis*-maleimide provides a thermoset with tunable distance between crosslinks and better control of mechanical properties.[58]

An alternative to peroxide homolysis, Aglietto *et al*. studied the C–H insertion of a carbene into polyolefins through thermal treatment of diazo compounds.[59] PEP was decorated with up to 6.0 mol% ester groups through EDA thermolysis after multiple additions of EDA at temperatures >200 °C (Figure 1.4A). In 2019, the Wulff group employed a novel *bis*-diazirine molecule capable of generating carbene species under mild and controllable conditions.[60] The carbene crosslinked PEs, *i*PP, PDMS, and paraffins through double C–H activation. Upon C–

A. Carbene insertion
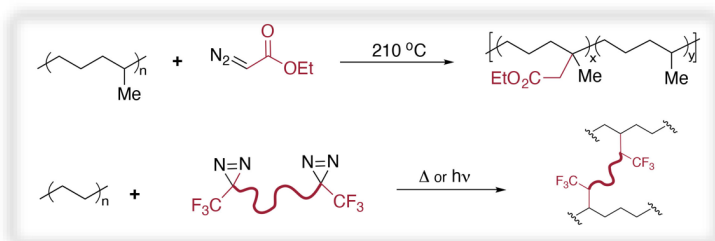
B. Hypervalent iodide catalysis
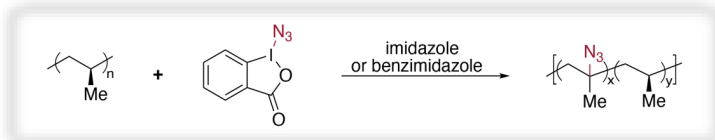
C. N-oxyl radical
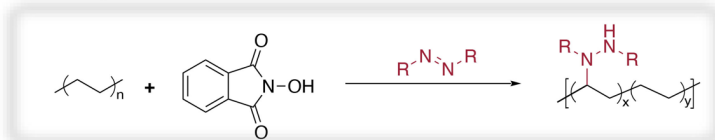
Figure 1.4 Metal-free polyolefin functionalization strategies that do not rely on HAT by the thermally initiated homolysis of a peroxide.

H crosslinking, the authors suggest PE fabric could be strengthened to improve its utility, offering a potential application to this research.

Alternatively, hypervalent iodide sources have proven useful for polyolefin functionalization.[61] Liu and Bielawski reported the azidation of polypropylene through a catalytic hypervalent iodide source (Figure 1.4B). This method worked on recalcitrant substrates including *i*PP to install versatile functionality. Like many methods on branched polyolefins that go through a radical intermediate, the authors observed a significant decrease in both polymer molecular weight and melting temperature (T_m) upon functionalization.

Chen and coworkers described a method to aminate PE using catalytic *N*-hydroxyphthalimide.[62] The authors hypothesized that the *N*-oxyl radical serves as the hydrogen atom abstracting reagent and the resultant carbon-centered radical on the polymer is trapped by an azodicarboxylate (Figure 1.4C).[63] Although the BDFE of the phthalimide *N*-oxyl radical has been measured to be considerably lower (85–90 kcal/mol) than aliphatic C–H bonds (96-101 kcal/mol), [64,65] the method achieved up to 10 mol% functionalization of PE when using 17 equivalents of azodicarboxylate reagent compared to repeat unit.

I-E. AMIDYL RADICALS AS A MEDIUM TOWARDS CHEMOSELECTIVE POLYOLEFIN PPM

Enhancing the properties of commodity polymers through operationally simple C–H functionalization methods is an emerging area of interest in the field of polymer science, with potential applications in sustainably upcycling plastic waste and generating new, functional materials with properties not accessible through traditional synthetic routes. Realizing the ultimate potential of polymer C–H functionalization will require contributions from many traditional chemical disciplines, including organic synthesis, organometallic chemistry, catalysis, and polymer science.

There remained a need in the community for a metal-free polyolefin C–H functionalization that installed polarity onto polyolefins under mild reaction conditions, using substoichiometric quantities of reagent, and without concurrent scission of the polymer backbone. Current methods are largely inefficient, resulting in superstoichiometric quantities of reagent or very low degrees of incorporation of the functionality, and do not take into account the endothermicity required for polyolefin hydrogen atom abstraction, leading to extraneous radical events. The ideal metal-free polyolefin C–H functionalization would be highly efficient, be easily translated into current industrial infrastructure, and be able to functionalize the polymer without concomitant chain scission or coupling.

With these parameters in mind, my dissertation develops amidyl radical-mediated C–H functionalization methods towards polar polyolefins. The central goal of this research is the development of a practical platform methodology to selectively functionalize commodity polyolefins through direct C–H transformation. In 2016, the Alexanian group reported C–H xanthylation of aliphatic small molecules.[66] We recognized the potential of this method for the C–H functionalization of polyolefins and began our studies towards upcycling commodity polyolefins via amidyl radical intermediates. In the following dissertation, Chapter II demonstrates that a *N*–xanthylamide reagent can regioselectively functionalize polyolefins under blue light irradiation. Chapter III communicates a thermal initiation strategy for polyolefin C–H xanthylation, as well as mechanism elucidation and translation to reactive extrusion. Chapter IV reports a general methodology that enables broad C–H diversification of polyolefins and upcycles plastic waste into new materials, like polyolefin ionomers.

REFERENCES

(1)   PlasticsEurope; EPRO. Plastics - the Facts 2019. **2019**.

(2)   Vollmer, I.; Jenks, M. J. F.; Roelands, M. C. P.; White, R. J.; van Harmelen, T.; de Wild, P.; van der Laan, G. P.; Meirer, F.; Keurentjes, J. T. F.; Weckhuysen, B. M. Beyond Mechanical Recycling: Giving New Life to Plastic Waste. *Angew. Chem. Int. Ed.* **2020**, *59*, 15402–15423.

(3)   Antelava, A.; Damilos, S.; Hafeez, S.; Manos, G.; Al-Salem, S. M.; Sharma, B. K.; Kohli, K.; Constantinou, A. Plastic Solid Waste (PSW) in the Context of Life Cycle Assessment (LCA) and Sustainable Management. *Environ. Manage.* **2019**, *64*, 230–244.

(4)   United States Environmental Protection Agency. Recycling and Composting Trends. *Natl. Overv. Facts Fig. Mater. Wastes, Recycl.* **2018**.

(5)   World Plastics Materials Demand 2015 by Types. *PlasticsEurope Market Research Group*, 2015, 3.

(6)   Williamson, J. B.; Lewis, S. E.; Johnson III, R. R.; Manning, I. M.; Leibfarth, F. C-H Functionalization of Commodity Polymers. *Angew. Chem. Int. Ed.* **2018**, *58*, 8654–8668.

(7)   Gutekunst, W. R.; Baran, P. S. C-H Functionalisation in Organic Synthesis Themed Issue. *Chem. Soc. Rev.* **2011**, *40*, 1845–2040.

(8)   Cernak, T.; Dykstra, K. D.; Tyagarajan, S.; Vachal, P.; Krska, S. W. The Medicinal Chemist's Toolbox for Late Stage Functionalization of Drug-like Molecules. *Chem. Soc. Rev.* **2016**, *45*, 546–576.

(9)   Wencel-Delord, J.; Glorius, F. C-H Bond Activation Enables the Rapid Construction and Late-Stage Diversification of Functional Molecules. *Nat. Chem.* **2013**, *5*, 369–375.

(10)   Davies, H. M. L.; Morton, D. Collective Approach to Advancing C-H Functionalization. *ACS Cent. Sci.* **2017**, *3*, 936–943.

(11)   Franssen, N. M. G.; Reek, J. N. H.; de Bruin, B. Synthesis of Functional 'Polyolefins': State of the Art and Remaining Challenges. *Chem. Soc. Rev.* **2013**, *42*, 5809–5832.

(12)   Novák, I.; Krupa, I.; Luyt, A. S. Modification of the Polarity and Adhesive Properties of Polyolefins through Blending with Maleic Anhydride Grafted Fischer-Tropsch Paraffin Wax. *J. Appl. Polym. Sci.* **2006**, *100*, 3069–3074.

(13)   Moad, G. Synthesis of Polyolefin Graft Copolymers by Reactive Extrusion. *Prog. Polym. Sci.* **1999**, *24*, 81–142.

(14)   Domski, G. J.; Rose, J. M.; Coates, G. W.; Bolig, A. D.; Brookhart, M. Living Alkene Polymerization: New Methods for the Precision Synthesis of Polyolefins. *Prog. Polym. Sci.* **2007**, *32*, 30–92.

(15)   Boaen, N. K.; Hillmyer, M. A. Post-Polymerization Functionalization of Polyolefins. *Chem. Soc. Rev.* **2005**, *34*, 267–275.

(16)   Chung, T. C. Synthesis of Functional Polyolefin Copolymers with Graft and Block Structures. *Prog. Polym. Sci.* **2002**, *27*, 39–85.

(17)   Ittel, S. D.; Johnson, L. K.; Brookhart, M. Late-Metal Catalysts for Ethylene Homo- and Copolymerization. *Chem. Rev.* **2000**, *100*, 1169–1203.

(18)   Ito, S.; Nozaki, K. Coordination – Insertion Copolymerization of Polar Vinyl Monomers By. *Chem. Rev.* **2010**, *10*, 315–325.

(19)   Carrow, B. P.; Nozaki, K. Transition-Metal-Catalyzed Functional Polyolefin Synthesis: Effecting Control through Chelating Ancillary Ligand Design and Mechanistic Insights. *Macromolecules* **2014**, *47*, 2541–2555.

(20)   Nakamura, A.; Anselment, T. M. J.; Claverie, J.; Goodall, B.; Jordan, R. F.; Mecking, S.; Rieger, B.; Sen, A.; van Leeuwen, P. W. N. M.; Nozaki, K. Ortho-Phosphinobenzenesulfonate: A Superb Ligand for Palladium-Catalyzed Coordination–Insertion Copolymerization of Polar Vinyl Monomers. *Acc. Chem. Res.* **2013**, *46*, 1438–1449.

(21)   Zhang, W.; Waddell, P. M.; Tiedemann, M. A.; Padilla, C. E.; Mei, J.; Chen, L.; Carrow, B. P. Electron-Rich Metal Cations Enable Synthesis of High Molecular Weight, Linear Functional Polyethylenes. *J. Am. Chem. Soc.* **2018**, *140*, 8841–8850.

(22)   Kenyon, P.; Wörner, M.; Mecking, S. Controlled Polymerization in Polar Solvents to Ultrahigh Molecular Weight Polyethylene. *J. Am. Chem. Soc.* **2018**, *140*, 6685–6689. jacs.8b03223.

(23)   Roudesly, F.; Oble, J.; Poli, G. Metal-Catalyzed C–H Activation/Functionalization: The Fundamentals. *J. Mol. Catal. A Chem.* **2017**, *426*, 275–296.

(24)   Gupta, M.; Hagen, C.; Flesher, R. J.; Kaska, W. C.; Jensen, C. M. A Highly Active Alkane Dehydrogenation Catalyst: Stabilization of Dihydrido Rhodium and Iridium Complexes by a P-C-P Pincer Ligand. *Chem. Commun.* **1996**, 2083–2084.

(25)   Liu, F.; Pak, E. B.; Singh, B.; Jensen, C. M.; Goldman, A. S. Dehydrogenation of n - Alkanes Catalyzed by Iridium "Pincer" Complexes : Regioselective Formation of α - Olefins. *J. Am. Chem. Soc.* **1999**, *121*, 4086–4087.

(26)   Choi, J.; MacArthur, A. H. R.; Brookhart, M.; Goldman, A. S. Dehydrogenation and Related Reactions Catalyzed by Iridium Pincer Complexes. *Chem. Rev.* **2011**, *111*,

1761–1779.

(27) Ray, A.; Zhu, K.; Kissin, Y. V.; Cherian, A. E.; Coates, G. W.; Goldman, A. S. Dehydrogenation of Aliphatic Polyolefins Catalyzed by Pincer-Ligated Iridium Complexes. *Chem. Commun.* **2005**, 3388–3390.

(28) Ray, A.; Kissin, Y. V.; Zhu, K.; Goldman, A. S.; Cherian, A. E.; Coates, G. W. Catalytic Post-Modification of Alkene Polymers. Chemistry and Kinetics of Dehydrogenation of Alkene Polymers and Oligomers with Pincer Ir Complexes. *J. Mol. Catal. A Chem.* **2006**, *256*, 200–207.

(29) Jia, X.; Qin, C.; Friedberger, T.; Guan, Z.; Huang, Z. Efficient and Selective Degradation of Polyethylenes into Liquid Fuels and Waxes under Mild Conditions. *Sci. Adv.* **2016**, *2*, 1–8.

(30) Boaen, N. K.; Hillmyer, M. A. Selective and Mild Oxyfunctionalization of Model Polyolefins. *Macromolecules* **2003**, *36*, 7027–7034.

(31) Bunescu, A.; Lee, S.; Li, Q.; Hartwig, J. F. Catalytic Hydroxylation of Polyethylenes. *ACS Cent. Sci.* **2017**, *3*, 895–903.

(32) Chen, L.; Malollari, K. G.; Uliana, A.; Sanchez, D.; Messersmith, P. B.; Hartwig, J. F. Selective, Catalytic Oxidations of C–H Bonds in Polyethylenes Produce Functional Materials with Enhanced Adhesion. *Chem* **2021**, *7*, 137–145.

(33) Díaz-Requejo, M. M.; Wehrmann, P.; Leatherman, M. D.; Trofimenko, S.; Mecking, S.; Brookhart, M.; Pérez, P. J. Controlled, Copper-Catalyzed Functionalization of Polyolefins. *Macromolecules* **2005**, *38*, 4966–4969.

(34) Díaz-Requejo, M. M.; Belderraín, T. R.; Nicasio, M. C.; Trofimenko, S.; Pérez, P. J. Cyclohexane and Benzene Amination by Catalytic Nitrene Insertion into C-H Bonds with the Copper-Homoscorpionate Catalyst TpBr3Cu(NCMe). *J. Am. Chem. Soc.* **2003**, *125*, 12078–12079.

(35) Chen, H.; Hartwig, J. F. Catalytic, Regiospecific End-Functionalization of Alkanes: Rhenium-Catalyzed Borylation under Photochemical Conditions. *Angew. Chem. Int. Ed.* **1999**, *38*, 3391–3393.

(36) F., H. J. Thermal, Catalytic, Regiospecific Functionalization of Alkanes. *Science* **2000**, *287*, 1995.

(37) Kondo, Y.; García-Cuadrado, D.; Hartwig, J. F.; Boaen, N. K.; Wagner, N. L.; Hillmyer, M. A. Rhodium-Catalyzed, Regiospecific Functionalization of Polyolefins in the Melt. *J. Am. Chem. Soc.* **2002**, *124*, 1164–1165.

(38) Bae, C.; Hartwig, J. F.; Chung, H.; Harris, N. K.; Switek, K. A.; Hillmyer, M. A. Regiospecific Side-Chain Functionalization of Linear Low-Density Polyethylene with

Polar Groups. *Angew. Chem. Int. Ed.* **2005**, *44*, 6410–6413.

(39)   Bae, C.; Hartwig, J. F.; Boaen Harris, N. K.; Long, R. O.; Anderson, K. S.; Hillmyer, M. A. Catalytic Hydroxylation of Polypropylenes. *J. Am. Chem. Soc.* **2005**, 127, 767–776.

(40)   Matsumura, S.; Hlil, A. R.; Lepiller, C.; Gaudet, J.; Guay, D.; Shi, Z.; Holdcroft, S.; Hay, A. S. Ionomers for Proton Exchange Membrane Fuel Cells with Sulfonic Acid Groups on the End-Groups: Novel Branched Poly(Ether-Ketone)s. *Am. Chem. Soc. Polym. Prepr. Div. Polym. Chem.* **2008**, *49*, 511–512.

(41)   Foster, G. N.; Wasserman, S. H.; Yacka, D. J. Oxidation Behavior and Stabilization of Metallocene and Other Polyolefins. *Angew. Makro. Chem.* **1997**, *252*, 11–32.

(42)   Mader, E. A.; Davidson, E. R.; Mayer, J. M. Large Ground-State Entropy Changes for Hydrogen Atom Transfer Reactions of Iron Complexes. *J. Am. Chem. Soc.* **2007**, *129*, 5153–5166.

(43)   Blanksby, S. J.; Ellison, G. B. Bond Dissociation Energies of Organic Molecules. *Acc. Chem. Res.* **2003**, *36*, 255–263.

(44)   Zhang, M.; Colby, R. H.; Milner, S. T.; Chung, T. C. M. Synthesis and Characterization of Maleic Anhydride Grafted Polypropylene with a Well-Defined Molecular Structure. *Macromolecules* **2013**, *46*, 4313 – 4323.

(45)   Gloor, P. E.; Tang, Y.; Kostanska, A. E.; Hamielec, A. E. Chemical Modification of Polyolefins by Free Radical Mechanisms: A Modelling and Experimental Study of Simultaneous Random Scission, Branching and Crosslinking. *Polymer (Guildf).* **1994**, *35*, 1012–1030.

(46)   Coiai, S.; Cicogna, F.; Yang, C.; Tempesti, V.; Carroccio, S. C.; Gorrasi, G.; Mendichi, R.; Dintcheva, N. T.; Passaglia, E. Grafting of Hindered Phenol Groups onto Ethylene/α-Olefin Copolymer by Nitroxide Radical Coupling. *Polymers (Basel).* **2017**, *9*, 1–19.

(47)   Cicogna, F.; Coiai, S.; Passaglia, E.; Tucci, I.; Ricci, L.; Ciardelli, F.; Batistini, A. Grafting of Functional Nitroxyl Free Radicals to Polyolefins as a Tool to Postreactor Modification of Polyethylene-Based Materials with Control of Macromolecular Architecture. *J. Polym. Sci. Part A Polym. Chem.* **2010**, *49*, 781–796.

(48)   Cicogna, F.; Domenichelli, I.; Coiai, S.; Bellina, F.; Lessi, M.; Spiniello, R.; Passaglia, E. Azo-Aromatic Functionalized Polyethylene by Nitroxide Radical Coupling (NRC) Reaction: Preparation and Photo-Physical Properties. *Polym. (United Kingdom)* **2016**, *82*, 366–377.

(49)   Domenichelli, I.; Banerjee, S.; Taddei, S.; Martinelli, E.; Passaglia, E.; Ameduri, B. Styrene and Substituted Styrene Grafted Functional Polyolefins *via* Nitroxide

Mediated Polymerization. *Polym. Chem.* **2018**, 307–314.

(50)   Ciardelli, F.; Aglietto, M.; Ruggeri, G.; Passaglia, E.; Castelvetro, V. Functionalization of Polyolefins in the Melt through Reaction with Molecules and Macromolecules. *Macromol. Symp.* **1997**, *118*, 311–316.

(51)   Ciardelli, F.; Aglietto, M.; Coltelli, M. B.; Passaglia, E.; Ruggeri, G.; Coiai, S. Functionalization of Polyolefins in the Melt. In *Modification and Blending of Synthetic and Natural Macromolecules*; Ciardelli, F., Penczek, S., Eds.; Springer, Dordrecht, 2004; pp 47–71.

(52)   Ciardelli, F.; Aglietto, M.; Passaglia, E.; Ruggeri, G.; Macromolecules, O. A.; Risorgimento, V. Molecular and Mechanistic Aspects of the Functionalization of Polyolefins with Ester Groups. *Macromol. Symp.* **1998**, *129*, 79–88.

(53)   Coiai, S.; Augier, S.; Pinzino, C.; Passaglia, E. Control of Degradation of Polypropylene during Its Radical Functionalisation with Furan and Thiophene Derivatives. *Polym. Degrad. Stab.* **2010**, *95*, 298–305.

(54)   Manning, S. C.; Moore, R. B. Functionalization of Polypropylene by Reactive Extrusion with Acidic Peroxides. *Am. Chem. Soc. Polym. Prepr. Div. Polym. Chem.* **1997**, *38*, 390–391.

(55)   Martell, J. M.; Verner, J. J.; Incavo, S. J. Clinical Performance of a Highly Cross-Linked Polyethylene at Two Years in Total Hip Arthroplasty: A Randomized Prospective Trial. *J. Arthroplasty* **2003**, *18*, 55–59.

(56)   Munier, C.; Gaillard-Devaux, E.; Tcharkhtchi, A.; Verdu, J. Durability of Cross-Linked Polyethylene Pipes under Pressure. *J. Mater. Sci.* **2002**, *37*, 4159–4163.

(57)   Chodák, I. Mechanical Properties of Crosslinked Polyolefin-Based Materials. *Prog. Polym. Sci.* **1995**, *20*, 1165–1199.

(58)   Romania, F.; Corrieri, R.; Bragab, V.; Ciardelli, F. Monitoring the Chemical Crosslinking of Propylene Polymers through Rheology. *Polymer (Guildf).* **2002**, *43*, 1115–1131.

(59)   Aglietto, M.; Alterio, R.; Bertani, R.; Galleschi, F.; Ruggeri, G. Polyolefin Functionalization by Carbene Insertion for Polymer Blends. *Polymer (Guildf).* **1989**, *30*, 1133–1136.

(60)   Lepage, M. L.; Simhadri, C.; Liu, C.; Takaffoli, M.; Bi, L.; Crawford, B.; Milani, A. S.; Wulff, J. E. A Broadly Applicable Cross-Linker for Aliphatic Polymers Containing C–H Bonds. *Science* **2019**, *366*, 875–878.

(61)   Liu, D.; Bielawski, C. W. Direct Azidation of Isotactic Polypropylene and Synthesis of 'Grafted to' Derivatives Thereof Using Azide-Alkyne Cycloaddition Chemistry.

Polym. Int. **2017**, *66*, 70–76.

(62) Zhou, H.; Wang, S.; Huang, H.; Li, Z.; Plummer, C. M.; Wang, S.; Sun, W. H.; Chen, Y. Direct Amination of Polyethylene by Metal-Free Reaction. *Macromolecules* **2017**, *50*, 3510–3515.

(63) Amaoka, Y.; Kamijo, S.; Hoshikawa, T.; Inoue, M. Radical Amination of C(sp^3)-H Bonds Using N -Hydroxyphthalimide and Dialkyl Azodicarboxylate. *J. Org. Chem.* **2012**, *77*, 9959–9969.

(64) Koshino, N.; Cai, Y.; Espenson, J. H. Kinetic Study of the Phthalimide N-Oxyl (PINO) Radical in Acetic Acid. Hydrogen Abstraction from C-H Bonds and Evaluation of O-H Bond Dissociation Energy of N-Hydroxyphthalimide. *J. Phys. Chem. A* **2003**, *107*, 4262–4267.

(65) Silva, G. Da; Bozzelli, J. W. Theoretical Study of the Oxidation Catalyst N-Hydroxyphthalimide (NHPI): Thermochemical Properties, Internal Rotor Potential, and Gas- And Liquid-Phase Bond Dissociation Energies. *J. Phys. Chem. C* **2007**, *111*, 5760–5765.

(66) Czaplyski, W. L.; Na, C. G.; Alexanian, E. J. C-H Xanthylation: A Synthetic Platform for Alkane Functionalization. *J. Am. Chem. Soc.* **2016**, *138*, 13854–13857.

CHAPTER II.

REGIOSELECTIVE POLYOLEFIN C–H XANTHYLATION VIA BLUE LIGHT IRRADIATION WITH A XANTHYLAMIDE REAGENT

● *regioselective* ● *mild conditions & no chain cleavage* ● *introduces diverse functionality*
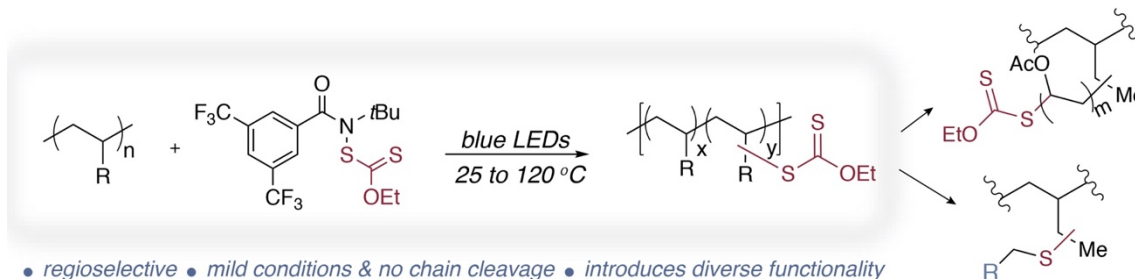
II-A. TANDEM AMIDYL RADICAL AND XANTHATE FOR SELECTIVE POLYOLEFIN C–H FUNCTIONALIZATION

This chapter was adapted in part from: J. B. Williamson, W. L. Czaplyski, E. J. Alexanian, F. A. Leibfarth. *Angew. Chem. Int. Ed.* **2018**, *57*, 6261.[1]

We envisioned a radical-mediated approach to branched polyolefin C–H functionalization that introduces a wide array of chemical functionality without the coincident chain degradation or interchain coupling typically observed during post-polymerization modification.[2] Key to our approach is the use of amidyl radicals as their associated N–H bond dissociation free energies (BDFE = 107–110 kcal/mol) are considerably higher than that of unactivated aliphatic C–H bonds (BDFE = 96–101 kcal/mol).[3] These electrophilic nitrogen-centered radicals participate in intermolecular C–H bond abstractions with regioselectivities dictated by the steric and electronic nature of the reagent.[4,5] The reagent-controlled selectivity of our approach disfavors the formation of tertiary radicals in the polymer backbone that are known to degrade material properties.[6,7] Furthermore, the efficient nature of hydrogen atom abstraction using heteroatom-centered

radicals does not require the use of large excesses of reagent to achieve relevant levels of polyolefin functionalization.[8,9]

As we have previously demonstrated in small molecule functionalization, C–H xanthylation offers a versatile platform for achieving a diverse set of C–H transformations.[10] Alkyl xanthates, therefore, represent a "universal" synthetic intermediate for, and if installed within an aliphatic polymer, could provide access to an array of advanced materials from commodity polyolefins.[11] Our modular approach is a departure from previous methodologies, which were each optimized for installation of a single functional group.[12–14]

II-B. POLYETHYLETHYLENE C–H XANTHYLATION VIA *N*-XANTHYLAMIDE

Our studies commenced with the use of commercially available *N*-xanthylamide **1** for the C–H xanthylation of branched polyolefins via the amidyl radical intermediate. We used polyethylethylene (PEE) with a number average molecular weight (M_n) of 3.6 kg/mol and a dispersity (Đ) of 1.26 as well-defined model branched polyolefin. This material was prepared by the reduction of a polybutadiene parent polymer with 90% 1,2 additions, which corresponds to approximately 40 ethyl branches per 100 carbons.[13] The well-defined structure of the
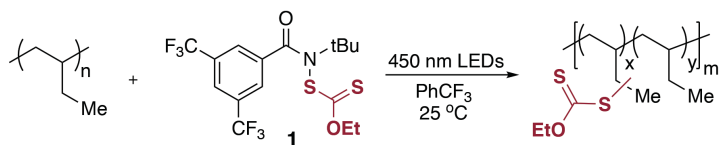
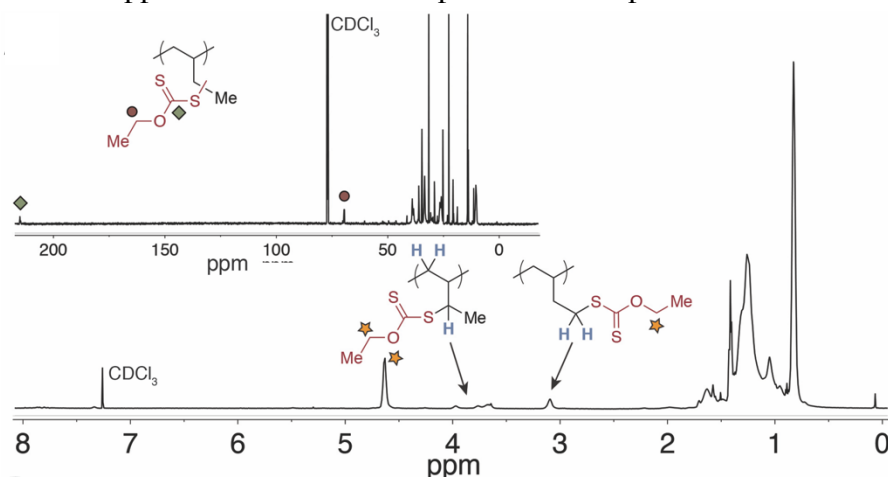| entry	equiv. **1**: repeat unit	percent xanthylation[a]	regioselectivity[a] 2°:1°	M_n (kg/mol)[b]	Đ
1	0	0	–	3.6	1.26
2	1:20	3	2.3:1	4.2	1.28
3	1:10	5	1.8:1	3.6	1.31
4	1:5	10	1.8:1	4.5	1.30
5	1:2	15	2.3:1	3.6	1.30
6	1:1	18	2.2:1	4.8	1.32
7[c]	1:10	6	1.8:1	4.3	1.33

Table 2.1 C–H xanthylation of PEE using *N*-xanthylamide **1**. Percent xanthylation is calculated as mol% with respect to repeat unit. [a]Percent xanthylation and regioselectivity determined by ^{1}H NMR. [b]M_n values obtained from GPC based on polystyrene standards. [c]Reaction performed in the absence of solvent at 60 °C.

branched polyolefin enabled the determination of subtle changes in the M_n and Đ under the reaction conditions.

We functionalized PEE with varying amounts of **1** in trifluorotoluene at room temperature under blue light irradiation at a concentration of [0.20 M] relative to **1** for 19 hours. Table 2.1 displays the results of a reaction screen for C–H xanthylation of PEE. The stoichiometry of **1** compared to the number of repeat units was varied and percent functionalization was analyzed by integration of the ¹H NMR spectra. As expected, increasing the concentration of **1** relative to repeat unit led to increased levels of polyolefin xanthylation (entries 3-6). These conditions allowed us to tune the level of polyolefin functionalization up to 18 mol%. The sole side product observed after reaction is the S–S dimer of ethyl xanthate, which is easily removed by polymer precipitation. Importantly, functionalization of PEE in the absence of solvent (**1** dissolved in pure polyolefin) performs equally well (entry 7).

II-C. CHARACTERIZATION OF XANTHYLATED POLYETHYLETHYLENE

¹H and ¹³C NMR provided quantitative evidence of polyolefin xanthylation (Figure 2.1). As compared to the parent PEE, new resonances appeared after reaction at δ 3.1, 3.7–4.0, and 4.6 ppm in the ¹H NMR spectrum. Comparison with small molecule standards and previously reported substrates confirmed that the protons *alpha* the sulfur atom of primary xanthates appear further upfield (3.1 ppm) than those

Figure 2.1 ¹H and ¹³C NMR spectra of PEE with 15 mol% xanthylation.

22

of secondary xanthates (3.7–4.0 ppm), while the resonance at 4.6 ppm corresponds to the

protons *alpha* to the oxygen atom.[10]

Heteronuclear single quantum coherence (HSQC) NMR between ^{1}H and ^{13}C confirmed the peak assignments (Figure 2.2). The difference between functionalization of secondary carbons located on the side-chain or backbone of PEE could not be determined by NMR, although we hypothesize that both are occurring under the reaction conditions. For the PEE functionalizations reported herein, we observed a preference of

Figure 2.2 HSQC spectrum of 15 mol % xanthylated PEE correlates the protons between δ 3.0 – 4.0 ppm in the ^{1}H NMR with peaks around δ 50 ppm in the ^{13}C NMR (encircled).

approximately two to one for secondary over primary xanthylation by ^{1}H NMR integration.

This polyolefin functionalization is considerably more selective for primary carbons than the functionalization of *n*-hexane alone, which occurs with 14:1 secondary:primary selectivity.[10] We hypothesize that this preference for
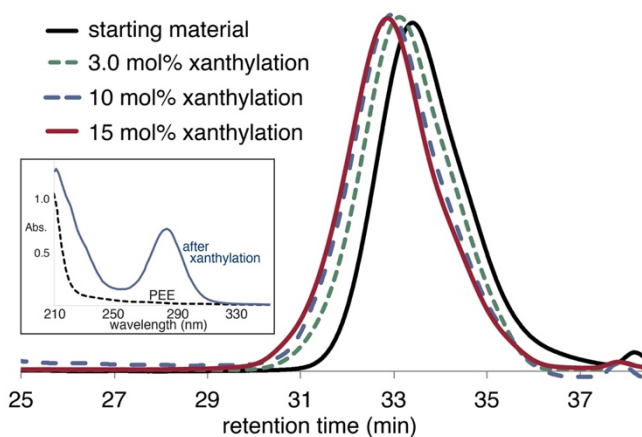
Figure 2.3 GPC Characterization of xanthylated PEE with a UV-vis spectrum taken at 33 min retention time.

23

primary xanthylation of the polymer is indicative of the increased steric hindrance of the polyolefin backbone shielding the methylene units of PEE.

Following polymer xanthylation, the GPC trace shifted slightly to higher retention time owing to the increase in both number-average (M_n) and weight-average (M_w) molecular weight upon addition of xanthate while the molecular weight distribution (MWD) remained relatively unchanged (Figure 2.3). These results are in stark contrast to traditional radical-based functionalization of branched polyolefins using peroxide initiators, which typically result in chain scission and a significant broadening of the MWD.[15] Only upon using high stoichiometries of reagent **1** compared to repeat unit (entry 6, Table 2.1) did we observe a small (<5%) high molecular weight shoulder in the GPC, which we attribute to radical–radical coupling of two polymer chains (Figure 2.4). Since there is little difference in mol % xanthylation between entries 5 and 6 (Table 2.1), we see little practical advantage to using high stoichiometries of **1** for polyolefin functionalization. The use of sub-stoichiometric amounts of reagent is a stark contrast to previous metal-free functionalization methods, which required large excesses of reagent to achieve modest levels (<10 mol%) of polyolefin functionality.
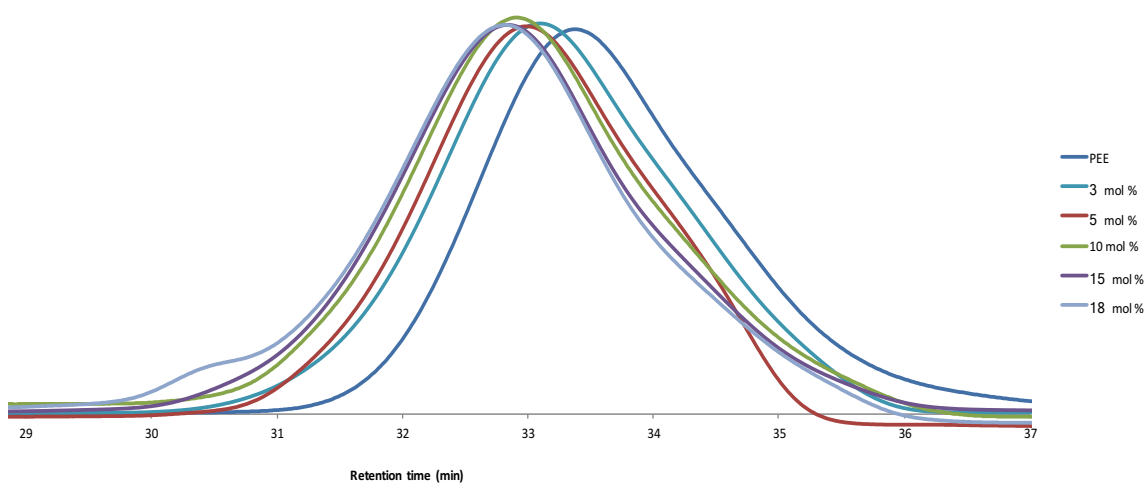
Retention time (min)

Figure 2.4 GPCs of xanthylated PEE with various mol % functionalization (mol % calculated based on repeat unit) shift to higher retention times as mol % xanthylation increased. The dispersity remained essentially unchanged. Each of the xanthylated polymers demonstrated the characteristic UV-Vis absorption of xanthate (283 nm) at the time of elution.

Analysis of the GPC photodiode array spectrum at a retention time of 33 minutes clearly showed the appearance of a new absorption peak centered at 283 nm (Figure 2.3, inset). The absorbance matches that of other aliphatic xanthates and provides further evidence that the reaction conditions are leading to polymer xanthylation.[16] Fourier transform infrared spectroscopy (FT-IR) also demonstrated the appearance of absorbances commensurate with
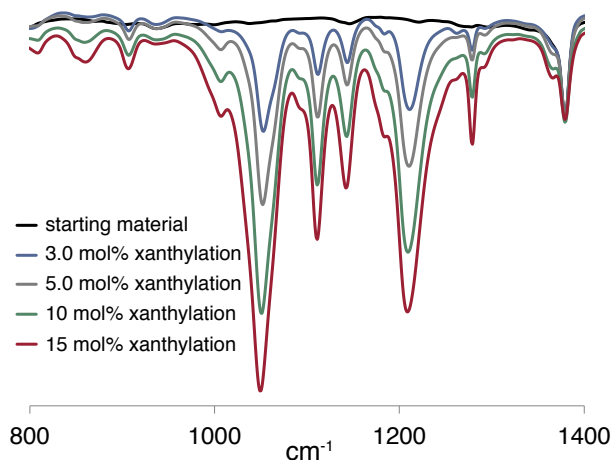
Figure 2.5 FT-IR spectra of polyethylethylene with varying mol % xanthylation. The peaks around 1215 and 1050 cm^{-1} are indicative of xanthate incorporation.

polymer-bound xanthate moieties at 1209 and 1050 cm^{-1} (Figure 2.5).[17] As expected, the intensity of these peaks increase as the mol % functionalization of PEE increases.

In order to probe the ability of **1** to xanthylate the tertiary C–H sites of PEE, we used
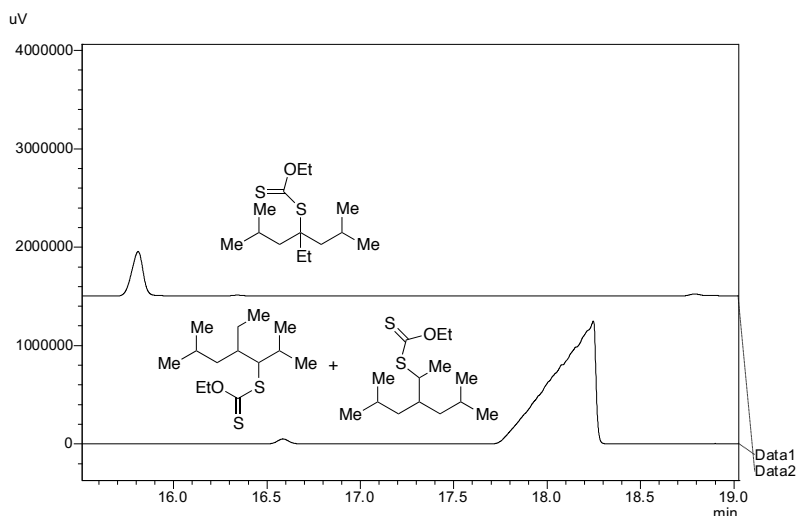
Figure 2.6 Gas Chromatography of xanthylated standards, indicating no tertiary backbone xanthylation. Top chromatogram: tertiary standard synthesized independently, with a retention time of 15.8 min. Bottom chromatogram: products from reaction of model substrate, 4-ethyl-2,6-dimethylheptane, with xanthylamide **1** and blue light irradiation, with retention times of 16.6 and 18 min.

the small molecule standard 4-ethyl-2,6-dimethylheptane as an analogue to the steric environment of the PEE backbone. We subjected this substrate to the reaction conditions used for PEE xanthylation and did not observe the product of tertiary

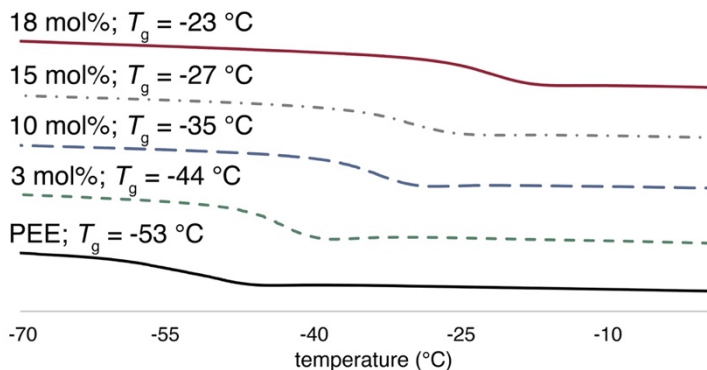xanthylation by gas chromatography, demonstrating that **1** favors secondary or primary C–H sites (Figure 2.6). Additionally, the rapid rate of radical xanthyl group-transfer is approximately four orders of magnitude faster than radical isomerization reactions that would lead to tertiary radicals capable of chain-degradation.[18,19]

The thermal properties of these functionalized polyolefins demonstrate the influence of xanthylation. Thermal gravimetric analysis (TGA) of unfunctionalized PEE showed a decomposition temperature (T_D), measured where the polymer lost 10% of its initial mass, at 412 °C. Each of the xanthylated polymers, however, demonstrate a partial mass loss starting at approximately 250 °C, with the

100
80
weight %
60
40
20
0

— starting material
— 3.0 mol% xanthylation
— 5.0 mol% xanthylation
— 10 mol% xanthylation
— 15 mol% xanthylation

100   200   300   400   500   600
temperature (°C)

Figure 2.7 TGA of xanthylated PEEs reveals a Chugaev or Chugaev-like elimination occurs on the polymer around 250 °C prior to depolymerization of the polymer around 400 °C. Weight loss is consistent with the degree of functionalization observed in the ^{1}H NMR.

magnitude of the mass loss increasing with an increase in the mol% xanthylation. Xanthates are well-known to undergo a thermal Chugaev elimination at elevated temperatures to yield an alkene and carbonyl sulfide, which we hypothesis is occurring on the polymer (Figure 2.7).[20]

18 mol%; T_g = -23 °C
15 mol%; T_g = -27 °C
10 mol%; T_g = -35 °C
3 mol%; T_g = -44 °C
PEE; T_g = -53 °C

-70   -55   -40   -25   -10
temperature (°C)

Figure 2.8 DSC curves displaying the T_g of xanthylated polyolefins. All DSC data taken from the 2nd heating cycle at a rate of 10 °C/min.

Xanthylation also significantly influences the glass transition temperature (T_g) of PEE as measured by differential scanning calorimetry (DSC), with data taken from the second

26

heating cycle using a ramp rate of 10 °C/min (Figure 2.8). Increased presence of the bulky

xanthate group along the backbone yields up to a 30 °C increase in the T_g of the amorphous

material, with the extent of the increase related to the mol% of xanthate groups incorporated.

This further confirms the impact of xanthylation on polyolefin properties and demonstrates

how this strategy can provide tunable control over the thermal properties of polyolefins.

II-D. XANTHATE AS AN INTERMEDIATE TOWARDS OTHER POLAR FUNCTIONALITY ON POLYOLEFINS

We view xanthylated polyolefins as a material platform for accessing diverse,

functional materials that unlock a range of new polymer properties (Figure 2.9). This is in

contrast to previous methods targeting the introduction of a single functional group, with new

C–H transformations required for each new desired derivative. This approach takes advantage

of the remarkable versatility of alkyl xanthates in both radical-mediated and polar bond-

forming reactions.[21–23] For example, reagents recently developed by Shen and co-workers

enable a one-step introduction of the trifluoromethylthio group (**2**).[24] This functional group,
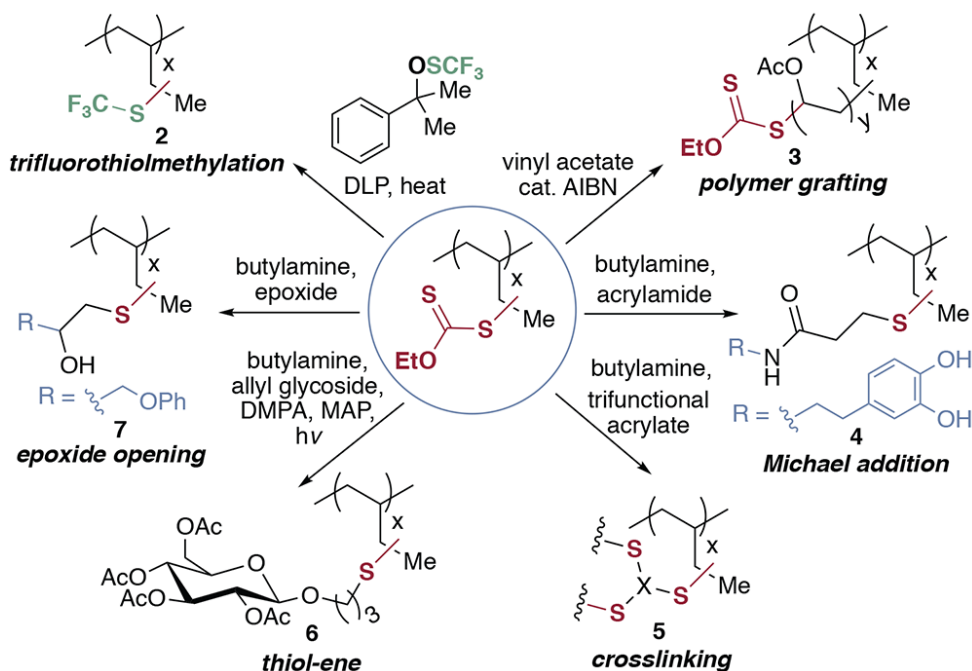
Figure 2.9 Diverse functionalized polyolefins from a single xanthylated polyolefin precursor.

27

well-known to modulate the lipophilicity of medicinal compounds, is underexplored in polymer chemistry. Furthermore, the xanthate group was used directly as a chain-transfer agent for the reversible addition–fragmentation chain-transfer (RAFT) polymerization of vinyl acetate (**3**).[25] Exposure of PEE with 6 mol% xanthylation to RAFT conditions led to a PEE-*graft*-poly(vinyl acetate) copolymer that displayed two distinct T_gs (Figure 2.10). Although a polyolefin backbone is not the ideal R group for the RAFT process, initiation still occurred and resulted in a material with a significantly lower M_n and Đ (2.02) than the same polymerization initiated in the absence of a macromolecular RAFT agent (3.06, Figure 2.11).
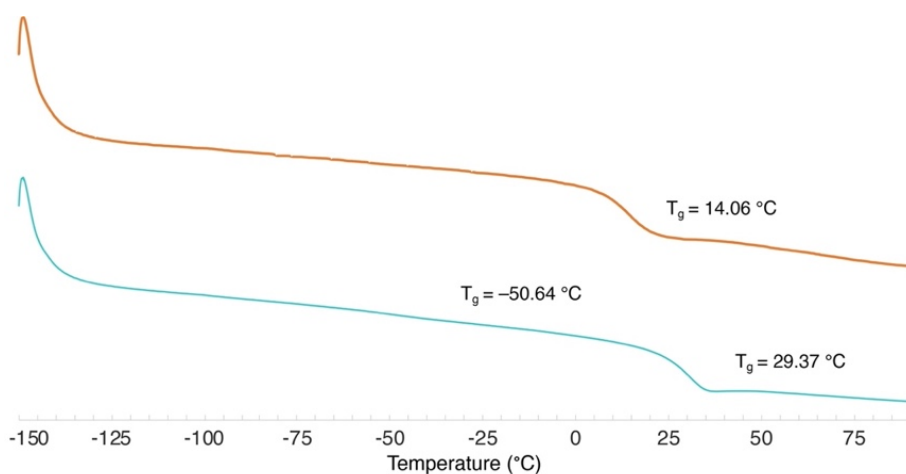

Figure 2.10 DSC of poly(ethyl ethylene–*graft*–vinyl acetate). the DSC demonstrates two distinct T_g values (blue) representing the polyolefin (-50.6 °C) and the poly(vinyl acetate) (26.4 °C). The DSC of PEE is shown in orange for reference.

Xanthates also enable facile access to the thiol functional group by aminolysis or hydrolysis. Characterization by ^{1}H and ^{13}C NMR, FT-IR, and GPC confirmed cleavage of the xanthylate upon aminolysis. The revealed thiol represents a valuable group for diversifying polyolefin functionality through a number of reactions, including thiol-ene chemistry as well as Michael addition and epoxide ring-opening.[26] Michael addition of the thiol to an acrylate or acrylamide can be used to install a range of valuable groups. For instance, adhesive catechol groups were incorporated into branched polyolefins through this methodology (**4**), which could act as a valuable compatibilizing group applications in composite materials.[27,28] Furthermore,

28

the long-standing challenge of crosslinking branched polyolefins can be addressed through the reaction of thiol-functionalized PEE with commercially available, multi-functional acrylates to form polyolefin thermosets or elastomers (**5**).[29] Thiol-ene functionalization works well
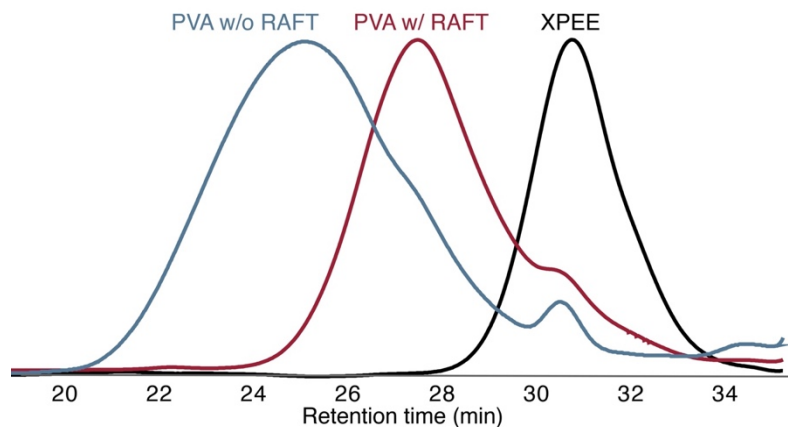

Figure 2.11 GPC overlay comparing the free-radical polymerization of vinyl acetate with and without a macromolecular chain-transfer agent. The blue trace is the result of a free radical polymerization of vinyl acetate initiated by AIBN and run at 80 °C for 19 hours (M_n = 52 kg/mol, PDI = 3.07). The black trace is a sample of xanthylated PEE containing 14 mol% xanthate moieties. The red trace is the result of the RAFT polymerization of vinyl acetate initiated with AIBN and run in the presence of xanthylated PEE (M_n = 17 kg/mol, PDI = 2.00).

in these systems to furnish materials such as glucose-functionalized PEE, whose saccharide group could act to improve the mixing of cellulose/polyolefin blends (**6**).[30] Finally, sequential addition of butylamine and phenyl glycidyl ether generated hydroxyl-containing PEE in a one-pot procedure (**7**).

II-E. XANTHYLATION OF HIGH MOLECULAR WEIGHT AND COMMODITY POLYOLEFINS

Successful polyolefin xanthylation demonstrated the mild functionalization conditions, regioselectivity, and versatility of this platform. Most
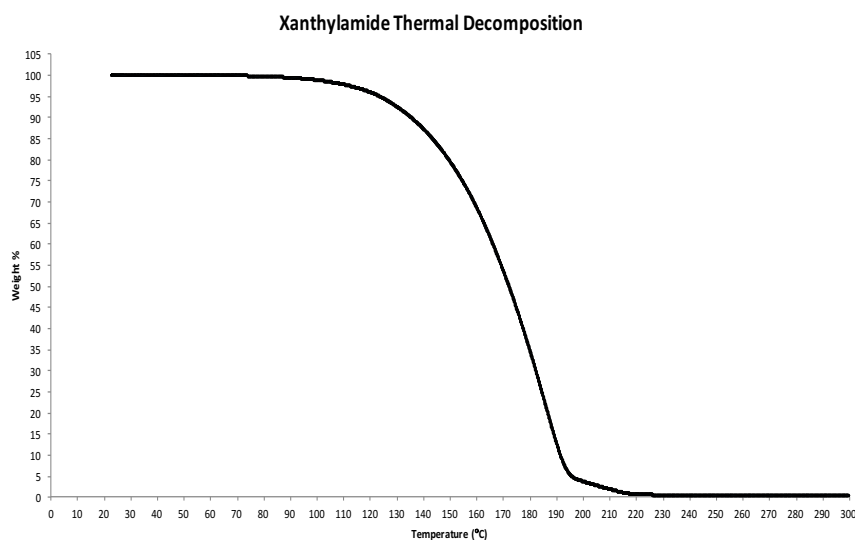
Figure 2.12 Thermal stability of xanthylamide

commercial polyolefins, however, are semicrystalline thermoplastics. Translation of homogeneous C–H functionalization chemistry to these intractable materials requires high temperature conditions at which they are soluble. Thermal analysis of **1** confirmed its stability up to 120 °C (Figure 2.12). The photochemical C–H xanthylation of PEE at 120 °C in 1,2-dichlorobenzene led to nearly identical results as compared to the room temperature reaction (Figure 2.13). For example, PEE reacted with 10 mol% **1** per repeat unit at 120 °C resulted in a material with 3.0 mol% xanthylation per repeat unit.
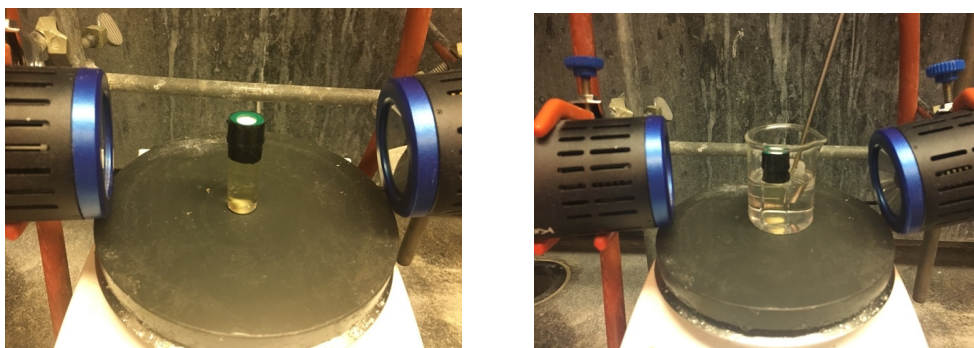
Figure 2.13 Photo of translating the reaction at room temperature to high temperatures to perform reactions on commodity polyolefins

We next turned our attention to the C–H xanthylation of commercially relevant polyolefins to demonstrate the scope of the method. A low molecular weight sample of semicrystalline polyethylene (T_m = 92 °C) underwent efficient xanthylation at elevated temperatures, resulting a slight increase in M_n and minimal change to the MWD (Figure 2.14). Commercial polyolefins are traditionally more challenging substrates. A sample of commercial high-density polyethylene (ExxonMobil™ HD6719; T_m = 131 °C) performed analogous to PEE under the reaction conditions, achieving 5 mol% xanthylation with only a 10 mol% loading of reagent **1**. This efficiency is in contrast to other metal-free methods, wherein a large excess of reagent is typically needed to achieve similar functionalization.[9,31]

We hypothesized that the regioselectivity of reagent **1** would enable the first metal-free C–H functionalization of branched, commercial polyolefins that does not cause coincident chain-scission. A commercial copolymer of ethylene and 1-hexene designated as linear low-density polyethylene (Dow™ DNDA-1081; T_m = 113 °C) with approximately two butyl branches per 100 carbons was subjected to our homogeneous reaction conditions at 120 °C. The polymer underwent xanthylation at commensurate levels to both PEE and HDPE with no evidence of chain

substrate	equiv. **1**: repeat unit	percent xanthylation[a]	before rxn M_n M_w (kg/mol)[b]		after rxn M_n M_w (kg/mol)[b]	
PE	1:10	8	4.5	9.6	4.7	10
HDPE	1:10	5	15	49	15	62
LLDPE	1:10	4	8.1	31	13	46
EP copolymer	1:10	3	463	490	521	605
hyperbranched PE	1:20	3	29	47	35	57
	1:10	7	29	47	36	65
	1:2	13	29	47	36	67

Table 2.2 Functionalization of high molecular weight and commodity polyolefins.

scission. To understand the performance of **1** with high molecular weight polyolefins, a multi-arm polyolefin elastomer derived from the hydrogenation of parent polyisoprene (PI) star polymer (Kraton™ G1750) was subjected to the reaction conditions at 60 °C. This material can be considered a perfectly alternating copolymer of ethylene and propylene, with 25 methyl branches for every 100 carbons. The peak in GPC corresponding to a molecular weight of 463 kg/mol for the starting material was most diagnostic. Reaction with 10 mol% of **1** resulted in 3 mol% xanthylation of the material with only a modest increase of molecular weight and no observable chain scission (Table 2.2). The ability for **1** to selectively modify such high molecular weight branched polyolefins without deleterious chain scission or crosslinking is unprecedented for polyolefin C–H functionalization and further demonstrates the efficiency

and selectivity of this methodology. Lastly, xanthylation of hyperbranched PE with an M_n of 29 kg/mol and 13 methyl branches per 100 carbons was studied.[32–34] Percent xanthylation increased as more of **1** is included in the reaction with a minimal effect on molecular weight. In the case of HDPE, LLDPE, hyperbranched PE, and hydrogenated PI, xanthylation resulted in a more significant increase in M_w compared to M_n. The lack of chain scission and increase in M_w is beneficial for increasing the melt strength of these polymers, which is especially attractive for film blowing of branched polyolefins.[35]

II-F. SUMMARY OF FINDINGS

In conclusion, we have demonstrated a new approach toward the functionalization of commercial polyolefins under mild and metal-free reaction conditions. This approach capitalizes on the regioselectivity of C–H xanthylation to avoid the long-standing problem of chain cleavage in radical-mediated functionalizations of branched polyolefins. Adjusting the stoichiometry of **1** enables the fine tuning of the level of polyolefin functionalization. The versatility of the xanthate functional group enables access to a wide variety of valuable functionalized polyolefins inaccessible using prior approaches. With the initial demonstrations of commercial polyolefin functionalization, we anticipate that this approach will enhance the utility of these lightweight thermoplastics where adhesion to or blending with polar materials provides improved properties in a variety of applications. Future studies will continue to explore the unique capabilities of our C–H functionalization platform as an enabling technology for the discovery of polyolefins with unique and valuable properties.

REFERENCES

(1)   Williamson, J. B.; Czaplyski, W. L.; Alexanian, E. J.; Leibfarth, F. A. Regioselective C–H Xanthylation as a Platform for Polyolefin Functionalization. *Angew. Chem. Int. Ed.* **2018**, *57*, 6261–6265. https://doi.org/10.1002/anie.201803020.

(2)   Boaen, N. K.; Hillmyer, M. A. Post-polymerization functionalization of polyolefins. *Chem. Soc. Rev.* **2005**, *34*, 267. https://doi.org/10.1039/b311405h.

(3)   Blanksby, S. J.; Ellison, G. B. Bond dissociation energies of organic molecules. *Acc. Chem. Res.* **2003**, *36*, 255–263. https://doi.org/10.1021/ar020230d.

(4)   Schmidt, V. A.; Quinn, R. K.; Brusoe, A. T.; Alexanian, E. J. Site-selective aliphatic C-H bromination using N -bromoamides and visible light. *J. Am. Chem. Soc.* **2014**, *136*, 14389–14392. https://doi.org/10.1021/ja508469u.

(5)   Quinn, R. K.; Könst, Z. A.; Michalak, S. E.; Schmidt, Y.; Szklarski, A. R.; Flores, A. R.; Nam, S.; Horne, D. A.; Vanderwal, C. D.; Alexanian, E. J. Site-Selective Aliphatic C-H Chlorination Using N-Chloroamides Enables a Synthesis of Chlorolissoclimide. *J. Am. Chem. Soc.* **2016**, *138*, 696–702. https://doi.org/10.1021/jacs.5b12308.

(6)   Gloor, P. E.; Tang, Y.; Kostanska, A. E.; Hamielec, A. E. Chemical modification of polyolefins by free radical mechanisms: a modelling and experimental study of simultaneous random scission, branching and crosslinking. *Polymer (Guildf)*. **1994**, *35*, 1012–1030. https://doi.org/10.1016/0032-3861(94)90946-6.

(7)   Hamielec, A. E.; Gloor, P. E.; Zhu, S. Kinetics of, free radical modification of polyolefins in extruders – chain scission, crosslinking and grafting. *Can. J. Chem. Eng.* **1991**, *69*, 611–618. https://doi.org/10.1002/cjce.5450690302.

(8)   Díaz-Requejo, M. M.; Wehrmann, P.; Leatherman, M. D.; Trofimenko, S.; Mecking, S.; Brookhart, M.; Pérez, P. J. Controlled, copper-catalyzed functionalization of polyolefins. *Macromolecules* **2005**, *38*, 4966–4969. https://doi.org/10.1021/ma050626f.

(9)   Zhou, H.; Wang, S.; Huang, H.; Li, Z.; Plummer, C. M.; Wang, S.; Sun, W. H.; Chen, Y. Direct Amination of Polyethylene by Metal-Free Reaction. *Macromolecules* **2017**, *50*, 3510–3515. https://doi.org/10.1021/acs.macromol.6b02572.

(10) Czaplyski, W. L.; Na, C. G.; Alexanian, E. J. C-H Xanthylation: A Synthetic Platform for Alkane Functionalization. *J. Am. Chem. Soc.* **2016**, *138*, 13854–13857. https://doi.org/10.1021/jacs.6b09414.

(11) Zard, S. Z. On the Trail of Xanthates: Some New Chemistry from an Old Functional Group. *Angew. Chem. Int. Ed.* **1997**, *36*, 672–685. https://doi.org/10.1002/anie.199706721.

(12) Bae, C.; Hartwig, J. F.; Chung, H.; Harris, N. K.; Switek, K. A.; Hillmyer, M. A. Regiospecific side-chain functionalization of linear low-density polyethylene with polar groups. *Angew. Chem. Int. Ed.* **2005**, *44*, 6410–6413. https://doi.org/10.1002/anie.200501837.

(13) Kondo, Y.; García-Cuadrado, D.; Hartwig, J. F.; Boaen, N. K.; Wagner, N. L.; Hillmyer, M. A. Rhodium-catalyzed, regiospecific functionalization of polyolefins in the melt. *J. Am. Chem. Soc.* **2002**, *124*, 1164–1165. https://doi.org/10.1021/ja016763j.

(14) Bae, C.; Hartwig, J. F.; Boaen Harris, N. K.; Long, R. O.; Anderson, K. S.; Hillmyer, M. A. Catalytic hydroxylation of polypropylenes. *J. Am. Chem. Soc.* **2005**, *127*, 767–776. https://doi.org/10.1021/ja044440s.

(15) Rätzsch, M.; Bucka, H.; Hesse, A.; Reichelt, N.; Borsig, E. Challenges in polypropylene by chemical modification. *Macromol. Symp.* **1998**, *129*, 53–77.

(16) Pomianowski, A.; Leja, J. Spectrophotometric Study of Xanthate and Dixanthogen Solutions. *Can. J. Chem.* **1963**, *41*, 2219–2230. https://doi.org/10.1139/v63-322.

(17) Poling, G. W.; Leja, J. Infrared Study of Xanthate Adsorption on Vacuum Deposited Films of Lead Sulfide and Metallic Copper Under Conditions of Controlled Oxidation. *J. Phys. Chem.* **1963**, *67*, 2121–2126. https://doi.org/10.1021/j100804a036.

(18) Coote, M. L.; Radom, L. Substituent effects in xanthate-mediated polymerization of vinyl acetate: Ab initio evidence for an alternative fragmentation pathway. *Macromolecules* **2004**, *37*, 590–596. https://doi.org/10.1021/ma035477k.

(19) Wang, K.; Villano, S. M.; Dean, A. M. Reactivity-Structure-Based Rate Estimation Rules for Alkyl Radical H Atom Shift and Alkenyl Radical Cycloaddition Reactions. *J. Phys. Chem. A* **2015**, *119*, 7205–7221. https://doi.org/10.1021/jp511017z.

(20) Chugaev, L. A new method for the preparation of unsaturated hydrocarbons. *Ber.* **1899**, *32*, 3332–3335.

(21) Quiclet-Sire, B.; Zard, S. Z. Some aspects of radical chemistry in the assembly of complex molecular architectures. *Beilstein J. Org. Chem.* **2013**, *9*, 557–576. https://doi.org/10.3762/bjoc.9.61.

(22) Quiclet-Sire, B.; Zard, S. Z. Riding the tiger: Using degeneracy to tame wild radical processes. *Pure Appl. Chem.* **1997**, *69*, 645–650. https://doi.org/10.1351/pac199769030645.

(23) Quiclet-Sire, B.; Zard, S. Z. Powerful Carbon-Carbon Bond Forming Reactions Based on a Novel Radical Exchange Process. *Chem. - A Eur. J.* **2006**, *12*, 6002–6016. https://doi.org/10.1002/chem.200600510.

(24)   Shao, X.; Xu, C.; Lu, L.; Shen, Q. Structure-reactivity relationship of trifluoromethanesulfenates: Discovery of an electrophilic trifluoromethylthiolating reagent. *J. Org. Chem.* **2015**, *80*, 3012–3021. https://doi.org/10.1021/jo502645m.

(25)   Stenzel, M. H.; Cummins, L.; Roberts, G. E.; Davis, T. P.; Vana, P.; Barner-Kowollik, C. Xanthate Mediated Living Polymerization of Vinyl Acetate : A Systematic Variation in MADIX / RAFT Agent Structure. *Macromol. Chem. Phys.* **2003**, *204*, 1160–1168.

(26)   Le Neindre, M.; Nicolaÿ, R. One-pot deprotection and functionalization of polythiol copolymers via six different thiol-X reactions. *Polym. Int.* **2014**, *63*, 887–893. https://doi.org/10.1002/pi.4665.

(27)   Kord Forooshani, P.; Lee, B. P. Recent approaches in designing bioadhesive materials inspired by mussel adhesive protein. *J. Polym. Sci. Part A Polym. Chem.* **2017**, *55*, 9–33. https://doi.org/10.1002/pola.28368.

(28)   Wang, C. X.; Braendle, A.; Menyo, M. S.; Pester, C. W.; Perl, E. E.; Arias, I.; Hawker, C. J.; Klinger, D. Catechol-based layer-by-layer assembly of composite coatings: A versatile platform to hierarchical nano-materials. *Soft Matter* **2015**, *11*, 6173–6178. https://doi.org/10.1039/c5sm01374g.

(29)   Lin, W.; Shao, Z.; Dong, J. Y.; Chung, T. C. M. Cross-linked polypropylene prepared by PP copolymers containing flexible styrene groups. *Macromolecules* **2009**, *42*, 3750–3754. https://doi.org/10.1021/ma9002775.

(30)   Kim, H. S.; Lee, B. H.; Choi, S. W.; Kim, S.; Kim, H. J. The effect of types of maleic anhydride-grafted polypropylene (MAPP) on the interfacial adhesion properties of bio-flour-filled polypropylene composites. *Compos. Part A Appl. Sci. Manuf.* **2007**, *38*, 1473–1482. https://doi.org/10.1016/j.compositesa.2007.01.004.

(31)   Aglietto, M.; Alterio, R.; Bertani, R.; Galleschi, F.; Ruggeri, G. Polyolefin functionalization by carbene insertion for polymer blends. *Polymer (Guildf).* **1989**, *30*, 1133–1136. https://doi.org/10.1016/0032-3861(89)90093-1.

(32)   Bézier, D.; Daugulis, O.; Brookhart, M. Oligomerization of Ethylene Using a Diphosphine Palladium Catalyst. *Organometallics* **2017**, *36*, 443–447. https://doi.org/10.1021/acs.organomet.6b00850.

(33)   Ittel, S. D.; Johnson, L. K.; Brookhart, M. Late-metal catalysts for ethylene homo- and copolymerization. *Chem. Rev.* **2000**, *100*, 1169–1203. https://doi.org/10.1021/cr9804644.

(34)   Tempel, D. J.; Johnson, L. K.; Huff, R. L.; White, P. S.; Brookhart, M. Mechanistic studies of Pd(II)-α-diimine-catalyzed olefin polymerizations. *J. Am. Chem. Soc.* **2000**, *122*, 6686–6700. https://doi.org/10.1021/ja000893v.

(35)   Yoshii, F.; Makuuchi, K.; Kikukawa, S.; Tanaka, T.; Saitoh, J.; Koyama, K. High-melt-strength polypropylene with electron beam irradiation in the presence of polyfunctional monomers. *J. Appl. Polym. Sci.* **1996**, *60*, 617–623. https://doi.org/10.1002/(sici)1097-4628(19960425)60:4<617::aid-app16>3.0.co;2-w.

CHAPTER III.

THERMAL POLYOLEFIN C–H FUNCTIONALIZATION VIA AN AMIDYL RADICAL: MECHANISTIC STUDIES AND APPLICATION IN REACTIVE EXTRUSION
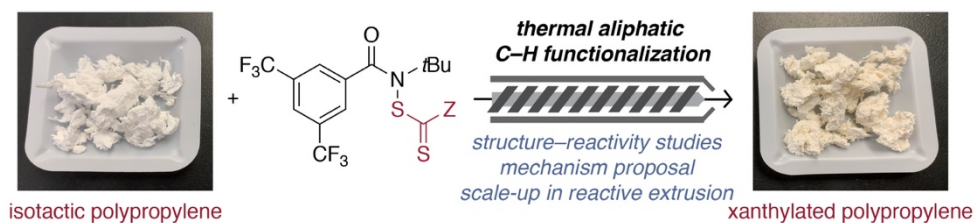

III-A. REQUIREMENT OF MECHANISTIC UNDERSTANDING AND THERMAL INITIATION

This chapter was adapted in part from: J. B. Williamson, C. G. Na, R. R. Johnson III, W. F. M. Daniel Jr., E. J. Alexanian, F. A. Leibfarth. *J. Am. Chem. Soc.* **2019**, *141*, 12815.[1]

In an effort to develop a metal-free post-polymerization modification (PPM) reaction that retains the beneficial thermomechanical properties of the parent polymer, we recently identified a sterically encumbered *N*-xanthylamide reagent that, upon photolysis, provided regioselective xanthyl group transfer to branched polyolefins without deleterious chain scission reactions.[2] In contrast to previously reported metal-free PPM approaches that rely on radicals generated from the thermal decomposition of peroxides to abstract hydrogen atoms[3–5], this reagent did not require an exogenous initiator, which suggests that the transformation proceeds through a fundamentally distinct pathway. The development of a thermal PPM process combined with a deeper understanding of the mechanism of this unique reagent was required to design improved reagents and identify reaction conditions that enable functionalization via reactive extrusion.

Our working mechanistic hypothesis is that thiocarbonylthio-amide reagents provide a privileged scaffold in that: 1) an amidyl radical is responsible for hydrogen atom abstraction and 2) is followed rapidly by the trapping of the polymer-centered radical by the thiocarbonyl group of the reagent (Figure 3.1). This results in a set of complex equilibria that we probe herein through systematic reagent design, crossover experiments, and kinetic studies. The culmination of the data presented provides the rational design of reagents and reaction conditions for the thermally initiated functionalization of branched polyolefins without coincident chain-scission. Key principles identified from systematic experiments facilitated the C–H xanthylation of isotactic polypropylene (*i*PP) within a twin-screw extruder. The resulting functionalized *i*PP demonstrated similar mechanical properties to the virgin polymer while exhibiting twice the adhesion strength to polar substrates. The fundamental understanding of the elementary steps in amidyl radical-mediated polyolefin functionalization provided in this report reveals key structure–reactivity relationships and serves as a platform for design of improved methods and translational technologies for polymer C–H functionalization.
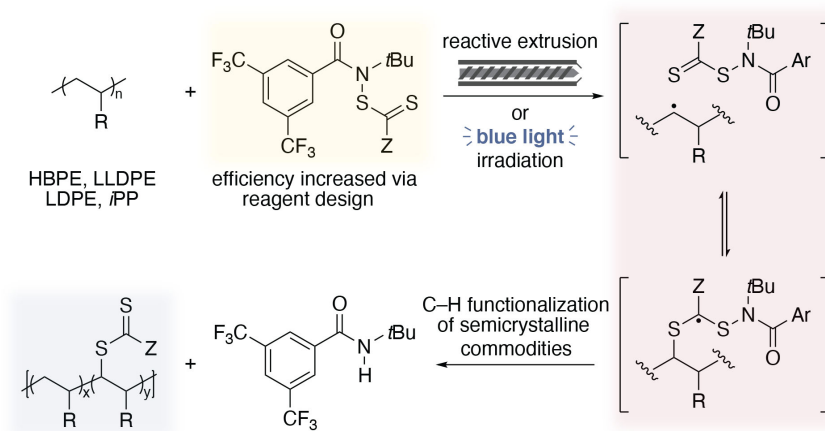
Figure 3.1. Outline of mechanistic analysis of thermal C–H thiocarbonylthiolation of polyolefins

III-B. STRUCTURE–REACTIVITY STUDIES OF AMIDYL REAGENTS ON SMALL MOLECULE SURROGATE

To develop structure–reactivity relationships for the thermally initiated C–H functionalization, cyclooctane was chosen as a small molecule surrogate to facilitate rapid and accurate characterization. Heating cyclooctane to 80 °C in benzene (0.15 M) with xanthylamide **1a** and 10 mol % azobisbutyronitrile (AIBN) successfully yielded xanthylated
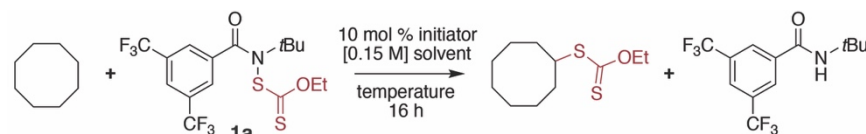
Initiator	Solvent	Temperature	N–S cleavage	Percent yield
AIBN	PhH	80 °C	24%	22%
DLP	PhH	80 °C	36%	25%
BPO	PhH	80 °C	26%	17%
BPO	PhCl	100 °C	63%	39%
(*t*BuO)$_2$	PhCl	130 °C	37%	23%
DCP	PhCl	110 °C	56%	37%
DCP	PhCl	130 °C	100%	66%

Figure 3.2 Optimization of the thermally initiated xanthylation of cyclooctane with **1a**. N–S cleavage and percent yield were determined by ^{1}H NMR analysis using hexamethyldisiloxane as an internal standard.

cyclooctane in a 22% yield (Figure 3.2). These conditions resulted in only 24% homolysis of the N–S bond in **1a**, which was monitored by conversion of **1a** to its respective parent amide by ^{1}H NMR. Alternative radical initiators, such as dilauroyl peroxide (DLP) and benzoyl peroxide (BPO), yielded similar results at 80 °C. In the case of BPO, increasing the reaction temperature resulted in an increase in yield. Further optimization found that the reaction performed best with dicumyl peroxide (DCP) at 130 °C. Upon product isolation, only xanthylated cyclooctane, *O,O*-diethyl dithiobis-(thioformate), and the parent amide were observed. This chemoselective C–H functionalization is attractive for translation to polymer substrates, since multiple products attached to the same polymer chain cannot be separated from one another.[6]

III-C. EXPANSION OF REAGENT SCOPE TO PROBE THE ELECTRONIC INFLUENCE OF THE Z GROUP
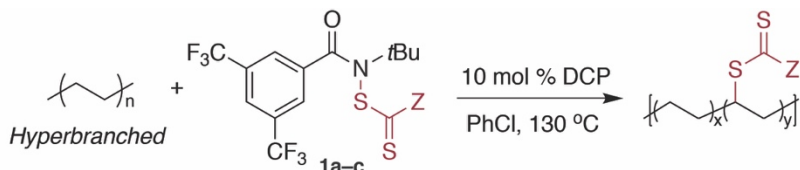
The electronic properties of thiocarbonylthio functional groups are known to play a large role in their reactivity. For example, these groups demonstrate different rates of chain-transfer in reversible addition–fragmentation chain-transfer (RAFT) radical
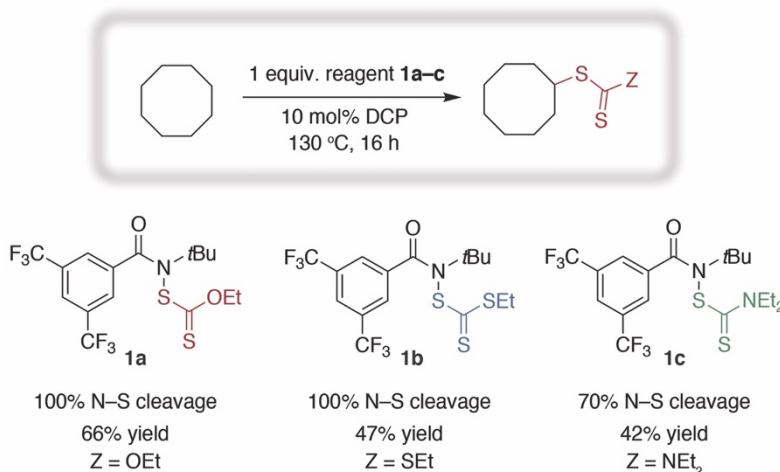
Figure 3.3 Structure–reactivity trends within the thermal C–H functionalization of cyclooctane. N–S cleavage and percent yield were determined by ^{1}H NMR analysis using hexamethyldisiloxane as an internal standard.

polymerization.[7–10] To probe the structure–reactivity properties of amidyl reagents with different thiocarbonylthio groups, we designed and synthesized **1a–c** (Figure 3.3).[11–13] Similar to RAFT polymerization, thiocarbonylthio groups can be conveniently described with respect to their Z groups: –OEt for **1a**, –SEt for **1b**, and –NEt$_2$ for **1c**. Despite differing only in the heteroatom of the Z group, reagents **1b** and **1c** provided lower yields of functionalized cyclooctane under analogous conditions to those of **1a**. Trithiocarbonylamide **1b** was observed to undergo complete N–S cleavage of **1b** to parent amide, but only a 47% yield of trithiocarbonylated cyclooctane was obtained. Dithiocarbamylamide **1c** did not completely convert to parent amide, but demonstrated similar yield as reagent **1b**.

III-D. THERMAL C–H FUNCTIONALIZATION OF HYPERBRANCHED POLYETHYLENE

To translate the results on cyclooctane to polymeric substrates, hyperbranched polyethylene (HBPE) was chosen as a model branched polyolefin for reaction optimization. HBPE with 10 methyl branches per 100 carbons was synthesized


Entry	Z	Theoretical mol % funct.	Actual mol % funct.[a]	Before[b]		After[b]	
				M_n	Đ	M_n	Đ
1	—OEt	10	4	35	1.03	48	1.11
2	—OEt	20	5	35	1.03	51	1.07
3	—OEt	50	7	35	1.03	53	1.09
4	—OEt	100	7	35	1.03	40	1.07
5	—SEt	10	3	42	1.05	45	1.12
6	—SEt	20	3	42	1.05	45	1.08
7	—SEt	50	3	42	1.05	45	1.06
8	—SEt	100	3	42	1.05	43	1.10
9	—NEt$_2$	10	1	35	1.17	35	1.22
10	—NEt$_2$	20	1	35	1.17	35	1.28
11	—NEt$_2$	50	1	35	1.17	35	1.27
12	—NEt$_2$	100	1	35	1.17	36	1.24

Table 3.1 Reagents **1a–c** were reacted with HBPE in the presence of DCP. [a]Determined by ^{1}H NMR in CDCl$_3$. [b]Determined by SEC against polystyrene standards in tetrahydrofuran.

using a previously reported Pd(II) α-diimine catalyst.[14] Polymers with different number-average molar mass (M_n) and narrow dispersities (Đ) were synthesized in order to determine the influence of reaction conditions on molecular weight and MWD. The use of amorphous HBPE enabled facile characterization of a branched polyolefin at room temperature. Under homogeneous conditions, HBPE was heated at 130 °C for 6–24 hours in the presence of **1a–c** and 10 mol % DCP in chlorobenzene at a concentration of 0.2 M with respect to reagent (Table 3.1). The stoichiometry of reagents **1a–c** was varied relative to repeat unit, with functionalization reported as mol % compared to the polymer repeat unit.

Polymer C–H functionalization was quantified by ^{1}H NMR integration of the methylene protons of the Z group (Figure 3.4). Theoretical maximum functionalization represents the stoichiometry of reagent relative to repeat unit (*i.e.*, a theoretical maximum of 10 mol % functionalization is addition of 1 equivalent of reagent per 10 repeat units). Exposing HBPE
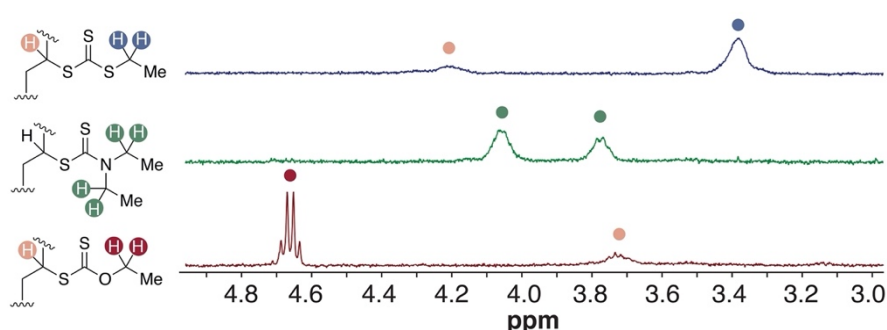
Figure 3.4 ^{1}H NMR of 1 mol % functionalized HBPE was taken in CDCl₃ and used to determine percent functionalization. The methine proton of dithiocarbamylated HBPE likely overlaps with the methylene protons of the diethylamine Z group

along with reagent **1a** at a theoretical maximum functionalization of 10 mol % resulted in 4 mol % polymer xanthylation (Entry 1, Table 3.1). By increasing the mol % theoretical maximum xanthylation, C–H functionalization of HBPE proved tunable in a range of 1–7 mol %. Despite the addition of more reagent, the ultimate mol % functionalization plateaued around 8 mol % for reagent **1a**. Reagents **1b** and **1c** also successfully functionalized HBPE, but the plateau of functionalization appeared at 3 mol % and 1 mol %, respectively. We note that even low degrees of functionalization can have a significant influence on the structure and properties of a high molecular weight polymer; for example, 1 mol % functionalization installs an average of 9 thiocarbonylthio groups on a polymer chain with an M_n of 25 kg/mol. In agreement with previous work, regioselectivity of
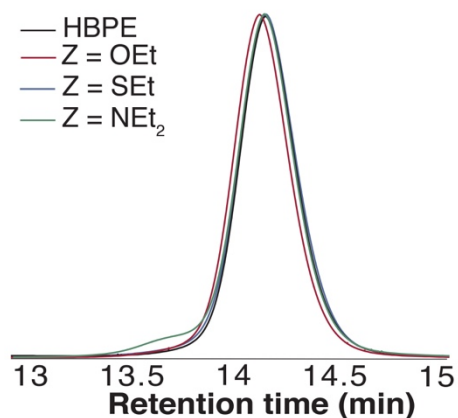
Figure 3.5 SEC traces obtained by the refractive index detector of 1 mol % functionalized HBPE

amidyl radical HAT was determined by ^{1}H NMR to be selective towards secondary carbon sites on HBPE.[2]

Changes in the MWD were analyzed by size exclusion chromatography (SEC). A sample of HBPE was functionalized with 1 mol % of each of the thiocarbonylthio groups, and the SEC trace of the polymers are shown in Figure 3.5. Xanthylated (from **1a**) and trithiocarbonylated (from **1b**) HBPE demonstrate MWD similar to that of the parent polymer, but dithiocarbamylated (from **1c**) HBPE shows evidence of polymer-chain coupling reactions, with a peak appearing at 13.6-minute retention time upon functionalization.

To assess the influence of the Z group on polymer thermal properties, 1 mol % functionalized HBPE of each Z group variant were analyzed via thermal gravimetric analysis (TGA) and differential scanning calorimetry (DSC). All the polymers demonstrated thermal stability up to 250 °C, at
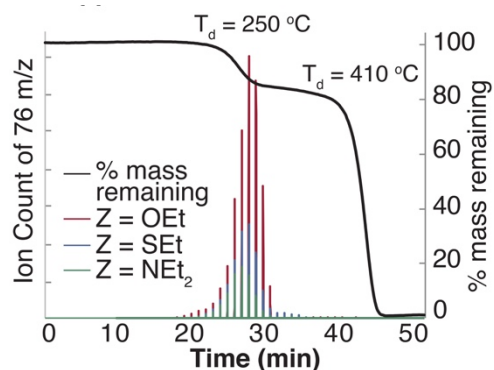
Figure 3.6 TGA–MS of 1 mol % functionalized HBPEs.

which point they underwent a partial mass loss before reaching a plateau and fully degrading at >400 °C (Figure 3.6). We hypothesized that this partial mass loss was the result of a Chugaev-type elimination.[15,16] To support this hypothesis, the evolution of volatile compounds accompanying the partial mass loss was analyzed by mass spectrometry (TGA–MS). A prominent peak at mass to charge (m/z) of 76.1 was evident in all of the samples, which we hypothesize is due to expulsion of carbon disulfide. Based on this data, we hypothesize the thiocarbonylthio groups are undergoing a Chugaev-like rearrangement to yield an olefin on the polymer backbone (Figure 3.7).[17]

i. Decomposition by a Chugaev-like elimination
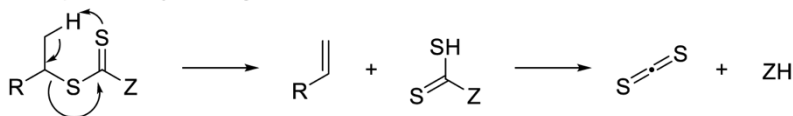
ii. Decomposition by C-S homolysis

further polymer decomposition
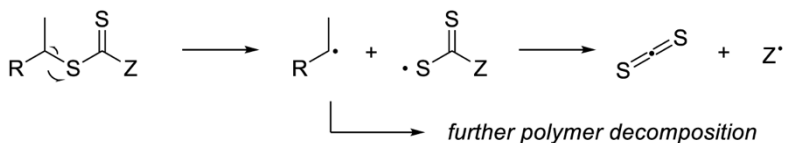
Figure 3.7 Two possible mechanisms for decomposition at 250 °C through (i) two-electron elimination or (ii) C–S bond homolysis

This hypothesis is also supported by the magnitude of mass loss for each of the functional polymers in TGA, which correlates to the loss of the entire thiocarbonylthio functional group. The DSC spectra for functional HBPE demonstrate that, with identical degrees of functionalization, the Z groups did not have a significant impact on the thermal properties. The parent polymer underwent glass transition at –69 °C, while the HBPEs with 1 mol % functionalization had glass transition temperatures (T_g) of –66 and –67 °C (Figure 3.8). HBPE also demonstrates a melting temperature at –42 °C, which does not change considerably upon 1 mol % functionalization. This melting exotherm, however, does disappear at higher mol % functionalization of xanthate and trithiocarbonate.
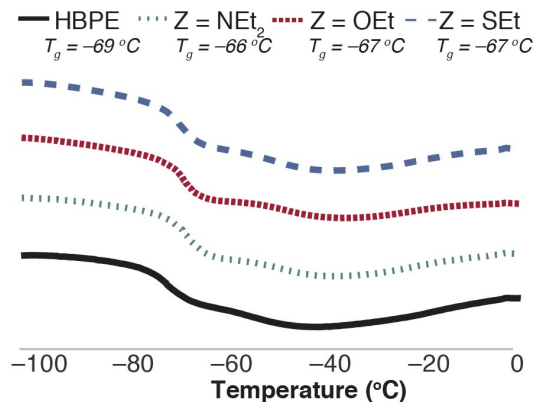
Figure 3.8 DSC of 1 mol% functionalized hyperbranched polyethylene samples.

III-E. CROSSOVER AND KINETIC EXPERIMENTS TOWARDS MECHANISM ELUCIDATION

The structure–reactivity experiments for polymer functionalization (Table 3.1) revealed key differences among the three reagents. One of the most instructive was that each reagent reached a maximum mol % functionalization despite further addition of reagent

relative to polymer repeat unit. For example, reagent **1a** achieved 8 mol % xanthylation of

HBPE when adding 50 mol % reagent; however, doubling the amount of reagent did not further

increase functionalization. In the case of **1c**, the maximum amount of dithiocarbamylation

plateaued at 1 mol % regardless of reagent stoichiometry. We observed a similar trend in our

previous work using a photochemical initiation strategy.[2] We hypothesized that this

phenomenon was the result of degenerative chain-transfer of the thiocarbonylthio groups

between polymer chains.[18,19] The equilibria of this chain-transfer process, therefore, would

result in reversible functionalization.

To test this hypothesis, we designed and conducted a number of crossover experiments

using polymer samples that had previously been functionalized with thiocarbonylthio groups.

Initially, a HBPE sample with 5.4 mol % xanthylation was heated in the presence of DCP as

an initiator with no additional reagent. A decrease in functionalization to 2.3 mol % was

observed (Table 3.2, entry 1). Subsequently, reagents containing Z groups not found on the functionalized polymer (**1b** and **1c**, respectively) were reacted with xanthylated HBPE (Table 3.2, entry 2-3). In both cases, the mol %
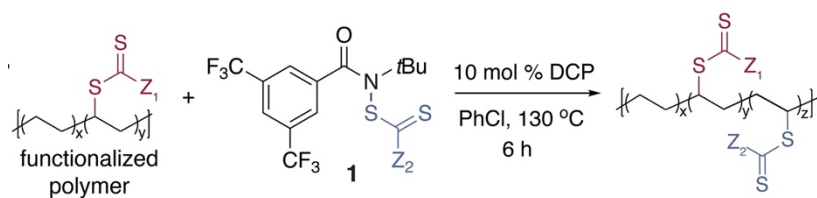
Entry	Z_1	polymer initial mol % funct[a]	Z_2	Ratio of **1** relative to r.u.[b]	Z_1 mol % funct[a]	Z_2 mol % funct[a]
1[c]	—OEt	5.4	N/A	1:10	2.3	N/A
2	—OEt	4.7	—SEt	1:10	2.9	2.6
3	—OEt	4.7	—NEt$_2$	1:10	2.7	2.4
4	—SEt	2.6	—OEt	1:10	0.9	3.0
5	—NEt$_2$	0.9	—OEt	1:10	0.2	3.0

Table 3.2 Crossover experiments of functionalized HBPE with another amide reagent. [a]Determined by ^{1}H NMR in CDCl$_3$. [b]Repeat unit. [c]No functionalized amide reagent was added to the reaction.

functionalization of xanthate decreased and the other thiocarbonylthio group was added to the

polymer. The same trends were observed if the HBPE was initially functionalized with

45

trithiocarbonate (entry 4) or dithiocarbamate (entry 5). These experiments demonstrate that polymer functionalization is reversible under the reaction conditions and the ultimate mol % functionalization is affected by the rate of degenerative chain-transfer.

The observation of reversible functionalization under the reaction conditions led us to probe the kinetics of group transfer for reagents **1a–c** under the reaction conditions. A solution of HBPE, reagent **1**, and DCP in chlorobenzene was separated into aliquots and reacted for different amounts of time to monitor the conversion of **1a–c** to the parent amide. As shown in Figure 3.9, reagent **1a** demonstrated considerably faster conversion than that of either **1b** or **1c**, resulting in a rate constant of 9 times and 6 times larger, respectively.
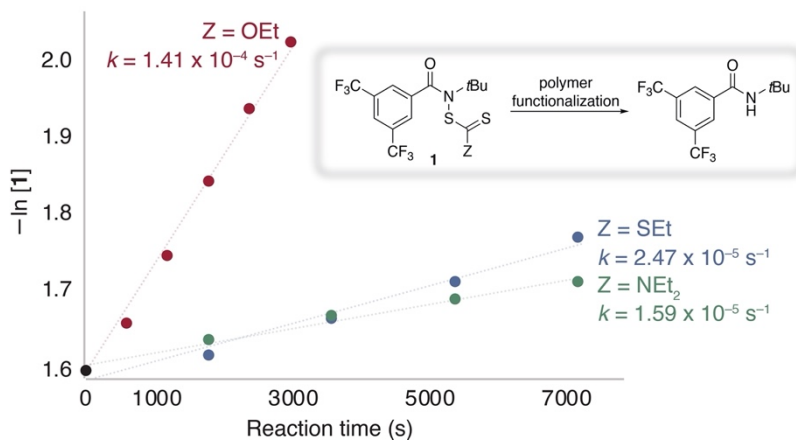
Figure 3.9 Kinetics of reagent conversion during functionalization of HBPE at a theoretical maximum of 10 mol % incorporation. Reaction progress determined by ^{1}H NMR.

The trend for rate of reagent consumption does follow the pattern of mol % polymer functionalization, with reagent **1a** demonstrating both the fastest rate and highest mol % polymer functionalization and **1c** representing the slowest rate and lowest mol % functionalization.

III-F. INFORMED MECHANISTIC HYPOTHESIS

To develop a more comprehensive understanding of this C–H functionalization method, our experimental observations were used to formulate a mechanistic hypothesis (Figure 3.10). Supported by previous literature, we hypothesize that thermolysis of dicumyl peroxide yields a methyl radical,[20,21] which is quickly trapped by the functionalized amide reagent to form the
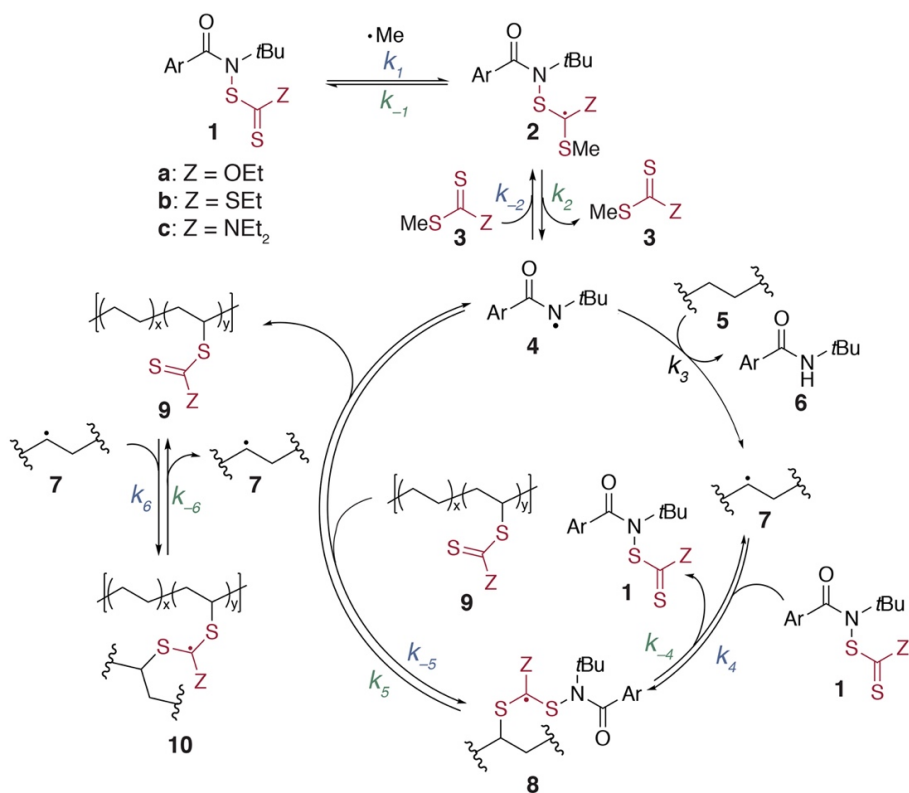
Figure 3.10 Proposed mechanism of amidyl radical-mediated polyolefin C–H functionalization. Polymer side chains omitted for clarity.

captodatively stabilized radical **2**. Fragmentation of intermediate **2** yields amidyl radical **4**.[11]

We hypothesize that **4** is responsible for HAT from the polymer backbone. HAT of aliphatic

C–H bonds by amidyl radicals is exergonic due to the large difference in BDFE of an amidyl

radical (BDFE of 107–110 kcal/mol) relative to C–H bonds (BDFE of 96–100 kcal/mol).[22]

Furthermore, polarity matching between the electrophilic amidyl radical and electron-rich

aliphatic C–H bonds is proposed to lower the kinetic barrier toward HAT.[23,24]

A hydrogen atom from polymer **5** undergoes HAT to furnish the parent amide **6**

concomitant with carbon-centered radical **7**. The production of **6** was monitored to determine

the overall rate of conversion of **1**→**6** (Figure 3.9). We hypothesize that step 3 is an irreversible

transformation due to the thermodynamics of this step. In the productive reaction pathway,

carbon-centered radical **7** reacts with reagent **1** to form the captodative radical **8**.

Fragmentation of **8** is not degenerative and, based on the kinetic experiments, the rate of fragmentation depends largely on the Z group. C–S homolysis can revert compound **8** back to the carbon-centered radical **7** (k_{-4}) or facilitate productive cleavage of intermediate **8** to yield functionalized polymer (**9**) and amidyl radical **4** (k_5). The crossover experiments detailed in Figure 6A demonstrate that both trapping of the polymer-centered radical (**7→8**) and fragmentation to yield functionalized polymer (**8→9**) are reversible. Even after formation of desired product **9,** the functionalized polymer can react with amidyl radical **4** and revert back to the carbon-centered radical **7** (k_{-5}).

In a separate experiment, we isolated xanthylated HBPE and added a radical initiator in the presence of a lower molecular weight polyolefin (Figure 3.11). After the reaction, both polymers exhibited UV-Vis absorptions consistent with xanthate functionalization, indicating
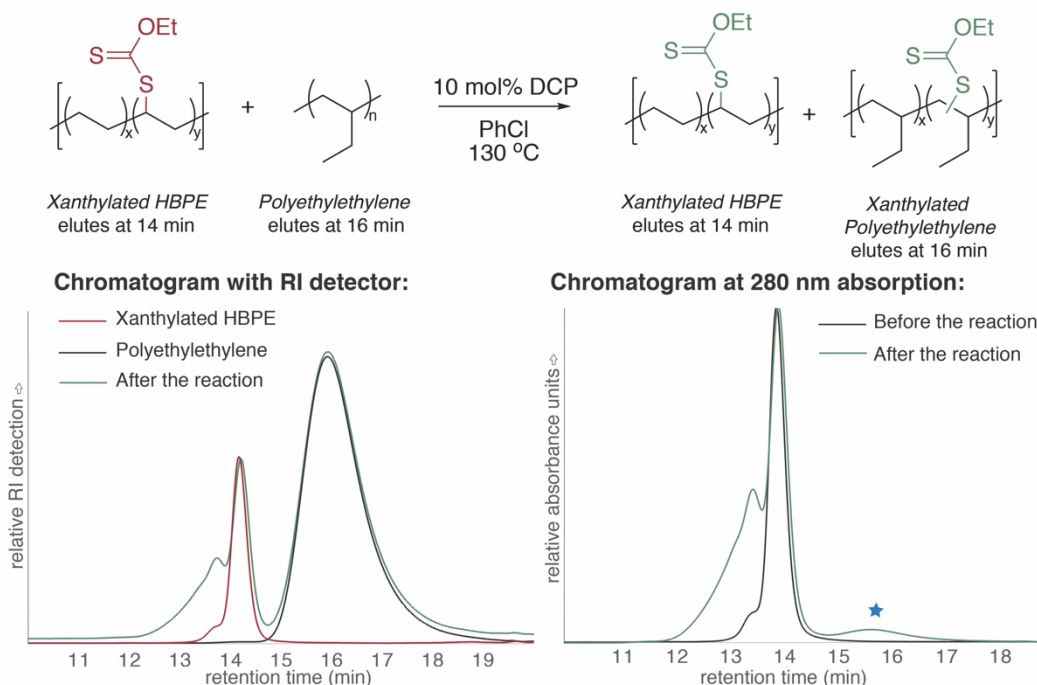
Figure 3.11 Crossover experiment for C–H xanthylation via separately xanthylated polyolefin. 4.5 mol% xanthylated HBPE was reacted with 10 mol% dicumyl peroxide as a radical source in the presence of polyethylethylene. Upon reaction, a new absorption at 280 nm at a retention time of 16 min (blue star) appears, indicative of xanthylation of polyethylethylene.

48

xanthate group transfer. From this experiment we confirmed that an "off-cycle" degenerative radical chain-transfer process is likely occurring that sequesters a portion of the polymer-centered radical into intermediate **10** (Figure 3.10). The culmination of these experiments describes the complexity of this C–H functionalization reaction and the many equilibria that must be considered when optimizing reactivity and/or designing new reagents.

Previous work understanding the rate of chain transfer of thiocarbonylthio groups in RAFT polymerization helps to conceptualize the experimental observations.[25,26] In RAFT polymerization, the choice of Z groups had pronounced effects on the rates of radical addition to thiocarbonylthio functional groups and the rate of fragmentation of
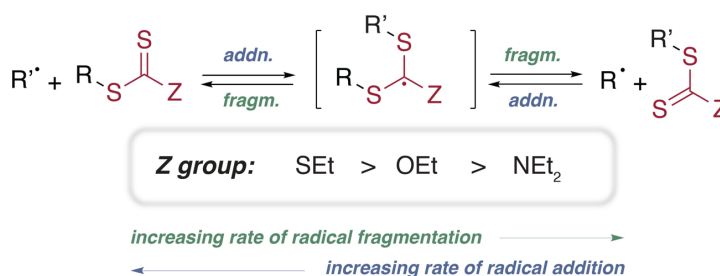
Figure 3.12 Relative rates of radical addition and fragmentation.
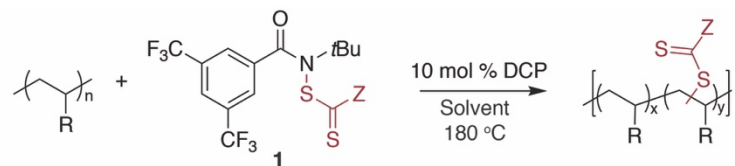
the captodatively stabilized species.[7] For the Z groups studied herein, the rate of radical addition (k_1, k_{-2}, k_4, k_{-5}, and k_6) decreases in the series SEt > OEt > NEt_2, whereas the rate of radical fragmentation (k_{-1}, k_2, k_{-4}, k_5, and k_{-6}) decreases in the series NEt_2 > OEt > SEt (Figure 3.12). For the dithiocarbamate functional group in **1c**, we hypothesize that the slower rate of radical addition leads to a longer lifetime of the polymer-centered radical **7** and an increased potential for radical–radical coupling. Significant chain-coupling observed in the SEC traces (Figure 3.5) supports this hypothesis. The trithiocarbonate group in **1b** presumably results in both an increase in k_4 and k_{-5}. The faster rate of radical addition leads to better control over the MWD of the functionalized polyolefin, which agrees with our experimental results. The faster rate of addition, however, results in a lower amount of overall polymer functionalization than **1a** even at high reagent loadings, presumably due to a faster rate for k_{-5}
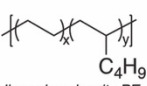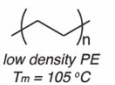
even after product **9** is formed. We hypothesize that the reagent **1a** is successful because it balances the rates of addition and fragmentation. In the conditions described herein, this enables the addition of 8 mol % xanthyl groups to HBPE.

III-G. FUNCTIONALIZATION OF SEMICRYSTALLINE BRANCHED POLYOLEFINS

With a more complete understanding of reagent design principles and reaction mechanism, the thermal functionalization of commercially available semicrystalline branched polyolefins was explored (Table 3.3). Reactions were conducted at 180 °C, a temperature typically used for the commercial PPM of polyolefins via reactive extrusion.[27–30] Xanthylation of Dow™ DNDA-1081 NT 7 linear low density polyethylene resin (LLDPE, 19 branches per 100 carbons) using reagent **1a** resulted in 3 mol % functionalization upon addition of 5 mol % of the reagent. At higher equivalents of reagent **1a**, mol % functionalization increased along with an observed increase in MWD. Based on the mechanistic understanding gained herein, we hypothesized that reagent **1b**, which has a faster rate of radical addition, would decrease the amount of deleterious chain coupling and chain scission side-reactions. The

Polyolefin	Z	Solvent	Ratio of 1 : r.u.[a]	mol % funct[b]	Before[c] M_n	Before[c] Đ	After[c] M_n	After[c] Đ	T_m[d]
linear low density PE T_m = 122 °C	—OEt	DCB	1:20	3	22	3.37	28	7.66	95
	—OEt	DCB	1:10	7	22	3.37	15	6.17	75
	—SEt	DCB	1:10	3	22	3.37	23	3.84	100
	—NEt_2	DCB	1:10	0	⸺	⸺	⸺	⸺	⸺
low density PE T_m = 105 °C	—OEt	DCB	1:20	3	41	9.54	41	23.35	84
	—OEt	DCB	1:10	5	41	9.54	39	13.15	73
	—SEt	DCB	1:10	3	41	9.54	43	17.94	85
	—NEt_2	DCB	1:10	0	⸺	⸺	⸺	⸺	⸺
isotactic PP T_m = 155 °C	—OEt	DCB	1:20	0	⸺	⸺	⸺	⸺	⸺
	—OEt	DCB	1:10	1	64	4.84	84	4.03	144
	—OEt	neat	1:20	1	64	4.84	63	9.72	137
	—OEt	neat	1:10	2	64	4.84	79	7.34	130

⸺ indicates not applicable

Table 3.3 Functionalization of commercial branched polyolefins. [a]Repeat unit. [b]Determined by ^{1}H NMR at 110 °C. [c]Determined by SEC at 120 °C. [d]Determined by DSC in the 2nd heating cycle.

experimental results confirmed our hypothesis; trithiocarbonate reagent **1b** led to moderate functionalization of LLDPE without significantly altering M_n or the Đ.

Functionalization of Dow™ polyethylene 4012 low density (LDPE, 49 branches per 100 carbons) is challenging due to its undefined structure and broad MWD (Đ = 9.54). Regardless, the trends observed in our mechanistic experiments held true, with reagent **1a** providing more efficient functionalization. The chemoselective functionalization provided by these reagents is notable, as even small amounts of chain coupling side reactions are known to cause gelation on substrates with high weight-average molecular weights (M_w). No functionalization was imparted using reagent **1c**, consistent with results on the HBPE model system.

Basell™ Profax 6301 polypropylene homopolymer (*i*PP) represents the most challenging semicrystalline polyolefin substrate for C–H functionalization, as it has a high melting temperature, high degree of crystallinity, high branch content (50 methyl branches per 100 carbons), and is prone to β-scission reactions. For this challenging substrate, polymer functionalization in solution was not observed in any of the conditions we tested using reagents **1a-c**. Using reagent **1a** under neat conditions (*i.e.* without solvent), however, resulted in 1 mol % xanthylation at a theoretical maximum functionalization of 5 mol %. High temperature ^{1}H NMR spectroscopy indicated that functionalization was highly regioselective for the primary C–H bonds on *i*PP (Figure 3.13). Most importantly, no evidence of β-scission of *i*PP was observed and the material maintained a high melting temperature.

III-H. C–H XANTHYLATION OF *i*PP WITHIN AN EXTRUDER

The culmination of mechanistic experiments, structure–reactivity studies, and functionalization experiments led us to design conditions for the functionalization of *i*PP by reactive extrusion. A powder formulation of *i*PP mixed with reagent **1a** and 10 mol % DCP at a stoichiometry corresponding to a theoretical maximum functionalization of 5 mol % was injected into a twin-screw extruder at 180 °C and allowed to circulate for 30 minutes. The extrusion process resulted in the C– I functionalization of *i*PP with 1 mol % xanthate groups and no observed *β*-scission (Figure 3.14). In fact, the shear mixing provided by the twin-screw extruder led to a MWD that better represented that of the parent *i*PP than analogous reactions conducted using mechanical stirring alone (Figure 3.15).[31]
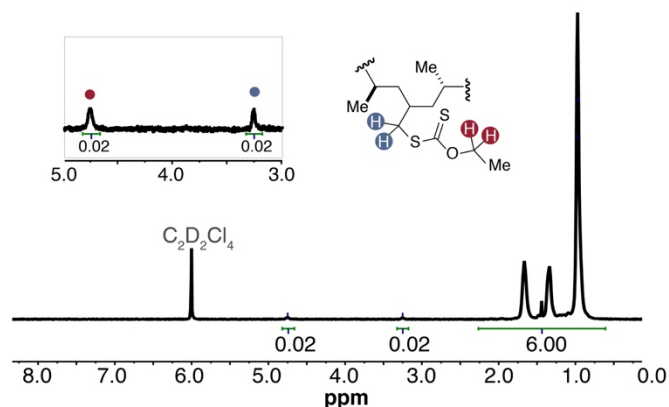
Figure 3.13 ^{1}H NMR at 110 °C in C$_2$D$_2$Cl$_4$ of xanthylated *i*PP via reactive extrusion or neat conditions
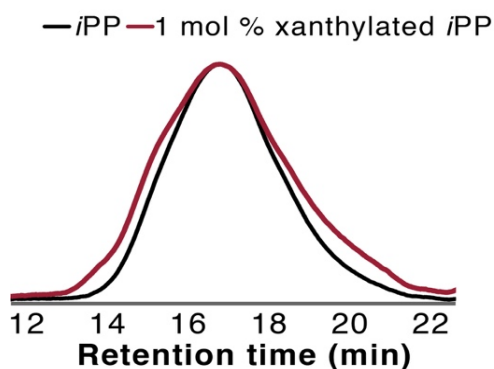
Figure 3.14 HT SEC at 120 °C in TCB of extruded product.

Scaling up the functionalization in an extruder achieved multigram quantities of xanthylated *i*PP and provided sufficient material for further structure–property evaluation. The crystalline nature of xanthylated *i*PP was confirmed by DSC. The xanthylated *i*PP had a high melting point (137 °C) and a percent crystallinity of 28%. Both of these values are modest decreases from the commercial Profax

6301 material tested under analogous conditions (T_m = 155 °C, 41% crystalline), which is commonly observed for semicrystalline polymers upon functionalization.[32,33]
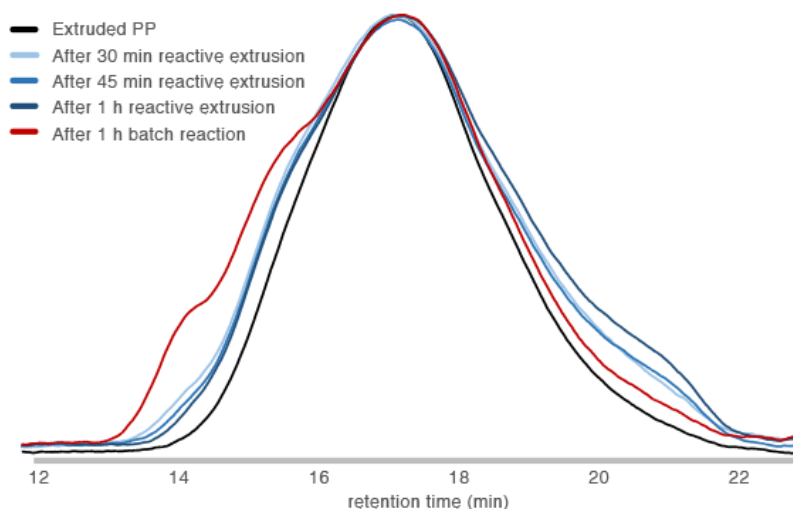
Figure 3.15 HT GPC at 120 °C in TCB of iPP after reactive extrusion vs. after batch reaction

III-J. STRUCTURE–PROPERTY STUDIES OF *i*PP AND 1 MOL % XANTHYLATED *i*PP (X*i*PP)

The large thermal processing window (above the T_m and below the T_d) of the xanthylated *i*PP enabled us to melt-press films of the material to probe the impact of functionalization on mechanical and adhesive properties. Tensile testing of dog bone-shaped samples cut from melt-pressed films of the parent Basell™ Profax 6301 *i*PP and 1 mol % xanthylated *i*PP by dynamic mechanical analysis in linear film tension mode yielded stress–strain curves that showed plastic deformation behavior consistent with semicrystalline thermoplastics (Figure 3.16). A similar Young's modulus (E) was observed for both *i*PP (E = 15 ± 1 MPa) and xanthylated *i*PP (E = 14 ± 2 MPa); the yield strength (σ_y) of *i*PP (σ_y = 35 ± 1 MPa) was slightly higher than that of xanthylated *i*PP (σ_y = 26 ± 3 MPa). The elongation at break value of *i*PP (ε_B = 570 ± 50%) was congruent to results with xanthylated *i*PP (ε_B = 430

53
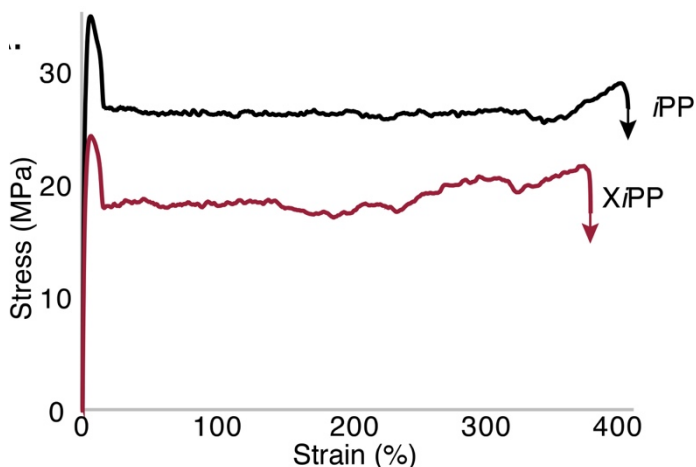
Figure 3.16 Overlay of stress–strain curves for *i*PP and X*i*PP measured by tensile testing (0.1 mm/s, room temperature, break point indicated by arrow).

± 120%). Strain stiffening was observed in films of *i*PP and xanthylated *i*PP, generating a stress at break of $\sigma_B = 31 \pm 2$ MPa and $\sigma_y = 24 \pm 6$ MPa respectively.

In addition to retaining the desirable thermomechanical properties of commercial polyolefin materials, we expected xanthylated *i*PP to exhibit significantly different adhesive properties due to the intrinsic polarity of the xanthate group. On this basis, we reasoned that xanthylated *i*PP should display superior adhesion to polar surfaces (*i.e.* glass) relative to polyolefin materials. To test this hypothesis, we prepared a single-lap joint between two glass slides, using *i*PP or xanthylated *i*PP, and subjected it to lap shear analysis (Figure 3.17). Xanthylated *i*PP demonstrated more than twice the adhesion strength to glass than did the *i*PP material, with apparent lap shear strengths of 120 ± 30 MPa and 48 ± 4 MPa, respectively.
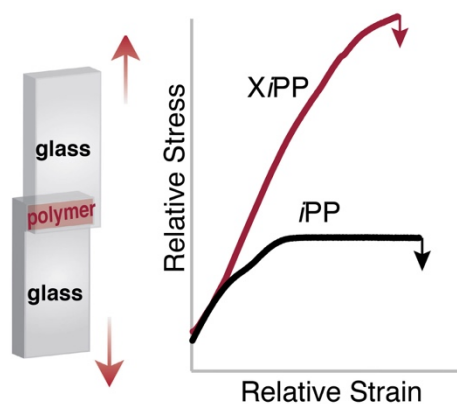
Figure 3.17 Relative shear stress–strain curves for *i*PP and X*i*PP single-lap joints measured by tensile testing (5 mm/min, room temperature).

These results prove the significant impact of imparting even small amounts of polar functionality onto polyolefins.

III-K. CONCLUSION

A thermally initiated, metal-free C–H functionalization of branched polyolefins is demonstrated using thiocarbonylthio amide reagents. Comprehensive experimental studies on

both small molecule and polyolefin substrates revealed key structure–reactivity relationships. Crossover and kinetic experiments provide information of the many competing equilibria that combine to determine the efficiency and magnitude of polymer functionalization. From these experimental studies, we developed a mechanistic hypothesis that informed the translation of these reagents for the successful chemoselective functionalization of commercial samples of semicrystalline polyolefins. Ultimately, the reactive extrusion of *i*PP on a decagram scale was demonstrated and resulted in functionalized *i*PP that adheres to polar substrates twice as strong as commercial *i*PP. We envision the results of this experimental and mechanistic study will serve as a comprehensive launching point for the continued improvement and implementation of polyolefin C–H functionalization in practical settings.

REFERENCES

(1)   Williamson, J. B.; Na, C. G.; Johnson, R. R.; Daniel, W. F. M.; Alexanian, E. J.; Leibfarth, F. A. Chemo- and Regioselective Functionalization of Isotactic Polypropylene: A Mechanistic and Structure–Property Study. *J. Am. Chem. Soc.* **2019**, *141*, 12815–12823. https://doi.org/10.1021/jacs.9b05799.

(2)   Williamson, J. B.; Czaplyski, W. L.; Alexanian, E. J.; Leibfarth, F. A. Regioselective C–H Xanthylation as a Platform for Polyolefin Functionalization. *Angew. Chem. Int. Ed.* **2018**, *57*, 6261–6265. https://doi.org/10.1002/anie.201803020.

(3)   Coiai, S.; Cicogna, F.; Yang, C.; Tempesti, V.; Carroccio, S. C.; Gorrasi, G.; Mendichi, R.; Dintcheva, N. T.; Passaglia, E. Grafting of hindered phenol groups onto Ethylene/α-Olefin copolymer by nitroxide radical coupling. *Polymers (Basel).* **2017**, *9*, 1–19. https://doi.org/10.3390/polym9120670.

(4)   Coiai, S.; Augier, S.; Pinzino, C.; Passaglia, E. Control of degradation of polypropylene during its radical functionalisation with furan and thiophene derivatives. *Polym. Degrad. Stab.* **2010**, *95*, 298–305. https://doi.org/10.1016/j.polymdegradstab.2009.11.014.

(5)   Porejko, S.; Gabara, W.; Kulesza, J. Grafting of maleic anhydride on polyethylene. II. Mechanism of grafting in a homogeneous medium in the presence of radical initiators. *J. Polym. Sci. Part A-1 Polym. Chem.* **1967**, *5*, 1563–1571. https://doi.org/10.1002/pol.1967.150050707.

(6)   Williamson, J. B.; Lewis, S. E.; Johnson III, R. R.; Manning, I. M.; Leibfarth, F. C-H Functionalization of Commodity Polymers. *Angew. Chem. Int. Ed.* **2018**, *58*, 8654–8668. https://doi.org/10.1002/anie.201810970.

(7)   Moad, G.; Rizzardo, E.; Thang, S. H. Radical addition-fragmentation chemistry in polymer synthesis. *Polymer (Guildf).* **2008**, *49*, 1079–1131. https://doi.org/10.1016/j.polymer.2007.11.020.

(8)   Chiefari, J.; Mayadunne, R. T. A.; Moad, C. L.; Moad, G.; Rizzardo, E.; Postma, A.; Skidmore, M. A.; Thang, S. H. Thiocarbonylthio Compounds (S=C(Z)S-R) in Free Radical Polymerization with Reversible Addition-Fragmentation Chain Transfer (RAFT Polymerization). Effect of the Activating Group Z. *Macromolecules* **2003**, *36*, 2273–2283. https://doi.org/10.1021/ma020883.

(9)   Mayadunne, R. T. A.; Rizzardo, E.; Chiefari, J.; Krstina, J.; Moad, G.; Postma, A.; Thang, S. H. Living Polymers by the Use of Trithiocarbonates as Reversible Addition–Fragmentation Chain Transfer (RAFT) Agents: ABA Triblock Copolymers by Radical Polymerization in Two Steps. *Macromolecules* **2000**, *33*, 243–245. https://doi.org/10.1021/ma991451a.

(10)   Mayadunne, R. T. A.; Rizzardo, E.; Chiefari, J.; Chong, Y. K.; Moad, G.; Thang, S. H. Living Radical Polymerization with Reversible Addition–Fragmentation Chain Transfer (RAFT Polymerization) Using Dithiocarbamates as Chain Transfer Agents. *Macromolecules* **1999**, *32*, 6977–6980. https://doi.org/10.1021/ma9906837.

(11)   Czaplyski, W. L.; Na, C. G.; Alexanian, E. J. C-H Xanthylation: A Synthetic Platform for Alkane Functionalization. *J. Am. Chem. Soc.* **2016**, *138*, 13854–13857. https://doi.org/10.1021/jacs.6b09414.

(12)   Na, C. G.; Alexanian, E. J. A General Approach to Site-Specific, Intramolecular C–H Functionalization Using Dithiocarbamates. *Angew. Chem. Int. Ed.* **2018**, *57*, 13106–13109. https://doi.org/10.1002/anie.201806963.

(13)   Smith, G. E. P.; Alliger, G.; Carr, E. L.; Young, K. C. Thiocarbamylsulfenamides 1. *J. Org. Chem.* **1949**, *14*, 935–945. https://doi.org/10.1021/jo01158a002.

(14)   Gottfried, A. C.; Brookhart, M. Living polymerization of ethylene using Pd(II) α-diimine catalysts. *Macromolecules* **2001**, *34*, 1140–1142. https://doi.org/10.1021/ma0015951.

(15)   Benkeser, R. A.; Hazdra, J. J. Factors Influencing the Direction of Elimination in the Chugaev Reaction. *J. Am. Chem. Soc.* **1959**, *81*, 228–231. https://doi.org/10.1021/ja01510a052.

(16)   Betou, M.; Male, L.; Steed, J. W.; Grainger, R. S. Carbamoyl Radical-Mediated Synthesis and Semipinacol Rearrangement of β-Lactam Diols. *Chem. - A Eur. J.* **2014**, *20*, 6505–6517. https://doi.org/10.1002/chem.201304982.

(17)   Chugaev, L. A new method for the preparation of unsaturated hydrocarbons. *Ber.* **1899**, *32*, 3332–3335.

(18)   Braunecker, W. A.; Matyjaszewski, K. Controlled/living radical polymerization: Features, developments, and perspectives. *Prog. Polym. Sci.* **2007**, *32*, 93–146. https://doi.org/10.1016/j.progpolymsci.2006.11.002.

(19)   Zard, S. Z. The Radical Chemistry of Thiocarbonylthio Compounds: An Overview. In *Handbook of RAFT Polymerization*; Barner-Kowollik, C., Ed.; Wiley-VCH Verlag GmbH & Co. KGaA: Weinheim, Germany, 2008.

(20)   Inoue, S.; Kumagai, T.; Tamezawa, H.; Aota, H.; Matsumoto, A.; Yokoyama, K.; Matoba, Y.; Shibano, M. Predominant methyl radical initiation preceded by β-scission of alkoxy radicals in allyl polymerization with organic peroxide initiators at elevated temperatures. *Polym. J.* **2010**, *42*, 716–721. https://doi.org/10.1038/pj.2010.66.

(21)   Norrish, R. G. W.; Searby, M. H. The photochemical decomposition of dicumyl peroxide and cumene hydroperoxide in solution. *Proc. R. Soc. London. Ser. A. Math.*

Phys. Sci. **1956**, *237*, 464–475. https://doi.org/10.1098/rspa.1956.0190.

(22) Blanksby, S. J.; Ellison, G. B. Bond dissociation energies of organic molecules. *Acc. Chem. Res.* **2003**, *36*, 255–263. https://doi.org/10.1021/ar020230d.

(23) P. Roberts, B. Polarity-reversal catalysis of hydrogen-atom abstraction reactions: concepts and applications in organic chemistry. *Chem. Soc. Rev.* **1999**, *28*, 25–35. https://doi.org/10.1039/A804291H.

(24) Hioe, J.; Zipse, H. Radical stability and its role in synthesis and catalysis. *Org. Biomol. Chem.* **2010**, *8*, 3609. https://doi.org/10.1039/c004166a.

(25) Jeffery, J.; Ercole, F.; Mayadunne, R. T. A.; Moad, G.; Rizzardo, E.; Le, T. P. T.; Chiefari, J.; Krstina, J.; Chong, Y. K. (Bill); Moad, C. L.; Thang, S. H.; Meijs, G. F. Living Free-Radical Polymerization by Reversible Addition–Fragmentation Chain Transfer: The RAFT Process. *Macromolecules* **2002**, *31*, 5559–5562. https://doi.org/10.1021/ma9804951.

(26) Zard, S. Z. Some intriguing mechanistic aspects of the radical chemistry of xanthates. *J. Phys. Org. Chem.* **2012**, *25*, 953–964. https://doi.org/10.1002/poc.2976.

(27) Manning, S. C.; Moore, R. B. Carboxylation of polypropylene by reactive extrusion with functionalized peroxides for use as a compatibilizer in polypropylene/polyamide-6,6 blends. *J. Vinyl Addit. Technol.* **2004**, *3*, 184–189. https://doi.org/10.1002/vnl.10187.

(28) Berzin, F.; Flat, J. J.; Vergnes, B. Grafting of maleic anhydride on polypropylene by reactive extrusion: Effect of maleic anhydride and peroxide concentrations on reaction yield and products characteristics. *J. Polym. Eng.* **2013**, *33*, 673–682. https://doi.org/10.1515/polyeng-2013-0130.

(29) Cicogna, F.; Coiai, S.; Passaglia, E.; Tucci, I.; Ricci, L.; Ciardelli, F.; Batistini, A. Grafting of Functional Nitroxyl Free Radicals to Polyolefins as a Tool to Postreactor Modification of Polyethylene-Based Materials with Control of Macromolecular Architecture. *J. Polym. Sci. Part A Polym. Chem.* **2010**, *49*, 781–796. https://doi.org/10.1002/pola.

(30) Assoun, L.; Manning, S. C.; Moore, R. B. Carboxylation of polypropylene by reactive extrusion with functionalised peroxides. *Polymer (Guildf).* **1998**, *39*, 2571–2577. https://doi.org/10.1016/S0032-3861(97)00584-3.

(31) Hopmann, C.; Adamy, M.; Cohnen, A. Introduction to Reactive Extrusion. In *Reactive Extrusion*; Beyer, G., Hopmann, C., Eds.; Wiley-VCH Verlag GmbH & Co. KGaA: Weinheim, Germany, 2017; pp 1–10. https://doi.org/10.1002/9783527801541.ch1.

(32) Bae, C.; Hartwig, J. F.; Boaen Harris, N. K.; Long, R. O.; Anderson, K. S.; Hillmyer,

M. A. Catalytic hydroxylation of polypropylenes. *J. Am. Chem. Soc.* **2005**, *127*, 767–776. https://doi.org/10.1021/ja044440s.

(33)   Bunescu, A.; Lee, S.; Li, Q.; Hartwig, J. F. Catalytic Hydroxylation of Polyethylenes. *ACS Cent. Sci.* **2017**, *3*, 895–903. https://doi.org/10.1021/acscentsci.7b00255.

CHAPTER IV.

A GENERAL STRATEGY FOR THE DIVERSIFICATION OF ALIPHATIC C–H BONDS VIA
RADICAL CHAIN TRANSFER
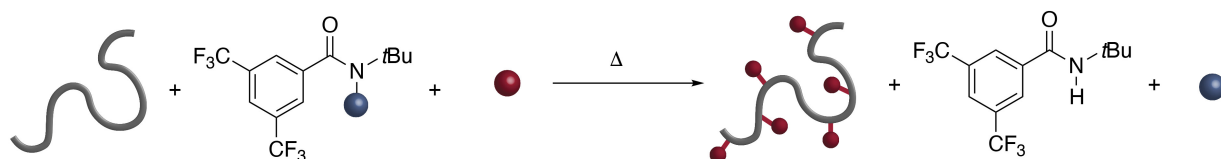
IV-A. A REMAINING NEED FOR DECOUPLING THE AMIDYL RADICAL FROM THE TRANSFERRED FUNCTIONALITY

The direct transformation of unreactive aliphatic C–H bonds to useful functionality represents a streamlined and sustainable approach to complex molecules and materials from readily available starting materials. Late-stage diversification of drug-like molecules, wherein structurally complex substrates are modified selectively to alter their function, has emerged as a powerful strategy to access new lead compounds for medicinal chemistry without resorting to *de novo* synthesis. The broad impact of late-stage diversification extends from such small molecule contexts to the end-of-life fate of plastic waste, where an estimated 95% of the economic value of plastics is lost after a single use.[1] Selective C–H functionalization of post-consumer plastic has the potential to differentiate its properties and enhance its value, thus contributing to a more sustainable plastics economy.[2,3] Currently, a number of transformations of aliphatic C–H bonds exist and are used for the late-stage diversification of drug-like molecules and commodity polymers, but the vast majority of these use either substrate-
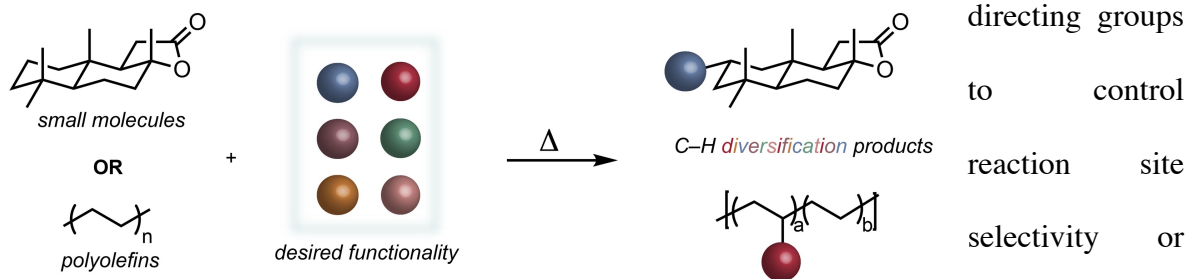
Figure 4.1 A universal approach to C–H functionalization would place an array of functionality selectively onto small molecules and commodity polymers.

directing groups to control reaction site selectivity or involve promiscuous reactive intermediates which significantly limit the substrate scope of these approaches.[3,4] A universal strategy for aliphatic C–H functionalization, wherein a wide array of functionality can be placed site-selectively in an intermolecular transformation on both complex organic substrates and commodity polymers, remains a grand challenge (Figure 4.1).

Efficient C–H functionalizations that occur under mild conditions and use substrate as the limiting reagent–an essential requirement to applications in medicinal chemistry and polymer functionalization–remain scarce. A notable exception is the use of high-valent transition metal-oxo complexes in aliphatic C–H functionalization, but this approach is limited by its modest scope of transformations and use of highly oxidizing intermediates.[5] Intermolecular alkylation of C–H bonds using rhodium catalysis is also well-developed[6,7], but the requirement for donor–acceptor diazo reagents significantly limits overall scope, and the use of a precious metal limits high-volume applications in polymer science. Furthermore, several valuable reactions, such as aliphatic C–H iodination, remain limited regardless of approach.

Recent studies have demonstrated the utility of heteroatom-centered radicals to facilitate several site-selective, intermolecular functionalizations of unactivated aliphatic C–H bonds on a variety of molecules and materials, constituting a complementary strategy to metal-catalyzed methods.[8–14] These reactions principally harness the ability of a tuned nitrogen-
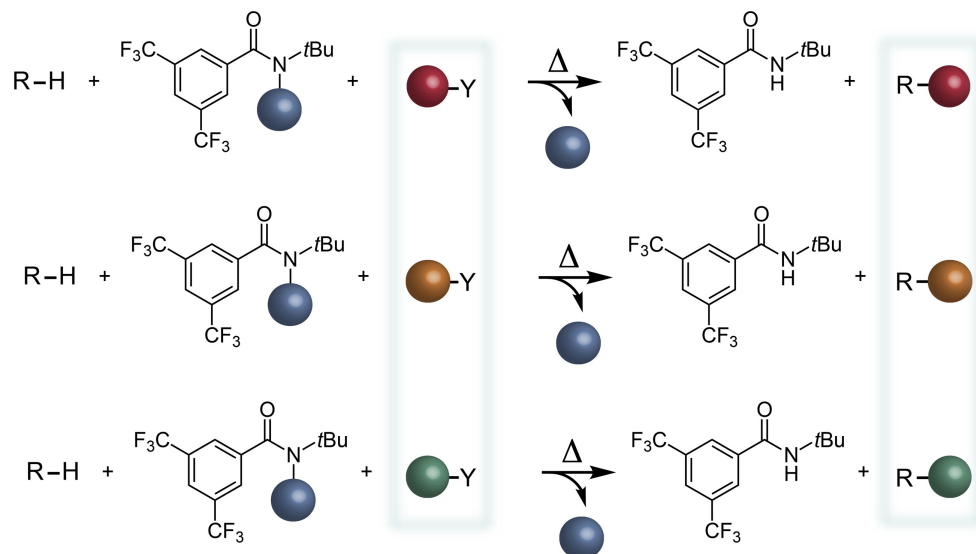
Figure 4.2 This work uses an *N*-functionalized amide and a diverse set of chain transfer agents to achieve C–H diversification.

centered radical to achieve facile hydrogen atom transfer (HAT) from strong, unactivated aliphatic C–H sites. A critical drawback to these previous studies which limits broad application of site-selective radical-chain C–H functionalizations is the requirement for direct group transfer of the functionality appended to nitrogen, which greatly restricts the diversity of products accessible via the HAT platform. With this in mind, we hypothesized that decoupling the formation of the heteroatom-centered radical responsible for HAT would unlock a universal C–H diversification applicable to a vast range of transformations (Figure 4.2). We identified an *O*-vinylhydroxyamide (**1**) as an ideal reagent that was capable of forming reactive nitrogen-centered radicals, but whose direct chain transfer kinetics allows exogenous radical traps to outcompete it for substrate functionalization (Figure 4.3). We hypothesized that such a versatile C–H diversification strategy would encompass many important transformations, including those inaccessible with current synthetic technology, and extend to applications in the transformation of post-consumer plastic waste to functional polyolefins.

IV-B. POLYOLEFIN C–H DIVERSIFICATION

The C–H functionalization approach promoted by **1** efficiently installs a wide variety of functionality onto commodity polyolefins (Figure 4.4). Linear low-density polyethylene (LLDPE) represents a branched substrate (melting temperature of 122 °C; 19 branches per 100 carbons) that typically undergoes deleterious β-scission or crosslinking events during radical functionalization.[15] The C–H diversification of LLDPE with substrate as limiting reagent was successful using 8 diverse trapping agents, in good to excellent yield. This includes the first example of a C–H iodination, which enables a range of challenging C–H transformations. All polymer functionalization reactions are targeting a maximum of 10 mol % repeat-unit modification in order to impart emergent polymer function while maintaining the beneficial thermomechanical properties of the material. Notably, the C–H functionalizations promoted by reagent **1** proceeded without the need for an exogenous initiator, which is an enabling aspect of the approach.
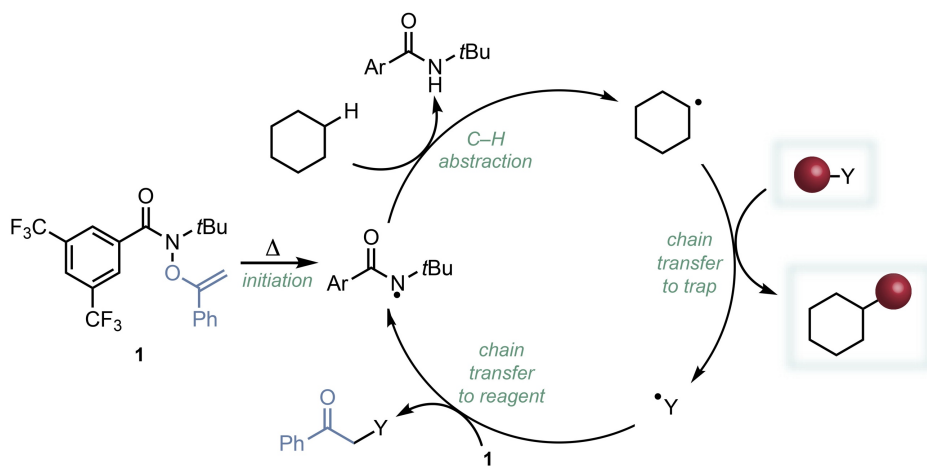
Figure 4.3 The mechanistic hypothesis for C–H diversification using *O*-alkenylhydroxamates. Ar = 3,5-bis(trifluoromethyl)phenyl.

As a representative reaction to access a nitrogen-functionalized polyolefin, cyanation of LLDPE with **1** under homogeneous conditions (130 °C in chlorobenzene) yielded efficient reactivity, site-selectivity for methylene carbons, and no discernable side reactions as

confirmed by size exclusion chromatography as well as a variety of 1D and 2D NMR techniques (see Spectral Information). In contrast, an analogous cyanation using dicumyl peroxide in place of **1** yielded no functionalization and a decrease in polymer molecular weight.

In addition to the polyolefin cyanation, the installations of fluoride, bromide, iodide, trifluoromethylthiol, thiophenol, azido, and phenyl tetrazolyl groups onto LLDPE were successful. Several of these polyolefin C–H transformations are without precedent and deliver novel products inaccessible by other means.[11,14,16] To further extend

Figure 4.4 C–H functionalization of commodity polyolefins. Gray spheres represent sites of minor functionalization.

the scope, C–H cyanation, thiophenolation, and iodination were successful on complementary substrates, including highly crystalline high-density PE (HDPE), highly branched low-density PE (LDPE; 49 branches per 100 carbons), post-industrial waste PE (PIPE) obtained from packaging forms, and post-consumer waste PE obtained from PE foam packaging (PCPE). Functionalization proceeded efficiently even with an undefined mix of additives observable in the infrared and NMR spectrum, indicating the potential for this method to place post-consumer waste at the start of a new plastics value chain.

The exceptional chemoselectivity of this chemistry is evident from the lack of tailing in the high-temperature size exclusion chromatograms (Figures 4.5) and the observation that the material remains a semicrystalline thermoplastic with a high melting point after functionalization (Figure 4.6). As expected, the percent crystallinity of the material decreases
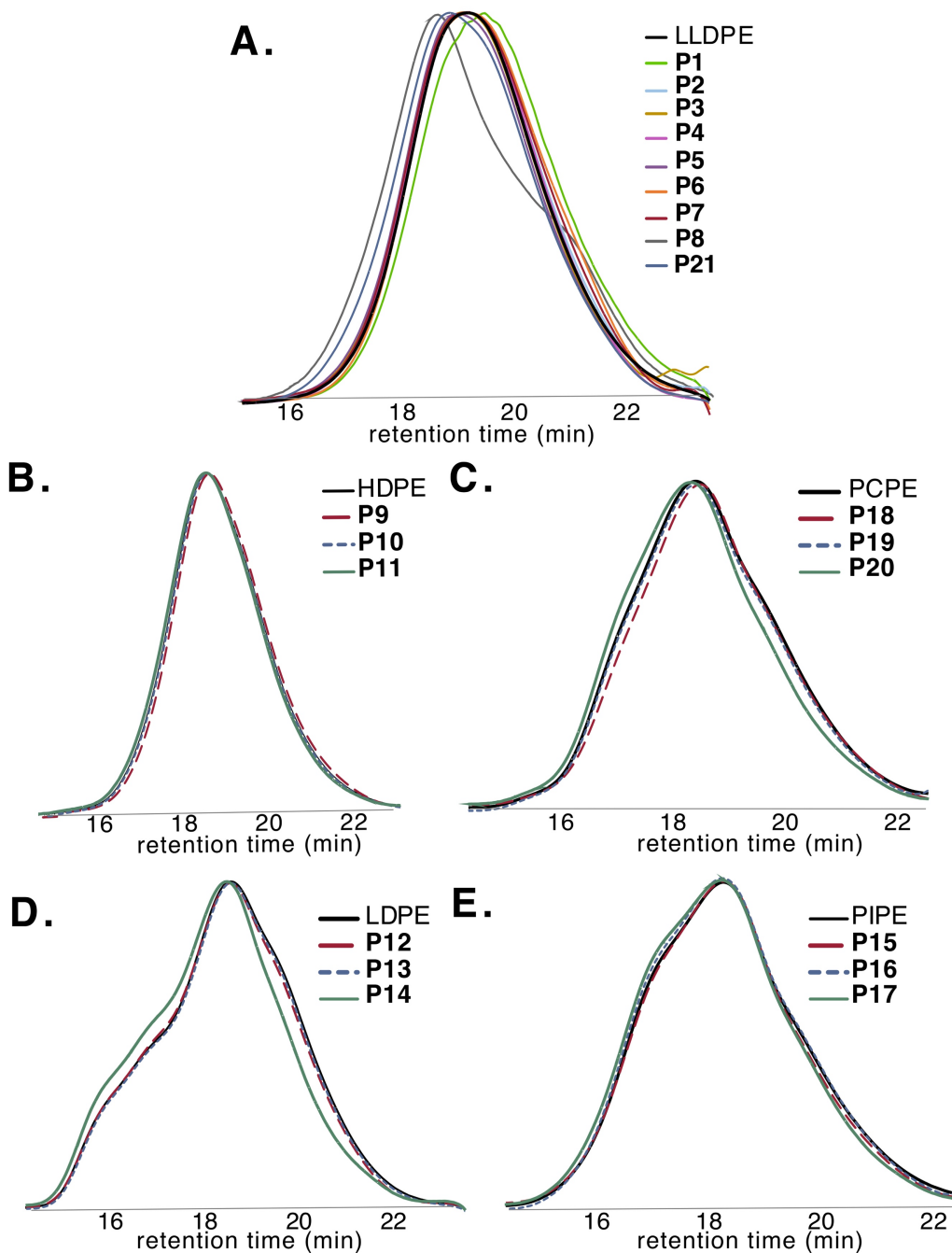
Figure 4.5 High temperature size exclusion chromatography confirms retention of MWD after functionalization.

65

as an increasing amount of functionality is added. The ability to add diverse functionality to linear and branched polyolefins enables access to material classes that are difficult or impossible to access through alternative methods.
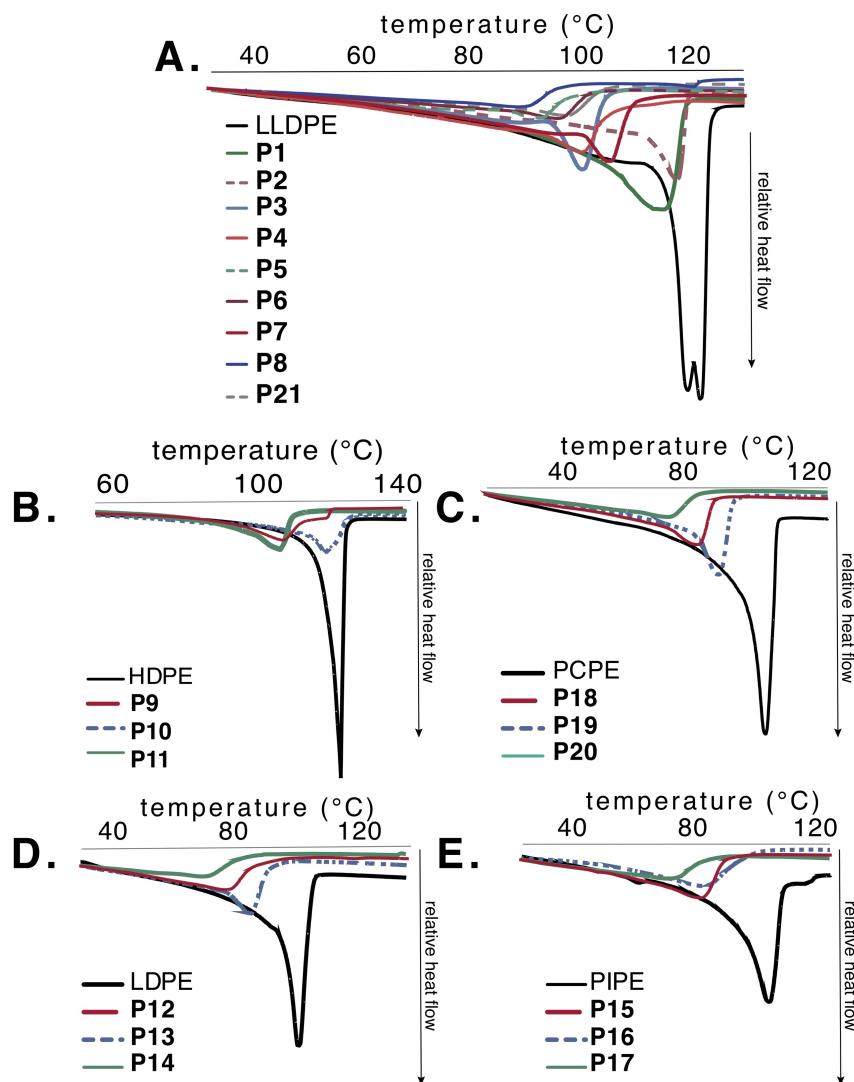
Figure 4.6 Differential scanning calorimetry of functionalized polyolefins shows decrease in crystallinity and T_m.

IV-C. POLYOLEFIN IONOMERS VIA C–H DIVERSIFICATION

The exceptional chemoselectivity of this method combined with the versatility of trapping reagents enables the pursuit of polyolefin materials inaccessible by Ziegler–Natta or related catalytic approaches. Commercial polyolefin ionomers, high-value thermoplastics

stabilized by ionic crosslinks used in packaging, structural adhesion, and ion-conducting membranes, are synthesized through radical copolymerization of acrylic acid and ethylene, which leads to a highly branched LDPE microstructure that limits the overall strength and toughness of the materials.[17] Given the structural fidelity and lack of long-chain branching evident from the high-temperature size exclusion chromatograms post-functionalization (Figures 4.5) and the observation that the material remains a semicrystalline thermoplastic with a high melting point (Figure 4.6), we envisioned creating ionomers from high-performance polyolefins through a post-functionalization approach (Figure 4.7).

The generality of the C–H functionalization mediated by **1** enabled the development of a 2-bromoethyl thiosulfonate radical trapping reagent that installed a primary bromide onto the polyolefin (**P21**). Displacement of the bromide by methyl imidazole yielded imidazolium-functionalized LLDPE (**P22**), which represents a formal copolymerization of α-olefins with an ion-containing vinyl monomer. The ionomer had distinct properties from the parent LLDPE, including solubility in polar aprotic
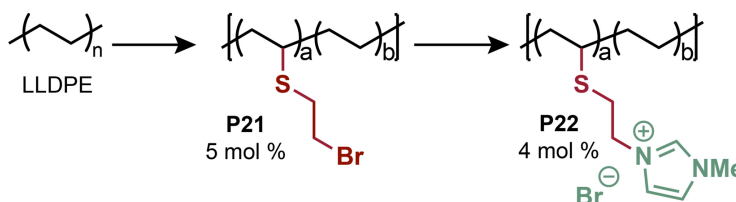
Figure 4.7 Polyolefin C–H functionalization enabled the production of ionomers from commercial plastics in a two-step synthetic route.

solvents, a decreased melting temperature, and enhanced clarity. Compression molding films of the LLDPE ionomer enabled uniaxial tensile testing to conduct a comparative experiment on the impact of ionic functionality on mechanical properties (Figure 4.8). Introduction of the imidazolium to only 4 mol% of the repeat units dramatically changed the material from a

thermoplastic to a tough elastomer. While yield stress and Young's modulus (E) of **P22** decreased considerably compared to the parent LLDPE, the strain at break (ε_B) more than doubled, leading to an increase in the tensile toughness (U_T) of 180% while maintaining a similar stress at break (σ_B). Collectively, the enhanced toughness and ductility of this ionomer demonstrates the value-added properties accessible from this versatile C–H functionalization of branched polyolefins.
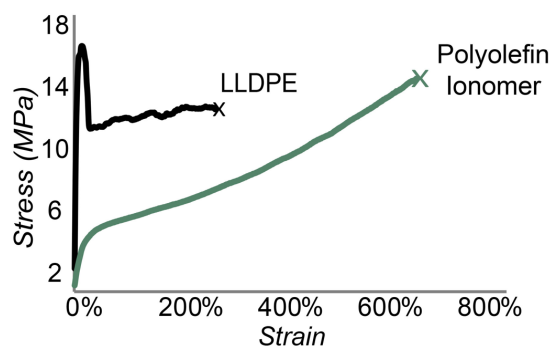
	LLDPE	Polyolefin Ionomer
σ_B (MPa)	13 ± 1	15 ± 1
ε_B	250 ± 51%	675 ± 69%
E (MPa)	27 ± 2	1.9 ± 0.2
U_T (MPa)	387 ± 74	696 ± 49

Figure 4.8 Tensile tests demonstrate the change in polymer properties upon functionalization. Strain rate = 1.0 mm/s, average values and standard deviations reported from data collected over three experiments.

IV-D. CONCLUSION

Our studies demonstrate the versatility of easily accessed, shelf-stable *O*-alkenylhydroxamate **1** in these transformations. Furthermore, there are no platforms for aliphatic C–H functionalization that rival the synthetic scope demonstrated herein with respect to both the diversity of accessible transformations and the viable substrates ranging from pure, linear polyolefins to post-consumer waste. While we targeted many synthetically valuable C–H transformations, additional processes are easily envisioned upon the use of alternative radical traps. We anticipate that the ability to selectively place versatile functionality on substrates >3500 carbon atoms under a universal conceptual approach will enhance the capabilities of late-stage diversification, while the materials made accessible by this platform method will provide solutions to challenges in medicinal chemistry and materials science.

REFERENCES

(1)   Ellen MacArthur Foundation. The New Plastics Economy: Rethinking the Future of Plastics. *World Econ. Forum* **2016**, No. January, 120.

(2)   Williamson, J. B.; Lewis, S. E.; Johnson III, R. R.; Manning, I. M.; Leibfarth, F. C-H Functionalization of Commodity Polymers. *Angew. Chem. Int. Ed.* **2018**, *58*, 8654–8668.

(3)   Britt, P. F. C.; Geoffrey, W.; Winey, K. I.; Byers, J.; Chen, E.; Coughlin, B.; Ellison, C.; Garcia, J.; Goldman, A.; Guzman, J.; Hartwig, J.; Helms, B.; Huber, G.; Jenks, C.; Martin, J.; McCann, M.; Miller, S.; O'Neill, H.; Sadow, A.; Scott, S.; Sita, L.; Vlachos, D.; Waymouth, R. Roundtable on Chemical Upcycling of Polymers. *United States Department of Energy*. **2019**.

(4)   Sambiagio, C.; Schönbauer, D.; Blieck, R.; Dao-Huy, T.; Pototschnig, G.; Schaaf, P.; Wiesinger, T.; Zia, M. F.; Wencel-Delord, J.; Besset, T.; Maes, B. U. W.; Schnürch, M. A Comprehensive Overview of Directing Groups Applied in Metal-Catalysed C–H Functionalisation Chemistry. *Chem. Soc. Rev.* **2018**, *47*, 6603–6743.

(5)   Chen, L.; Malollari, K. G.; Uliana, A.; Sanchez, D.; Messersmith, P. B.; Hartwig, J. F. Selective, Catalytic Oxidations of C–H Bonds in Polyethylenes Produce Functional Materials with Enhanced Adhesion. *Chem* **2021**, *7*, 137–145.

(6)   Hou, W.; Yang, Y.; Wu, Y.; Feng, H.; Li, Y.; Zhou, B. Rhodium(III)-Catalyzed Alkylation of Primary C(sp^3)–H Bonds with α-Diazocarbonyl Compounds. *Chem. Commun.* **2016**, *52*, 9672–9675.

(7)   Chan, W.-W.; Lo, S.-F.; Zhou, Z.; Yu, W.-Y. Rh-Catalyzed Intermolecular Carbenoid Functionalization of Aromatic C–H Bonds by α-Diazomalonates. *J. Am. Chem. Soc.* **2012**, *134*, 13565–13568.

(8)   Na, C. G.; Ravelli, D.; Alexanian, E. J. Direct Decarboxylative Functionalization of Carboxylic Acids Via. *J. Am. Chem. Soc.* **2020**, *142*, 44–49.

(9)   Schmidt, V. A.; Quinn, R. K.; Brusoe, A. T.; Alexanian, E. J. Site-Selective Aliphatic C-H Bromination Using N -Bromoamides and Visible Light. *J. Am. Chem. Soc.* **2014**, *136*, 14389–14392.

(10)   Czaplyski, W. L.; Na, C. G.; Alexanian, E. J. C-H Xanthylation: A Synthetic Platform for Alkane Functionalization. *J. Am. Chem. Soc.* **2016**, *138*, 13854–13857.

(11)   Williamson, J. B.; Czaplyski, W. L.; Alexanian, E. J.; Leibfarth, F. A. Regioselective C–H Xanthylation as a Platform for Polyolefin Functionalization. *Angew. Chem. Int. Ed.* **2018**, *57*, 6261–6265.

(12) Williamson, J. B.; Na, C. G.; Johnson, R. R.; Daniel, W. F. M.; Alexanian, E. J.; Leibfarth, F. A. Chemo- and Regioselective Functionalization of Isotactic Polypropylene: A Mechanistic and Structure–Property Study. *J. Am. Chem. Soc.* **2019**, *141*, 12815–12823.

(13) Li, H.; Ma, P.; Chen, Y.; Zhou, H.; Huang, H.; Liu, L.; Li, L.; Plummer, C. M. Regioselective Post-Functionalization of Isotactic Polypropylene by Amination in the Presence of N -Hydroxyphthalimide. *Polym. Chem.* **2018**, *10*, 619–626.

(14) Plummer, C. M.; Zhou, H.; Zhu, W.; Huang, H.; Liu, L.; Chen, Y. Mild Halogenation of Polyolefins Using an *N* -Haloamide Reagent. *Polym. Chem.* **2018**, *9*, 1309–1317.

(15) Hamielec, A. E.; Gloor, P. E.; Zhu, S. Kinetics of, Free Radical Modification of Polyolefins in Extruders – Chain Scission, Crosslinking and Grafting. *Can. J. Chem. Eng.* **1991**, *69*, 611–618.

(16) Liu, D.; Bielawski, C. W. Direct Azidation of Isotactic Polypropylene and Synthesis of 'Grafted to' Derivatives Thereof Using Azide-Alkyne Cycloaddition Chemistry. *Polym. Int.* **2017**, *66*, 70–76.

(17) Wakabayashi, K.; Register, R. A. Micromechanical Interpretation of the Modulus of Ethylene–(Meth)Acrylic Acid Copolymers. *Polymer (Guildf).* **2005**, *46*, 8838–8845.

APPENDIX A: *SUPPORTING INFORMATION FOR CHAPTER II*

A.1 GENERAL METHODS AND MATERIALS

All post-polymerization modifications were performed under inert atmosphere using standard glove box and Schlenk-line techniques. Xanthylamide and TES-protected N-(2-[3,4-dihydroxyphenyl]ethyl)acrylamide were prepared using previously reported methods. Predominantly (90%) 1,2-polybutadiene was purchased from Sigma-Aldrich and hydrogenated according to known procedure. Hyperbranched polyethylene (13% branched) was obtained from collaborators and synthesized there according to known procedure. Polyethylene, and polyisobutylene were obtained from Sigma-Aldrich and pre-purified via two precipitations prior to use. 1,2-dichlorobenzene was degassed with argon through multiple freeze-pump-thaw cycles. Trifluorotoluene was distilled over calcium hydride and stored in a glove box. Reagents, unless otherwise specified, were purchased and used without further purification.

Proton and carbon magnetic resonance spectra (^{1}H NMR and ^{13}C NMR) were recorded on a Bruker model DRX 400 MHz, Bruker 500 MHz, Varian Inova 600, or Bruker AVANCE III 600 MHz CryoProbe spectrometer with solvent resonance as the internal standard (^{1}H NMR: CDCl$_3$ at 7.26 ppm; ^{13}C NMR: CDCl$_3$ at 77.16 ppm). ^{1}H NMR data are reported as follows: chemical shift, multiplicity (s = singlet, d = doublet, t = triplet, q = quartet, m = multiplet, dd = doublet of doublets, bs = broad singlet), coupling constants (Hz), and integration. Infrared (IR) spectra were obtained using PerkinElmer Frontier FT-IR spectrometer. Small molecule mass spectra obtained using a Thermo LTqFT mass spectrometer with electrospray introduction and external calibration at the University of North Carolina's Department of Chemistry Mass Spectrometry Core Laboratory.

Gel permeation chromatography (GPC) spectra were obtained using Waters 2695 separations module liquid chromatograph, Waters 2414 refractive index detector at room temperature, and Waters 2996 photodiode array detector with styragel HR columns. Tetrahydrofuran was the mobile phase and the flow rate was set to 1 mL/min. The instrument was calibrated using polystyrene standards in the range of 580 to 892,800 Da. Polyethylene were analyzed with high-temperature GPC (140 °C, TCB) against polystyrene standards at the University of Akron.

Differential scanning calorimetry (DSC) was used to determine the thermal characteristics of the polyolefins and graft copolymers using a TA Instruments DSC (Discovery Series). The DSC measurements were performed on 2 – 10 mg of polymer samples at a temperature ramp rate of 10 °C/min unless otherwise noted. Data was taken from the second thermal scanning cycle. Thermal gravimetric analysis was obtained using a TA Instruments TGA (Discovery Series) in the temperature range of 40-600 °C at a temperature ramp rate of 10 °C/min. GC spectra were obtained using a Shimadzu GC-2010 gas chromatograph with a Shimadzu AOC-20s Autosampler, and Shimadzu SHRXI-5MS GC column. Irradiation of xanthylation reactions was performed using Kessil KSH150B Blue 36W LED Grow Lights. UV light reactions were performed in a Luzchem LZC-ORG photoreactor containing UV-A lamps.

A.2 DEPT EXPERIMENT
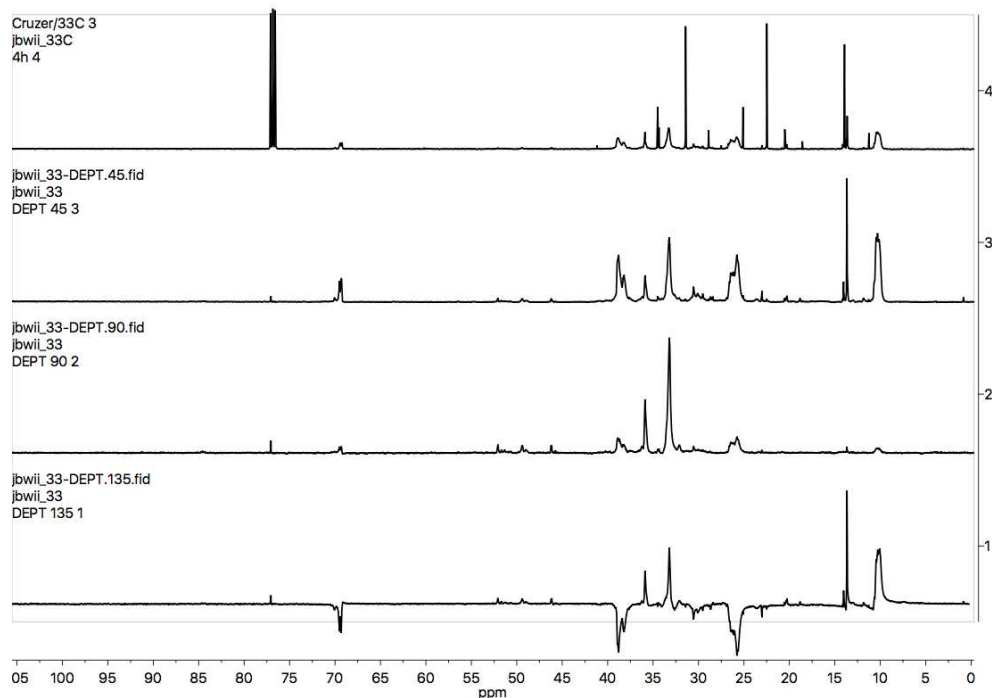
Distortionless Enhancement by Polarization Transfer (DEPT) NMR experiment was conducted on 15 mol % xanthylated PEE. The top spectrum (4) is the ^{13}C NMR of the sample, and the peak at δ 70 ppm is the carbon *alpha* to the xanthate group. The 2nd spectra (3) is a DEPT 45 experiment, where all protonated carbon resonances appear with positive intensity (quaternary carbons are not observed). The peak at δ 70 ppm remains unchanged in this spectrum, indicating that the xanthate is not appended to a quaternary carbon and that tertiary xanthylation of the polymer does not occur. The 3rd spectra (2) is a DEPT 90 experiment, where only methine carbons are displayed. The peak at δ 70 ppm appears, so secondary xanthylation is occurring. The 4th spectra (1) is a DEPT 135 experiment, where methine and methyl groups appear positive and methylene groups appear negative. The peak at δ 70 ppm is inverted, so primary xanthylation is occurring.

A.3 INDEPENDENT SYNTHESIS OF XANTHATE STANDARDS

Overview of experiment: If tertiary xanthylation were observed, it would occur via the abstraction of a tertiary C–H bond by the amidyl radical to generate a tertiary radical, the presence of which could lead to β-scission of the polymer backbone with deleterious impact on the molecular weight of the final material. In order to confirm that no tertiary xanthylation occurs under the reaction conditions, we synthesized a small molecule model substrate, 4-ethyl-2,6-dimethylheptane (**S1**), and subjected it to xanthylation using xanthylamide **1**. The products of this reaction, multiple mono-xanthylated substrates that differ in site of xanthylation, were analyzed by gas chromatography against a tertiary xanthate standard (**S3**). The standard was independently synthesized via decarbonylation of the corresponding acyl xanthate to afford the single product regioisomer. In Figure 2.6, the products of xanthylation of **S1** are shown not to contain any tertiary xanthylation product, as there was no compound eluted around 15.9 min, where the tertiary standard **S3** eluted.
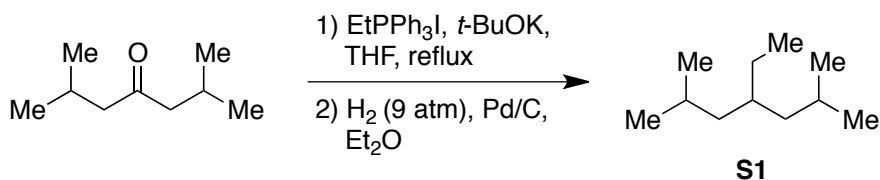
Synthesis of model small molecule substrate 4-ethyl-2,6-dimethylheptane (S1): To a solution of ethyltriphenylphosphonium iodide (8.37 g, 20 mmol) in THF (66 mL) was added potassium *tert*-butoxide (2.24 g, 20 mmol) portionwise followed by 2,6-dimethylheptan-4-one (3.52 mL, 20 mmol). The resultant orange mixture was heated at reflux for 24 h, then cooled to room temperature, diluted with hexanes (100 mL), and stirred for 2 h. The mixture was passed over a pad of Celite and concentrated *in vacuo*. The product was then dissolved in hexanes, passed over a short silica pad, and concentrated *in vacuo* to yield the olefin (2.9 g, 94% yield), which was used without further purification.

To a solution of olefin (2.9 g, 18.8 mmol) in diethyl ether (2 mL) was added 10% palladium on carbon (600 mg). The reaction was pressurized with H_2 (9 atm) and stirred at room temperature overnight. After depressurization, the solution was passed over a pad of silica and Celite and carefully concentrated *in vacuo* to afford the alkane as a clear liquid (1.56 g, 53% yield):

^{1}H NMR (600 MHz, CDCl$_3$) δ 1.62 (dt, *J* = 13.6, 6.7 Hz, 2H), 1.39 – 1.32 (m, 1H), 1.28 – 1.22 (m, 2H), 1.08 (dt, *J* = 13.8, 6.9 Hz, 2H), 1.02 – 0.98 (m, 2H), 0.86 (d, *J* = 6.6 Hz, 12H), 0.82 (t, *J* = 7.4 Hz, 3H). **^{13}C NMR (151 MHz, CDCl$_3$)** δ 43.65, 33.81, 26.12, 25.20, 23.17, 22.82, 10.32. **HRGC-MS (EI)** Exact mass calcd for C_9H_{18} $[M–C_2H_6]^+$, 126.1409. Found 126.1402.
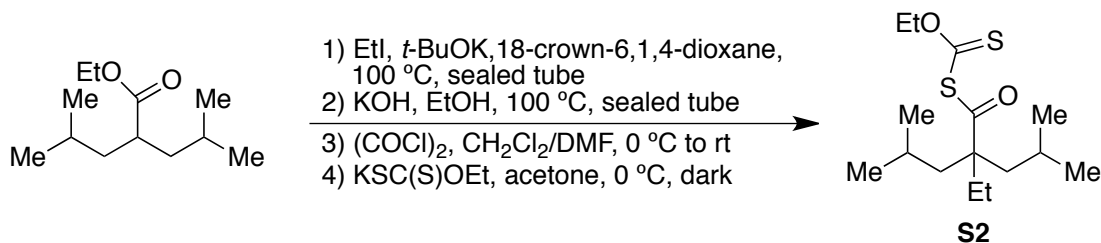
Synthesis of tertiary xanthate standard: To a solution of 4-methyl-2-(2-methylpropyl)-pentanoic acid ethyl ester[1] (1.5 g, 7.5 mmol) in 1,4-dioxane (8 mL) in a pressure tube was added 18-crown-6 (20 mg, 0.08 mmol), iodoethane (6 mL, 75 mmol), and potassium *tert*-butoxide (2.5 g, 22.5 mmol). The tube was sealed and heated at 100 °C for 16 h, then cooled to room temperature. The mixture was passed over a short silica plug and concentrated to afford the alkylated ester as a clear oil (1.7 g, 90% yield), which was used without further purification.

To a solution of the alkylated ester (1.7 g, 7.4 mmol) in ethanol (3 mL) in a pressure tube was added potassium hydroxide (2.5 g, 44.4 mmol). The tube was sealed and heated at 100 ˚C for 24 h, then cooled to room temperature. The mixture was washed 3x with Et_2O to remove unreacted ester, acidified to pH 2 with concentrated hydrochloric acid, and then extracted 3x with Et_2O. The combined organic extracts were dried with $MgSO_4$ and concentrated *in vacuo* to afford the acid as a pale brown oil (450 mg, 30% yield), which was used without further purification.

To a solution of acid (200 mg, 1 mmol) in CH_2Cl_2 (4 mL) at 0 ˚C was added DMF (2 drops) followed by oxalyl chloride (169 μL, 2 mmol). The solution was warmed to room temperature and stirred for 4 h until effervescence ceased, after which it was concentrated *in vacuo*. The residue was taken up in acetone (4 mL) and cooled to 0 ˚C. Potassium ethyl xanthate (152 mg, 0.95 mmol) was added in one portion, and the suspension was stirred for 2 h at 0 ˚C and then concentrated *in vacuo*. The residue was dissolved in CH_2Cl_2/H_2O, and the aqueous phase was extracted 2x with CH_2Cl. The combined organic phases were washed with brine, dried with $MgSO_4$, and concentrated *in vacuo*. The residue was purified by flash column chromatography (5% Et_2O in hexanes) to afford the acyl xanthate as a bright yellow oil (105 mg, 35% yield):

^{1}H NMR (400 MHz, CDCl$_3$) δ 4.63 (q, *J* = 7.0 Hz, 2H), 1.71 (q, *J* = 7.4 Hz, 2H), 1.65 – 1.56 (m, 3H), 1.54 (d, *J* = 6.3 Hz, 1H), 1.49 (d, *J* = 5.6 Hz, 1H), 1.47 – 1.38 (m, 4H), 0.89 (d, *J* = 6.5 Hz, 12H), 0.81 (t, *J* = 7.4 Hz, 3H). **^{13}C NMR (101 MHz, CDCl$_3$)** δ 205.42, 199.51, 70.78, 58.38, 44.39, 25.64, 24.54, 24.31, 24.07, 13.50, 8.01. **HRMS (ES+)** Exact mass calcd for $C_{15}H_{28}O_2S_2Na$ [M+Na]$^+$, 327.1423. Found 327.1418.
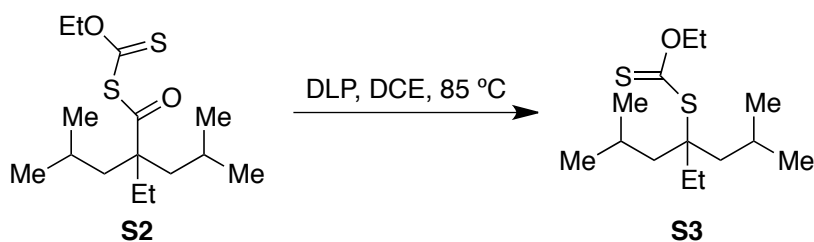
Acyl xanthate (50 mg, 0.16 mmol) was dissolved in 1,2-dichloroethane (0.2 mL) in an argon-filled glovebox and added dilauroyl peroxide (1.6 mg, 0.004 mmol). The vial was sealed with a Teflon-lined screw cap, sealed with Teflon tape, and placed under a balloon of argon outside the glovebox. The solution was heated at 85 ˚C for 30 min until bubbling ceased, after which the solution was cooled to room temperature and concentrated *in vacuo*. The residue was purified by flash column chromatography (0 – 5% Et_2O in hexanes) to afford the tertiary xanthate as a pale yellow oil (12 mg, 27% yield) contaminated with an inseparable, xanthate-derived impurity. The NMR spectra are also complicated due to the presence of rotamers:

¹H NMR (400 MHz, CDCl₃) δ 4.67 – 4.65 (m, 2H), 1.81 – 1.76 (m, 4H), 1.68 – 1.64 (m, 2H), 1.50 – 1.42 (m, 8H), 0.95 (d, J = 6.5 Hz, 12H), 0.92 (t, J = 7.4 Hz, 3H).

¹³C NMR (151 MHz, CDCl₃) δ 214.86, 207.61, 71.80, 71.15, 69.40, 64.75, 44.89, 31.11, 29.86, 29.14, 25.26, 25.24, 24.67, 13.98, 13.77. **HRMS (ES+)** Exact mass calcd for $C_{14}H_{29}OS_2$ [M+H]⁺, 277.1654. Found 277.1657.
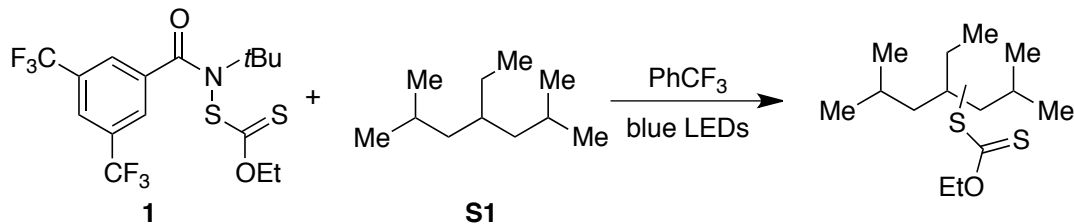
Xanthylation of small molecule standard: A 1 dram vial was charged with xanthylamide **1** (173 mg, 0.4 mmol), 4-ethyl-2,6-dimethylheptane **S1** (188 mg, 1.2 mmol), and PhCF₃ (0.4 mL) in an argon-filled glovebox. The vial was fitted with a PTFE lined screw cap, sealed with Teflon tape, and removed from the glovebox. The vial suspended above an Ecoxotic PAR38 23 W blue LED such that the bottom of the vial was directly aligned with and 1 cm above one of the five LEDs, and the apparatus was covered with aluminum foil. The reaction was irradiated for 15 h and then diluted with CH_2Cl_2 for GC analysis (Figure 2.6).

A.4 SYNTHESIS OF XANTHYLATED POLYOLEFINS VIA C–H XANTHYLATION

General Procedure A (room temperature reactions): The required amount of polyolefin, xanthylamide, and trifluorotoluene were added to a one dram reaction vial equipped with a magnetic stir bar under inert atmosphere. The reaction vial was sealed and placed on a magnetic stir plate. Two Kessil-brand "Tuna Blue" aquarium lights were placed 2 inches from the vial (Figure 2.13) and the reaction mixture was irradiated for 19h. After completion of the reaction, the solution was concentrated *in vacuo* and precipitated in cold MeOH to yield the xanthylated polyolefin as a viscous liquid.

General Procedure B (heated reactions neat or with solvent): The required amount of polyolefin, xanthylamide, and optionally solvent were added to a one dram reaction vial equipped with a magnetic stir bar under inert atmosphere. The reaction vial was sealed and placed on a magnetic stir plate in a small beaker of oil at the desired temperature (Figure 2.13). Two Kessil-brand "Tuna Blue" aquarium lights were placed 2 inches from the vial and the reaction mixture was irradiated for 19h. After completion of the reaction, the solution was concentrated *in vacuo* and precipitated in cold MeOH to yield the xanthylated polyolefin as a viscous liquid.
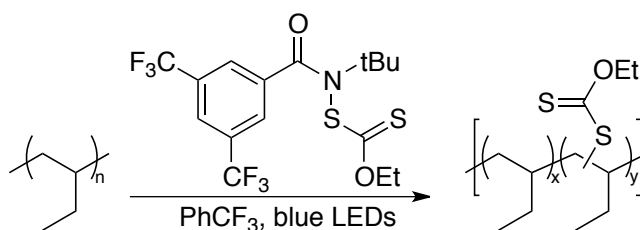
Xanthylated Polyethylethylene: Polyethylethylene (M_n = 3.6 kg/mol, PDI = 1.23) and xanthylamide were reacted according to General Procedure A or B, both worked well (Figure 2.S1). Polyethylethylene (56 mg, 0.89 mmol repeat unit) reacted with xanthylamide (193 mg, 0.45 mmol) in trifluorotoluene (2.25 mL) upon blue light irradiation for 19h. The resulting material was 15 mol % xanthylated polyethylethylene. Similar characterization data was obtained using other stoichiometric ratios of xanthylamide to repeat unit. See accompanying tables and figures for more information.

The following was gathered using 15 mol % xanthylated polyethylethylene:

¹H NMR (600 MHz, CDCl₃) δ 4.64 (bs), 3.98 (bs), 3.77 (bs), 3.69 (bs), 3.10 (bs), 1.64 (bs), 1.41 (t, J = 1 Hz), 1.25 (bs), 1.05 (bs), 0.83 (bs). **¹³C NMR (125 MHz, CDCl₃)** δ 215.1, 69.6,

69.4, 41.4, 39.2, 39.0, 38.9, 38.5, 38.4, 37.9, 36.5, 36.1, 36.1, 36.1, 36.0, 34.7, 34.6, 33.8, 33.5,

33.4, 33.1, 32.9, 32.0, 31.6, 30.7, 30.3, 29.8, 29.4, 29.1, 29.0, 28.9, 28.6, 27.7, 26.9, 26.8, 26.7,

26.4, 26.1, 26.0, 25.9, 25.3, 23.3, 23.2, 22.7, 22.7, 22.6, 20.7, 20.5, 18.8, 14.3, 14.2, 14.1, 13.8,

12.0, 11.5, 10.9, 10.7, 10.5, 10.3, 10.2. **IR (neat, ATR, cm⁻¹)** 735, 907, 1007, 1051, 1111,

1143, 1210, 1279, 1379, 1461, 2855, 2874, 2918, 2959. **GPC (THF)** M_n = 4.8 kg/mol, PDI =

1.32, UV-Vis (nm) = 224, 283 at 33 min. **DSC (°C):** T_g = -27 °C.

Determination of percent functionalization of polyethylethylene: Upon purification, the percent

xanthylation of polyethylethylene can be determined through integration of the ¹H NMR.

Considering the composition of the polymer, the peaks between 0.8 – 1.6 ppm were set to total

to 8 protons. The methylene protons of the ethoxy group that appear at 4.6 ppm are used to

determine mol % xanthylation per repeat unit. Regioselectivity is determined by integration of

the two signals corresponding to primary and secondary xanthylation. For instance, protons

alpha to primary xanthates appear between 3.0 – 3.5 ppm and protons *alpha* to secondary

xanthates appear between 3.5 – 4.0 ppm.
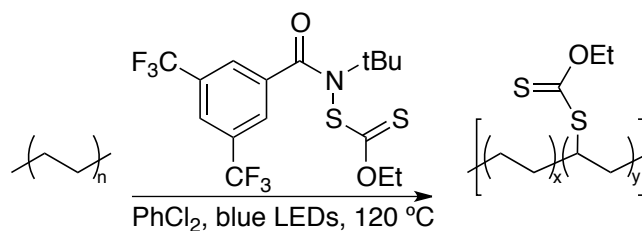
Xanthylated Polyethylene: Polyethylene (M_n = 4.5 kg/mol, PDI = 2.13, 50 mg, 1.79 mmol

repeat unit) and xanthylamide (77 mg, 0.179 mmol) were reacted according to General

Procedure B in dichlorobenzene (3.6 mL). The reaction yielded 9 mol % xanthylated

polyethylene:

¹H NMR (600 MHz, CDCl₃) δ 4.64 (q, J = 1 Hz), 3.69 (bs), 1.64 (bs), 1.57 (d, J = 3 Hz), 1.42 (t, J = 1 Hz), 1.38 (bs), 1.25 (bs), 0.89 (bs), 0.83 (bs). **¹³C NMR (125 MHz, CDCl₃)** δ 215.2, 69.6, 51.5, 34.1, 29.8, 29.7, 29.6, 28.8, 26.8, 13.9. **IR (neat, ATR, cm⁻¹)** 2925, 2853, 1464, 1207, 1111, 1047. **GPC (TCB, 140 °C)** M_n = 4.7 kg/mol, PDI = 2.20.

Determination of percent functionalization of polyethylene: Upon purification, the percent xanthylation of polyethylene can be determined through integration of the ¹H NMR. Considering the composition of the polymer, the peaks between 0.8 – 1.6 ppm were set to total to 4 protons. The methylene protons of the ethoxy unit that appear at 4.6 ppm are used to determine mol % xanthylation per repeat unit.
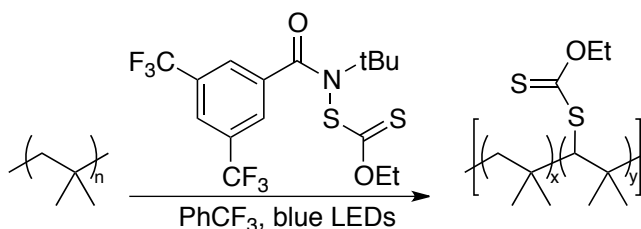
Xanthylated Polyisobutylene: Polyisobutylene (M_n = 1.7 kg/mol, PDI = 1.67, 100 mg, 1.79 mmol repeat unit) and xanthylamide (77 mg, 0.179 mmol) were reacted according to General Procedure A in PhCF₃ (3.6 mL), yielding 2 mol % xanthylated polyisobutylene:

¹H NMR (600 MHz, CDCl₃) δ 5.30 (s), 5.22 (s), 4.91 (s), 4.85 (s), 4.64 (m), 3.85 (bs), 3.76 (bs), 3.72 (bs), 2.09 (s), 2.00 (s), 1.88 (dd, J = 1 Hz, 2Hz), 1.78 (s), 1.57 (d, J = 1 Hz), 1.51 (s), 1.43 (s), 1.41 (bs), 1.38 (m), 1.33 (s), 1.31 (m), 1.27 (m), 1.11 (bs), 1.10 (s), 1.07 (m), 1.02 (s), 0.99 (s), 0.97 (s), 0.96 (s), 0.89 (t, J = 1 Hz), 0.87 (s), 0.86 (s), 0.85 (s). **¹³C NMR (125 MHz, CDCl₃)** δ 59.5, 59.4, 58.8, 58.2, 38.2, 38.1, 38.1, 37.8, 32.6, 32.4, 31.2, 31.2, 31.1, 30.8. **IR**

(neat, ATR, cm⁻¹) 681, 736, 804, 849, 905, 923, 951, 1048, 1111, 1142, 1182, 1229, 1279, 1366, 1389, 1471, 1655, 1711, 2895, 2952. **GPC (THF)** M_n = 2.6 kg/mol, PDI = 1.35, UV-Vis (nm) = 212, 282 at 35 min.

Determination of percent functionalization of polyisobutylene: Upon purification, the percent xanthylation of polyisobutylene can be determined through integration of the ¹H NMR. Considering the composition of the polymer, the peaks between $0.8 - 2.1$ ppm were set to total to 8 protons. The methylene protons of the ethoxy unit that appear at 4.6 ppm are used to determine mol % xanthylation per repeat unit.
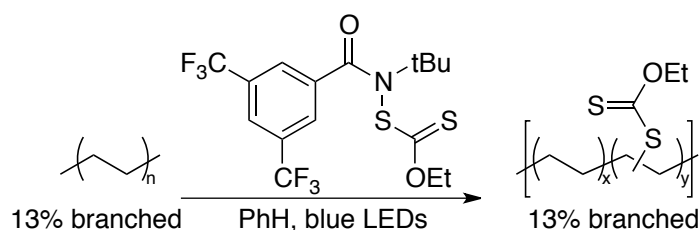
Xanthylated Hyperbranched Polyethylene: Hyperbranched polyethylene[4] (M_n = 29 kg/mol, PDI = 1.56, mg, 1.07 mmol repeat unit, 13% branched) and xanthylamide (23 mg, 0.05 mmol) were added to a reaction vial with a stir bar. The mixture was submitted to the glove box, where dry benzene was added (0.3 mL). The mixture was then stirred and irradiated with Kessil blue lights for 19h. The polymer was purified via precipitation in cold MeOH to yield xanthylated polyolefin.

The following was gathered for 3 mol % xanthylated hyperbranched polyethylene:

¹H NMR (600 MHz, CDCl₃) δ 4.64 (s), 3.78 (bs), 3.70 (bs), 3.13 (bs), 1.64 (bs), 1.56 (s), 1.51 (s), 1.42 (s), 1.22 (bs), 1.09 (bs), 0.89 (s), 0.84 (s). **¹³C NMR (125 MHz, CDCl₃)** δ 215.1, 77.3, 77.0, 76.8, 69.5, 45.9, 39.3, 38.9, 37.8, 37.4, 37.2, 36.8, 36.7, 34.9, 34.4, 34.2, 33.7, 33.4, 33.3, 32.8, 32.4, 32.0, 32.0, 30.2, 30.1, 29.9, 29.8, 29.5, 29.4, 29.0, 28.8, 27.6, 27.2, 26.8, 25.9, 25.5, 23.8, 23.2, 23.1, 22.7, 20.5, 19.8, 19.3, 14.6, 14.2, 13.8, 11.4, 10.9. **IR (neat, ATR, cm⁻¹)** 2945, 2922, 2853, 1459, 1377, 1209, 1118, 1065, 1052, 722. **GPC (THF)** M_n = 34 kg/mol, PDI = 1.66, UV-Vis (nm) = 228, 283 at 28 min.

Determination of percent functionalization of hyperbranched polyethylene: Upon purification, the percent xanthylation of hyperbranched polyethylene can be determined through integration of the ¹H NMR. Considering the composition of the polymer, the peaks between 0.8 – 1.6 ppm were set to total to 4 protons. The methylene protons of the ethoxy unit that appear at 4.6 ppm are used to determine mol % xanthylation per repeat unit.

A.5 FURTHER DERIVATIZATION OF XANTHATE PRODUCTS
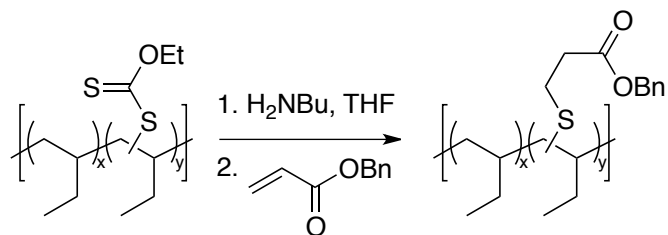
Thiol-acrylate procedure: A solution of 13 mol % xanthylated polyethylethylene (66 mg, 0.15 mmol xanthate) in 1 mL THF and butylamine were separately degassed with argon for 30 min. Butylamine (38 μL, 0.38 mmol) was added to the polymer solution at room temperature and allowed to stir at room temperature overnight. Benzyl acrylate (0.11 mL, 0.77 mmol) was degassed with argon for 30 min and then added to the solution. The mixture was left to stir

overnight at room temperature. The reaction was concentrated *in vacuo* and the desired

polymer was collected through precipitation in cold MeOH:

¹H NMR (600 MHz, CDCl₃) δ 7.35 (m, 5H, *J* = 3 Hz), 5.14 (s, 2H), 2.79 (bs, 2H), 2.65 (bs,

2H), 1.27 (bs), 0.89 (t), 0.84 (bs). **¹³C NMR (125 MHz, CDCl₃)** δ 172, 136, 129, 128.4, 128.3,

128.2, 66, 49, 39, 38, 36, 35, 33, 32, 27, 26, 25, 23, 14, 11, 10. **IR (neat, ATR, cm⁻¹)** 696, 735,

751, 803, 1029, 1140, 1183, 1215, 1238, 1279, 1347, 1379, 1459, 1740, 2855, 2874, 2919,

2959. **GPC (THF)** M_n = 5.9 kg/mol, PDI = 1.32, UV-Vis (nm) = 214 at 33 min.
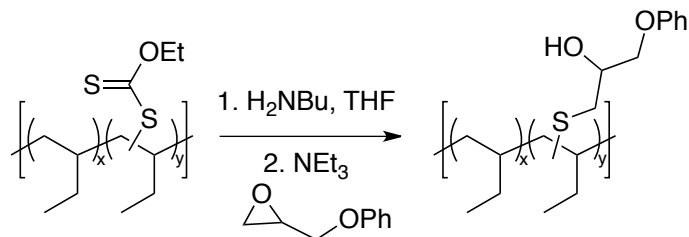
Thiol-epoxy procedure: To a 1-dram vial, 13 mol % xanthylated polyethylethylene (84 mg,

0.20 mmol xanthate) in THF (1 mL) was added and degassed with argon for 30 min. Degassed

butylamine (48 μL, 0.49 mmol) was added to the solution. The reaction was stirred at room

temperature for 20 hours. Glycidyl phenyl ether (0.14 mL, 0.98 mmol) and triethylamine (0.14

mL, 0.98 mmol) were degassed and added to the reaction and stirred at room temperature for

24 h. The solution was concentrated *in vacuo* and precipitated in MeOH to afford the desired

polymer:

¹H NMR (CDCl₃, 600 MHz) δ 7.28 (t, 2H, J = 1 Hz), 6.96 (t, 1H, J = 1 Hz), 6.92 (d, 2H, J =

1 Hz), 4.07 (bs, 1H), 4.04 (bs, 2H), 3.38 (bs, 0.15H), 2.92 (t, 0.23H), 2.84 (bs, 0.92H), 2.77 (t,

0.41H), 2.72 (bs, 0.88H), 2.55 (bs, 0.33H), 1.59 (bs, 2H), 1.25 (bs, 43H), 1.05(bs, 13H), 0.82

(bs, 27H). **¹³C NMR (CDCl₃, 125 MHz)** δ 158, 130, 121, 115, 70, 69, 50, 45, 39, 38, 36, 33, 27, 26, 23, 14, 11, 10. **IR (neat, ATR, cm⁻¹)**: 690, 747, 752, 815, 910, 1043, 1079, 1143, 1173, 1245, 1280, 1300, 1380, 1461, 1496, 1589, 1601, 2856, 2874, 2921, 2959. **GPC (THF)**: $M_n =$ 6.5 kg/mol, PDI = 1.278, UV-Vis (nm) = 272.4 at 33 min.
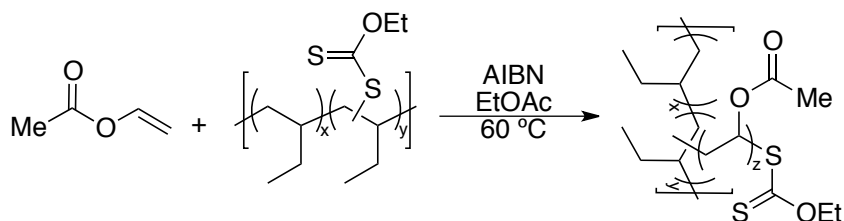
RAFT polymerization of vinyl acetate: A reaction vial was charged with vinyl acetate (0.90 mL, 9.79 mmol), AIBN (2.5 mg, 0.015 mmol), and 14 mol % xanthylated polyethylethylene (63 mg, 0.15 mmol xanthate) in EtOAc (0.9 mL) and degassed by 4 freeze-pump-thaw cycles. The reaction was sealed and placed in an oil bath at 60 °C. After 18 h, the reaction was stopped by cooling in an ice bath. The reaction was concentrated *in vacuo* and the resulting polymer was purified through multiple washes with hexanes to yield a clear, viscous oil:

¹H NMR (600 MHz, CDCl₃) δ 4.91 (bs), 4.85 (bs), 4.61 (bs), 2.00 (t, $J = 2$ Hz), 1.82 (bs), 1.82 (bs), 1.73 (bs), 1.23 (bs), 0.94 (bs), 0.86 (d, $J = 1$ Hz), 0.82 (t, $J = 1$ Hz), 0.80 (bs). **¹³C NMR (125 MHz, CDCl₃)** δ 170.5, 170.4, 170.3, 170.3, 68.0, 67.9, 66.9, 66.7, 66.7, 66.6, 66.3, 66.0, 39.9, 39.5, 39.1, 38.7, 36.0, 34.6, 34.5, 33.4, 31.6, 29.0, 25.3, 25.2, 22.6, 21.1, 21.0, 20.9, 20.8, 20.7, 18.8, 14.1, 13.8, 11.4. **IR (neat, ATR, cm⁻¹)** 606, 632, 735, 797, 947, 1020, 1045, 1112, 1230, 1371, 1437, 1732, 2855, 2872, 2925, 2961. **GPC (THF)** $M_n = 16.7$ kg/mol, PDI = 2.00,

UV-Vis (nm) = 221, 282 at 33 min. **DSC (°C, 40 °C/min)** T_g (2 observed) = -50.64 and 26.37

°C.
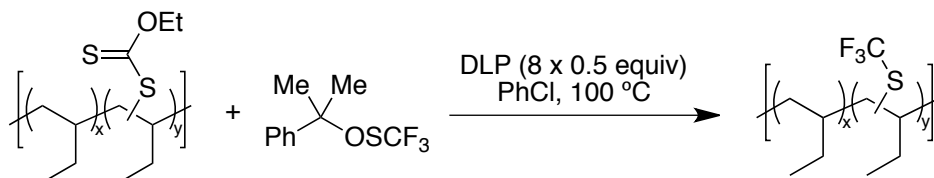
Trifluoromethylthiolation procedure: In a 2-dram vial, 12 mol % xanthylated

polyethylethylene (50 mg, 0.084 mmol xanthate), ((2-phenylpropan-2-

yl)oxy)(trifluoromethyl)sulfane[5] (60 mg, 0.25 mmol), and dilauroyl peroxide (16 mg, 0.04

mmol) were dissolved in chlorobenzene (4 mL) in an argon-filled glovebox. The vial was

sealed with a Teflon-lined screw cap, sealed with Teflon tape, and heated at 100 ˚C under a

balloon of argon. Additional dilauroyl peroxide (16 mg, 0.04 mmol) was added every 30

minutes for a total of eight additions. After the last addition, the reaction mixture was heated

for an additional 30 minutes, then cooled to room temperature and concentrated *in vacuo*. The

polymer was purified via precipitation three times from methanol to afford

trifluoromethylthiolated polyethylethylene as a yellow solid (29 mg, 60% yield):

¹H NMR (600 MHz, CDCl₃) δ 3.48 (br. s), 3.26 (q, *J* = 7.66 Hz), 1.56 (br. s), 1.25 (br. s), 1.05

(br. s), 0.83 (br. s). **¹³C NMR (151 MHz, CDCl₃)** δ 134.57, 132.79, 132.54, 130.77, 130.52,

125.16, 39.29, 39.25, 39.19, 39.10, 39.02, 38.97, 38.63, 38.53, 36.23, 36.19, 36.17, 36.14,

33.63, 33.53, 33.49, 32.09, 32.08, 31.11, 30.87, 29.86, 29.82, 29.81, 29.53, 26.79, 26.55, 26.14,

26.03, 25.95, 23.35, 22.86, 14.30, 10.83, 10.79, 10.75, 10.72, 10.62, 10.45, 10.34. **¹⁹F NMR**

(376 MHz, CDCl₃) δ -39.41, -39.56, -39.81, -39.86, -39.88, -40.20, -40.25, -40.34, -41.93, -

41.96. **IR (neat, ATR, cm⁻¹)** 2962, 2924, 2857, 1463, 1381, 1264, 1114, 742. **GPC (THF)** M_n = 5.2 kg/mol, PDI = 1.22, UV-Vis (nm) = 212 at 33 min.
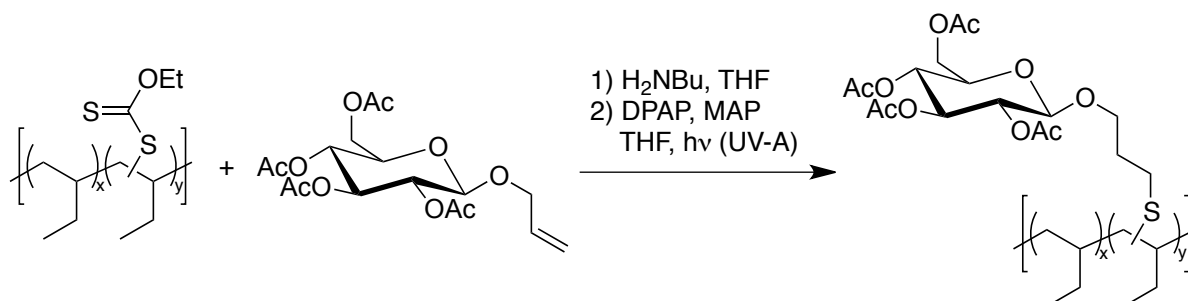
Thiol-ene procedure: In a 1-dram vial, 11 mol % xanthylated polyethylethylene (60 mg, 0.095 mmol xanthate) was dissolved in THF (1 mL) in an argon-filled glovebox. The vial was fitted with a rubber septum, sealed with Teflon tape, and removed from the glovebox. Butylamine (94 μL, 0.95 mmol) was added, causing a deep yellow color to persist. The solution was stirred for 20 h and then concentrated to dryness *in vacuo* and further dried via high-vacuum. The vial was brought back into the glovebox, and the residue was added to a 20 mL scintillation vial containing the allyl glycoside[6] (111 mg, 0.29 mmol), 2,2-dimethoxy-2-phenylacetophenone (2.3 mg, 0.009 mmol), 4'-methoxyacetophenone (1.4 mg, 0.009 mmol), and THF (15 mL). The scintillation vial was sealed with Teflon tape, removed from the glovebox, and irradiated with UV-A light for 24 h. The solution was concentrated *in vacuo* and washed with methanol ten times to afford the thiol-ene polymer adduct as a yellow solid (38 mg, 43% yield):

¹H NMR (600 MHz, CDCl₃) δ 5.23 – 5.16 (m), 5.12 – 5.03 (m), 5.01 – 4.95 (s), 4.55 (d, *J* = 8.0 Hz), 4.49 (d, *J* = 8.0 Hz), 4.34 (dd, *J* = 13.2, 4.8 Hz), 4.29 – 4.24 (m), 4.12 (dd, *J* = 11.1, 3.5 Hz), 3.93 (br. s), 3.71 – 3.66 (m), 3.62 (br. s), 3.48 (br. s), 2.54 (br. s), 2.08 (s), 2.04 (s), 2.02 (s), 2.00 (s), 1.25 (br. s), 1.04 (br. s), 0.82 (br. s). **¹³C NMR (126 MHz, CDCl₃)** δ 170.81,

170.42, 169.54, 169.47, 101.10, 99.69, 72.99, 71.93, 71.43, 70.17, 68.55, 62.07, 51.02, 39.20, 38.59, 36.23, 33.59, 30.86, 29.86, 26.75, 26.11, 23.34, 20.89, 20.82, 20.76, 14.34, 10.79, 10.50. **IR (cm⁻¹)** 2962, 2926, 1758, 1464, 1381, 1226, 1045. **GPC (THF)** M_n = 6.2 kg/mol, PDI = 1.32, UV-Vis (nm) = 212 at 33 min.
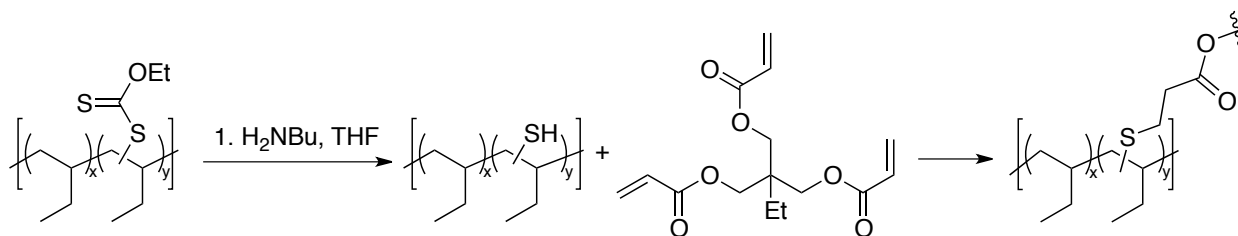
Thiol-triacrylate procedure: With a trifunctional acrylate, the goal was to generate a perfectly elastomeric network of the polyolefin. A solution of 14 mol % xanthylated polyethylethylene (50 mg, 0.098 mmol xanthate, 1 equiv) in THF (0.7 mL) was degassed with argon for 30 min. Degassed butylamine (12 μL, 0.12 mmol, 1.2 equiv) was added to the reaction mixture and allowed to stir at RT overnight. Trimethylolpropane triacrylate (11 μL, 0.039 mmol, 1.2 equiv per functional group) was degassed with argon for 30 min and then added to the solution. The mixture was left to stir overnight at RT. The reaction was concentrated *in vacuo*. After the reaction, the resulting material was an insoluble polymer network. Analysis by IR confirmed the expected carbonyl peaks and the lack of xanthate absorbances, demonstrating that the desired reaction went to completion:

IR (neat, ATR, cm⁻¹): 2959, 2915, 2858, 2855, 1740, 1461, 1379, 1279, 1241, 1174, 1142, 1070, 1016, 994, 913, 782.
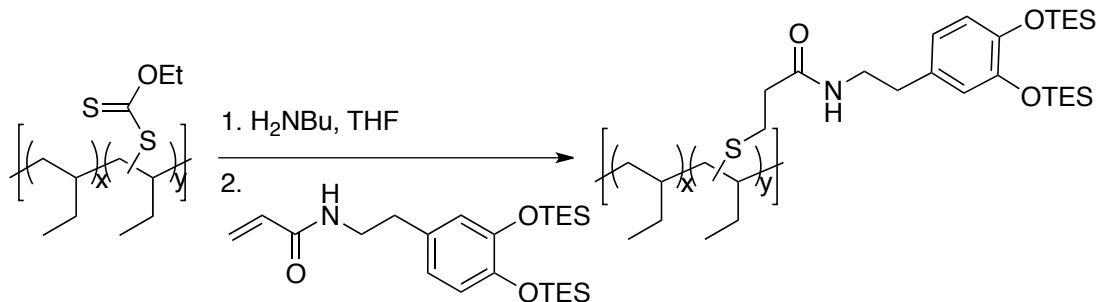
Thiol-acrylamide procedure: A solution of 14 mol % xanthylated polyethylethylene (47 mg, 0.11 mmol xanthate) in THF (0.8 mL) was bubbled with argon for 30 min. Degassed butylamine (28 μL, 0.29 mmol) was added to the reaction mixture and the solution was allowed to stir RT overnight. TES-protected N-(2-[3,4-dihydroxyphenyl]ethyl)acrylamide[6] (249 mg, 0.57 mmol) in THF (0.5 mL) was degassed with argon for 30 min and then added to the solution. The mixture was left to stir overnight at RT. The reaction was concentrated *in vacuo*. The desired polymer was collected through precipitation in cold MeOH as a clear, viscous oil:

¹H NMR (600 MHz, CDCl₃) δ 6.73 (m, J = 2 Hz), 6.63 (m, J = 2 Hz), 3.66 (bs), 3.45 (bs), 2.89 (bs), 2.83 (bs), 2.77 (bs), 2.68 (bs), 2.51 (bs), 2.39 (bs), 1.60 (bs), 1.25 (bs), 1.05 (bs), 0.98 (bs), 0.83 (bs), 0.76 (bs), 0.74 (bs), 0.73 (bs). **¹³C NMR (125 MHz, CDCl₃)** δ 146.8, 121.0, 120.5, 39.1, 38.4, 36.1, 33.4, 30.7, 29.7, 26.0, 23.2, 14.2, 10.4, 6.7, 5.1, 5.1, 1.0. **IR (cm⁻¹)** 2959, 2918, 2874, 2854, 1740, 1649, 1512, 1461, 1379, 1279, 1279, 1262, 1240, 1143, 1052, 1019, 801, 749. **GPC (THF)** M_n = 6.7 kg/mol, PDI = 1.44, UV-Vis (nm) = 225, 280 at 33 min.

A.6 GPCS FOR CHAPTER II
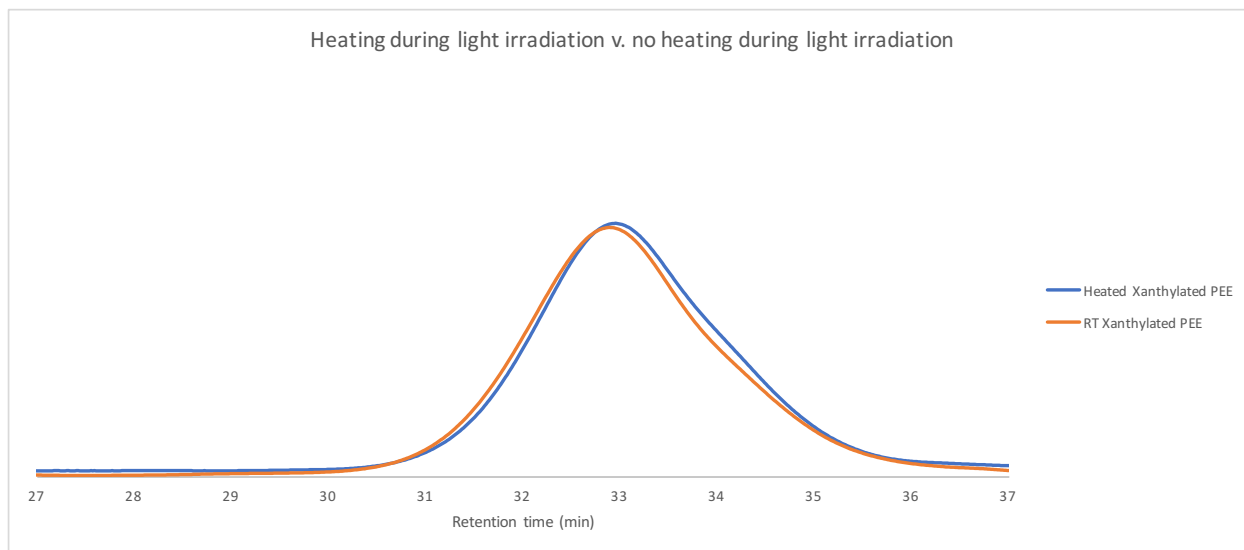
GPC overlay of PEE after xanthylation reaction at room temperature (orange, M_n = 4.5 kg/mol, PDI = 1.31) or at 120 °C in 1,2-dichlorobenzene (blue, M_n = 4.6 kg/mol, PDI = 1.33). Heating the reaction mixture did not significantly alter the molecular weight or dispersity. This indicates that General Procedure A and General Procedure B deliver similar polymer products.
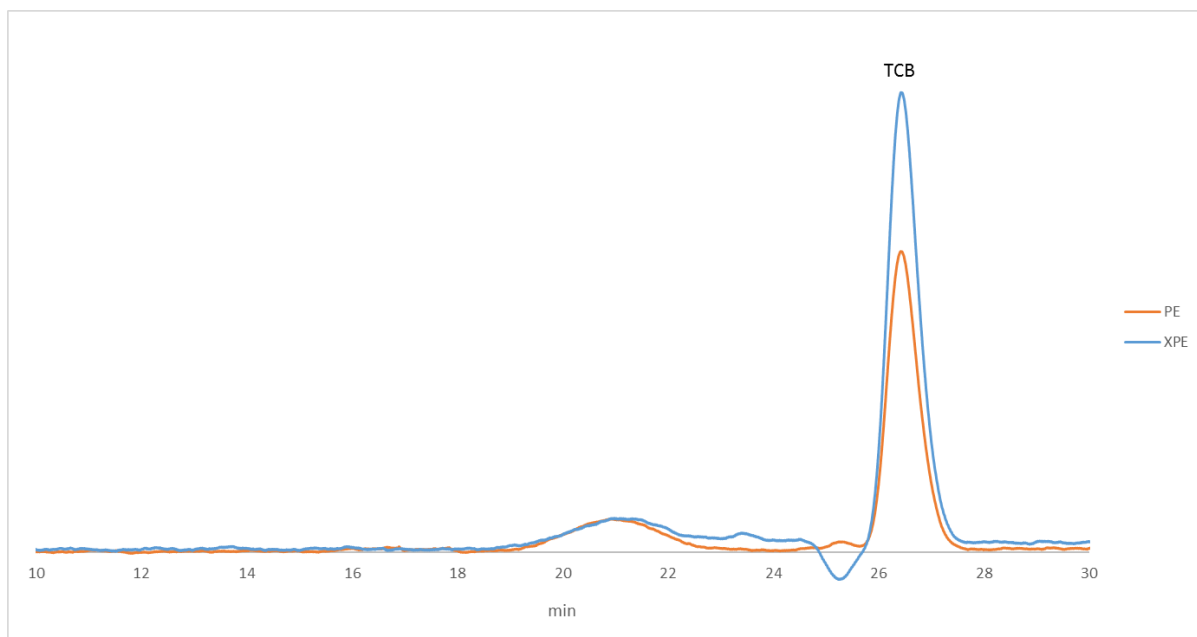
Due to the insolubility of polyethylene in THF, this polyolefin had to be analyzed by high temperature size exclusion chromatography at the University of Akron. High temperature GPC

at 140 °C in TCB of polyethylene after xanthylation (M_n = 4.7 kg/mol, PDI = 2.2) mimics the same molecular weight distribution as the parent material (M_n = 4.5 kg/mol, PDI = 2.1). This indicates that C–H xanthylation is a viable post-polymerization modification for commodity polyolefins.
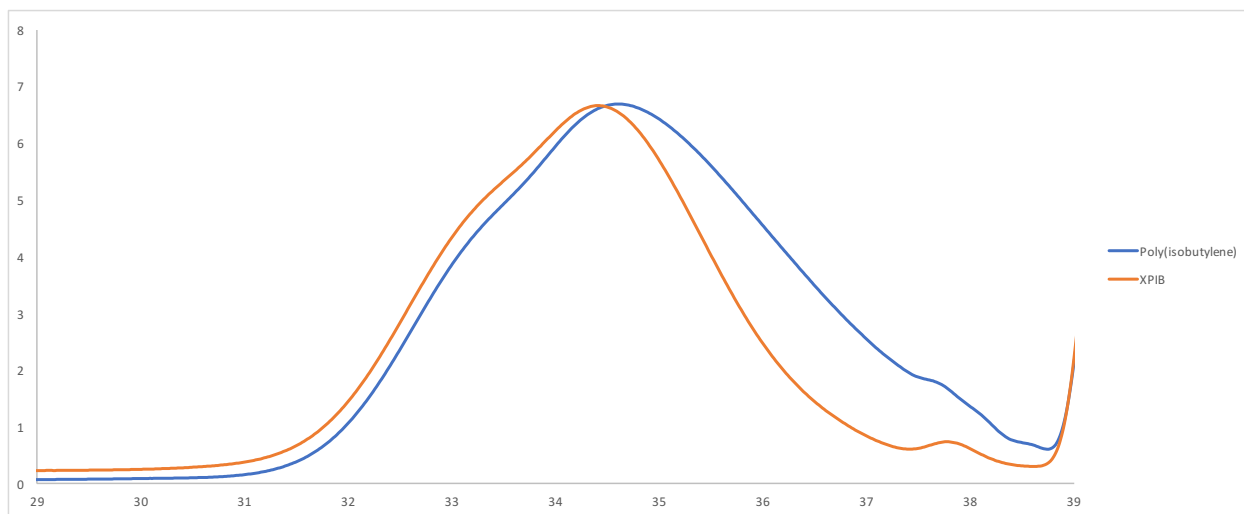
Poly(isobutylene) (M_n = 1.7 kg/mol, PDI = 1.67) was xanthylated to reveal xanthylated poly(isobutylene) (M_n = 2.6 kg/mol, PDI = 1.35). Unique to this experiment, we see that the molecular weight dispersity decreases after xanthylation. We hypothesize that this is due to the low molecular weight of this sample. We commonly observe an increase in solubility once a polyolefin has been xanthylated. The lower molecular weight polymers that would elute around 37 min, once xanthylated, could then be soluble in MeOH during the precipitation. This is represented in the GPC trace as the right side of the curve is identical in shape to the starting material, but the left side is abbreviated.
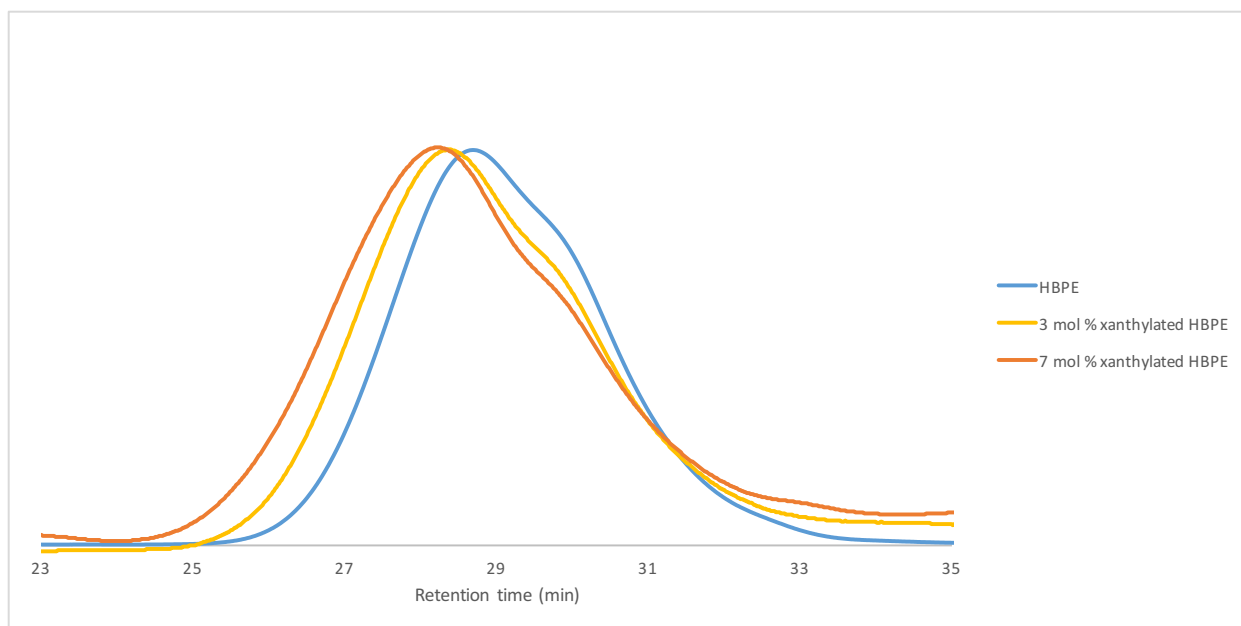
Xanthylated hyperbranched polyethylene (M_n = 29 kg/mol, PDI = 1.56) shifted to a higher molecular weight upon 3 mol % xanthylation (M_n = 34 kg/mol, PDI = 1.66) and 7 mol % xanthylation (M_n = 36 kg/mol, PDI = 1.82), but maintained nearly the same shape and dispersity. This indicates that C–H xanthylation is also chemoselective for functionalization rather than chain coupling or chain scission in higher molecular weight materials.
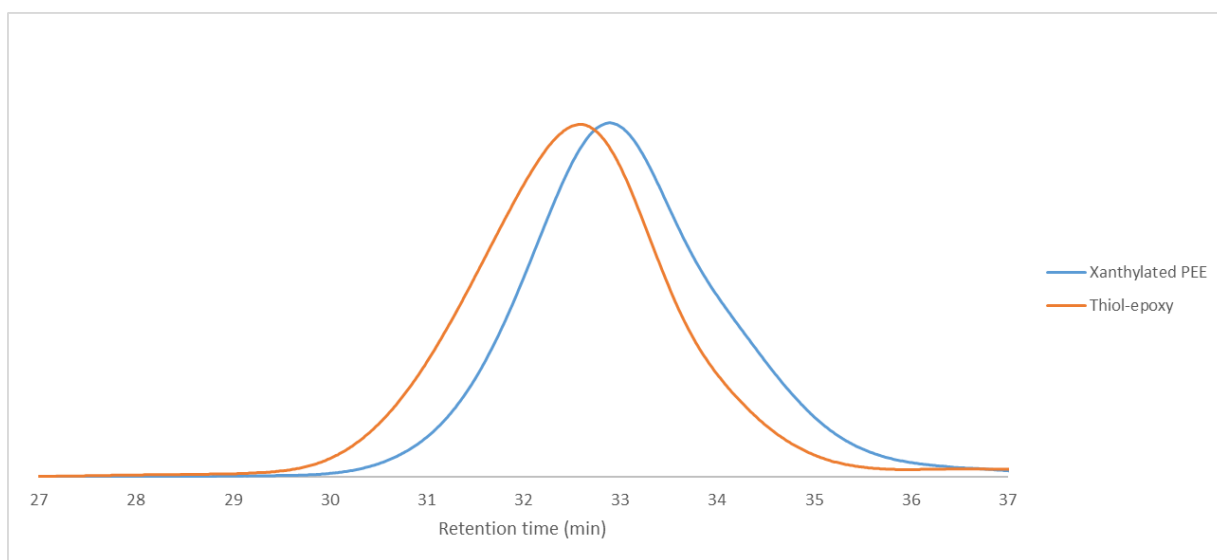
Xanthylated polyethylethylene (M_n = 4.9 kg/mol, PDI = 1.28) was transformed using glycidyl phenyl ether. Adding more mass to the polymer backbone, the molecular weight of the polyolefin increased, but the dispersity remained unchanged (M_n = 6.5 kg/mol, PDI = 1.28). The UV-Vis spectrum demonstrated the conversion of xanthate to thiol through the disappearance of the xanthate absorption at 283 nm and the appearance of aromatic absorptions at 272 nm.
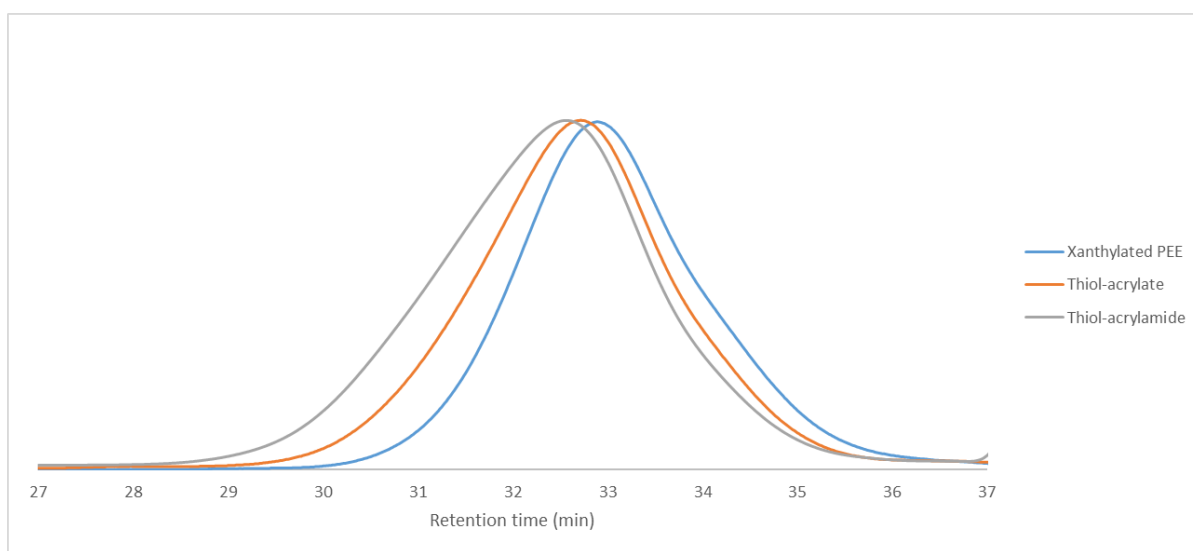
Xanthylated polyethylethylene (M_n = 4.9 kg/mol, PDI = 1.28) was transformed using a thiol-Michael addition with benzyl acrylate and a dopamide-derived acrylamide. The result of thiol-acrylate reaction showed M_n = 5.9 kg/mol and PDI = 1.32, so the molecular weight distribution was relatively unchanged. Acrylamides are known to crosslink polymers, so we were enthused that the molecular weight distribution was able to be maintained (M_n = 6.7 kg/mol, PDI = 1.44).
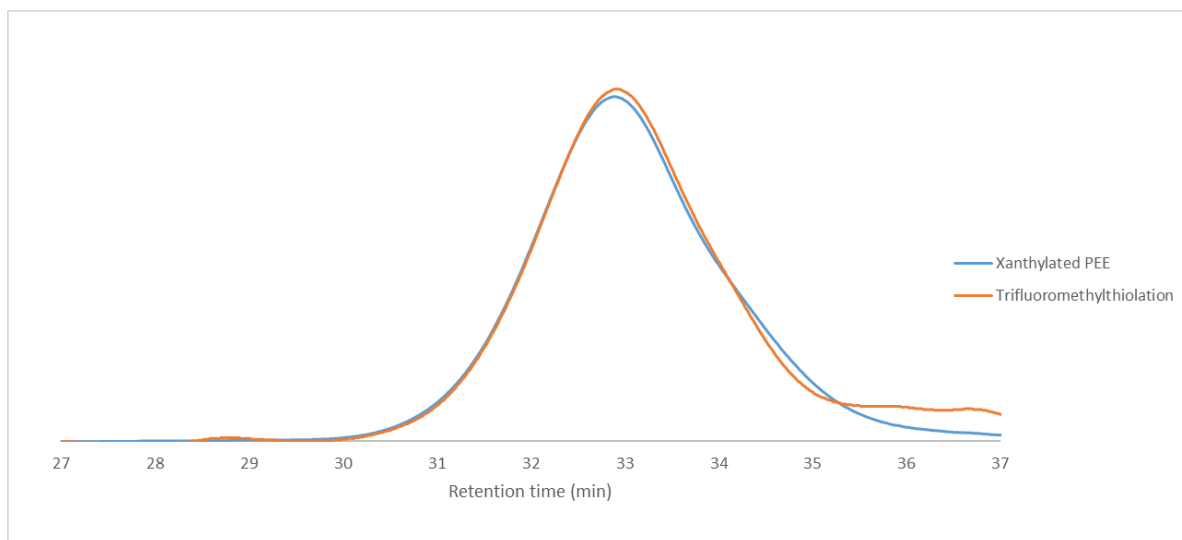
Even in radical-based transformations, such as trifluoromethylthiolation shown above, we were able to control the molecular weight distribution. The xanthylated material (M_n = 4.9 kg/mol, PDI = 1.26) had nearly the identical molecular weight distribution as the final trifluoromethylthiolated material (M_n = 5.2 kg/mol, PDI = 1.22). Our platform strategy is robust in radical and polar C–H transformations.

94
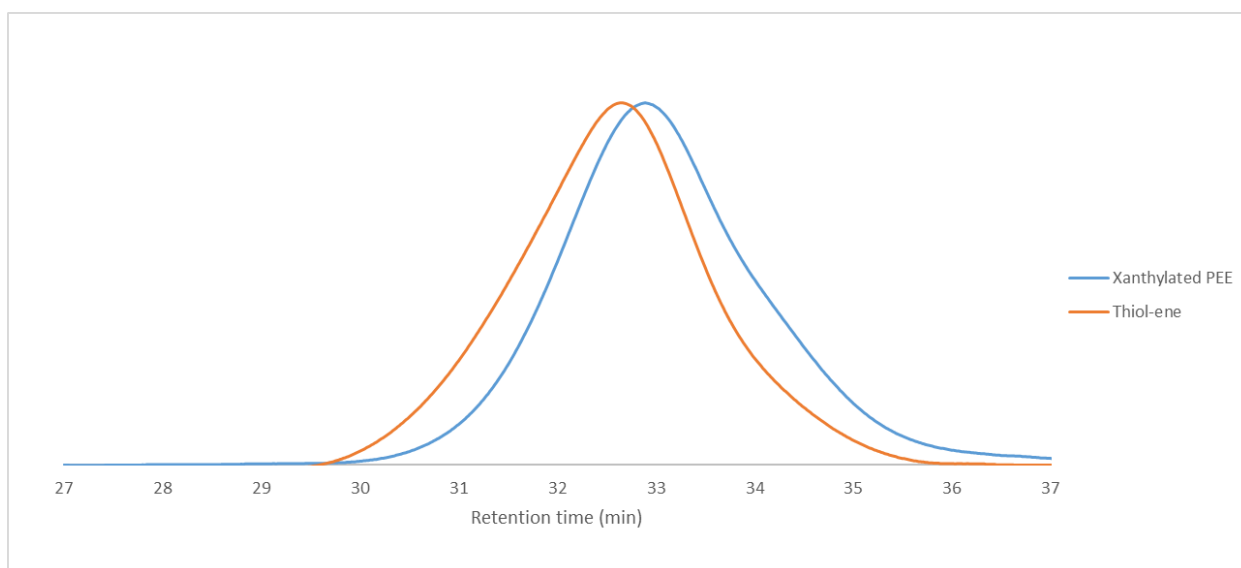
Photochemical thiol-ene reactions occur via radical pathways. Xanthylated polyethylethylene (M_n = 5.0 kg/mol, PDI = 1.25) underwent controlled conversion from the xanthate to thiol and then subsequent thiol-ene reaction with an allylglycoside without significant change in dispersity (M_n = 6.2 kg/mol, PDI = 1.32). As expected, the molecular weight of the polyolefin increased, as a great deal of mass was added.

A.7 NMRS FOR CHAPTER II

OEt

13% branched

9.5 9.0 8.5 8.0 7.5 7.0 6.5 6.0 5.5 5.0 4.5 4.0 3.5 3.0 2.5 2.0 1.5 1.0 0.5 0.0 -0.5
ppm
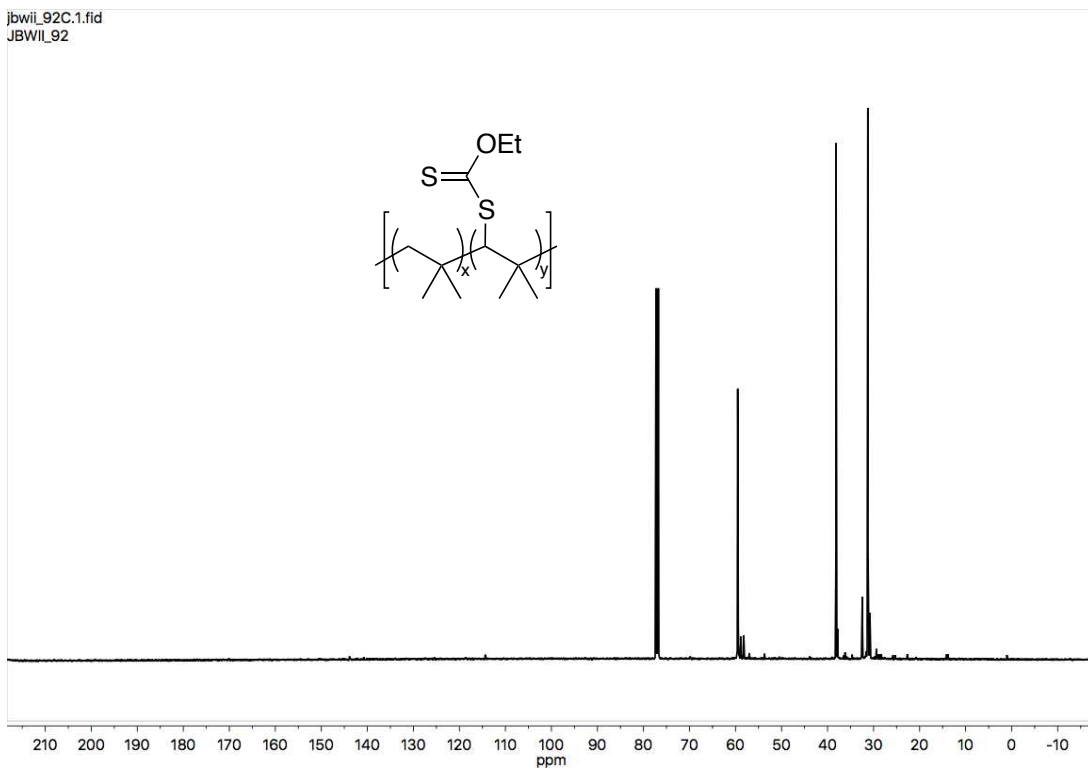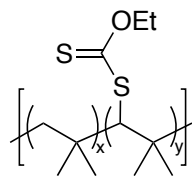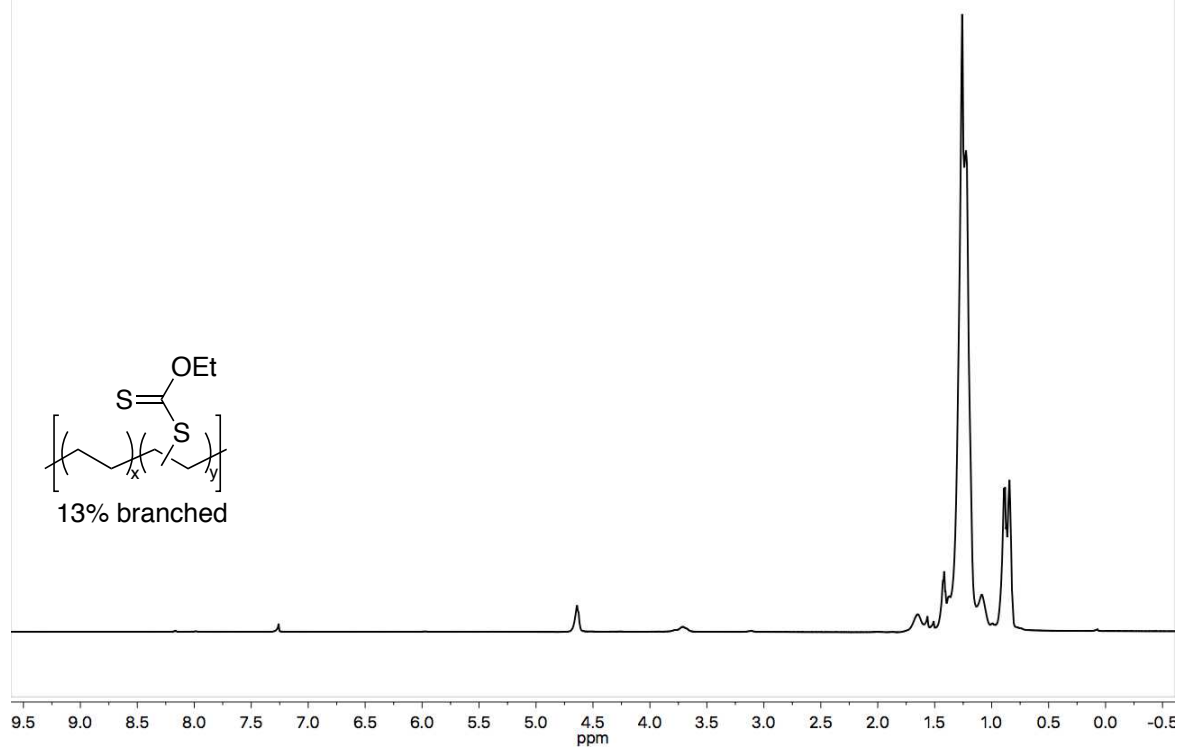
jbwiii_26.1.fid
jbwiii_26C
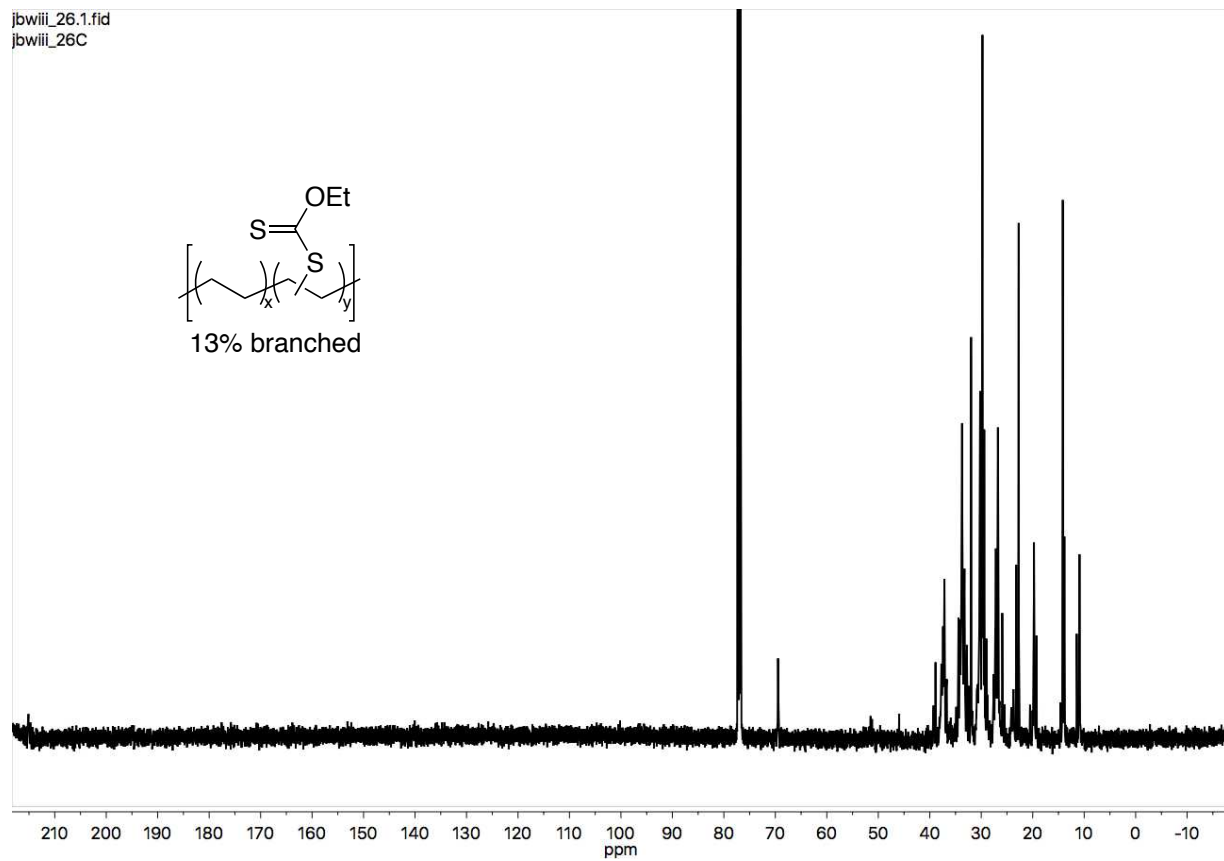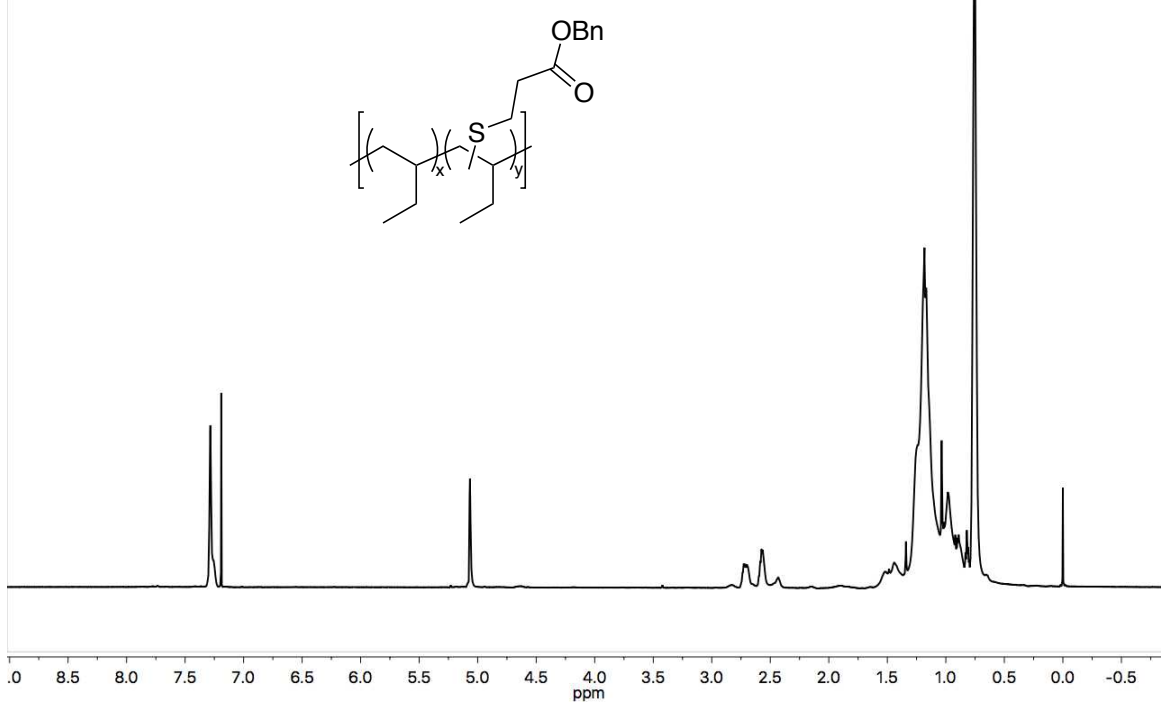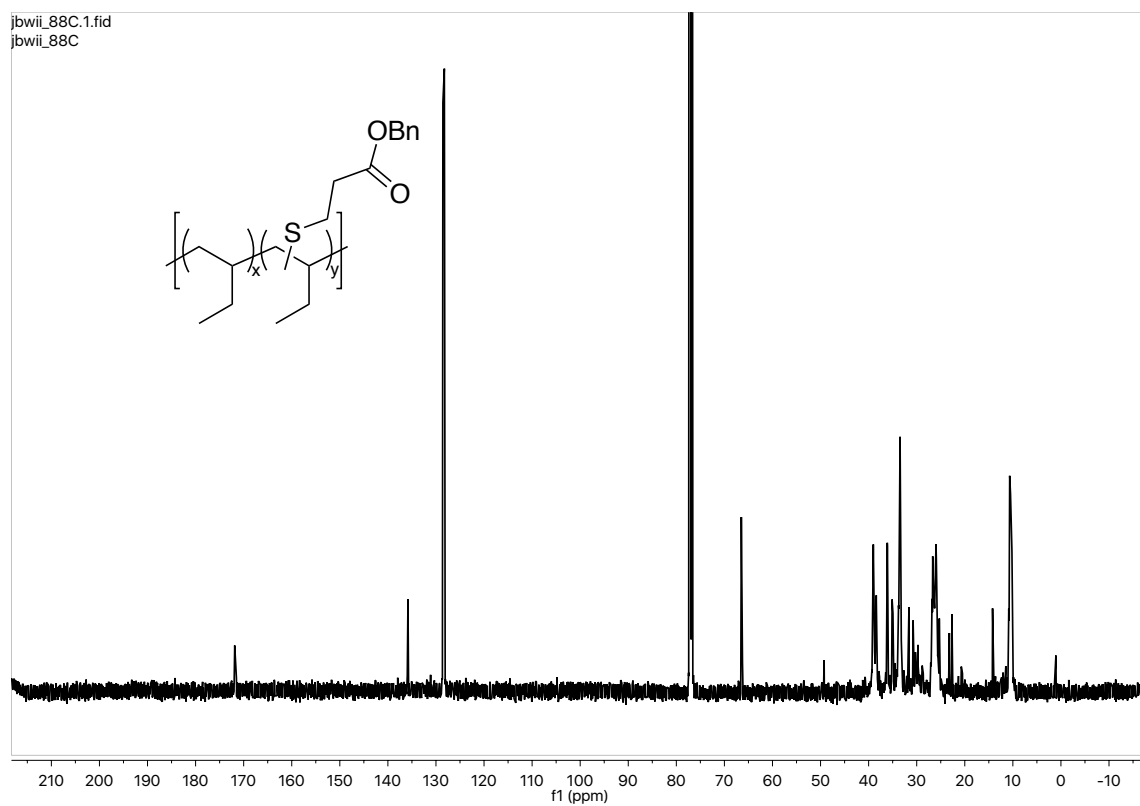
OEt

13% branched

210 200 190 180 170 160 150 140 130 120 110 100 90 80 70 60 50 40 30 20 10 0 -10
ppm

OBn

O

S

x y

| | | | | | | | | | | | | | | | | | | |
.0 8.5 8.0 7.5 7.0 6.5 6.0 5.5 5.0 4.5 4.0 3.5 3.0 2.5 2.0 1.5 1.0 0.5 0.0 -0.5
ppm

jbwii_88C.1.fid
jbwii_88C

OBn

O

S

x y

210 200 190 180 170 160 150 140 130 120 110 100 90 80 70 60 50 40 30 20 10 0 -10
f1 (ppm)

HO OPh

S

f1 (ppm)
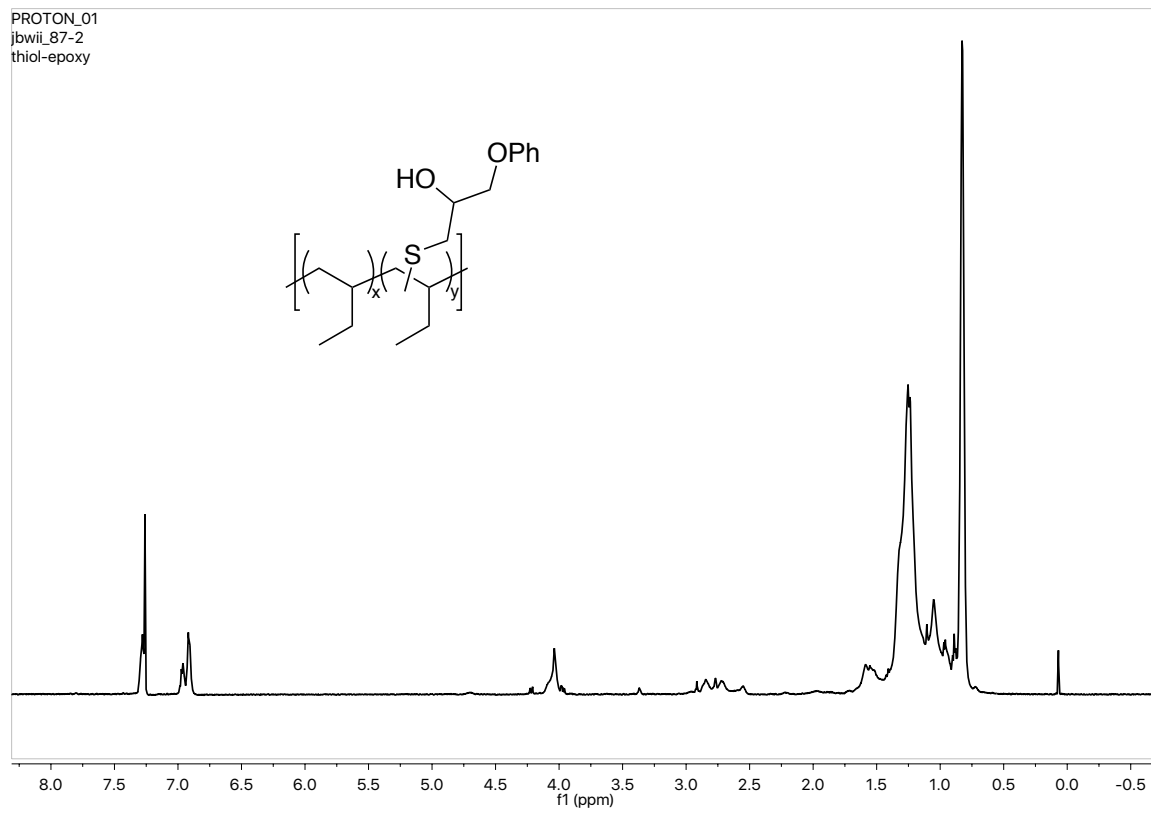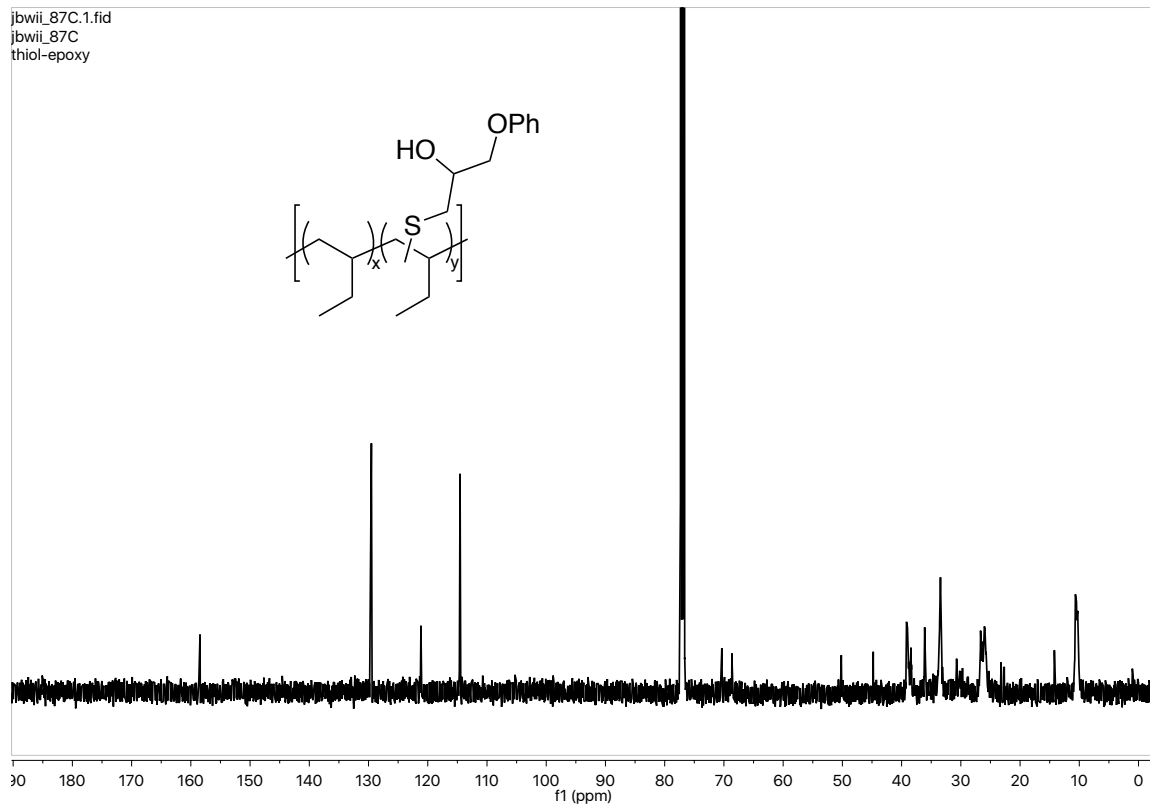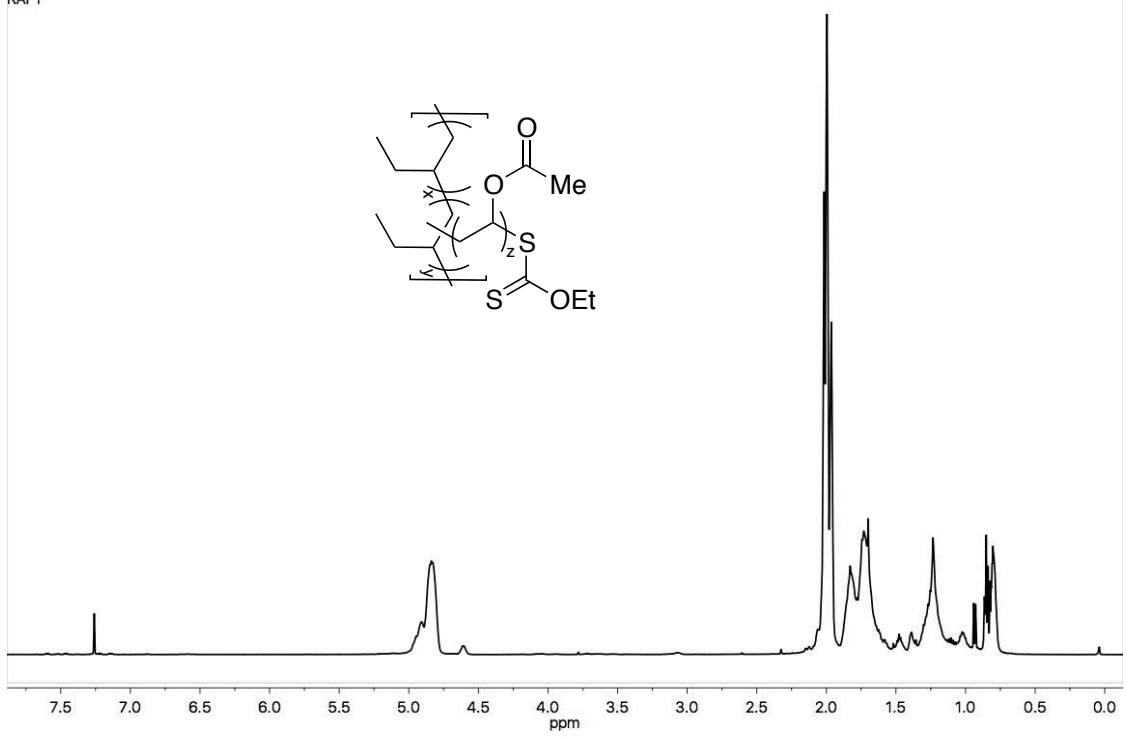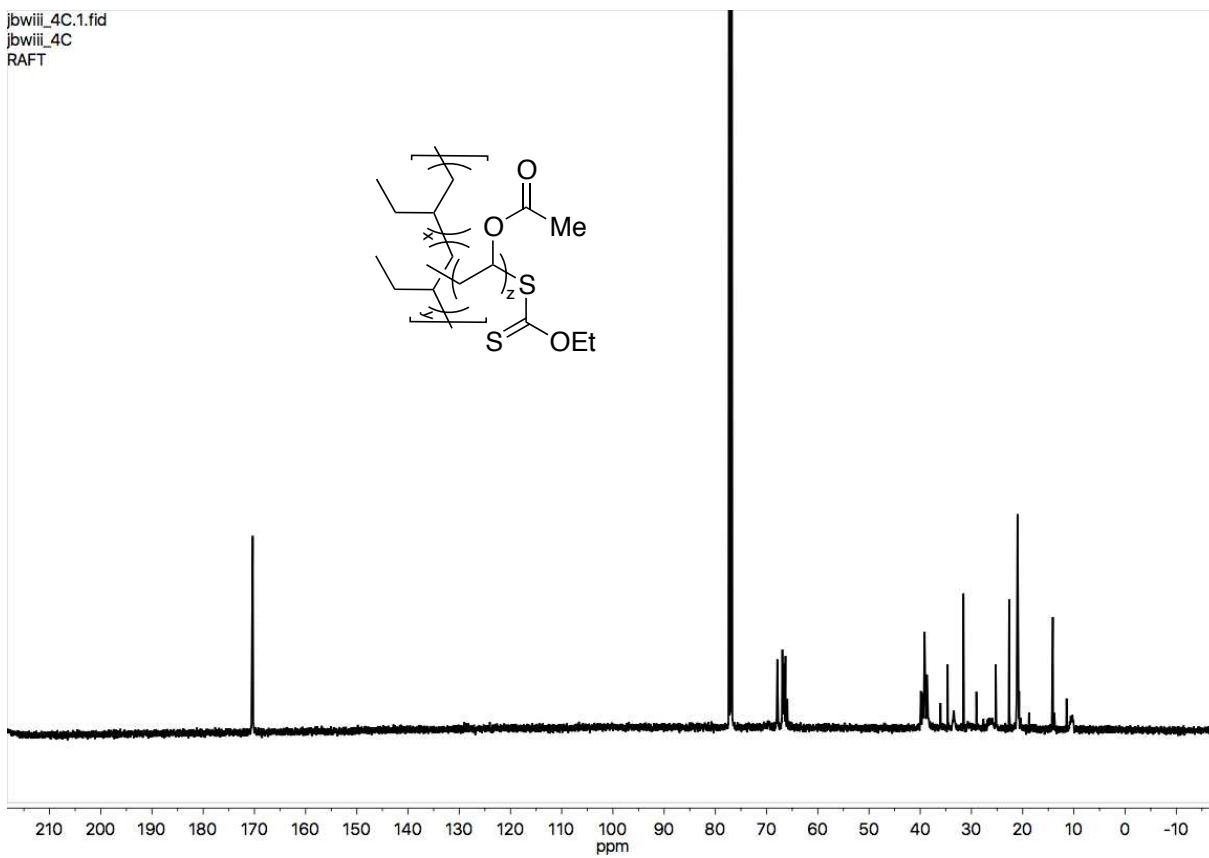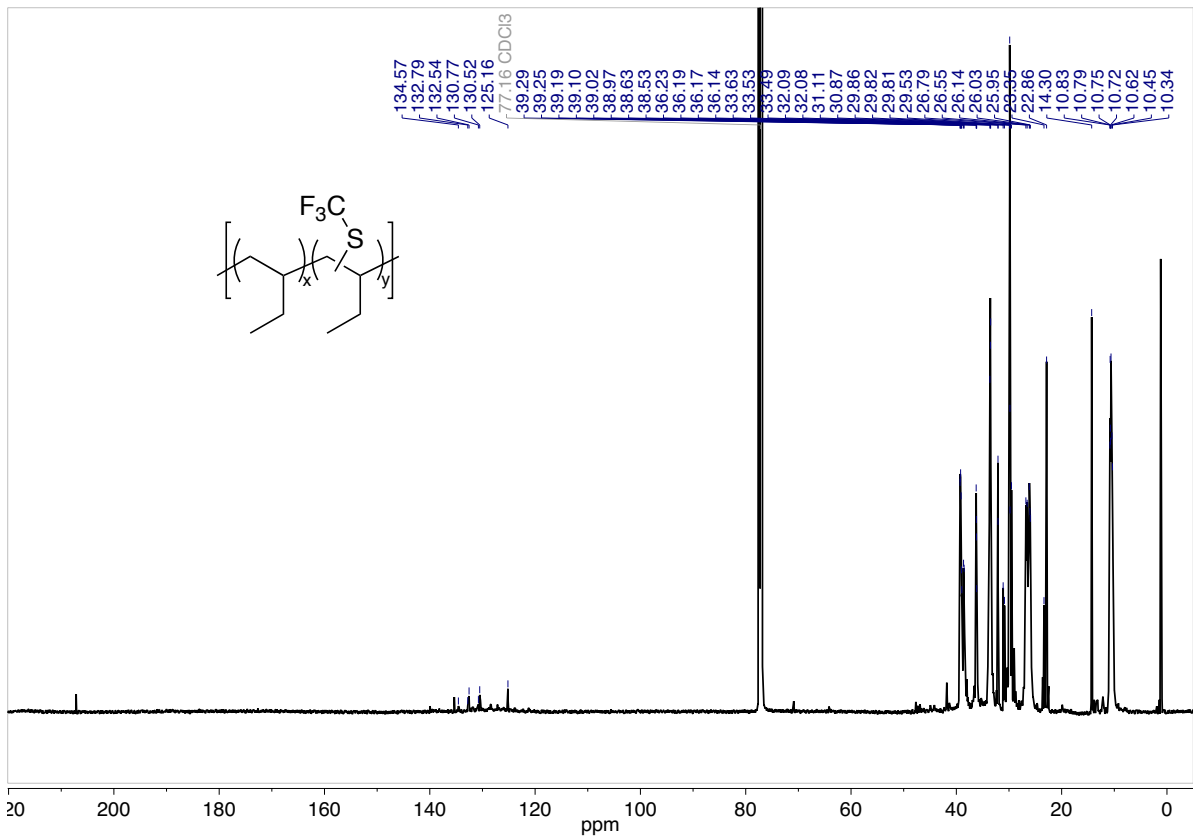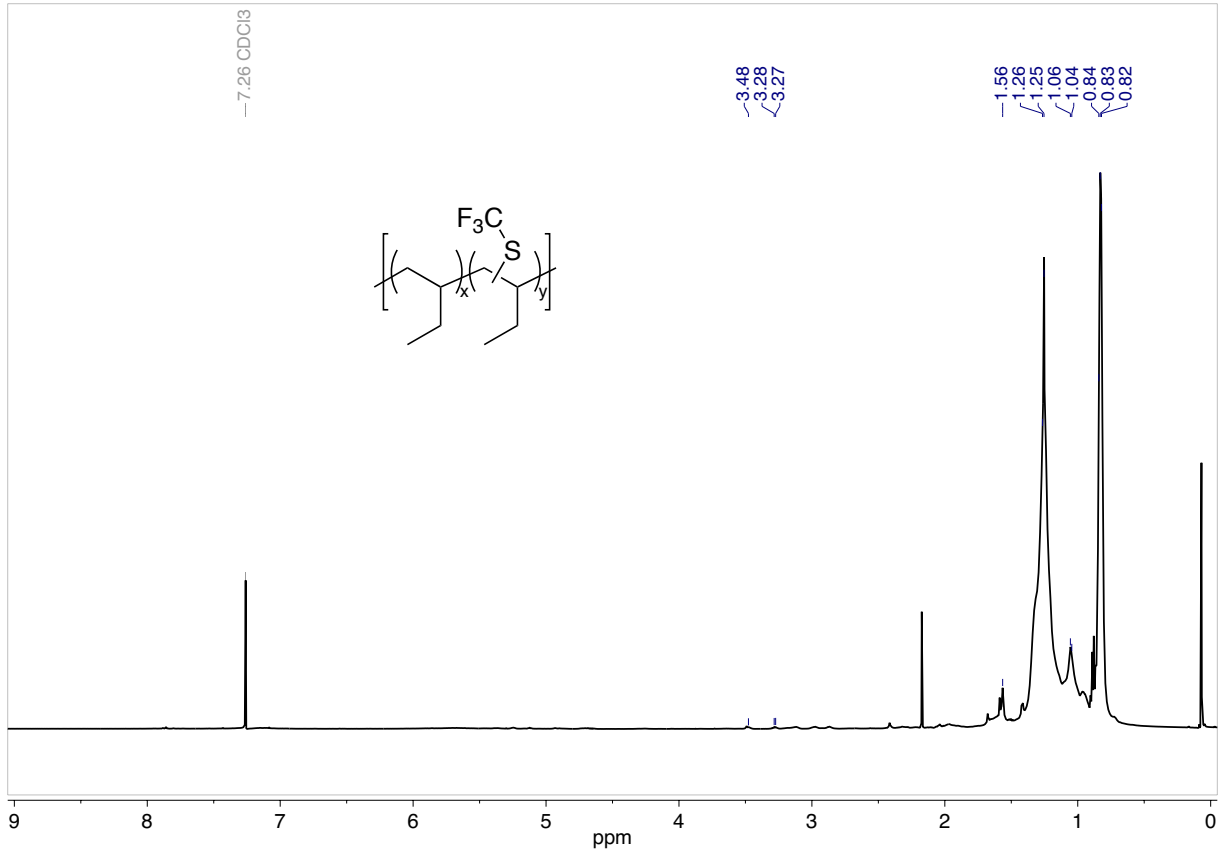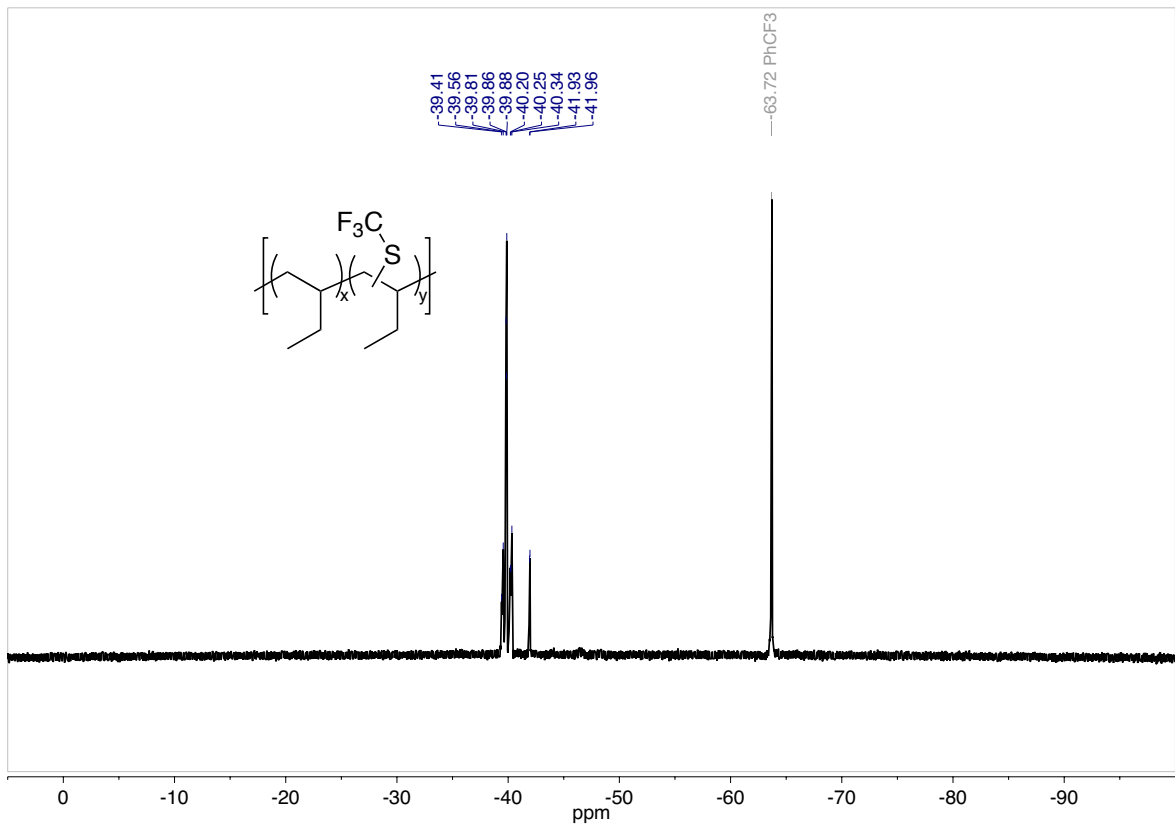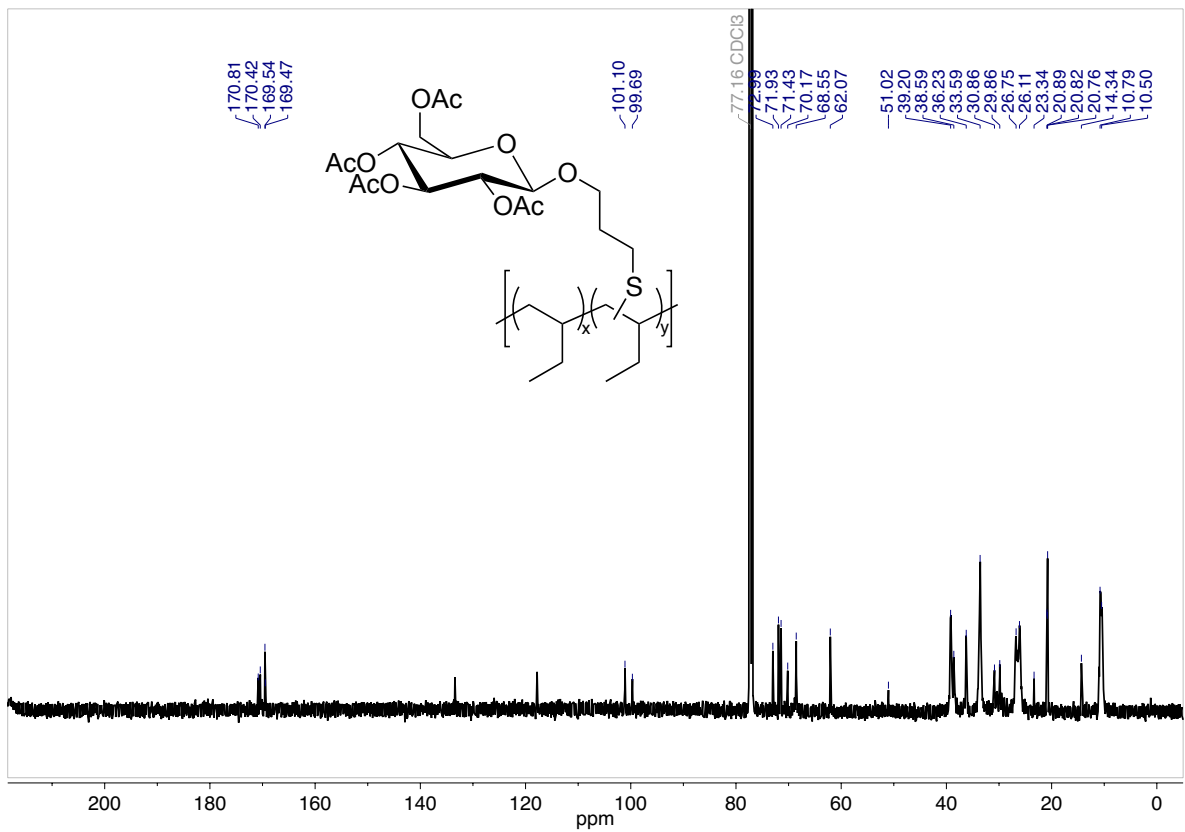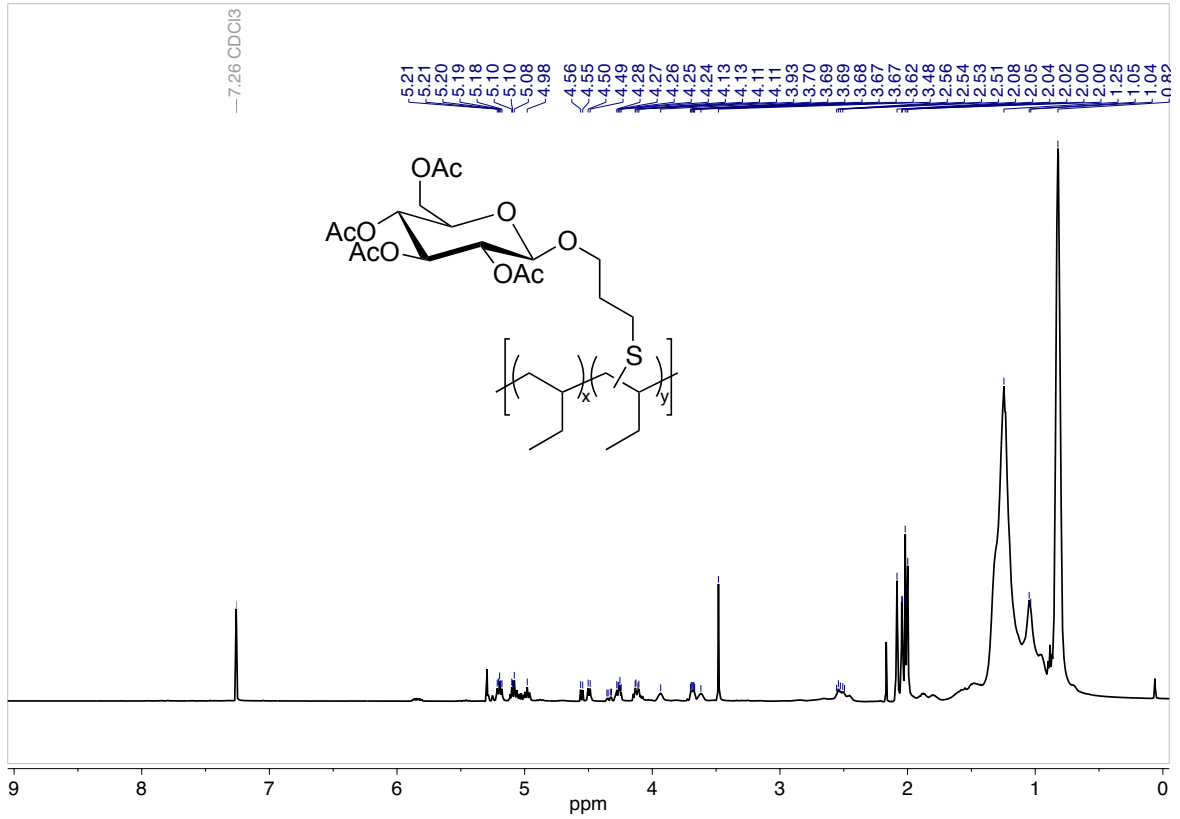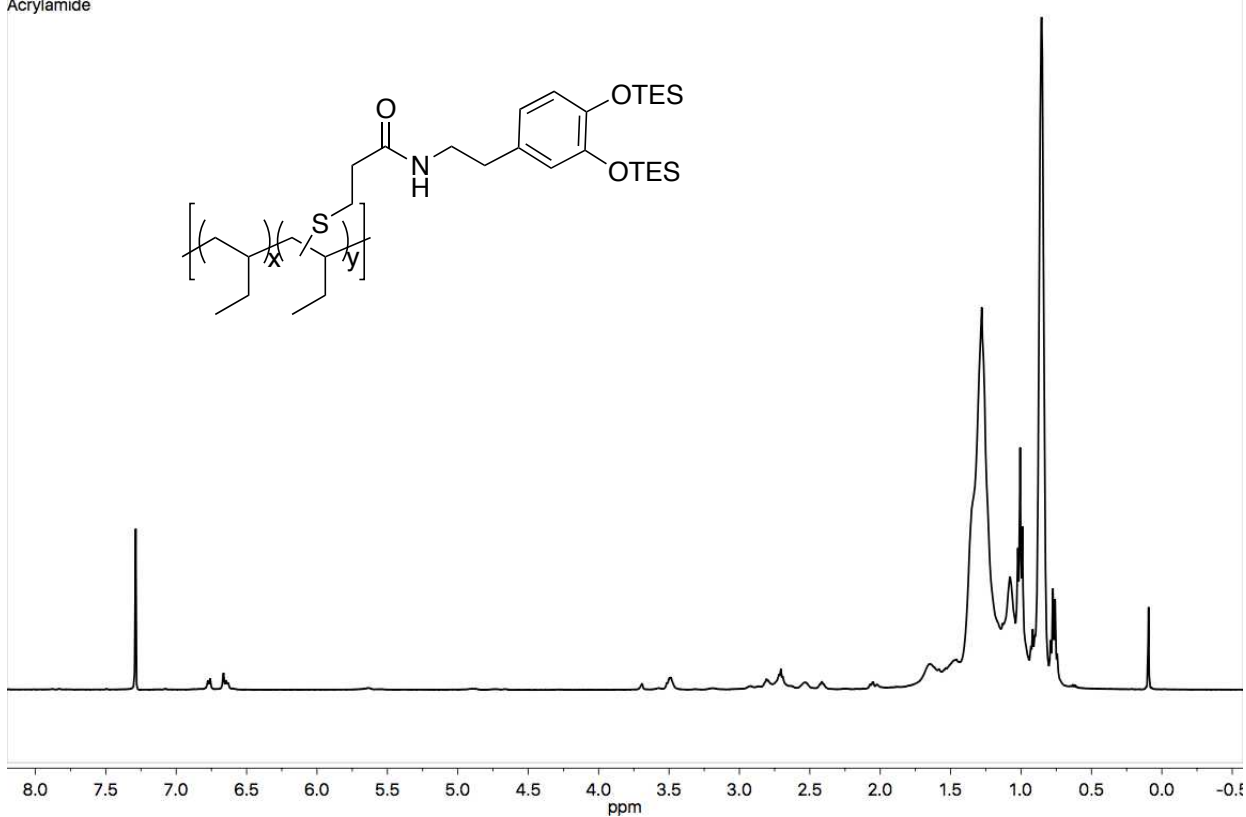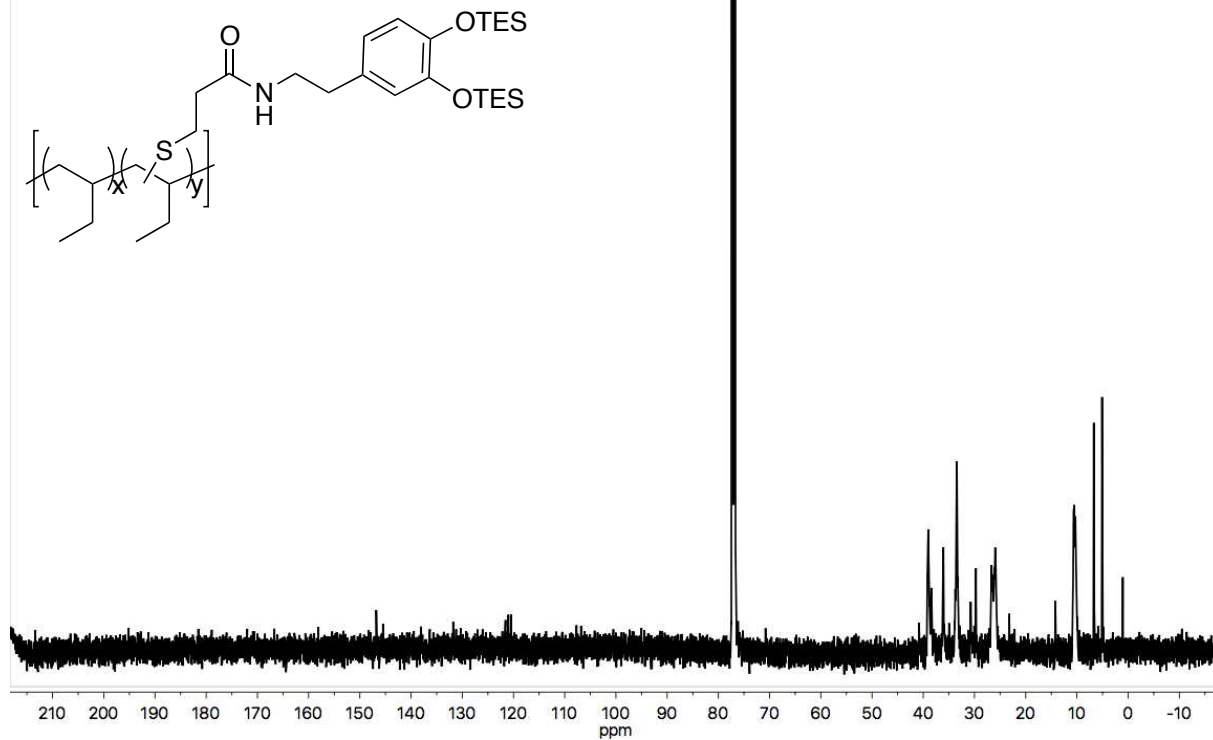
B.1 GENERAL METHODS AND MATERIALS

All post-polymerization modifications were performed under inert atmosphere using standard glove box and Schlenk-line techniques. Xanthylamide[1] and hyperbranched polyethylene (HBPE)[2] were prepared using previously reported methods. Commercial polyolefins were obtained from their respective companies and purified prior to use by precipitation into methanol. The company and lot number are named in the individual procedures. Acetonitrile, diethyl ether, and dichloromethane were dried by passage through a column of neutral alumina under nitrogen prior to use. 1,2-Dichlorobenzene was degassed with argon through multiple freeze-pump-thaw cycles. Chlorobenzene and benzene were distilled over calcium hydride, degassed through three freeze-pump-thaw cycles, and stored in a glove box. Reagents, unless otherwise specified, were purchased and used without further purification.

Proton and carbon magnetic resonance spectra (^{1}H NMR and ^{13}C NMR) were recorded on a Bruker model DRX 400 MHz, Bruker 500 MHz, Varian Inova 600, or Bruker AVANCE III 600 MHz CryoProbe spectrometer with solvent resonance as the internal standard (^{1}H NMR: CDCl$_3$ at 7.26 ppm; ^{13}C NMR: CDCl$_3$ at 77.16 ppm). ^{1}H NMR data are reported as follows: chemical shift, multiplicity (s = singlet, d = doublet, t = triplet, q = quartet, m = multiplet, dd = doublet of doublets, dt = doublet of triplets, bs = broad singlet), coupling constants (Hz), and integration. Infrared (IR) spectra were obtained using PerkinElmer Frontier FT-IR spectrometer. Mass spectra were obtained using a Q Exactive HF-X mass spectrometer with electrospray introduction and external calibration. Thin layer chromatography (TLC) was performed on SiliaPlate 250μm thick silica gel plates provided by Silicycle. Visualization was

accomplished with short wave UV light (254 nm), iodine, aqueous basic potassium permanganate solution, or aqueous acidic ceric ammonium molybdate solution followed by heating. Flash chromatography was performed using SiliaFlash P60 silica gel (40-63 μm) purchased from Silicycle.

Gel permeation chromatography (GPC) spectra were obtained using Waters 2695 separations module liquid chromatograph, Waters 2414 refractive index detector at room temperature, and Waters 2996 photodiode array detector with styragel HR columns. Tetrahydrofuran was the mobile phase and the flow rate was set to 1 mL/min. The instrument was calibrated using polystyrene standards in the range of 580 to 892,800 Da. Commercial polyolefin samples were analyzed at the Center for the Science and Technology Advancement of Materials and Interfaces (STAMI) using a Tosoh EcoSEC-HT (high temperature) GPC with refractive index detection against polystyrene standards in 1 mg/mL solutions of trichlorobenzene (TCB) at 120 °C.

Differential scanning calorimetry (DSC) was used to determine the thermal characteristics of the polyolefins and graft copolymers using a TA Instruments DSC (Discovery Series). The DSC measurements were performed on 1 – 10 mg of polymer samples at a temperature ramp rate of 10 °C/min. Data was taken from the second thermal scanning cycle. Thermal gravimetric analysis (TGA) was obtained using a TA Instruments TGA (Discovery Series) in the temperature range of 40 – 600 °C at a temperature ramp rate of 10 °C/min. Irradiation of xanthylation reactions was performed using Kessil KSH150B Blue 36W LED Grow Lights.

B.2 ADDITIONAL DATA

Dithiocarbamylation of hyperbranched polyethylene:
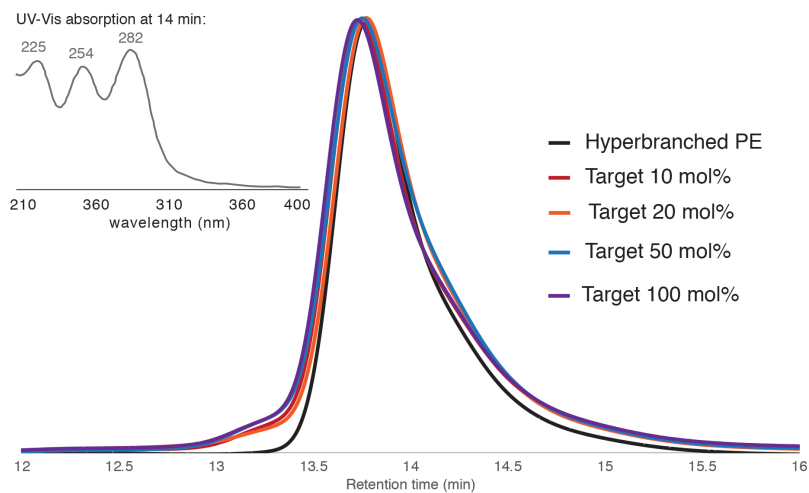
UV-Vis absorption at 14 min:

- Hyperbranched PE
- Target 10 mol%
- Target 20 mol%
- Target 50 mol%
- Target 100 mol%

Trithiocarbonylation of hyperbranched polyethylene:

UV-Vis absorption at 14 min:

- Hyperbranched PE
- Target 10 mol%
- Target 20 mol%
- Target 50 mol%
- Target 100 mol%

Xanthylation of hyperbranched polyethylene:

UV-Vis absorption at 29 min:

- Hyperbranched PE
- Target 10 mol%
- Target 20 mol%
- Target 50 mol%
- Target 100 mol%
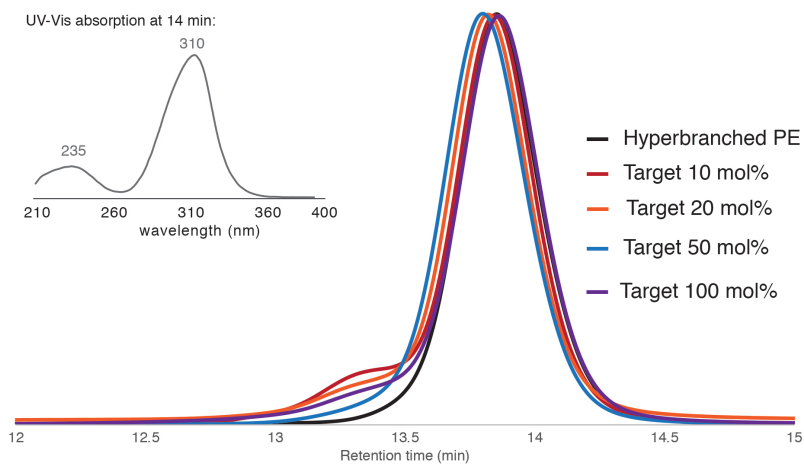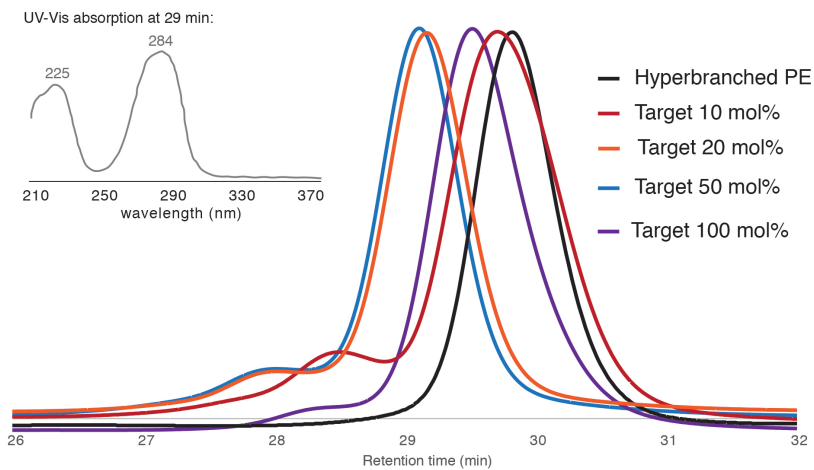
Gel permeation chromatography with tandem photodiode array (PDA) detector monitored the eluent polymers upon functionalization. The UV-Vis spectra (inset) reinforces that the polymers are indeed functionalized with dithiocarbamate (absorptions of 254 and 282 nm)[3], trithiocarbonate (absorption of 310 nm)[4], and xanthate (absorption of 284 nm)[4]. The size exclusion chromatograph depicts larger changes in molecular weight and dispersity in higher loadings of xanthylamide than in higher loadings of trithiocarbonylamide and diethyl dithiocarbamylamide. A small, high molecular weight species is observed during trithiocarbonylation, but it is diminished when more equivalents of trithiocarbonylamide are added. Hardly any change in molecular weight distribution is observed when changing the stoichiometry of diethyl dithiocarbamylamide and repeat unit; however, in all reactions, a small shoulder at shorter retention times was present. For quantitative values for the molecular weight and dispersity, see Table 3.1 in the main text.
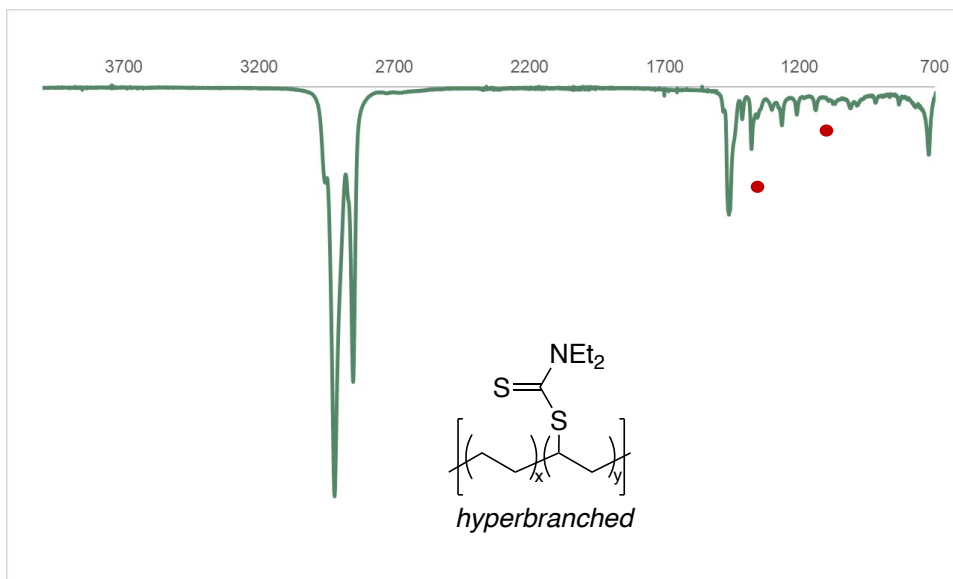
Infrared spectroscopy of dithiocarbamylated HBPE reveals key absorptions at 1265 and 1069 cm^{-1}.[5] The 1450 – 1550 cm^{-1} stretch associated with R_2N–CS_2 was not visible at low degrees of

functionalization. The 1265 peak reflects the C=S bond character present. The C–N bond is visible by the absorption at 1069 cm^{-1}.
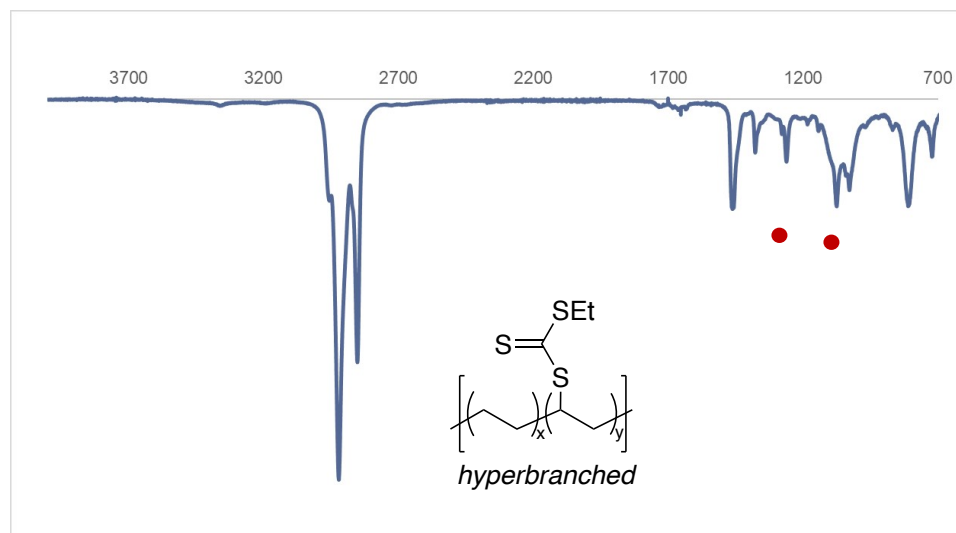
Infrared spectroscopy of trithiocarbonylated HBPE displays with key absorptions at 1262 and 1076 cm^{-1}, consistent with the literature.[4]
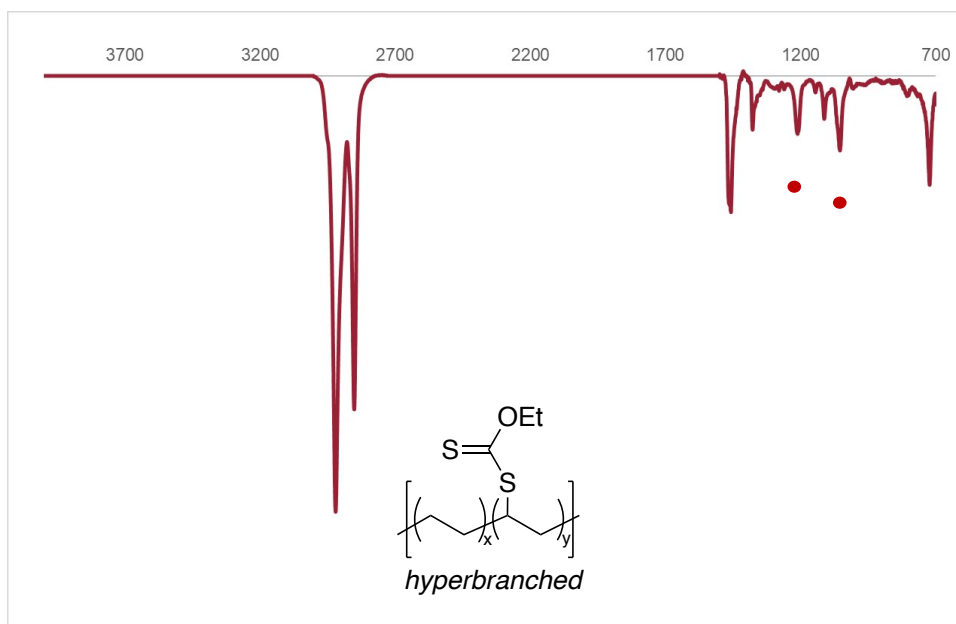
Infrared spectroscopy of xanthylated HBPE contains key peaks at 1212 and 1054 cm^{-1}.[4] This spectra is identical to those reported for photochemical initiation.[6]

B.3 SYNTHESIS OF AMIDYL REAGENTS
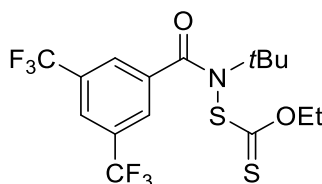
N-(tert-butyl)-N-((ethoxycarbonothioyl)thio)-3,5-bis(trifluoromethyl)benzamide was prepared as described from a previous report.[1]
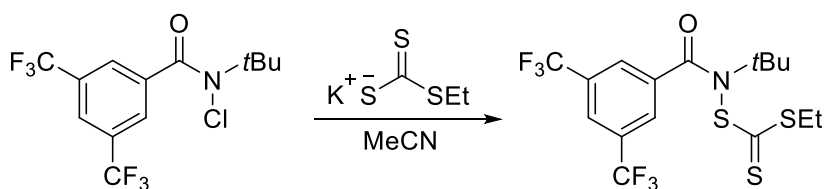
N-(tert-butyl)-N-(((ethylthio)carbonothioyl)thio)-3,5-bis(trifluoromethyl)benzamide: With the laboratory and hood lights off, potassium ethyl carbonotrithioate[7] (9.70 g, 55.0 mmol) was suspended in MeCN (2.5 L) in a 5 L round-bottomed flask. To this suspension was added a solution of *N*-chloroamide[1] (19.1 g, 55.0 mmol) in MeCN (500 mL) via cannula wire over 20 min. The flask was foil wrapped and stirred for 16 h, at which point the suspension was concentrated *in vacuo*. The residue was taken up in CH$_2$Cl$_2$/H$_2$O (1:1, 1 L total volume), and the layers were separated. The organic layer was washed with brine, dried with MgSO$_4$, and concentrated *in vacuo*. The resultant yellow mixture was purified by careful flash column chromatography (1 – 5% EtOAc in hexanes) to afford *N*-trithiocarbonylamide as a bright yellow solid (6.67 g, 27% yield):

¹H NMR (600 MHz, CDCl₃) δ 7.92 – 7.90 (m, 2H), 7.85 (dt, J = 2.0, 1.0 Hz, 1H), 3.40 – 3.24 (m, 2H), 1.66 (s, 9H), 1.31 (t, J = 7.4 Hz, 3H). **¹³C NMR (151 MHz, CDCl₃)** δ 226.46, 172.74, 140.06, 131.31 (q, J = 33.7 Hz), 126.66 (d, J = 3.9 Hz), 125.75 (q, J = 273.4 Hz), 123.45 (p, J = 3.9 Hz), 65.40, 30.98, 29.42, 12.96. **HRMS (ES+)** Exact mass calcd for $C_{16}H_{18}F_6NOS_3$ [M+H]⁺ 450.04547. Found 450.0440.
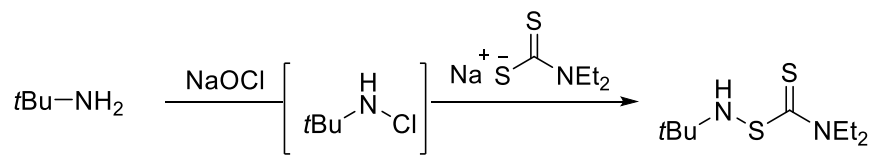
N-(((tert-butylamino)thio)carbonothioyl)-N-ethylethanamine: Adapted from an analogous literature procedure.[8] *Tert*-butylamine (37 mL, 0.35 mol) was treated with sodium hypochlorite (230 mL, ~1.5 M in H₂O from Sigma Aldrich) at 0 °C. After 5 to 10 minutes of stirring, a solution of sodium diethylcarbamodithioate trihydrate (67.6 g, 0.30 mol, 2.0 M in H₂O) was added dropwise, and the reaction mixture was allowed to come to room temperature overnight. The mixture was diluted with water and Et₂O, and the layers were separated. The aqueous phase was extracted twice with Et₂O, and the combined organic phase was washed with brine, dried over anhydrous MgSO₄, filtered, and concentrated *in vacuo*. The crude mixture was purified by column chromatography (2.5 to 5% EtOAc/hex) to give the thiocarbamylsulfenamide (10.89 g, 16% yield).

Warning: Rapid addition of the salt solution can cause an exotherm and gas evolution resulting from the decomposition of the reagents.

¹H NMR (600 MHz, CDCl₃) δ 4.11 (s, 1H), 3.99 (q, *J* = 7.1 Hz, 2H), 3.66 (q, *J* = 7.0 Hz, 2H), 1.32 – 1.22 (m, 6H), 1.14 (s, 9H). **¹³C NMR (151 MHz, CDCl₃)** δ 203.52, 50.14, 45.63, 29.08, 28.94, 12.93, 12.91, 11.81. **HRMS (ES+)** Exact mass calcd for $C_9H_{21}N_2S_2$ [M+H]⁺, 221.1146. Found 221.1137.
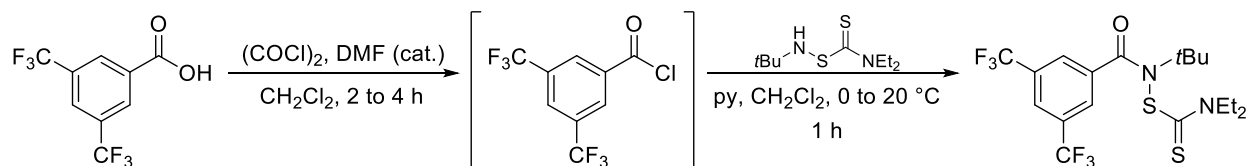
3,5-bis(trifluoromethyl)benzoyl chloride: To a solution of 3,5-bis(trifluoromethyl)benzoic acid (12.9 g, 50.0 mmol) in CH₂Cl₂ (125 mL) at 0 °C was added oxalyl chloride (4.8 mL, 55.0 mmol) dropwise followed by 1 to 2 drops of DMF. The resulting solution was stirred for 2-4 h and then concentrated to remove excess oxalyl chloride to give the acid chloride in quantitative yield, which was used without further purification.

N-(tert-butyl)-N-((diethylcarbamothioyl)thio)-3,5-bis(trifluoromethyl)benzamide: N-(((tert-butylamino)thio)carbonothioyl)-*N*-ethylethanamine (6.61 g, 30.0 mmol) was charged to a round-bottomed flask with a stir bar and was dissolved in CH₂Cl₂ (100 mL). Pyridine (4.0 mL, 50.0 mmol) was added dropwise at 0 °C, followed by a solution of the benzoyl chloride (2 M in CH₂Cl₂). The reaction mixture was allowed to warm to room temperature and was stirred until completion as determined by GC-MS (1-2 h). The reaction mixture was diluted with CH₂Cl₂ and washed with water. The aqueous layer was extracted with CH₂Cl₂ (x 2). The combined organic phase was then washed with 2 M NaOH solution and brine, then dried over anhydrous MgSO₄. The solid was filtered, and the filtrate was concentrated *in vacuo*. The

resulting residue was purified by flash column chromatography on silica (2.5 – 5% EtOAc in hexanes) to afford *N*-diethyldithiocarbamyl amide as a white solid (12.3 g, 89% yield).

¹H NMR (600 MHz, CDCl₃) δ 8.00 – 7.97 (m, 2H), 7.79 – 7.77 (m, 1H), 3.88 (s, 1H), 3.77 (s, 1H), 3.39 (s, 1H), 3.29 (s, 1H), 1.64 (s, 9H), 1.14 (s, 3H), 0.94 (s, 3H). **¹³C NMR (151 MHz, CDCl₃)** δ 195.81, 173.79, 141.02, 130.64 (q, *J* = 33.6 Hz), 126.69 (d, *J* = 3.9 Hz), 122.34 (p, *J* = 3.8 Hz), 64.72, 50.65, 45.85, 29.54, 12.62, 11.28. **HRMS (ES+)** Exact mass calcd for $C_{18}H_{23}F_6N_2OS_2$ [M+H]⁺, 461.1156. Found 461.1139.

B.4 SYNTHESIS OF FUNCTIONALIZED CYCLOOCTANES

General Procedure I (product functionalization using light initiation): A 1-dram vial was charged with an amidyl reagent (0.15 mmol, 1.0 equiv) and trifluorotoluene (0.15 mL) in an argon-filled glovebox. The vial was fitted with a PTFE-lined screw cap, sealed with Teflon tape, and removed from the glovebox. Cyclooctane (14 μL, 0.15 mmol, 1.0 equiv) was added by syringe. The vial was suspended above an Ecoxotic PAR38 23 W blue LED such that the bottom of each vial was directly aligned with and 1 cm above one of the five LEDs, and the apparatus was covered with aluminum foil. The reaction was irradiated for 15 h, and then was concentrated *in vacuo* and analyzed by ¹H NMR.

General Procedure II (product functionalization using heat and initiator):

A 1-dram vial equipped with a stir bar was charged with an amidyl reagent (0.15 mmol, 1.0 equiv), dicumyl peroxide (4.1 mg, 0.015 mmol, 0.10 equiv), and chlorobenzene (0.30 mL) in an argon-filled glovebox. The vial was fitted with a PTFE lined screw cap, sealed with Teflon

tape, and removed from the glovebox. Cyclooctane (14 μL, 0.15 mmol, 1.0 equiv) was added by syringe. The vial was placed on a block plate at 130 °C to stir overnight. Upon completion, the reaction was concentrated *in vacuo* for 15 h, and then was concentrated *in vacuo* and analyzed by ^{1}H NMR.
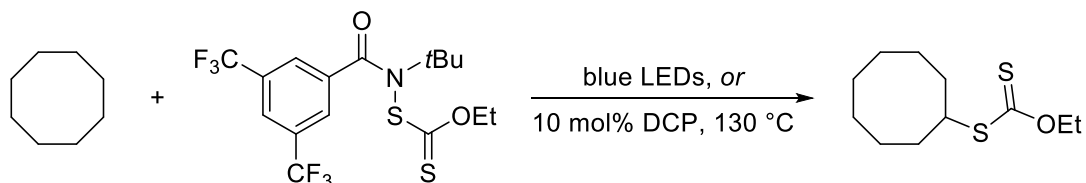
S-cyclooctyl O-ethyl carbonodithioate: Prepared according to General Procedures I and II using *N*-xanthylamide, giving 85% and 66% NMR yield, respectively.
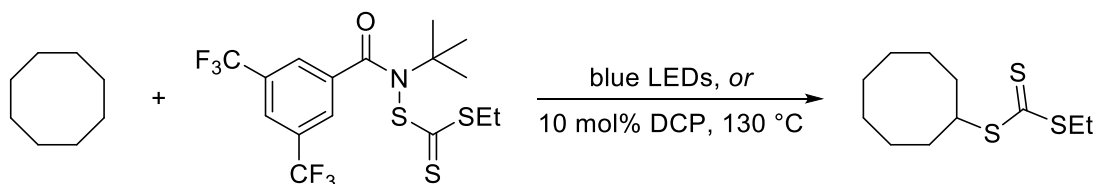
Cyclooctyl ethyl carbonotrithioate: Prepared according to General Procedures I and II, giving 48% and 47% NMR yield, respectively. An analytical sample was obtained after purification by column chromatography (2.5% EtOAc in hexanes).

^{1}**H NMR (600 MHz, CDCl$_3$)** δ 4.29 (tt, *J* = 9.5, 3.9 Hz, 1H), 3.34 (q, *J* = 7.4 Hz, 2H), 2.05 (ddt, *J* = 14.4, 8.9, 3.6 Hz, 2H), 1.79 (dddd, *J* = 14.5, 9.4, 8.4, 3.0 Hz, 2H), 1.75 – 1.66 (m, 2H), 1.66 – 1.50 (m, 8H), 1.34 (t, *J* = 7.4 Hz, 3H).^{13}**C NMR (151 MHz, CDCl$_3$)** δ 224.06, 51.03, 31.77, 31.04, 26.98, 26.06, 25.52, 13.24. **HRMS (ES+)** Exact mass calcd for C$_{11}$H$_{20}$S$_3$Na [M+Na]$^+$, 271.0625. Found 271.0628.
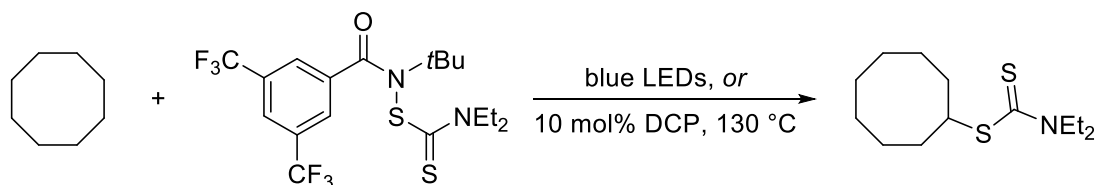
Cyclooctyl diethylcarbamodithioate: Prepared according to General Procedures I and II, giving 11% and 42% NMR yield, respectively. An analytical sample was obtained after purification by column chromatography (2.5% EtOAc in hexanes).

¹H NMR (600 MHz, CDCl₃) δ 4.14 (tt, J = 9.5, 4.0 Hz, 1H), 4.00 (q, J = 7.1 Hz, 2H), 3.71 (q, J = 7.1 Hz, 2H), 2.09 (ddt, J = 14.4, 9.0, 3.6 Hz, 2H), 1.79 (dddd, J = 14.4, 9.5, 8.2, 3.0 Hz, 2H), 1.74 – 1.67 (m, 2H), 1.67 – 1.55 (m, 6H), 1.55 – 1.48 (m, 2H), 1.25 (t, J = 7.1 Hz, 6H).**¹³C NMR (151 MHz, CDCl₃)** δ 195.76, 51.68, 49.13, 46.73, 32.38, 27.16, 26.08, 25.62, 12.50, 11.76. **HRMS (ES+)** Exact mass calcd for $C_{13}H_{26}NS_2$ [M+H]⁺, 260.1507. Found 260.1496.

B.5 SYNTHESIS OF FUNCTIONALIZED POLYOLEFINS

General Procedure A (amorphous reactions): The required amount of polyolefin, amidyl reagent, peroxide, and chlorobenzene were added to a 1-dram reaction vial equipped with a magnetic stir bar under inert atmosphere. The reaction vial was sealed and placed on a magnetic stir plate in a pie block to stir for 30 min, ensuring complete dissolution of the polymer prior to heating. The temperature was set to 130 °C and the reaction mixture was heated for 6 to 19 hours, depending on the reagent loading (see Table B.1). After the reaction was complete, the solution was concentrated *in vacuo* and precipitated in cold methanol to yield the functionalized HBPE as a viscous liquid.

General Procedure B (semi-crystalline reactions): The required amount of polyolefin was pre-dissolved in half the total volume of solvent by heating the solution for 30 min above the material's melting temperature with magnetic stirring. The pre-dissolved polyolefin, amidyl reagent, and peroxide were then combined in a 1-dram reaction vial and diluted with the other half volume of solvent in a nitrogen-filled glovebox. The vial was equipped with a magnetic stir bar under inert atmosphere and sealed with electrical tape. The reaction was heated and stirred on a magnetic stir plate at the desired temperature. After completion of the reaction, the solution was precipitated into methanol to yield the functionalized commodity polyolefins as a fluffy, whitish yellow powder.

General Procedure C (neat reactions): The required amount of polyolefin, amidyl reagent, and peroxide were added to a reaction vial. The reagents were dissolved in dry dichloromethane to ensure sufficient mixing of the peroxide and amidyl reagent. Dichloromethane was removed *in vacuo* by rotary evaporation and then high vacuum on a double manifold Schlenk line. The reaction vial was backfilled with nitrogen after 20 min of sufficient vacuum and sealed with electrical tape. The reaction vial was heated and stirred on a magnetic stir plate in a pie block set to the desired temperature (130 or 180 °C). After completion of the reaction, the mixture was cooled to room temperature. Precipitation from dichlorobenzene at 180 °C into methanol yielded pure functionalized polyolefin.
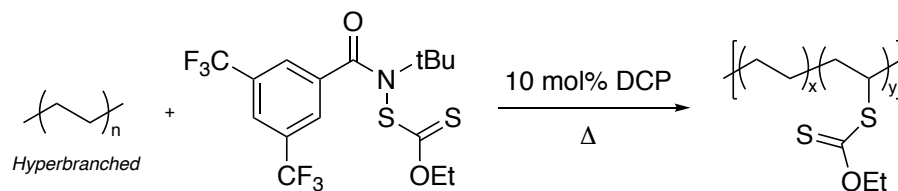
Xanthylated HBPE: HBPE, xanthylamide, and dicumyl peroxide were reacted according to General Procedure A and C. HBPE (M_n = 27 kg/mol, Đ = 1.04, 10% branched, 40 mg, 1.43 mmol) reacted with xanthylamide (8 mg, 0.018 mmol) and dicumyl peroxide (0.5 mg, 0.002 mmol) in chlorobenzene (0.1 mL) upon heating at 130 °C for 1 h. The resultant material was 1 mol% xanthylated HBPE. Similar characterization data was obtained using other stoichiometric ratios of xanthylamide to repeat unit (see Table B.1 for exact conditions). See accompanying tables and figures for more information. This material was previously characterized in another paper via blue light irradiation.[6]

The following was gathered using 1 mol% xanthylated HBPE:

¹H NMR (500 MHz, CDCl₃) δ 4.67 (m), 3.73 (bs), 1.68 (bs), 1.61 (bs), 1.57 (bs), 1.28 (bs), 1.24 (bs), 1.10 (bs), 0.91 (bs) 0.87 (bs), 0.85 (bs). **IR (neat, ATR, cm⁻¹)** 2920, 2852, 1457, 1377, 1212, 1063, 1054, 723. **GPC (THF)** M_n = 28 kg/mol, Đ = 1.04; UV-Vis at 14 min = 228, 283 nm. **TGA (°C)** T_d = 4 wt% lost at 252 °C with terminal onset at 412 °C. **UV-Vis (nm):** 225, 283. **DSC (°C):** parent T_g = –69, product T_g = –67.

Determination of percent functionalization of HBPE: Upon purification, the percent xanthylation of HBPE can be determined through integration of the ¹H NMR. Considering the composition of the polymer, the peaks between 0.8 – 2.0 ppm were set to total to 4 protons. The methylene protons of the ethoxy group that appear at 4.7 ppm are used to determine mol%

xanthylation per repeat unit. Regioselectivity was determined by integration of the two signals corresponding to primary and secondary xanthylation. For instance, protons *alpha* to primary xanthates appear between 3.0 – 3.5 ppm and protons *alpha* to secondary xanthates appear between 3.5 – 4.0 ppm.
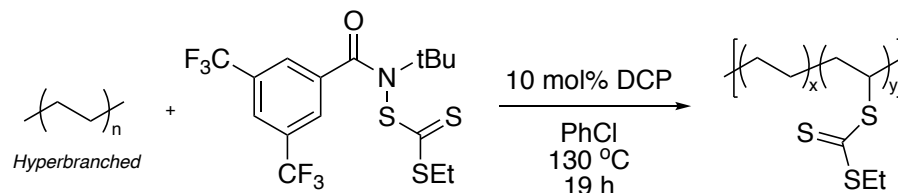
Trithiocarbonylated HBPE: HBPE (M_n= 32 kg/mol, $Đ$ = 1.07, mg, 1.07 mmol repeat unit, 10% branched), trithiocarbonylamide (96 mg, 0.214 mmol), and dicumyl peroxide (6 mg, 0.0214 mmol) were reacted according to General Procedure A in chlorobenzene (1.0 mL). The solution was stirred and heated at 130 °C for 19h. The polymer was purified via precipitation in cold methanol to yield 32 mg of 3 mol% trithiocarbonylated polyolefin. Similar characterization data was obtained using other stoichiometric ratios of trithiocarbonylamide to repeat unit. See accompanying tables and figures for more information.

The following was gathered for 3 mol% trithiocarbonylated HBPE:

¹H NMR (400 MHz, CDCl₃) δ 4.30 (bs), 4.21 (bs), 3.38 (q, J = 7.3 Hz), 1.69 (bs), 1.56 (bs), 1.37 (bs), 1.28 (bs), 1.24 (bs), 1.11 (bs), 0.91 (bs), 0.87 (bs), 0.86 (bs). **¹³C NMR (125 MHz, CDCl₃)** δ 52.2, 46.8, 38.9, 37.2, 34.4, 33.7, 32.0, 31.0, 29.8, 26.8, 25.9, 22.7, 19.8, 19.3, 14.2, 13.1, 10.9, 1.04. **IR (neat, ATR, cm⁻¹)** 2921, 2853, 1458, 1378, 1262, 1076, 1028, 809, 721.

GPC (THF) M_n = 39 kg/mol, $Đ$ = 1.08; UV-Vis at 14 min = 212, 234, 308 nm. **TGA (°C)** T_d = 10 wt% lost at 243 °C and terminal onset at 436 °C. **DSC (°C)** parent T_g = –69, product T_g = –67.

Determination of percent functionalization of HBPE: Upon purification, the percent trithiocarbonylation of HBPE can be determined through integration of the ^{1}H NMR. Considering the composition of the polymer, the peaks between 0.8 – 2.0 ppm were set to total to 4 protons. The methylene protons of the thioethoxy unit that appear at 3.4 ppm are used to determine mol% functionalization per repeat unit. Regioselectivity could not be determined as the functionalization peaks overlap in resonance with the primary trithiocarbonylation signal. Protons *alpha* to secondary trithiocarbonates appear between 4.2 – 4.3 ppm and estimate to encompass roughly 80% of functionalization.
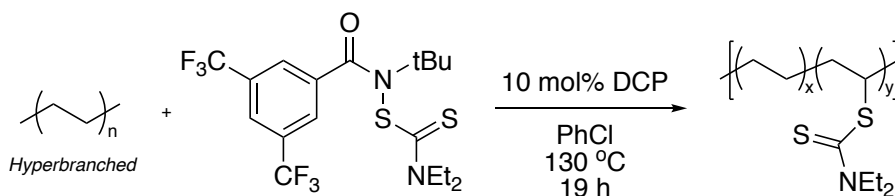
Diethyl Dithiocarbamylated HBPE: HBPE (M_n = 32 kg/mol, $Đ$ = 1.07, 50 mg, 1.79 mmol repeat unit, 10% branched), diethyl dithiocarbamylamide (409 mg, 0.89 mmol), and dicumyl peroxide (24 mg, 0.089 mmol) were reacted according to General Procedure A in dry chlorobenzene (4.5 mL). The mixture was stirred and heated at 130 °C for 19h. The polymer was purified via precipitation in cold methanol to yield 43 mg of 1 mol% dithiocarbamylated polyolefin. Similar characterization data was obtained using other stoichiometric ratios of

dithiocarbamylamide to repeat unit. See accompanying tables and figures for more information.

The following was gathered for 1 mol% dithiocarbamylated HBPE:

¹H NMR (400 MHz, CDCl₃) δ 4.05 (q, J = 7.4 Hz), 3.77 (q, J = 6.2 Hz), 1.71 (bs), 1.58 (bs), 1.28 (bs), 1.24 (bs), 1.11 (bs), 0.92 (bs), 0.91 (bs), 0.89 (bs), 0.87 (bs), 0.86 (bs), 0.84 (bs). **¹³C NMR (125 MHz, CDCl₃)** δ 49.2, 46.6, 39.2, 38.9, 37.7, 37.4, 37.2, 37.1, 36.8, 36.7, 36.1, 34.9, 34.4, 34.1, 33.7, 33.4, 33.2, 32.8, 32.4, 32.0, 32.0, 30.9, 30.7, 30.5, 30.2, 30.1, 30.1, 29.9, 29.8, 29.8, 29.7, 29.5, 29.4, 29.0, 27.6, 27.5, 27.2, 26.8, 26.4, 25.9, 25.5, 24.1, 23.7, 23.2, 23.1, 22.8, 22.7, 19.8, 19.7, 19.3, 14.6, 14.2, 14.2, 12.5, 11.7, 11.5, 10.9, 10.9, 1.0. **IR (neat, ATR, cm⁻¹)** 2921, 2852, 1462, 1378, 1265, 1211, 1139, 1069, 989, 921, 917, 832, 722. **GPC (THF)** M_n = 36 kg/mol, $Đ$ = 1.09; UV-Vis at 14 min = 228, 254, 282 nm. **TGA (°C)** T_d = 4 wt% lost at 229 °C with terminal onset at 409 °C. **DSC (°C)** parent T_g = –69, product T_g = –66.

Determination of percent functionalization of HBPE: Upon purification, the percent dithiocarbamylation of HBPE can be determined through integration of the ¹H NMR. Considering the composition of the polymer, the peaks between 0.8 – 2.0 ppm were set to total to 4 protons. The methylene protons of the diethyl amine unit appear as rotamers at 3.8 and 4.0 ppm and were used to determine mol% functionalization per repeat unit. Regioselectivity could not be determined as the functionalization peaks overlap in resonance with secondary carbon functionalization signals and the overall percent functionalization was too low to observe good signal-to-noise ratios.
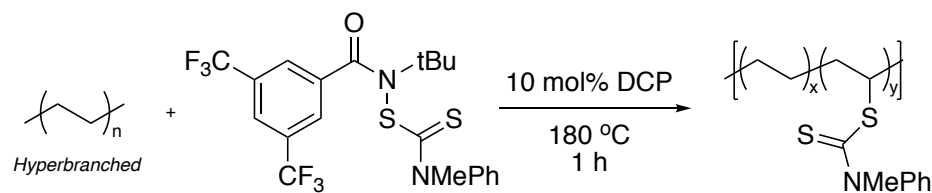
Methyl Aniline Dithiocarbamylated HBPE: HBPE (M_n = 27 kg/mol, Đ = 1.04, 40 mg, 1.43 mmol repeat unit, 10% branched), methyl aniline dithiocarbamylamide (35 mg, 0.0714 mmol), and dicumyl peroxide (1.4 mg, 0.007 mmol) were reacted according to General Procedure C. The mixture was heated at 180 °C for 1 h. The polymer was purified via precipitation in cold methanol to yield 38 mg of 1 mol% dithiocarbamylated polyolefin. Similar characterization data was obtained using other stoichiometric ratios of amide to repeat unit.

The following was gathered for 1 mol% dithiocarbamylated HBPE:

¹H NMR (400 MHz, CDCl₃) δ 7.43 (bs, 3H), 7.22 (bs, 2H), 4.03 (bs), 3.95 (bs), 3.75 (bs, 3H), 3.66 (bs), 3.56 (bs), 3.49 (bs), 1.58 (bs), 1.54 (bs), 1.26 (bs), 1.22 (bs), 1.08 (bs), 0.88 (bs), 0.85 (bs). **¹³C NMR (125 MHz, CDCl₃)** δ 129.6, 128.6, 127.0, 39.2, 38.9, 37.7, 37.4, 37.2, 37.1, 36.8, 36.7, 36.1, 34.8, 34.4, 34.1, 33.7, 33.4, 33.2, 32.8, 32.4, 32.0, 32.0, 30.9, 30.7, 30.5, 30.2, 30.1, 29.9, 29.8, 29.8, 29.7, 29.5, 29.4, 29.0, 27.6, 27.5, 27.2, 26.8, 26.4, 25.9, 25.4, 24.1, 23.7, 23.2, 23.1, 22.8, 22.7, 19.8, 19.7, 19.3, 14.6, 14.2, 14.2, 11.5, 10.9, 1.0. **IR (neat, ATR, cm⁻¹)** 2921, 2852, 1469, 1457, 1364, 1350, 1280, 1262, 1098, 960, 955, 766, 694, 633. **GPC (THF)** M_n = 27 kg/mol, Đ = 1.08; UV-Vis at 14 min = 212, 252, and 281 nm. **TGA (°C)** T_d = 230 °C with 10 wt% lost, terminal onset at 415 °C. **DSC (°C)** parent T_g = –69, product T_g = –63.

Determination of percent functionalization of HBPE: Upon purification, the percent methyl aniline dithiocarbamylation of HBPE can be determined through integration of the ^{1}H NMR. Considering the composition of the polymer, the peaks between 0.8 – 2.0 ppm were set to total to 4 protons. The methyl protons of the methyl aniline unit appear as a singlet at 3.75 were used to determine mol% functionalization per repeat unit. The integration agreed with that of the phenyl moiety at   7.22 and 7.43 ppm. Regioselectivity could not be determined as overall percent functionalization was too low to observe good signal-to-noise ratios.

Z group	Equiv. of amidyl reagent relative to repeat unit	Temperature (°C)	Solvent	Time (h)	Mol% funct.
OEt	1:80	130	PhCl	1	1
OEt	1:40	130	PhCl	2.5	2
OEt	1:20	130	PhCl	1.5	3
OEt	1:10	130	PhCl	6	4
OEt	1:10	180	$PhCl_2$	1	4
OEt	1:5	130	PhCl	6	6
OEt	1:2	130	PhCl	19	8
SEt	1:20	130	PhCl	1	1
SEt	1:10	130	PhCl	19	3
NEt_2	1:10	130	PhCl	19	1
NMePh	1:20	180	none	1	1
NMePh	1:10	180	none	1	1

NMePh	1:5	180	none	2	2
NMePh	1:2	180	none	2	2

Table B.1 Varying in the reaction temperature and time influenced the chemoselectivity of the reaction. Listed are the optimized reaction conditions to obtain a particular percent functionalization without significant chain coupling. Assume that all higher equivalents of amide were conducted for 19 h in chlorobenzene (PhCl) at 130 °C and with 10 mol% peroxide relative to amide.
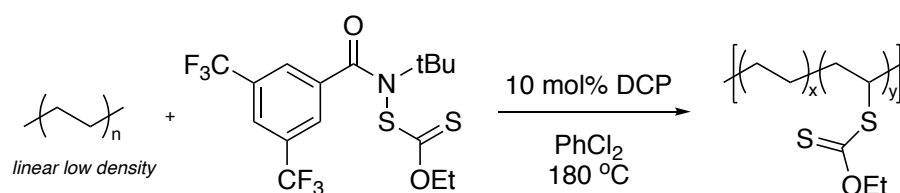
Xanthylated Linear Low Density Polyethylene: DOW™ DNDA-1081 NT 7 Linear Low Density Polyethylene Resin (M_n = 22 kg/mol, Đ = 3.37, 40 mg, 1.43 mmol repeat unit), xanthylamide (30 mg, 0.0070 mmol), and dicumyl peroxide (2 mg, 0.007 mmol) were reacted according to General Procedure B in dichlorobenzene (0.4 mL). The reaction was heated and stirred at 180 °C for 1h. The crude mixture was precipitated from solution into methanol at room temperature to afford 3 mol% xanthylated linear low density polyethylene. This material was previously characterized in another paper via blue light irradiation.[6] Changing the reaction stoichiometry to 10 repeat units per xanthylamide equivalent increased the percent functionalization to 7 mol%.

The following was gathered for 3 mol% xanthylated linear low density polyethylene:

¹H NMR (500 MHz, C₂D₂Cl₄, 110 °C) δ 4.76 (m), 3.75 (bs), 1.74 (bs), 1.49 (bs), 1.47 (bs), 1.44 (bs), 1.36 (bs), 0.97 (bs). **IR (neat, ATR, cm⁻¹)** 2917, 2849, 1469, 1465, 1207, 1117, 1110, 1050, 720. **GPC (TCB, 120 °C)** M_n = 28 kg/mol, Đ = 7.66. **TGA (°C)** T_d = 240 °C with 11 wt% loss, terminal onset at 411 °C. **DSC (°C)** parent T_m = 125, product T_m = 95.

Determination of percent functionalization of linear low density polyethylene: Upon purification, the percent xanthylation of linear low density polyethylene can be determined through integration of the ¹H NMR. Considering the composition of the polymer, the peaks between 0.9 – 1.8 ppm were set to total to 4 protons. The methylene protons of the ethoxy unit that appear at 4.8 ppm are used to determine mol% xanthylation per repeat unit.
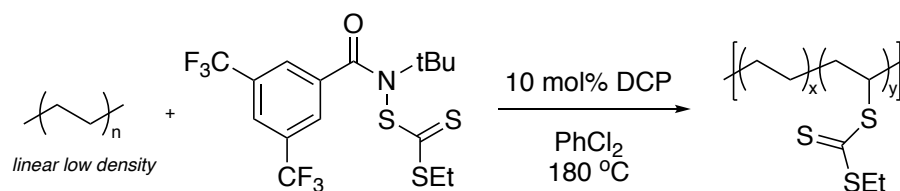
Trithiocarbonylated Linear Low Density Polyethylene: DOW™ DNDA-1081 NT 7 Linear Low Density Polyethylene Resin (M_n = 22 kg/mol, Đ = 3.37, 20 mg, 0.714 mmol repeat unit), trithiocarbonylamide (30 mg, 0.0.070 mmol), and dicumyl peroxide (2 mg, 0.007 mmol) were reacted according to General Procedure B in dichlorobenzene (0.4 mL). The reaction was heated and stirred at 180 °C for 1h. The crude mixture was precipitated from solution into methanol at room temperature to afford 3 mol% trithiocarbonylated linear low density polyethylene:

¹H NMR (500 MHz, C₂D₂Cl₄, 110 °C) δ 4.29 (bs), 3.47 (m), 1.82 (bs), 1.53 (bs), 1.47 (bs), 1.41 (bs), 1.36 (bs), 1.02 (bs). **IR (neat, ATR, cm⁻¹)** 2983, 2916, 2849, 1473, 1464, 1383, 1250, 1085, 1074, 1028, 958, 812, 720. **GPC (TCB, 120 °C)** M_n = 23 kg/mol, $Đ$ = 3.84. **TGA (°C)** T_d = 220 °C with 13 wt% loss, terminal onset at 433 °C. **DSC (°C)** parent T_m = 122, product T_m = 100.

Determination of percent functionalization of linear low density polyethylene: Upon purification, the percent trithiocarbonylation of linear low density polyethylene can be determined through integration of the ¹H NMR. Considering the composition of the polymer, the peaks between 0.9 – 1.8 ppm were set to total to 4 protons. The methylene protons of the thioethoxy unit that appear at 3.5 ppm are used to determine mol% trithiocarbonylation per repeat unit.
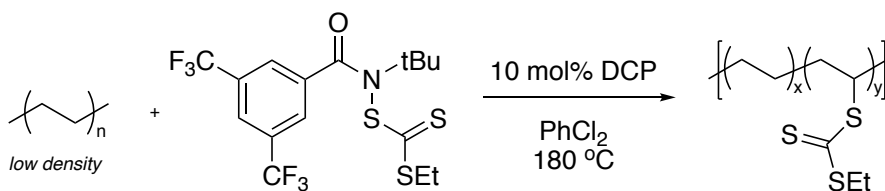
Trithiocarbonylated Low Density Polyethylene: Dow™ Polyethylene 4012 Low Density (M_n = 41 kg/mol, $Đ$ = 89.46, 20 mg, 0.714 mmol repeat unit), trithiocarbonylamide (32 mg, 0.0714 mmol), and dicumyl peroxide (2 mg, 0.007 mmol) were reacted according to General Procedure B in dichlorobenzene (0.4 mL). The reaction was heated and stirred at 180 °C for 1h. The crude mixture was precipitated from solution into methanol at room temperature to yield 3 mol% trithiocarbonylated low density polyethylene:

¹H NMR (500 MHz, C₂D₂Cl₄, 110 °C) δ 4.28 (bs), 3.47 (bs), 1.83 (bs), 1.78 (bs), 1.61 (bs), 1.52 (bs), 1.47 (bs), 1.41 (bs), 1.37 (bs), 1.02 (bs). **IR (neat, ATR, cm⁻¹)** 2934, 2917, 2849, 1473, 1464, 1374, 1279, 1269, 1149, 1085, 1075, 1067, 969, 809, 720. **GPC (TCB, 120 °C)** M_n = 43 kg/mol, Đ = 17.95. **TGA (°C)** T_d = 233 °C with 14 wt% loss, terminal onset at 422 °C. **DSC (°C)** parent T_m = 105, product T_m = 85.

Determination of percent functionalization of low density polyethylene: Upon purification, the percent trithiocarbonylation of low density polyethylene can be determined through integration of the ¹H NMR. Considering the composition of the polymer, the peaks between 0.9 – 1.8 ppm were set to total to 4 protons. The methylene protons of the thioethoxy unit that appear at 3.5 ppm are used to determine mol% trithiocarbonylation per repeat unit.
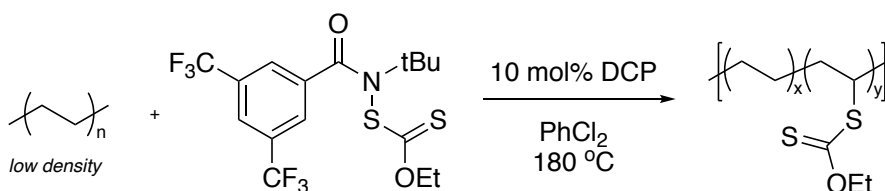
Xanthylated Low Density Polyethylene: Dow™ Polyethylene 4012 Low Density (M_n = 41 kg/mol, Đ = 9.46, 40 mg, 1.43 mmol repeat unit), xanthylamide (30 mg, 0.0714 mmol), and dicumyl peroxide (2 mg, 0.007 mmol) were reacted according to General Procedure B in dichlorobenzene (0.4 mL). The reaction was heated and stirred at 180 °C for 1h. The crude mixture was precipitated from solution into methanol at room temperature to yield 3 mol% xanthylated low density polyethylene. Doubling the quantity of xanthylamide and dicumyl peroxide in the reaction resulted in 5 mol% functionalization.

The following was gathered for 3 mol% xanthylated low density polyethylene:

¹H NMR (500 MHz, C₂D₂Cl₄, 110 °C) δ 4.77 (bs), 1.78 (bs), 1.61 (bs), 1.49 (bs), 1.40 (bs), 1.01 (bs). **IR (neat, ATR, cm⁻¹)** 2917, 2850, 1467, 1378, 1279, 1208, 1118, 1064, 1050, 720. **GPC (TCB, 120 °C)** M_n = 26 kg/mol, Đ = 12.09. **TGA (°C)** T_d = 241 °C with 10 wt% loss, terminal onset at 423 °C. **DSC (°C)** parent T_m = 105, product T_m = 84.

Determination of percent functionalization of low density polyethylene: Upon purification, the percent xanthylation of low density polyethylene can be determined through integration of the ¹H NMR. Considering the composition of the polymer, the peaks between 0.9 – 1.8 ppm were set to total to 4 protons. The methylene protons of the ethoxy unit that appear at 4.7 ppm are used to determine mol% xanthylation per repeat unit.
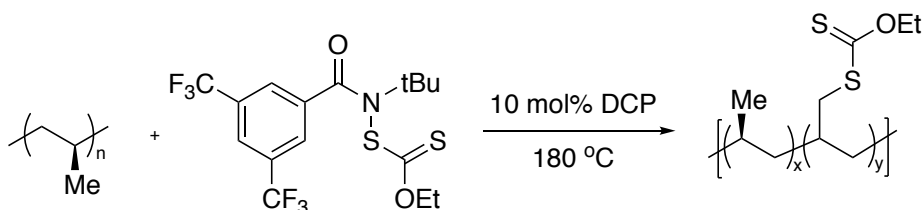
Xanthylated Polypropylene: Basell™ Profax 6301 polypropylene homopolymer (M_n = 64 kg/mol, Đ = 4.84, 3.33 g, 0.079 mol repeat unit), xanthylamide (1.67 g, 0.004 mol), and dicumyl peroxide (90 mg, 0.33 mmol) were reacted according to General Procedure C. The reaction was heated at 180 °C for 1h and afforded 1 mol% xanthylated polypropylene. General Procedure B at a target of 10 mol% xanthylation also achieved 1 mol% functionalization after reacting at 180 °C for 1h.

The following was gathered for 1 mol% xanthylated polypropylene:

¹H NMR (500 MHz, C₂D₂Cl₄, 110 °C) δ 4.75 (m), 3.25 (bs), 1.66 (bs), 1.35 (bs), 0.99 (bs).

IR (neat, ATR, cm⁻¹) 2923, 2918, 2839, 1457, 1376, 1360, 1215, 1167, 1113, 1052, 974, 972, 841. **GPC (TCB, 120 °C)** M_n = 67 kg/mol, $Đ$ = 9.44. **TGA (°C)** T_d = 245 °C with 3 wt% loss, terminal onset at 374 °C. **DSC (°C)** parent T_m = 155, product T_m = 137.

Determination of percent functionalization of isotactic polypropylene: Upon purification, the percent xanthylation of polypropylene can be determined through integration of the ¹H NMR. Considering the composition of the polymer, the peaks between 0.9 – 2.0 ppm were set to total to 6 protons. The methylene protons of the ethoxy unit that appear at 4.8 ppm are used to determine mol% xanthylation per repeat unit.

B.6 CROSSOVER EXPERIMENTS

Overview of experiment: If the functionalization step was reversible, it would occur via the abstraction of a thiocarbonylthio group by a propagating radical, either polymer-centered or initiating. In order to confirm that the plateau of functionalization achievable is due to the functionalization step exchanging thiocarbonylthio moieties between polymer chains, we reacted functionalized polymer in reaction conditions of a different amidyl reagent and observed changes in the degree of functionalization of the initial Z group and the newly installed Z group.
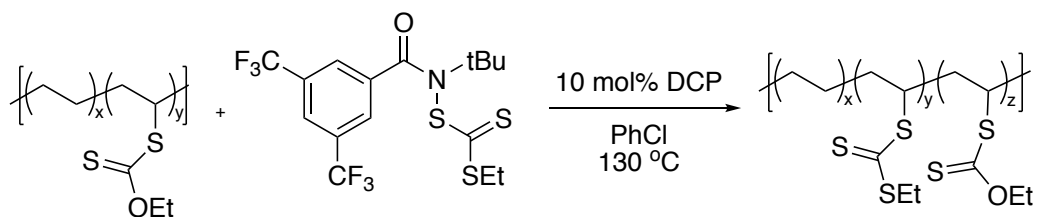
Xanthylation of HBPE reverted by trithiocarbonylamide: Xanthylated HBPE (4.5 mol%, M_n = 40 kg/mol, $Đ$ = 1.07, 10 mg, 0.35 mmol) was reacted with trithiocarbonylamide (16 mg, 0.04 mmol) and dicumyl peroxide (1 mg, 0.004 mmol) according to General Procedure A in dry chlorobenzene (0.2 mL). The reaction was heated and stirred at 130 °C for 6 h. The reaction afforded 3 mol% xanthylated and 2.5 mol% trithiocarbonylated HBPE:

¹H NMR (500 MHz, CDCl₃) δ 4.64 (m), 4.27 (bs), 4.17 (bs), 3.78 (bs), 3.70 (bs), 1.65 (bs), 1.55 (bs), 1.51 (bs), 1.42 (bs), 1.35 (bs), 1.25 (bs), 1.21 (bs), 1.06 (bs), 0.88 (bs), 0.83 (bs). **GPC (THF)** M_n = 38 kg/mol, $Đ$ = 1.13; UV-Vis at 29 min = 285, 310 nm.
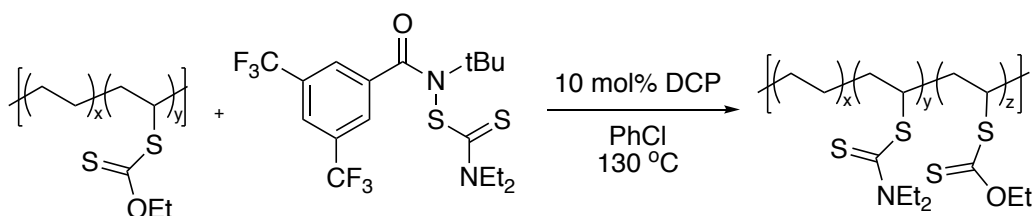
Xanthylation of HBPE reverted by dithiocarbamylamide: Xanthylated HBPE (4.5 mol%, M_n = 40 kg/mol, $Đ$ = 1.07, 9 mg, 0.32 mmol) was reacted with dithiocarbamylamide (15 mg, 0.0321 mmol) and dicumyl peroxide (0.8 mg, 0.003 mmol) according to General Procedure A in dry chlorobenzene (0.15 mL). The reaction was heated and stirred at 130 °C for 6 h. The reaction afforded 2.5 mol% dithiocarbamylated and 2.5 mol% xanthylated HBPE:

¹H NMR (500 MHz, CDCl₃) δ 4.64 (m), 4.03 (bs), 3.74 (bs), 3.67 (bs), 1.65 (bs), 1.55 (bs), 1.42 (bs), 1.25 (bs), 1.21 (bs), 1.06 (bs), 0.88 (bs), 0.83 (bs). **GPC (THF)** M_n = 47 kg/mol, $Đ$ = 1.59; UV-Vis at 30 min = 224, 254, 283 nm.
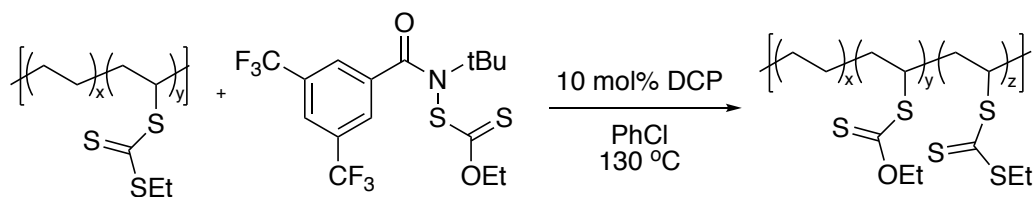
Trithiocarbonylation of HBPE reverted by xanthylamide: Trithiocarbonylated HBPE (3 mol%,

M_n = 33 kg/mol, $Đ$ = 1.07, 23 mg, 0.82 mmol) was reacted with xanthylamide (36 mg, 0.082

mmol) and dicumyl peroxide (2 mg, 0.008 mmol) according to General Procedure A in dry

chlorobenzene (0.4 mL). The reaction was heated and stirred at 130 °C for 6 h. The reaction

was concentrated *in vacuo* and then precipitated from hexanes into methanol at 0 °C. The

reaction afforded 1 mol% trithiocarbonylated and 3 mol% xanthylated HBPE:

¹H NMR (500 MHz, CDCl₃) δ 4.63 (m), 4.16 (bs), 3.71 (bs), 3.35 (bs), 3.12 (bs), 2.99 (bs),

1.66 (bs), 1.59 (bs), 1.55 (bs), 1.51 (bs), 1.42 (bs), 1.26 (bs), 1.22 (bs), 1.08 (bs), 0.88 (bs),

0.84 (bs). **GPC (THF)** M_n = 39 kg/mol, $Đ$ = 1.20; UV-Vis at 30 min = 288, 310 nm.
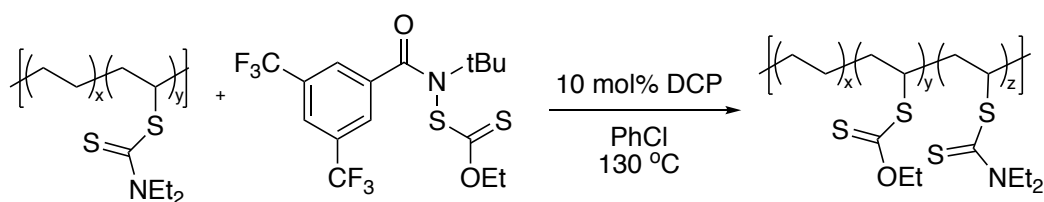
Dithiocarbonylation of HBPE reverted by xanthylamide: Dithiocarbamylated HBPE (1 mol%,

M_n = 32 kg/mol, $Đ$ = 1.08, 9 mg, 0.32 mmol) was reacted with xanthylamide (14 mg, 0.032

mmol) and dicumyl peroxide (0.8 mg, 0.003 mmol) according to General Procedure A in dry

chlorobenzene (0.2 mL). The reaction was heated and stirred at 130 °C for 6 h. The reaction afforded 0.5 mol% dithiocarbamylated and 3 mol% xanthylated HBPE:

¹H NMR (500 MHz, CDCl₃) δ 4.65 (m), 4.04 (bs), 3.77 (bs), 3.71 (bs), 1.67 (bs), 1.58 (bs), 1.43 (bs), 1.28 (bs), 1.24 (bs), 1.10 (bs), 0.90 (bs), 0.85 (bs). **GPC (THF)** M_n = 37 kg/mol, Đ = 1.18; UV-Vis at 30 min = 223, 283 nm.

B.7 KINETIC EXPERIMENTS

Overview of experiment: The consumption of amidyl reagent and subsequent turnover to its respective parent amide is a good indicator of reaction progress. To better understand the influence of the Z group on the overall rate of reaction, we conducted kinetic experiments that would later confirm the rate of addition and fragmentation significantly influence the overall rate of the reaction.

Monitoring Kinetics of Dithiocarbamylation of HBPE: HBPE (M_n = 33 kg/mol, Đ = 1.06, 56 mg, 2.0 mmol), diethyl dithiocarbamylamide (92 mg, 0.2 mmol), and dicumyl peroxide (5 mg, 0.02 mmol) were added to a reaction vial equipped with a magnetic stir bar. In a nitrogen-filled glovebox, chlorobenzene (1.0 mL) was added and the mixture was stirred for 30 min. Aliquots of 0.2 mL were distributed across 5 vials under inert atmosphere. The individual aliquots were heated and stirred at 130 °C for up to 2.5 h, with an aliquot removed every 30 min. The crude solution was concentrated *in vacuo* and a crude NMR was taken to determine N–S conversion to parent amide from functionalized amide. GPC was obtained in THF with a tandem PDA detector.

Time (h)	N–S conversion	M_n (kg/mol)	Đ	UV-Vis at 30 min (nm)
0	0	33	1.06	none
0.5	4	33	1.08	225, 254, 282
1	7	33	1.08	225, 254, 282
1.5	9	33	1.08	225, 254, 282
2	11	34	1.08	225, 254, 282
2.5	11	35	1.07	225, 254, 282

Monitoring Kinetics of Trithiocarbonylation of HBPE: HBPE (M_n = 31 kg/mol, Đ = 1.02, 56 mg, 2.0 mmol), trithiocarbonylamide (90 mg, 0.2 mmol), and dicumyl peroxide (5 mg, 0.02 mmol) were added to a reaction vial equipped with a magnetic stir bar. In a nitrogen-filled glovebox, chlorobenzene (1.0 mL) was added and the mixture was stirred for 30 min. Aliquots of 0.2 mL were distributed across 5 vials under inert atmosphere. The individual aliquots were heated and stirred at 130 °C for up to 2.5 h, with an aliquot removed every 30 min. The crude solution was concentrated *in vacuo* and a crude NMR was taken to determine N–S conversion to parent amide from functionalized amide. GPC was obtained in THF with a tandem PDA detector.

Time (h)	N–S conversion	M_n (kg/mol)	Đ	UV-Vis at 30 min (nm)
0	0	31	1.02	none

0.5	2	31	1.03	none
1	10	31	1.03	309
1.5	11	31	1.04	310
2	16	31	1.04	310
2.5	19	31	1.04	310

Monitoring Kinetics of Xanthylation of HBPE: HBPE (M_n = 31 kg/mol, $Đ$ = 1.02, 60 mg, 2.14 mmol), xanthylamide (93 mg, 0.214 mmol), and dicumyl peroxide (6 mg, 0.021 mmol) were added to a reaction vial equipped with a magnetic stir bar. In a nitrogen-filled glovebox, chlorobenzene (1.0 mL) was added and the mixture was stirred for 30 min. Aliquots of 0.2 mL were distributed across 5 vials under inert atmosphere. The individual aliquots were heated and stirred at 130 °C for up to 50 min, with an aliquot removed every 10 min. The crude solution was concentrated *in vacuo* and a crude NMR was taken to determine N–S conversion to parent amide from functionalized amide. GPC was obtained in THF with a tandem PDA detector.

Time (min)	N–S conversion	M_n (kg/mol)	$Đ$	UV-Vis at 30 min (nm)
0	0	31	1.02	none
10	6	31	1.03	283
20	14	31	1.03	283
30	22	31	1.04	281
40	29	31	1.04	283

| 50 | 35 | 32 | 1.05 | 285 |

B.8 REACTIVE EXTRUSION CONDITIONS
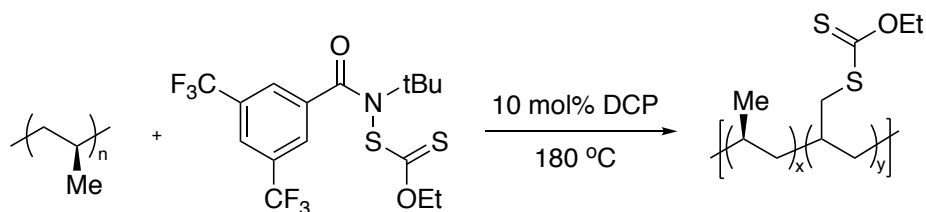
Basell™ Profax 6301 polypropylene homopolymer (M_n = 64 kg/mol, Đ = 4.84, 10 g, 0.238 mol) was mixed with xanthylamide (5 g, 0.012 mol) and dicumyl peroxide (270 mg, 0.001 mol) in an Erlenmeyer flask. The solids were dissolved slightly with dichloromethane to mix the amidyl reagent with the peroxide. Solvent was removed *in vacuo* overnight. The total mass (15 g) of the solid mixture was divided into two samples of 10 grams and 5 grams. To an Xplore twin-screw extruder was added the 10-gram sample. The screws were turned at 50 rpm, the heat profile was set around 187 °C, and the melt temperature was 182 °C. The sample was loaded into the extruder in 105 seconds and the extruder was filled with nitrogen. Aliquots were extruded after 30 min, 45 min, and 1 hour of heating. The crude material was precipitated from dichlorobenzene at 180 °C into methanol at room temperature.

The following was collected after 30 min and then extruded to yield 1 mol% xanthylated polypropylene (1.20 g):

¹H NMR (500 MHz, C₂D₂Cl₄, 110 °C) δ 4.72 (bs, 2H), 3.24 (bs, 1H), 1.65 (m), 1.34 (dt, J = 6.10, 12.5 Hz), 0.96 (d, J = 19.9 Hz). **IR (neat, ATR, cm⁻¹)** 2923, 2918, 2839, 1456, 1376, 1214, 1168, 1053, 998, 973, 899, 841. **GPC (TCB, 120 °C)** M_n = 49 kg/mol, Đ = 8.27. **TGA**

(°C) T_d = 261 °C with 2 wt% loss, terminal onset at 375 °C. **DSC (°C)** parent T_m = 158, product T_m = 146.

The following was collected after 45 min and then extruded to yield 1 mol% xanthylated polypropylene (0.71 g):

¹H NMR (500 MHz, C₂D₂Cl₄, 110 °C) δ 4.73 (bs, 2H), 3.24 (bs, 1H), 1.66 (dt, J = 6.88, 13.7 Hz), 1.34 (dt, J = 6.10, 12.7 Hz), 0.96 (d, J = 6.55 Hz). **IR (neat, ATR, cm⁻¹)** 2923, 2918, 2839, 1457, 1376, 1214, 1169, 1113, 1052, 975, 973, 899, 841. **GPC (TCB, 120 °C)** M_n = 43 kg/mol, Đ = 8.81. **TGA (°C)** T_d = 224 °C with 2 wt% loss, terminal onset at 361 °C. **DSC (°C)** parent T_m = 158, product T_m = 143.

The following was collected after 1 hour and then extruded to yield 1 mol% xanthylated polypropylene (1.12 g):

¹H NMR (500 MHz, C₂D₂Cl₄, 110 °C) δ 4.73 (bs, 2H), 3.24 (bs, 1H), 1.66 (dt, J = 6.88, 13.7 Hz), 1.34 (dt, J = 6.10, 12.7 Hz), 0.96 (d, J = 6.55 Hz). **IR (neat, ATR, cm⁻¹)** 2923, 2918, 2839, 1456, 1376, 1213, 1167, 1113, 1053, 974, 972, 841. **GPC (TCB, 120 °C)** M_n = 37 kg/mol, Đ = 9.01. **TGA (°C)** T_d = 250 °C with 2 wt% loss, terminal onset at 343 °C. **DSC (°C)** parent T_m = 158, product T_m = 145.

The remaining 5-gram sample was added to a reaction vial and submitted to the glovebox to be degassed. In the glovebox, the vial was sealed with electrical tape. The reaction was heated at 180 °C for 1 hour. The resultant material was precipitated from dichlorobenzene at 180 °C into methanol at room temperature to yield 1 mol% xanthylated polypropylene (0.55 g):

¹H NMR (500 MHz, C₂D₂Cl₄, 110 °C) δ 4.72 (bs, 2H), 3.24 (bs, 1H), 1.66 (dt, J = 6.88, 13.7 Hz), 1.34 (dt, J = 6.10, 12.7 Hz), 0.96 (d, J = 6.55 Hz). **IR (neat, ATR, cm⁻¹)** 2923, 2918, 2839, 1457, 1376, 1360, 1215, 1167, 1113, 1052, 974, 972, 841. **GPC (TCB, 120 °C)** M_n = 67 kg/mol, Đ = 9.44. **TGA (°C)** T_d = 245 °C with 3 wt% loss, terminal onset at 374 °C. **DSC (°C)** parent T_m = 158, product T_m = 143.

B.9 LAP SHEAR AND TENSILE PULL TESTING CONDITIONS

Polymer films (0.1 – 0.3 mm) suitable for dynamic mechanical analysis (DMA) were prepared by melt-pressing using a PHI Manual Compression Press. Basell™ Profax 6301 polypropylene homopolymer (PP, M_n = 64 kg/mol, Đ = 4.84) and 1 mol% xanthylated polypropylene (XPP, M_n = 43 kg/mol, Đ = 8.81) samples between two Kapton films (pre-treated with Frekote 770-NC) were placed between steel electrically heated plates at force 5000 psi and 180 °C for 3 minutes. Brass shims of 4 to 12 mil thickness were used to control ultimate film thickness. Films were removed from the melt press at the indicated temperature and quenched to room temperature by rapid heat transfer to an aluminum surface. Specimens for analysis were cut into dog-bones using an ISO 527 Type 5B cutting die to standard dimensions. Test specimens were mounted to screw-tight grips (30 cN.m). Tensile stress and strain were measured to the point of break at room temperature using an extension speed of 0.1 mm/s with an approximate loading gap of 16 mm on a TA instruments DMA 850 in linear film tension mode. Measurements were repeated for at least 3 specimens and the values reported are averaged from the measured data (Table B.2).

Polymer	σ_y (MPa)	E (MPa)	ε_y	σ_B (Mpa)	ε_B
PP	35	14	6%	33	583%
PP	36	15	7%	29	508%
PP	34	15	8%	32	605%
PP average	*35*	*15*	*7%*	*31*	*570%*
PP st. dev.	*1*	*1*	*1%*	*2*	*50%*
XPP	31	12	7%	33	604%
XPP	23	17	7%	22	346%
XPP	25	15	6%	20	344%
XPP	25	13	6%	20	420%
XPP average	*26*	*14*	*7%*	*24*	*430%*
XPP st. dev.	*3*	*2*	*1%*	*6*	*120%*

Table B.2 DMA results from thin film tensile axial pull of 0.3 mm thick iPP and X*i*PP samples at a rate of 0.1 mm/s

For lap shear analysis, glass slides (76.2 x 6.35 x 3.175 mm) were initially treated with piranha solution. Lap bonds were formed by placing a 0.1 mm film of either PP or XPP between two glass slides and heating the sample to 160 °C for 15 min. After cooling to room temperature, test specimens were affixed to hand-tightened rubber grips on an Instron 5566 Universal Testing Machine. Lap shear stress and strain were measured at room temperature using an extension speed of 5.0 mm/min. Measurements were repeated for at least 3 specimens and the values reported are averaged from the measured data.

Polymer	σ_y (MPa)
PP	46
PP	51
XPP	170
XPP	*141*
XPP	*124*
XPP	77
XPP	101
XPP	77
XPP	121
PP average	*48 ± 4*
XPP average	*120 ± 30*

Table B.3 Lap shear stress/strain data of isotactic polypropylene (stress at break = 48 ± 4 MPa) and post-xanthylation (stress at break = 120 ± 30 MPa).

A visualization of the large-scale functionalization of *i*PP (left) and after reactive extrusion (right).

REFERENCES

(1)   Czaplyski, W. L.; Na, C. G.; Alexanian, E. J. *J. Am. Chem. Soc.* **2016**, *138*, 13854–13857.

(2)   Gottfried, A. C.; Brookhart, M. *Macromolecules* **2001**, *34*, 1140–1142.

(3)   Rofouei, M. K.; Tajarrod, N.; Masteri-Farahani, M.; Zadmard, R. *J. Fluoresc.* **2015**, *25*, 1855–1866.

(4)   Pretsch, E.; Bühlmann, P.; Badertscher, M. *Structure determination of organic compounds: Tables of spectral data*; 2009.

(5)   Liu, L. N.; Dai, J. G.; Zhao, T. J.; Guo, S. Y.; Hou, D. S.; Zhang, P.; Shang, J.; Wang, S.; Han, S. *RSC Adv.* **2017**, *7*, 35075–35085.

(6)   Williamson, J. B.; Czaplyski, W. L.; Alexanian, E. J.; Leibfarth, F. A. *Angew. Chemie Int. Ed.* **2018**, *57*, 6261–6265.

(7)   Abel, B. A.; McCormick, C. L. *Macromolecules* **2016**, *49*, 465–474.

(8)   Na, C. G.; Alexanian, E. J. *Angew. Chemie - Int. Ed.* **2018**, *57*, 13106–13109.

B.11 GPCS FOR CHAPTER III
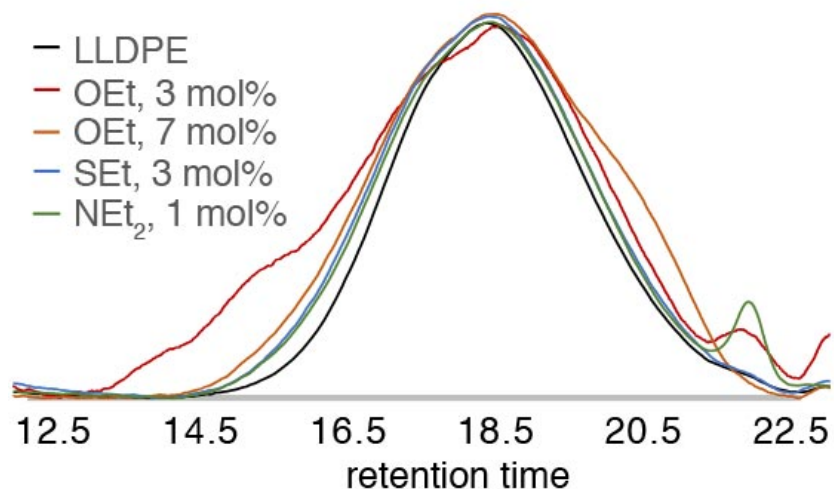
HT GPC at 120 °C in TCB of LLDPE prior to functionalization (M_n = 22 kg/mol, Đ = 3.37)

and after functionalization are pictured above. Trithiocarbonylation has a very similar

molecular weight distributions (M_n = 23 kg/mol, Đ = 3.84). Consistent with other results,

xanthylation induced a slight change in the MWD (M_n = 28 kg/mol, Đ = 7.66) and

dithiocarbamylation did not functionalize the polymer (M_n = 26 kg/mol, Đ = 3.45).
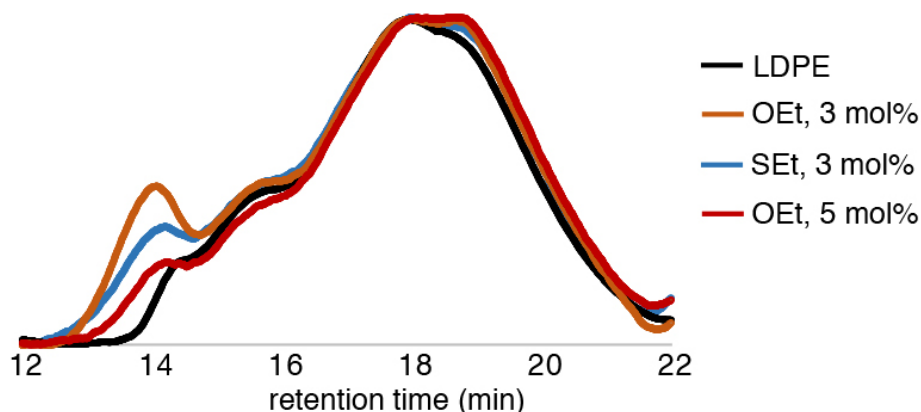
HT GPC at 120 °C in TCB of LDPE prior to dithiocarbamylation (M_n = 41 kg/mol, Đ = 9.46)

and after 3 mol% trithiocarbonylation have very similar molecular weight distributions (M_n =

43 kg/mol, Đ = 17.94). Xanthylation resulted in a polymer with 3 mol% incorporation (M_n =

41 kg/mol, Đ = 23.69) at a target of 5 mol% functionalization and a polymer with 5 mol%

incorporation (M_n = 39 kg/mol, Đ = 13.14) at a target of 10 mol% functionalization.
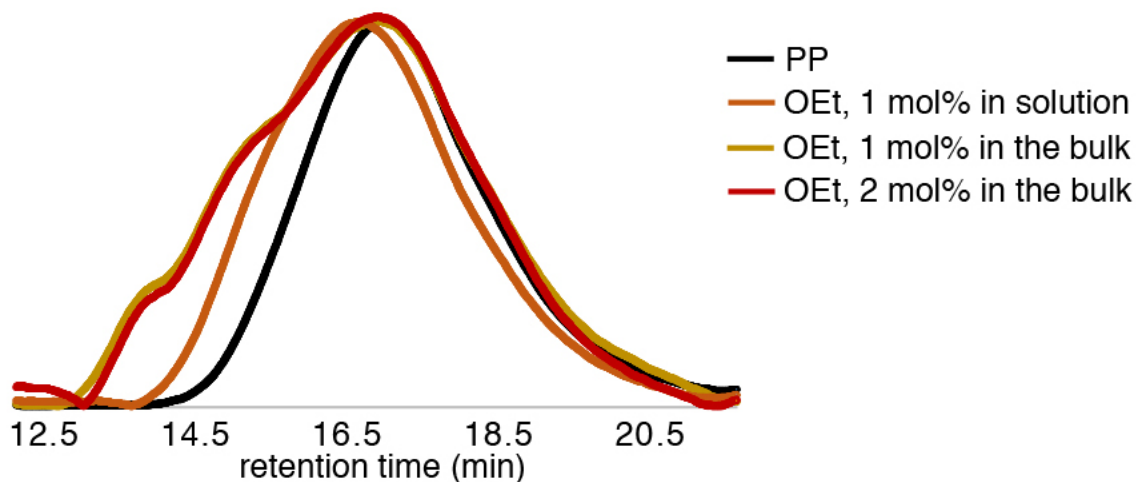
HT GPC at 120 °C in TCB of polypropylene prior to xanthylation (M_n = 64 kg/mol, Đ = 4.84)

and after 1 mol% xanthylation have very similar molecular weight distributions (M_n = 83

kg/mol, Đ = 4.17) when reacted in solution. Under neat conditions, C–H xanthylation was also

successful, as the reaction conditions did not degrade the M_n of the parent materia, with 1

mol% xanthylation at a 1:20 reagent loading relative to repeat unit (M_n = 67 kg/mol, Đ = 9.44)

and with 2 mol% xanthylation at a 1:10 reagent loading relative to repeat unit (M_n = 76 kg/mol,

Đ = 8.51).

B.12 NMRS FOR CHAPTER III
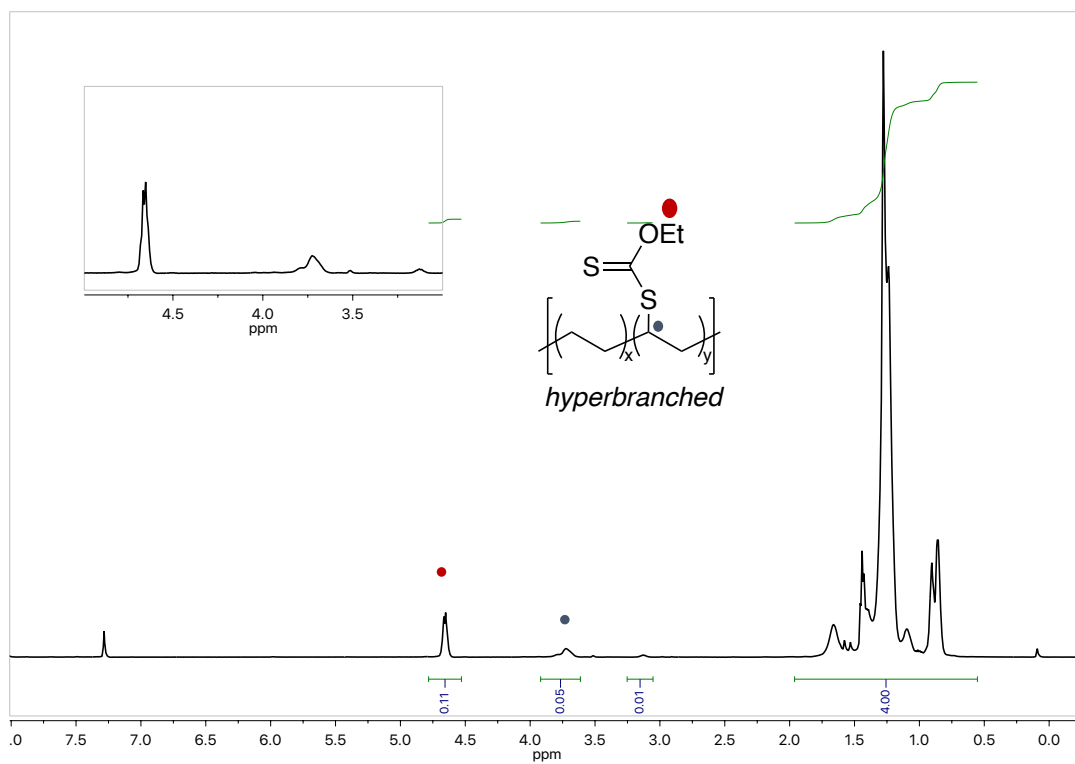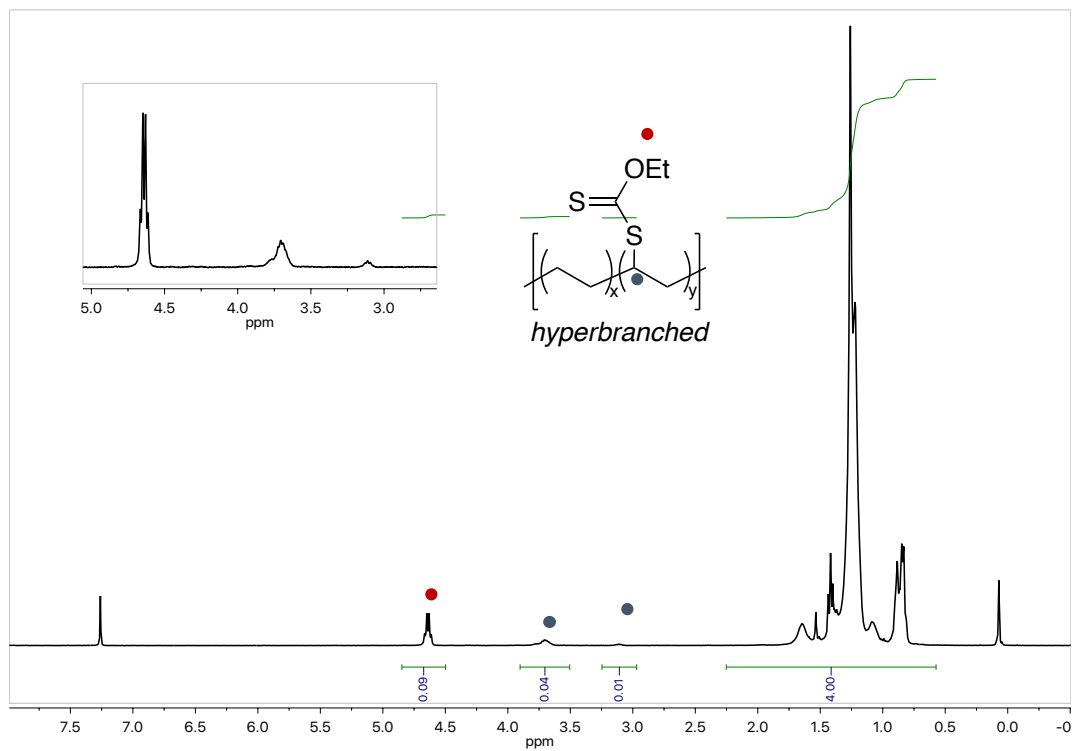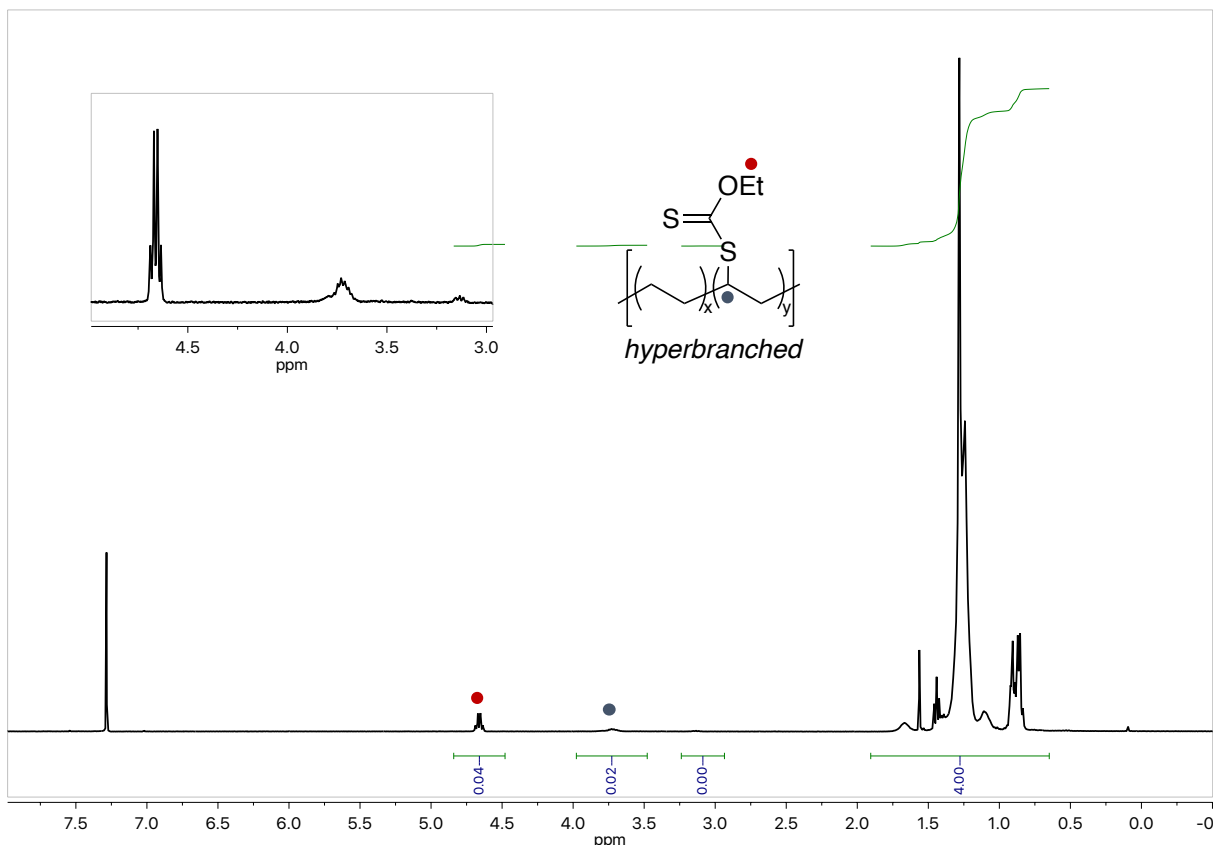
¹H NMR (top to bottom) of the 5.5 mol%, 4.5 mol%, and 2 mol% xanthylated HBPE, respectively. While these are not all the degrees of functionalization achievable, this collection demonstrates that degrees of functionalization clearly vary by ¹H NMR, even at low mol% incorporation. Xanthylated HBPE was previously characterized by photochemical initiation in this same method.[2] The percent functionalization was determined through the integration of peaks around δ 4.6 ppm corresponding to the methylene protons of the ethoxy Z group. Regioselectivity could be evaluated through the relative ratio of secondary xanthylation, with *alpha* polyolefin protons appearing at δ 3.7 ppm, and primary xanthylation, with *alpha*

polyolefin protons appearing at δ 3.2 ppm. In most cases, regioselectivity of thermal C–H xanthylation of HBPE was 8:1 for secondary carbons.
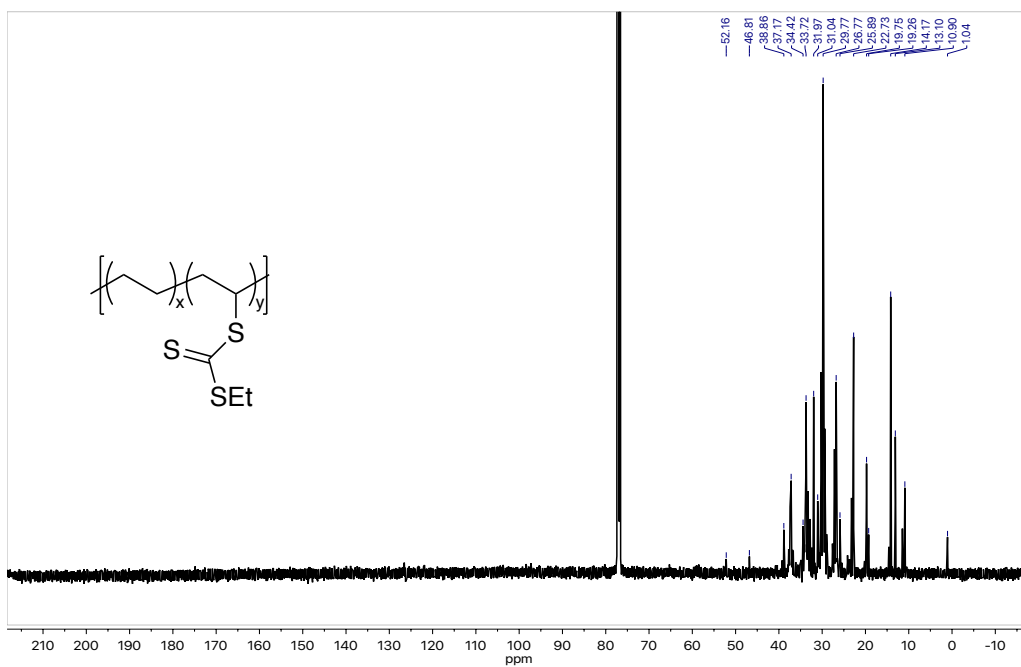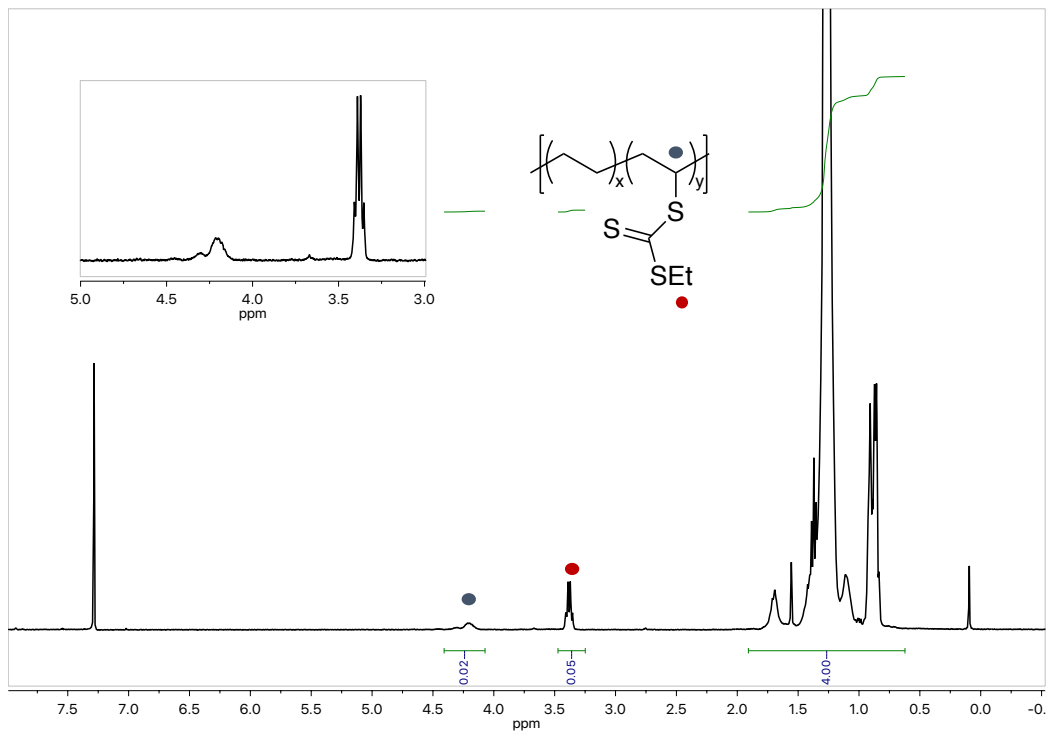
¹H NMR (top) and ¹³C NMR (bottom) of the 2.5 mol% trithiocarbonylated HBPE. Protons *alpha* trithiocarbonates resonated at δ 4.2 ppm and the methylene protons of the ethanethiol group resonated at δ 3.3 ppm in the ¹H NMR spectra. In the ¹³C NMR, a signature ¹³C–S bond can be surmised from the peak at δ 52 ppm. The modest degree of functionalization hampered resolution of the thiocarbonyl carbon peak in the NMR.
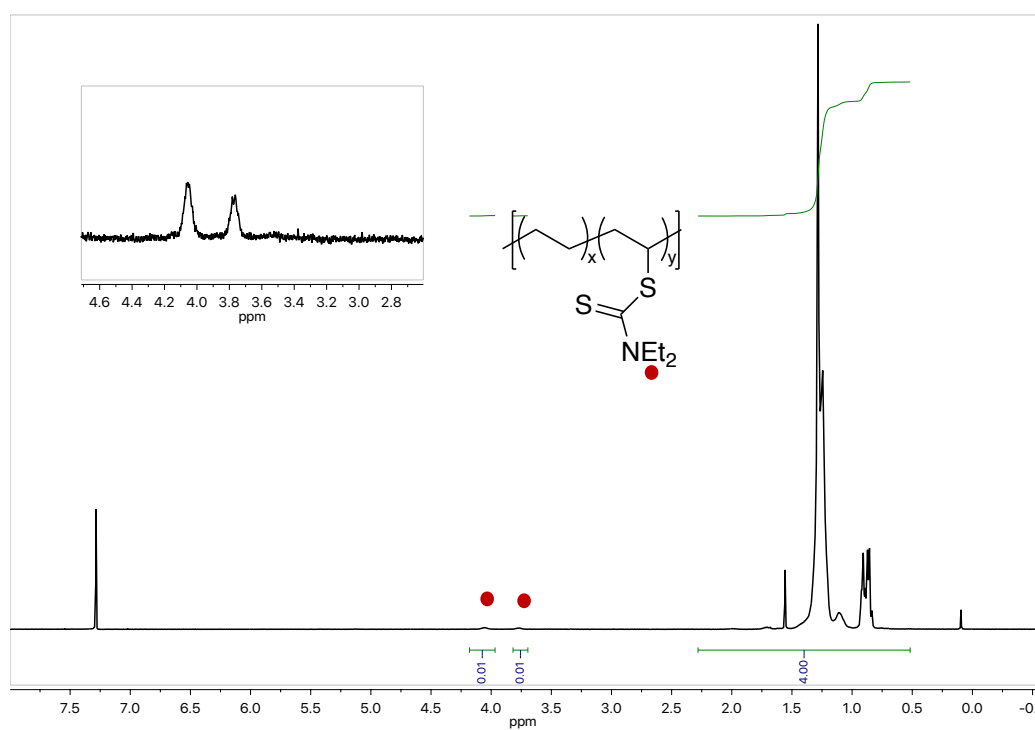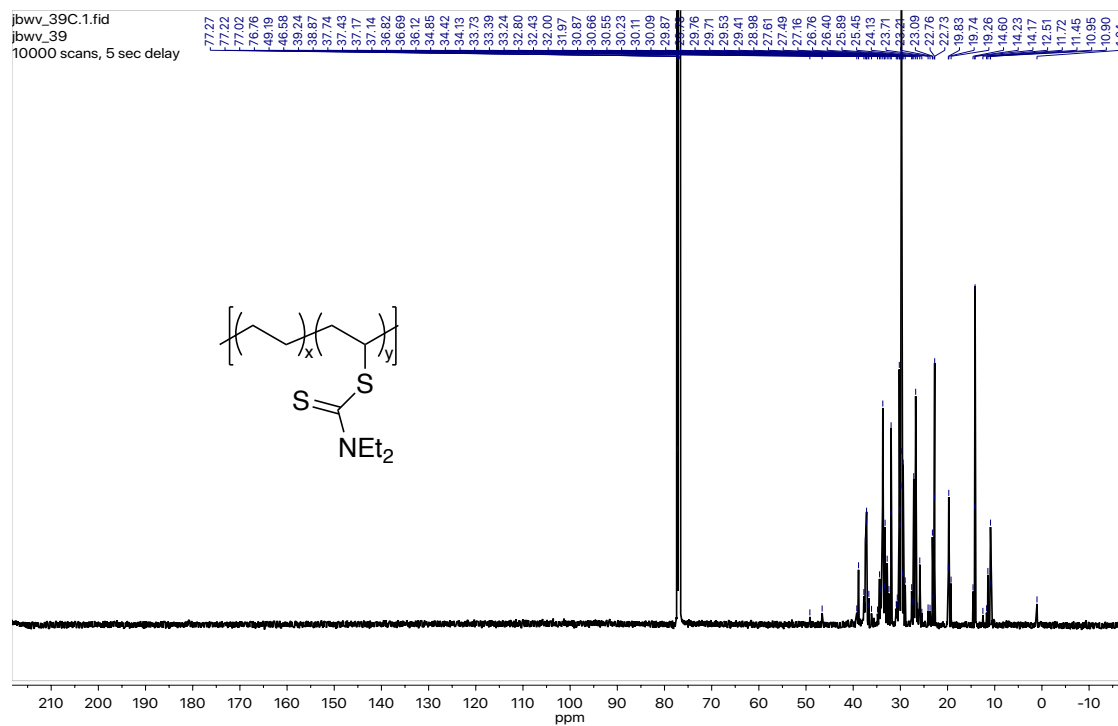
¹H NMR (top) and ¹³C NMR (bottom) of the 1 mol% dithiocarbamylated HBPE. In the ¹H NMR, percent functionalization was determined through the integration of rotameric methylene protons of the diethyl amine Z group at δ 3.7 and 4.0 ppm. ¹³C NMR further supports functionalization with a peak at δ 49 ppm, consistent with C–N bonds.
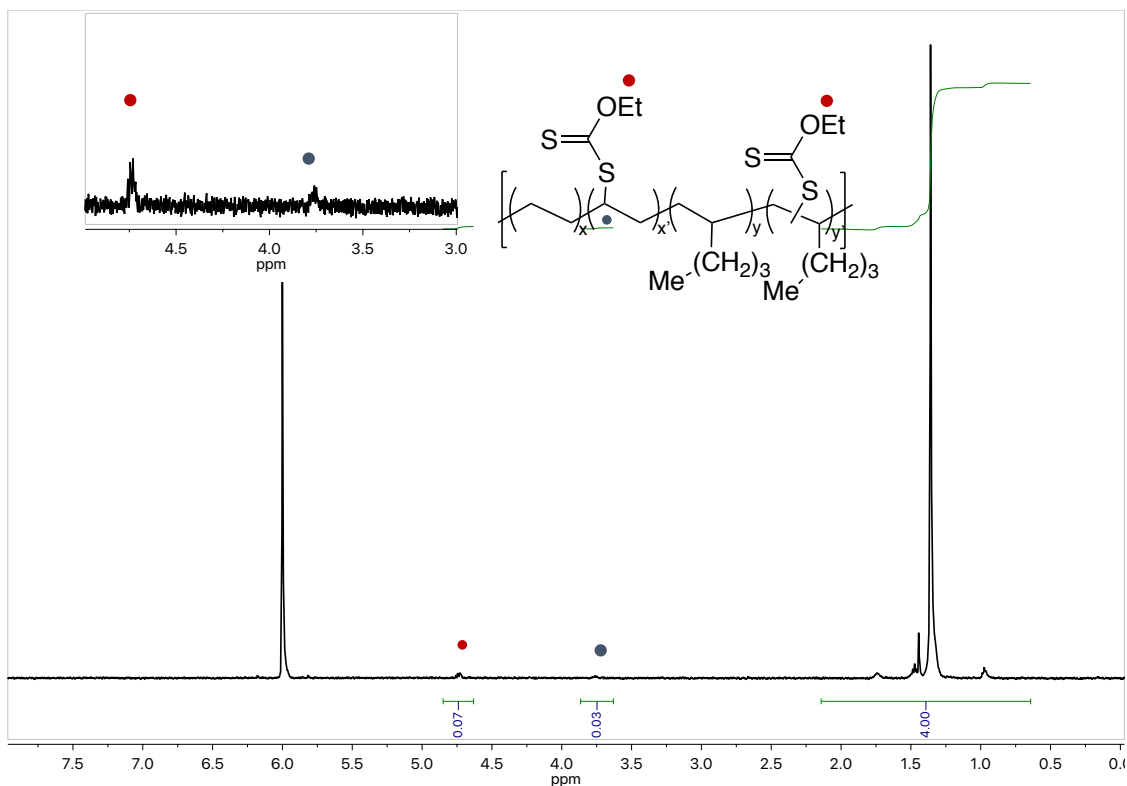
¹H NMR of 3.5 mol% xanthylated linear low density polyethylene at 110 °C in CD$_2$Cl$_4$. ¹³C NMR of this material was previously reported via photochemical initiation. The degree of functionalization was confirmed by methylene protons of the ethoxy unit at δ 4.7 and protons *alpha* xanthate at δ 3.7 ppm. This reaction seems to be regioselective for the secondary sites over the primary branching sites.
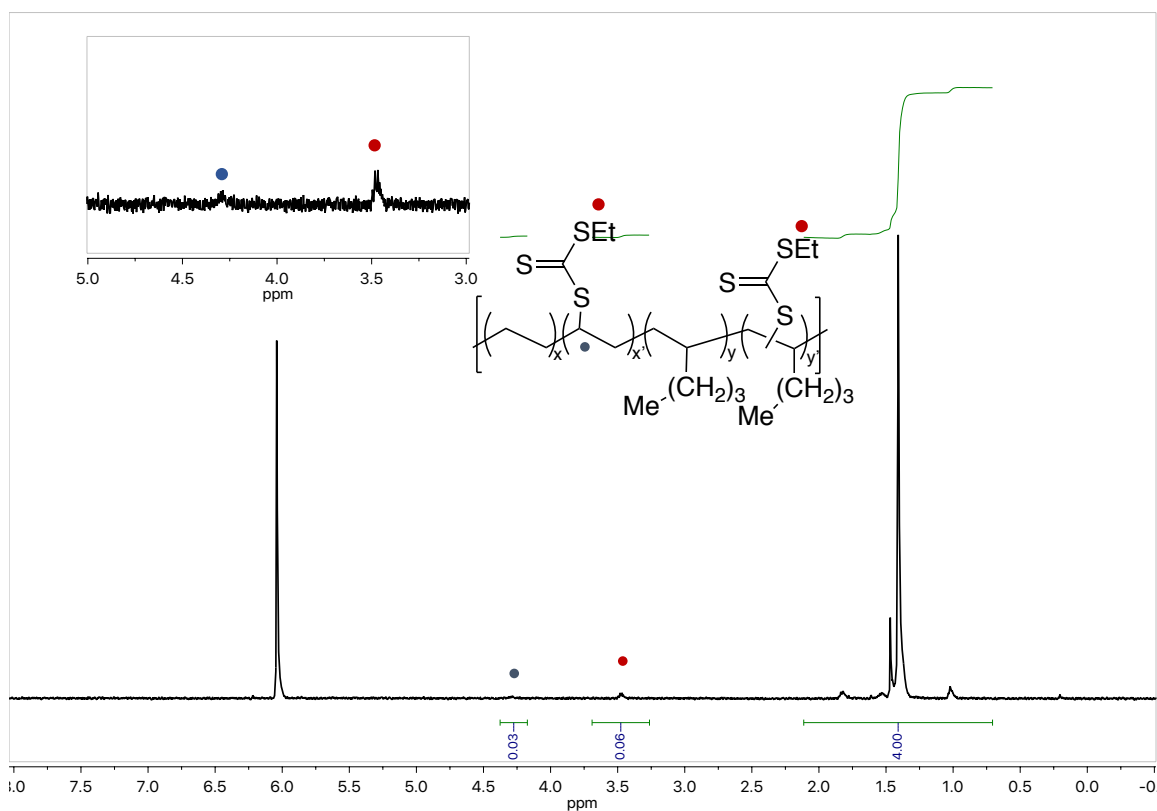
^{1}H NMR of trithiocarbonylated linear low density polyethylene at 110 °C in CD$_2$Cl$_4$ revealed key peaks at δ 3.5 and 4.2 ppm. Thermal gravimetric analysis depicts a 13 wt% loss at 220 °C, consistent with 3 mol% trithiocarbonates incorporated and decomposing via a Chugaev elimination.
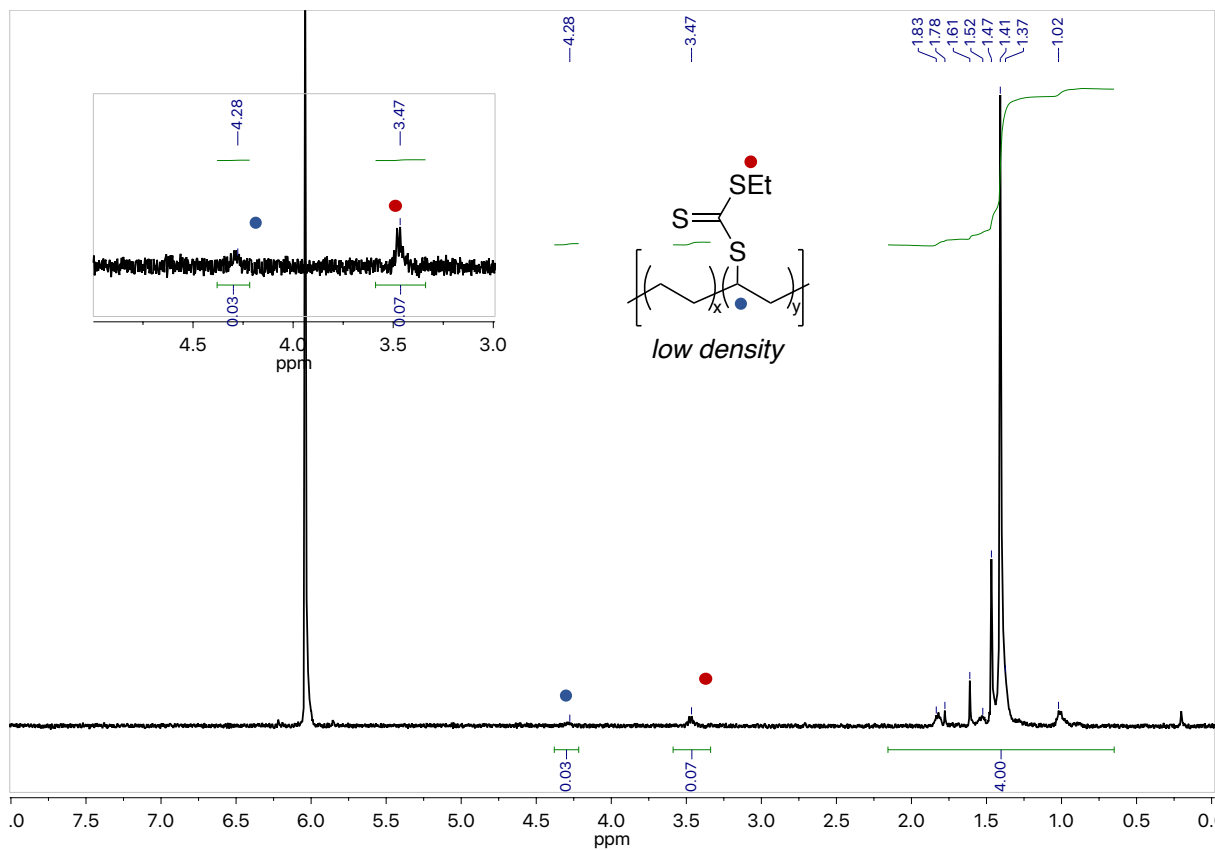
^{1}H NMR of trithiocarbonylated low density polyethylene at 110 °C in CD$_2$Cl$_4$ indicates successful incorporation of the polar moiety. The functionalization peak is present at δ 3.5 ppm, corresponding to the ethanethiol methylene protons, and further evidence is provided at δ 4.2 ppm, corresponding to polymeric protons *alpha* the trithiocarbonate group.
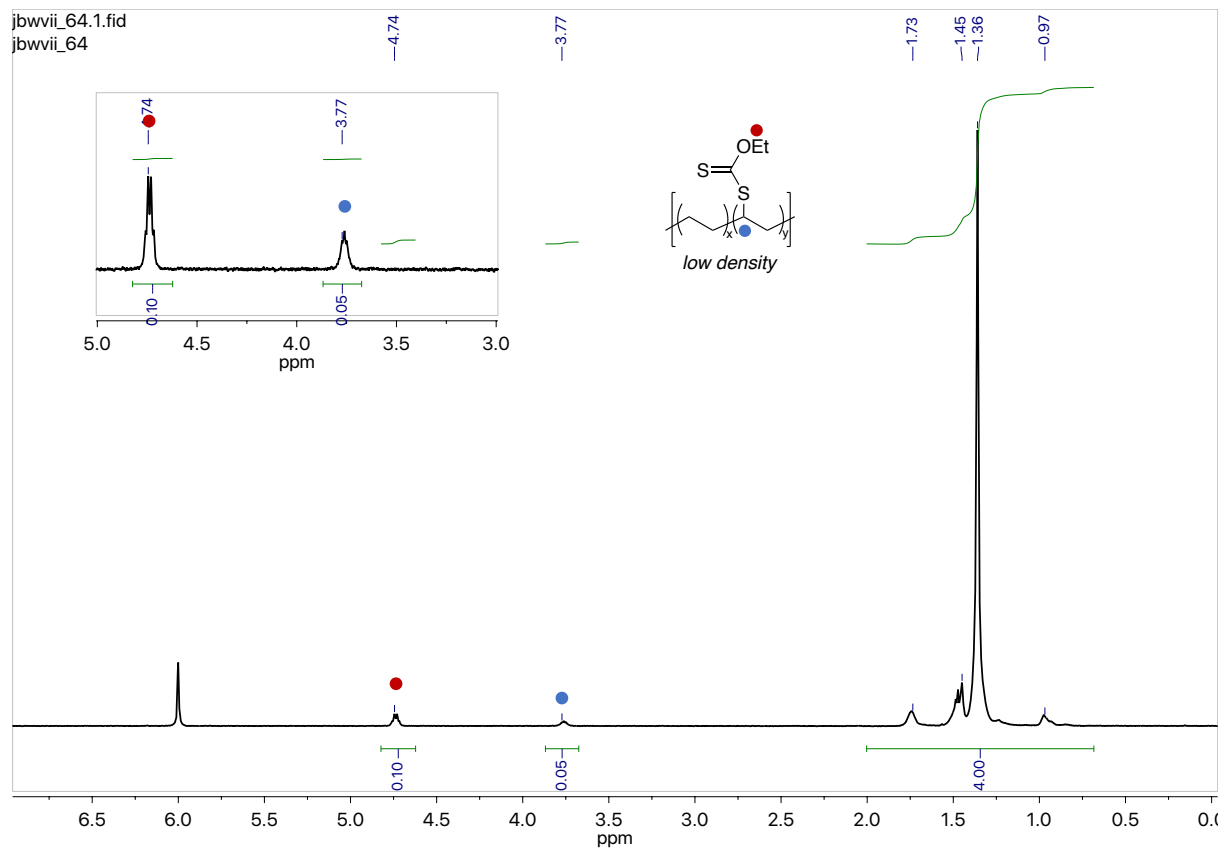
¹H NMR of xanthylated low density polyethylene at 110 °C in CD₂Cl₄ indicates successful incorporation of the polar moiety. The functionalization peak is present at δ 4.7 ppm, corresponding to the ethoxy methylene protons, and further evidence is provided at δ 3.8 ppm, corresponding to secondary polymeric protons *alpha* the xanthate group.
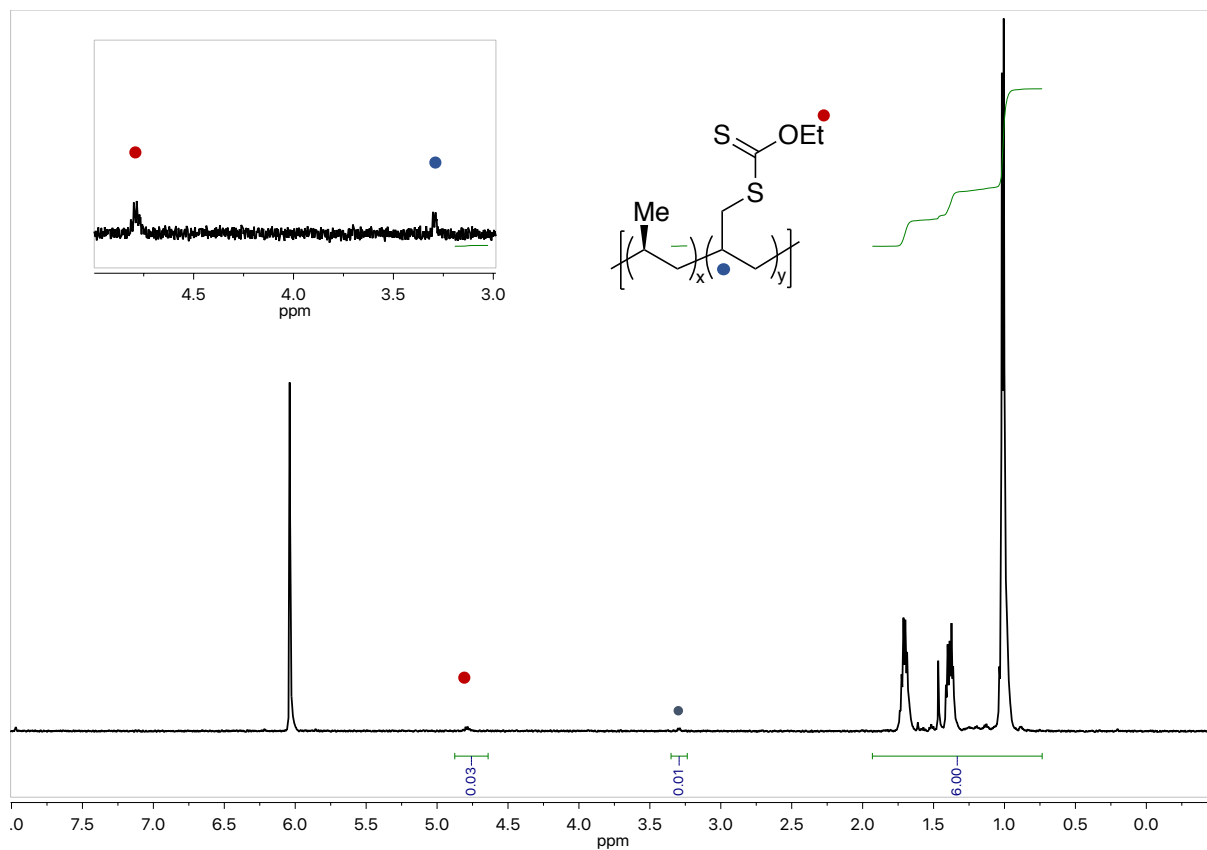
Xanthylation of polypropylene was proven by ^{1}H NMR at 110 °C in CD_2Cl_4. The methylene protons of the ethoxy unit were present at δ 4.8 ppm. The protons on the polymer that are *alpha* the xanthate moiety resonate at δ 3.4 ppm, suggesting xanthylation is only occurring at primary carbon sites. The ^{1}H NMRs of the products of reactive extrusion were identical to the one shown above.
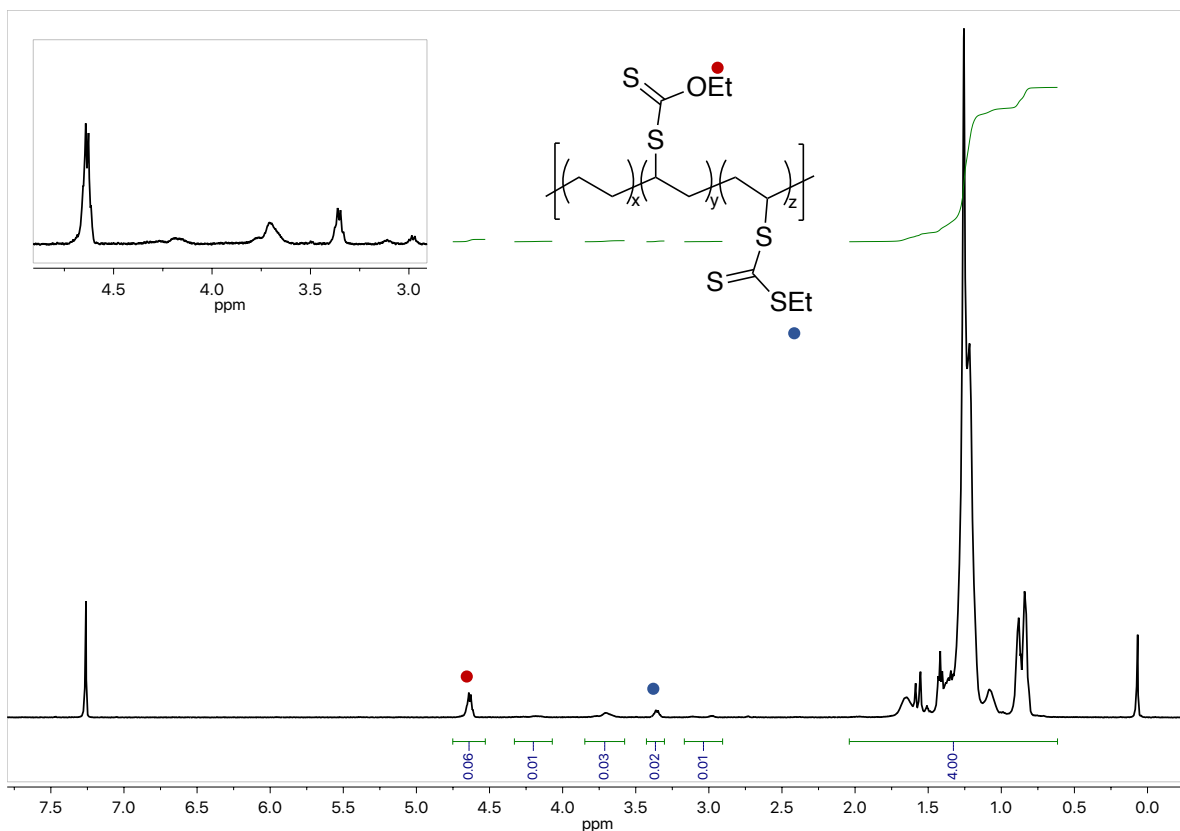
^{1}H NMR was taken of trithiocarbonylated and then xanthylated HBPE in CDCl$_3$. Initially, HBPE was functionalized at 3 mol% trithiocarbonylation, indicated by the peak at δ 3.3 ppm consistent with the methylene protons of the ethanethiol. Upon reacting trithiocarbonylated HBPE in a thermal C–H xanthylation reaction, the degree of trithiocarbonylation decreased from 3 to 1 mol% functionalization, seen in the peaks at 3.3 and 4.2 ppm. The reaction installed new xanthate moieties (3 mol%) with resonances at δ 3.0, 3.7, and 4.6 ppm. The removal of previously functionalized sites proves the reaction to be reversible at the functionalization step.
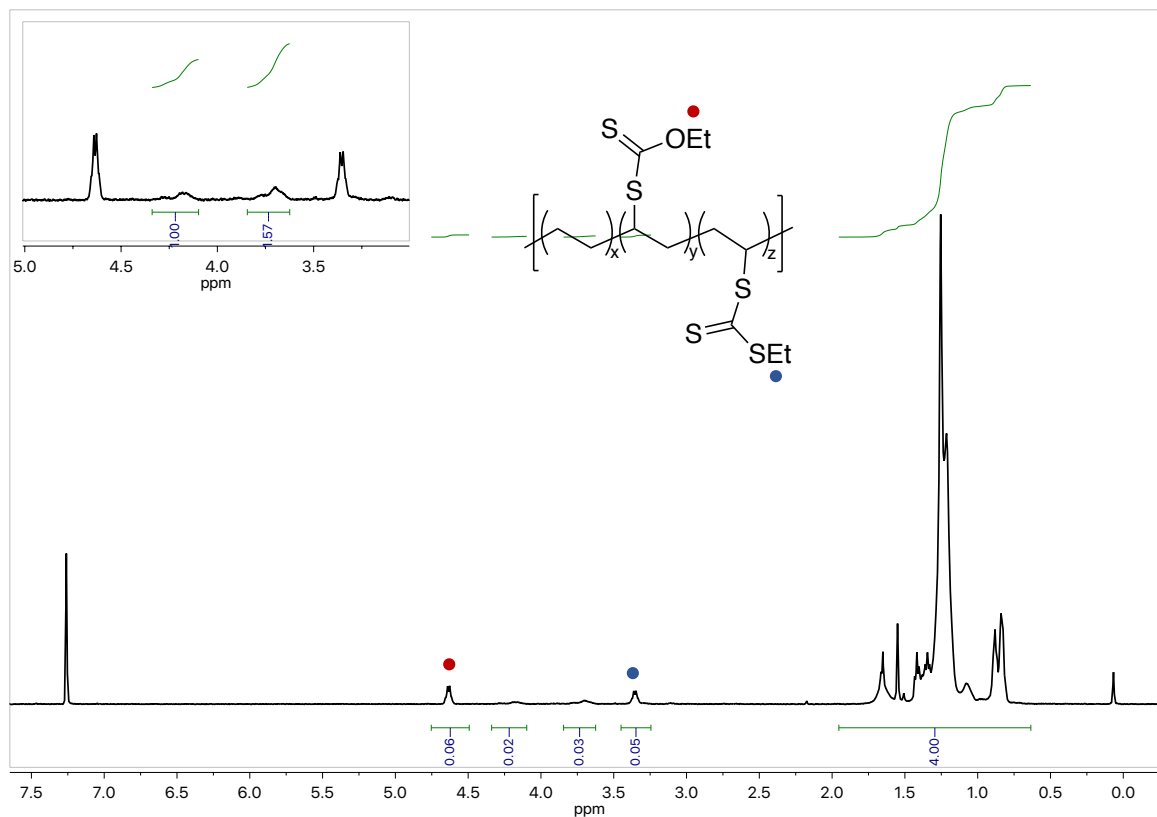
¹H NMR of xanthylated and then trithiocarbonylated HBPE in CDCl₃ was taken. Initially, HBPE was functionalized at 4.5 mol% xanthylation, indicated by the peak at δ 4.7 ppm consistent with the methylene protons of the ethoxy. Upon reacting xanthylated HBPE in a thermal C–H trithiocarbonylation reaction, the degree of xanthylation dropped from 4.5 to 3 mol% functionalization, seen through the peaks at δ 3.6 and 4.6 ppm. The reaction installed new trithiocarbonyl moieties (2.5 mol%) with resonances at δ 3.4 and 4.2 ppm. The removal of previously functionalized sites proves the reaction to be reversible at the functionalization step.
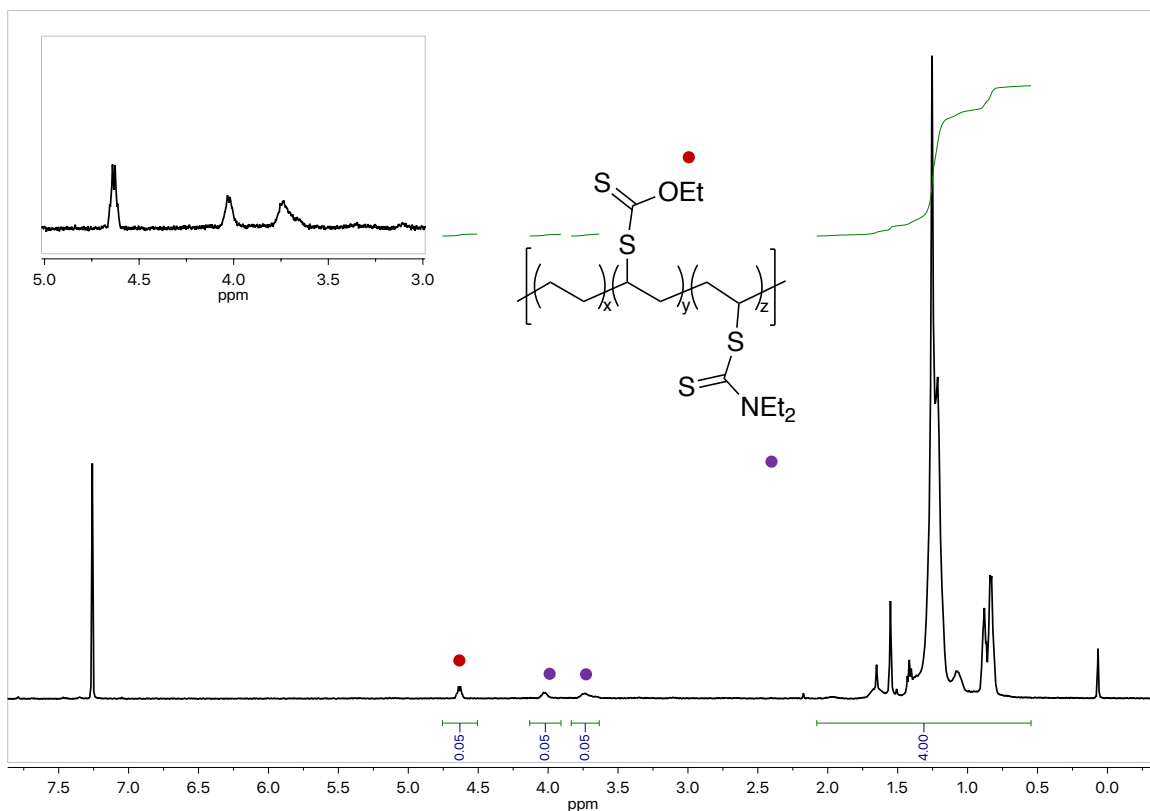
^{1}H NMR of xanthylated and then dithiocarbamylated HBPE in CDCl$_3$ was taken. Initially, HBPE was functionalized at 4.5 mol% xanthylation, indicated by the peak at δ 4.7 ppm consistent with the methylene protons of the ethoxy. Upon reacting xanthylated HBPE in a thermal C–H dithiocarbonylation reaction, the degree of xanthylation decreased from 4.5 to 2.5 mol% functionalization, seen through the peaks at δ 4.6 ppm. The reaction installed new dithiocarbamyl moieties (2.5 mol%) with resonances at δ 3.7 and 4.0 ppm. The removal of previously functionalized sites proves the reaction to be reversible at the functionalization step.
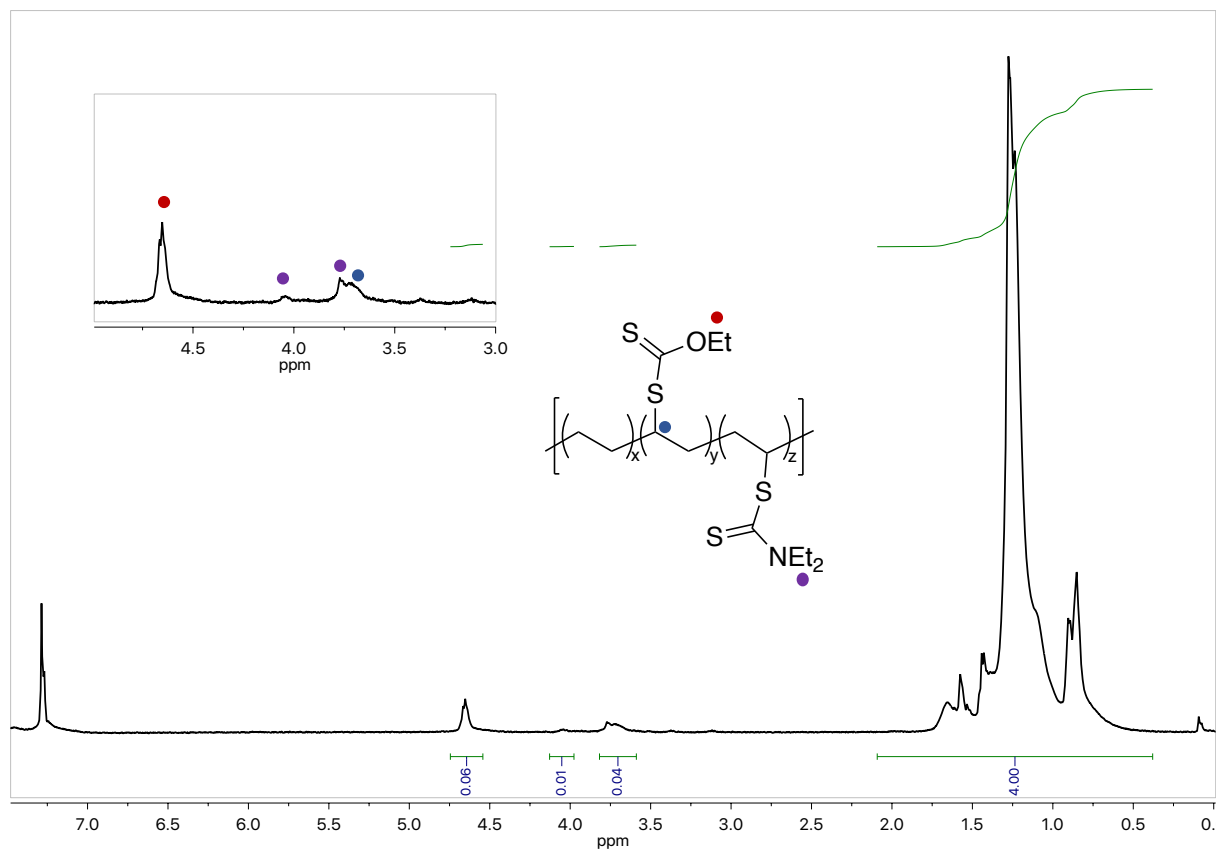
^{1}H NMR of dithiocarbamylated and then xanthylated HBPE in CDCl$_3$ was taken. Initially, HBPE was functionalized at 1 mol% dithiocarbamylated, indicated by the peaks at δ 3.7 and 4.0 ppm consistent with the methylene protons of the diethyl amine. Upon reacting dithiocarbamylated HBPE in a thermal C–H xanthylation reaction, the dithiocarbamylation decreased from 1 to 0.5 mol% functionalization, seen through the peaks at δ 3.7 and 4.0 ppm. The δ 3.7 peak was complicated by protons *alpha* xanthate also appearing in this region, so the peak at δ 4.0 ppm determined percent functionalization. The reaction installed new xanthate moieties (3 mol%) with resonances at δ 4.6 ppm. The removal of previously functionalized sites proves the reaction to be reversible at the functionalization step.

195.76

77.16 CDCl3

51.68
49.13
46.73

32.38
27.16
26.08
25.62

12.50
11.76

f1 (ppm)
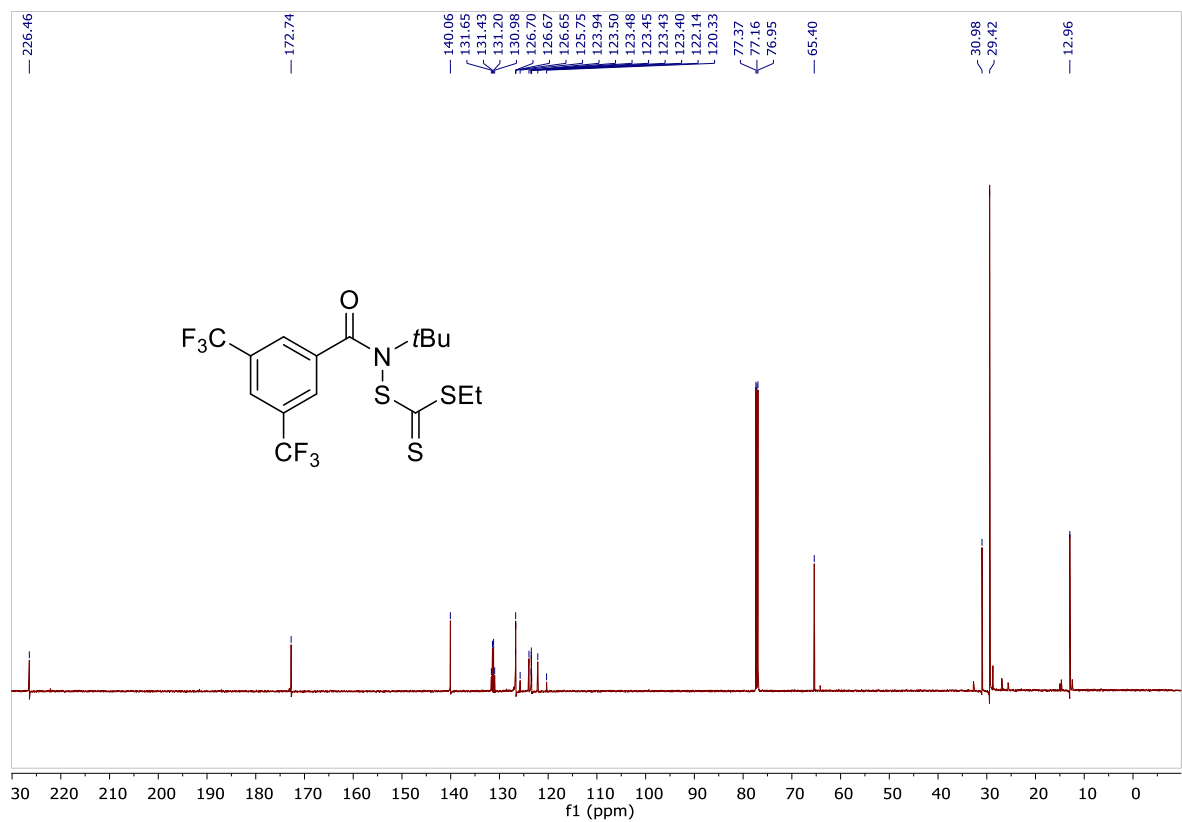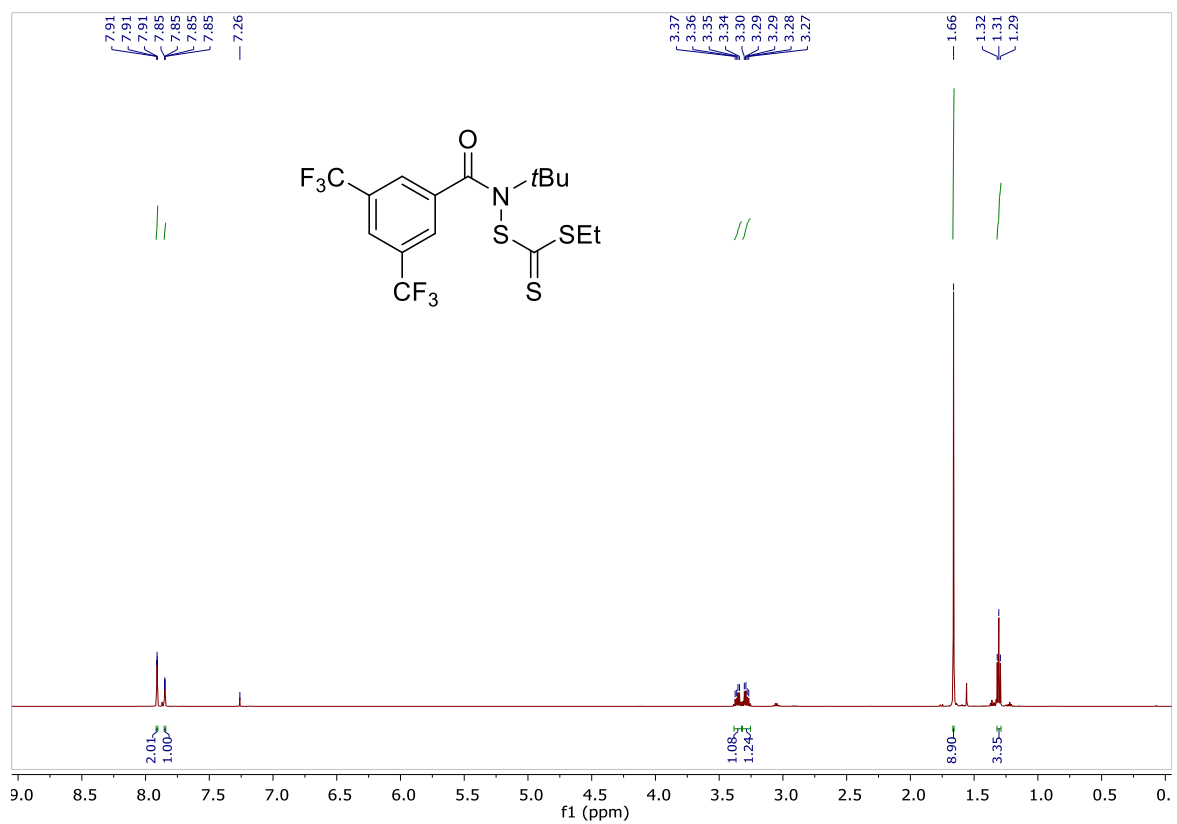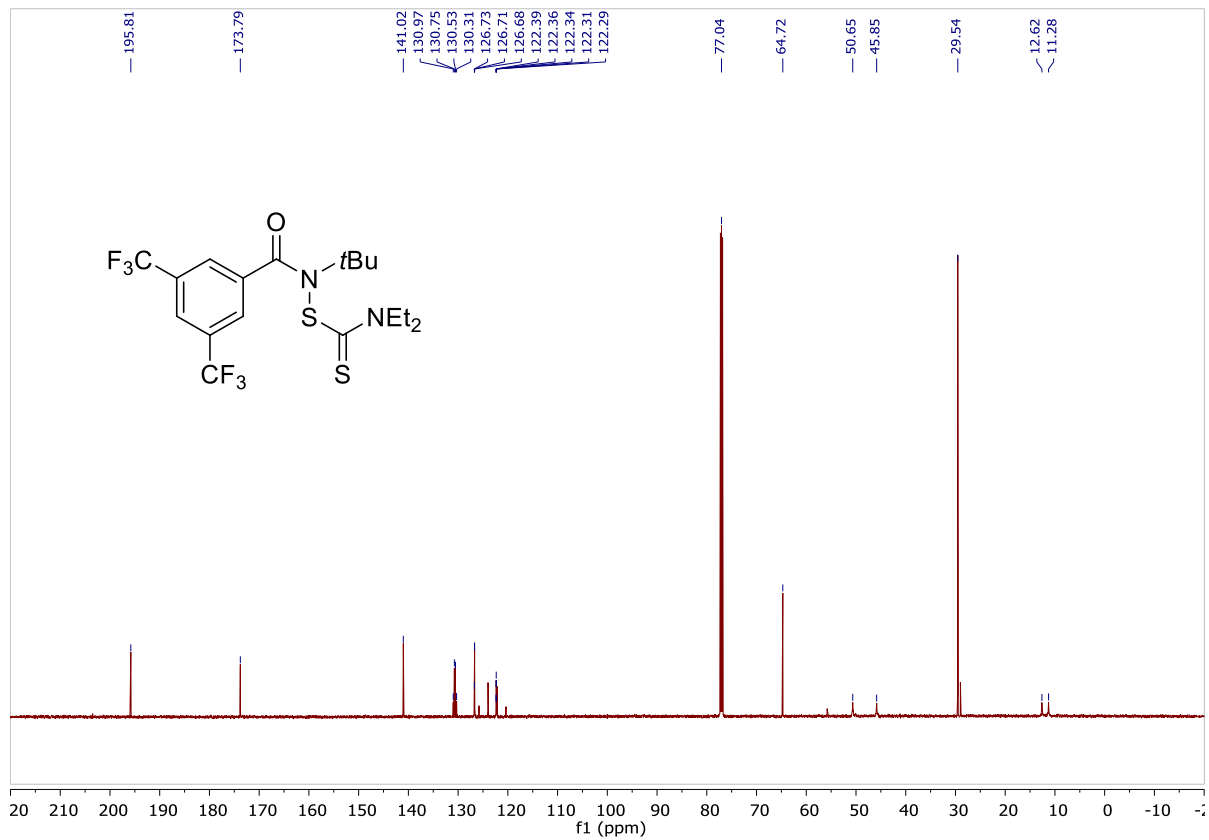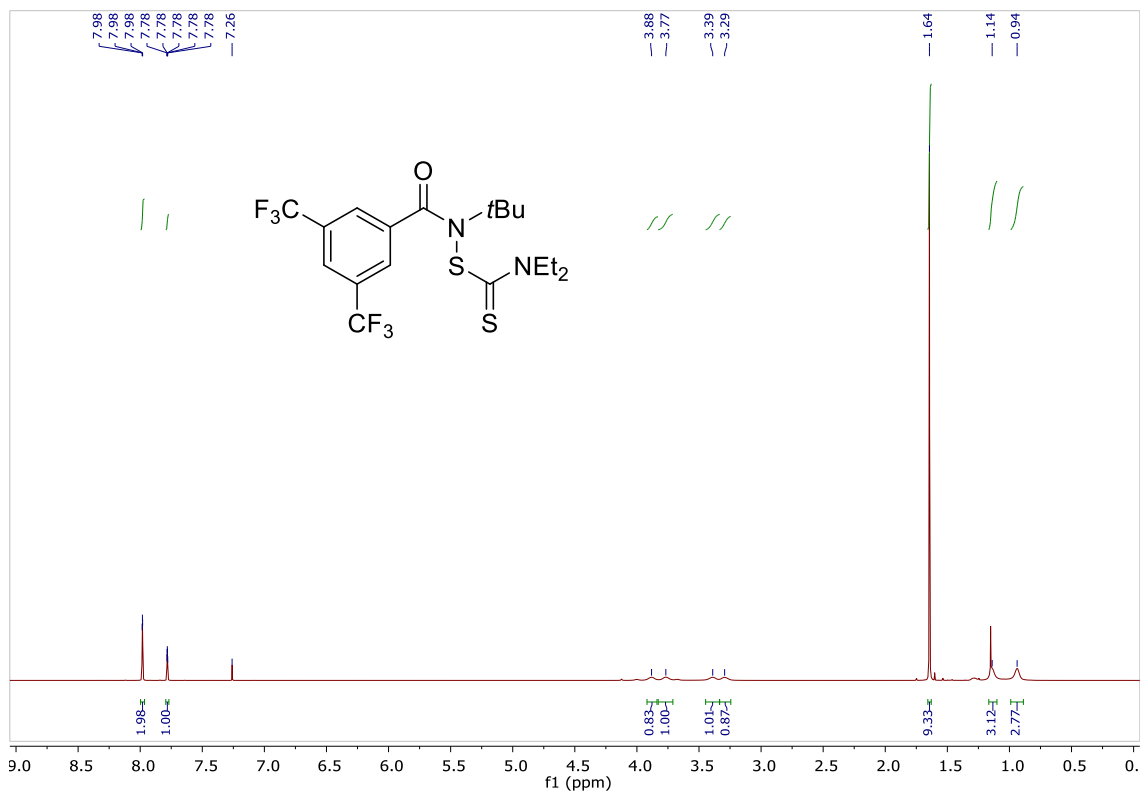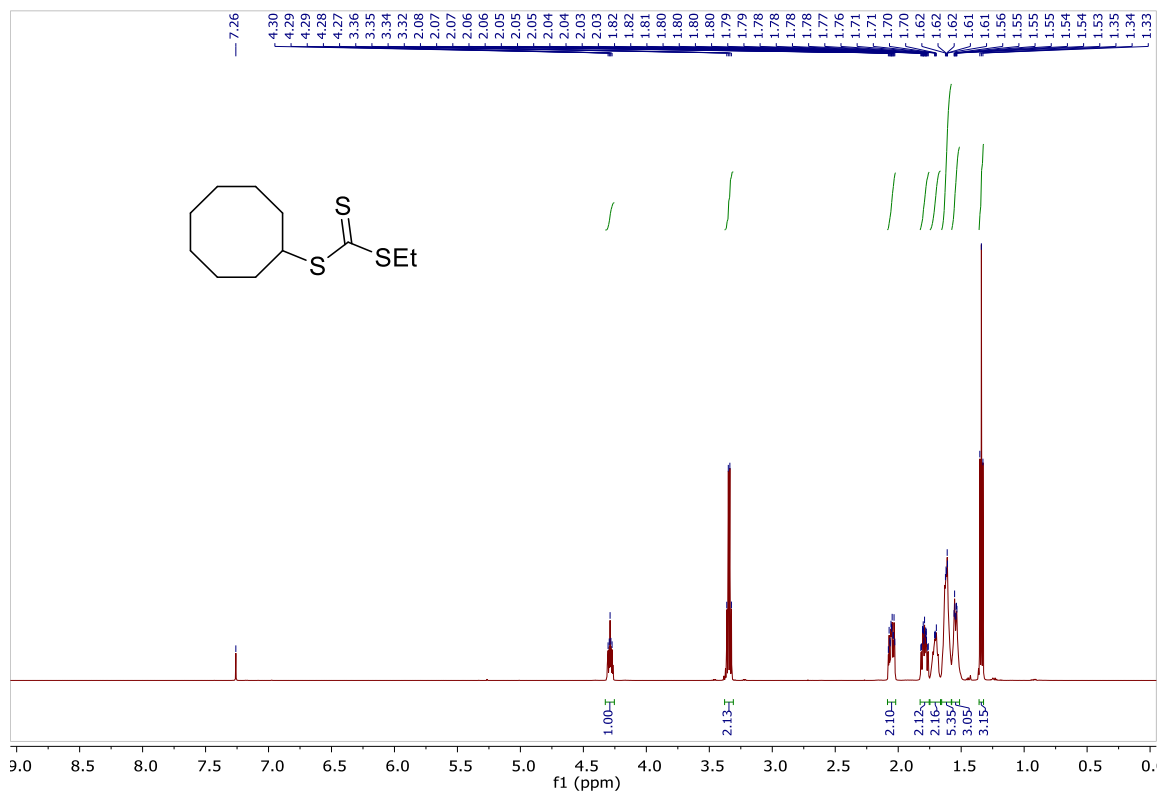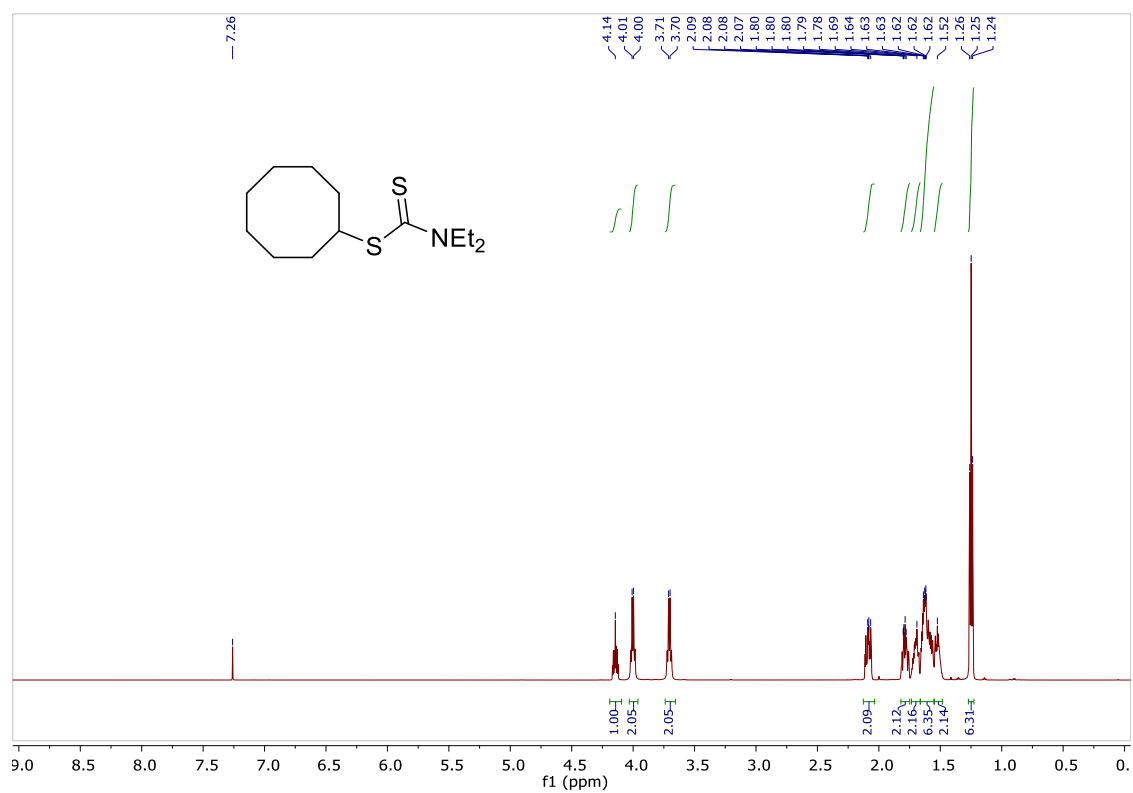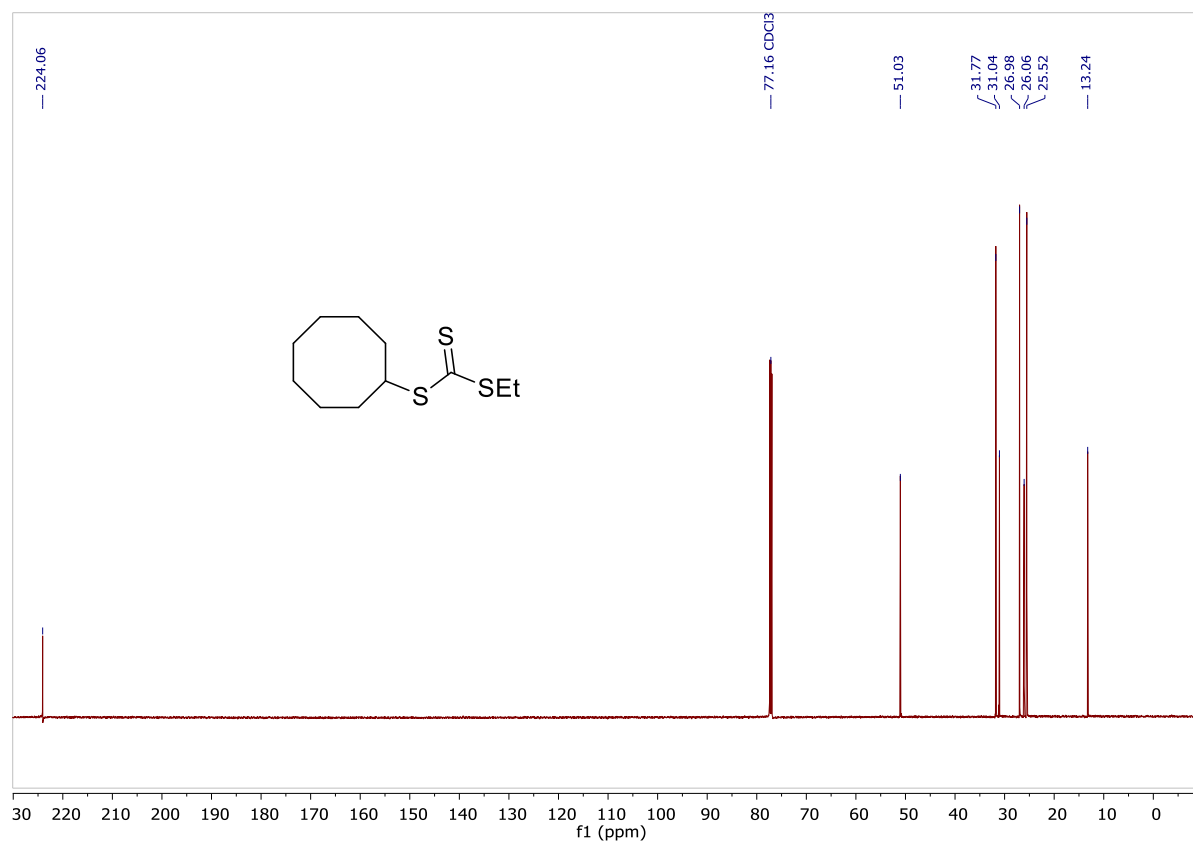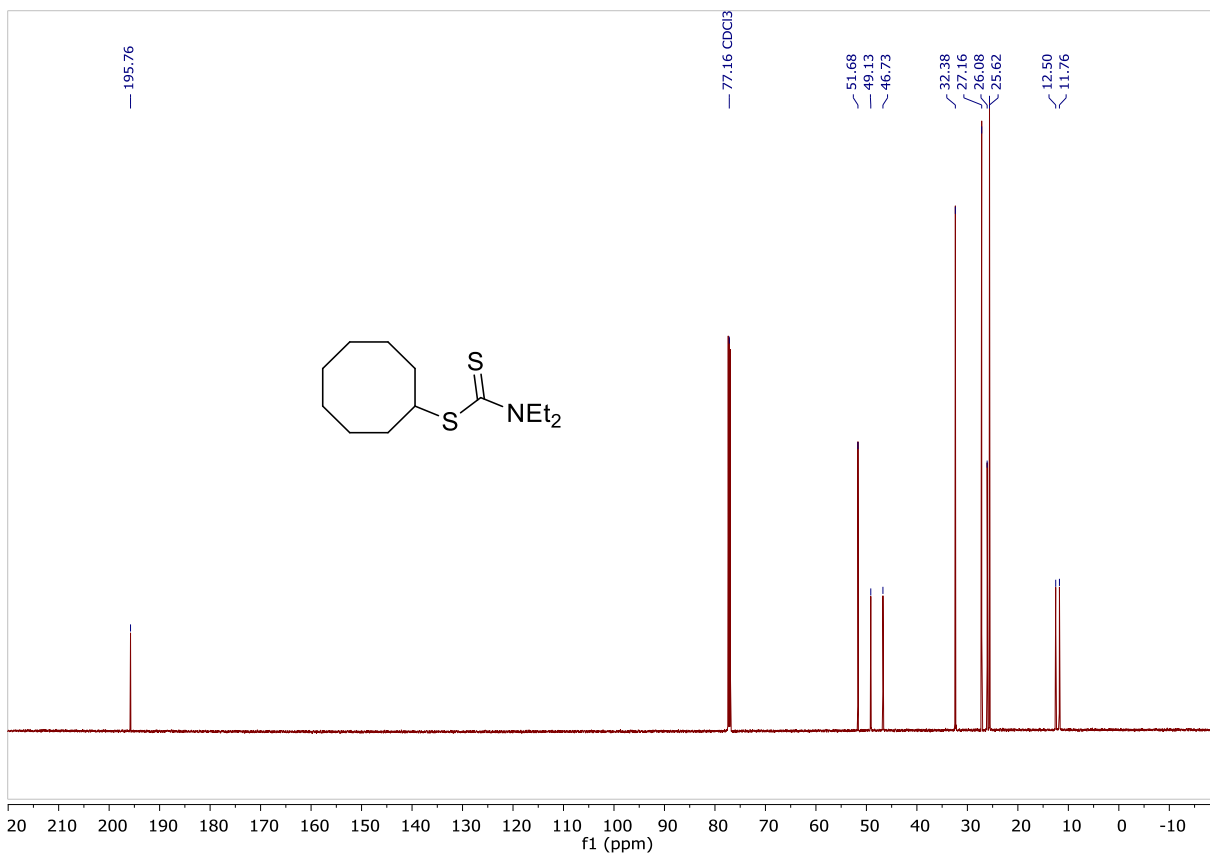
C.1 GENERAL METHODS AND MATERIALS

All post-polymerization modifications were performed under inert atmosphere using standard glove box and Schlenk-line techniques. Commercial polyolefins were obtained from their respective companies and purified prior to use by precipitation into methanol or acetone. The company and lot number are named in the individual procedures. 1,2-Dichlorobenzene was degassed with argon through multiple freeze-pump-thaw cycles. Chlorobenzene was distilled over calcium hydride, degassed through three freeze-pump-thaw cycles, and stored in a glove box. Reagents, unless otherwise specified, were purchased and used without further purification.

Proton, carbon, and fluorine magnetic resonance spectra (^{1}H NMR, ^{13}C NMR, and ^{19}F NMR) were recorded on a Bruker model DRX 400 MHz, Bruker 500 MHz, or Bruker AVANCE III 600 MHz CryoProbe spectrometer with solvent resonance as the internal standard (^{1}H NMR: CDCl$_3$ at 7.26 ppm; ^{13}C NMR: CDCl$_3$ at 77.16 ppm). ^{1}H NMR data are reported as follows: chemical shift, multiplicity (s = singlet, d = doublet, t = triplet, q = quartet, m = multiplet, dd = doublet of doublets, dt = doublet of triplets, bs = broad singlet), coupling constants (Hz), and integration. High temperature NMR (HT NMR) was recorded on a Bruker 500 MHz spectrometer at 110 °C with solvent resonance as the internal standard (^{1}H NMR: C$_2$D$_2$Cl$_4$ at 6.00 ppm; ^{13}C NMR: C$_2$D$_2$Cl$_4$ at 73.78 ppm). In all experiments, an ethylene glycol standard confirmed the temperature of the NMR, roughly 116 °C in all cases, and the delay time was set to 5 sec (d1 = 5). Infrared (IR) spectra were obtained using PerkinElmer Frontier FT-IR spectrometer. Thin layer chromatography (TLC) was performed on SiliaPlate 250μm thick silica gel plates provided by Silicycle. Visualization was accomplished with short wave

UV light (254 nm) and iodine. Flash chromatography was performed using a Biotage™ Isolera auto-column with silica gel purchased from Biotage. Light irradiation of reactions was performed using Kessil A160WE Tuna Blue LED Lights.

High temperature gel permeation chromatography (HT GPC) spectra were obtained using a Tosoh EcoSEC-HT GPC using TSKgel GMH_{HR}-M columns. Trichlorobenzene (TCB) with 200 ppm dibutylhydroxytoluene (BHT) was the mobile phase and the flow rate was set to 1 mL/min. The instrument was calibrated using polystyrene standards in the range of 580 to 5,480,000 Da. A calibration curve was created using refractive index detection against the polystyrene standards in 2 mg/mL solutions of trichlorobenzene (TCB) at 140 °C for polyethylenes. A tandem multi-angle light scattering (MALS) detector could also be employed on the HT GPC via a Wyatt DAWN 8 heated flow cell instrument.

Differential scanning calorimetry (DSC) was used to determine the thermal characteristics of the polyolefins using a TA Instruments DSC (Discovery Series). The DSC measurements were performed on 1 – 10 mg of polymer samples at a temperature ramp rate of 10 °C/min. Data was taken from the second thermal scanning cycle. Thermal gravimetric analysis (TGA) was obtained using a TA Instruments TGA (Discovery Series) in the temperature range of 40 – 600 °C at a temperature ramp rate of 10 °C/min. The temperature of decomposition (T_d) was defined by the temperature at which 10% of total mass was lost.

C.2 POLYMER C–H DIVERSIFICATION

General Polymer Procedure (130 °C): The polyolefin (40 mg) was pre-dissolved in 0.2 mL of chlorobenzene by heating the solution for 30 min at 130 °C with magnetic stirring. The pre-dissolved polyolefin, amidyl reagent, and radical trap were then combined in a 1-dram reaction

vial and diluted with 0.5 mL of chlorobenzene in a nitrogen-filled glovebox. The vial was equipped with a magnetic stir bar under inert atmosphere and sealed with electrical tape. The reaction was heated and stirred on a magnetic stir plate at the desired temperature. After completion of the reaction, the solution was precipitated into acetone and collected via Büchner filtration with nylon filter paper to yield the functionalized commodity polyolefins.
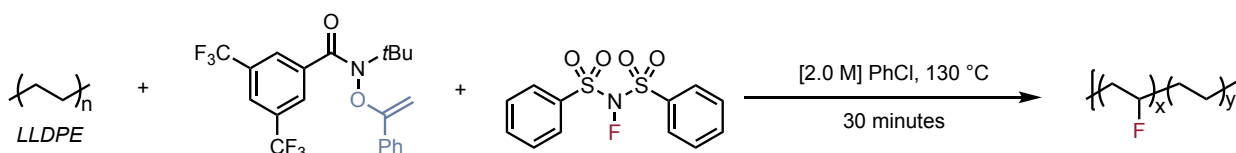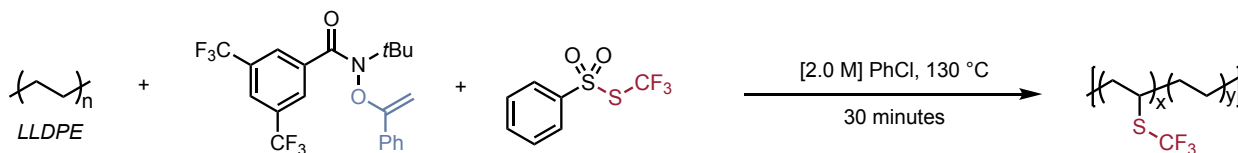

Fluorinated LLDPE (P1): DOW™ DNDA-1081 NT 7 Linear Low Density Polyethylene Resin, (1-phenylvinyloxy)amide, and *N*-fluorobenzenesulfonimide were reacted according to General Procedure I. LLDPE (RI M_n = 19 kg/mol, RI Đ = 4.76, MALS dn/dc = 0.105, M_n = 1.58 x 10^4 g/mol ± 3.74%, MALS Đ = 2.97 ± 3.77%, 19% branched, 40 mg, 0.143 mmol) reacted with (1-phenylvinyloxy)amide (62 mg, 0.14 mmol) and *N*-fluorobenzenesulfonimide (90 mg, 0.28 mmol) in chlorobenzene (0.7 mL) upon heating at 130 °C for 30 min. The resultant material (26 mg) was 5 mol % fluorinated LLDPE. Collection of the filtrate revealed 85% conversion of the functionalized amide to the parent amide by ^{19}F NMR.

The following was gathered using 5 mol % fluorinated LLDPE:

^{1}H NMR (500 MHz, C$_2$D$_2$Cl$_4$, 110 °C) δ 4.60 (bs), 4.50 (bs), 1.73 (bs), 1.56 (bs), 1.41 (bs), 1.02 (bs). **^{19}F NMR (400 MHz, C$_2$D$_2$Cl$_4$, 80 °C)** δ −179.53 (bs). **IR (neat, ATR, cm^{-1})** 2917, 2850, 1472, 1374, 1279, 1169, 1140, 1087, 1069, 1000, 864, 750, 719. **GPC (TCB, 140 °C):** RI M_n = 17 kg/mol, RI Đ = 4.76; MALS dn/dc = 0.105, M_n = 2.96 x 10^4 g/mol ± 3.38%,

MALS $Đ = 3.58 \pm 3.42\%$. **TGA (°C)** parent $T_d = 428$, product $T_d = 294$. **DSC (°C):** parent T_m = 125 with 41% crystallinity ($\Delta H = 122$ J/g), product $T_m = 112$ with 30% crystallinity ($\Delta H = 86$ J/g).

Determination of percent fluorination of LLDPE: Upon purification, the percent fluorination of LLDPE can be determined through integration of the ^{1}H NMR. Considering the composition of the polymer, the peaks between 0.8 – 2.0 ppm were set to total to 4 protons. The protons *alpha* the incorporated fluorine group that appear between 4.4–4.6 ppm are used to determine mol % fluorination per repeat unit. Only secondary C–H fluorination was observed.
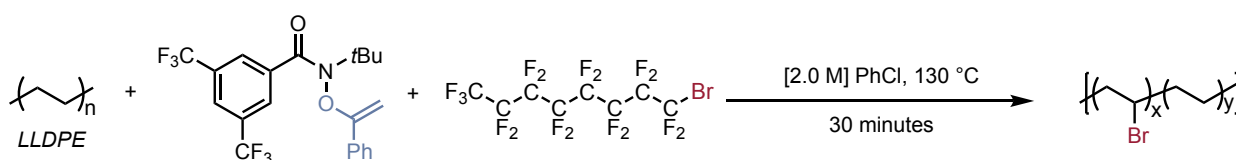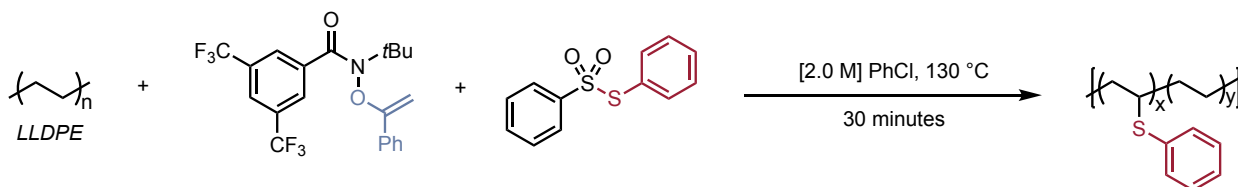

Brominated LLDPE (P2): DOW™ DNDA-1081 NT 7 Linear Low Density Polyethylene Resin, (1-phenylvinyloxy)amide, and 1-bromoheptadecafluorooctane were reacted according to General Procedure I. LLDPE ($M_n = 19$ kg/mol, $Đ = 4.76$, 19% branched, 40 mg, 1.4 mmol) reacted with (1-phenylvinyloxy)amide (62 mg, 0.14 mmol) and 1-bromoheptadecafluorooctane (74 µL, 0.29 mmol) in chlorobenzene (0.4 mL) upon heating at 130 °C for 30 min. The resultant material (30 mg) was 4 mol % brominated LLDPE. Collection of the filtrate revealed 77% conversion of the functionalized amide to the parent amide by ^{19}F NMR.

The following was gathered using 4 mol % brominated LLDPE:

¹H NMR (500 MHz, C₂D₂Cl₄, 110 °C) δ 4.11 (bs), 1.89 (bs), 1.61 (bs), 1.46 (bs), 1.35 (bs), 0.96 (bs). **IR (neat, ATR, cm⁻¹):** 2916, 2849, 1464, 1463, 1242, 1240, 1142, 813, 722, 719.

GPC (TCB, 140 °C) M_n = 20 kg/mol, Đ = 4.58. **TGA (°C)** parent T_d = 428, product T_d = 270.

DSC (°C): parent T_m = 125 with 41% crystallinity (ΔH = 122 J/g), product T_m = 119 with 18% crystallinity (ΔH = 53.2 J/g).

Determination of percent bromination of LLDPE: Upon purification, the percent bromination of LLDPE can be determined through integration of the ¹H NMR. Considering the composition of the polymer, the peaks between 0.8 – 2.0 ppm were set to total to 4 protons. The protons *alpha* the incorporated bromine group that appear at 4.1 ppm are used to determine mol % bromination per repeat unit. Only secondary C–H bromination was observed.
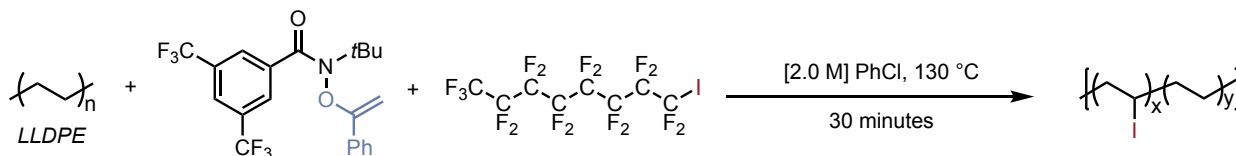
Iodinated LLDPE (P3): DOW™ DNDA-1081 NT 7 Linear Low Density Polyethylene Resin, (1-phenylvinyloxy)amide, and 1-iodoperfluorooctane were reacted according to General Polymer Procedure. LLDPE (M_n = 19 kg/mol, Đ = 4.76, 19% branched, 40 mg, 1.43 mmol) reacted with (1-phenylvinyloxy)amide (62 mg, 0.14 mmol) and 1-iodoperfluorooctane (81 µL, 0.29 mmol) in chlorobenzene (0.7 mL) upon heating at 130 °C for 30 min. The resultant material (39 mg) was 4 mol % iodinated LLDPE. Collection of the filtrate revealed 79% conversion of the functionalized amide to the parent amide by ¹⁹F NMR.

The following was gathered using 4 mol % iodinated LLDPE:

¹H NMR (500 MHz, C₂D₂Cl₄, 110 °C) δ 4.21 (bs), 1.95 (bs), 1.79 (bs), 1.57 (bs), 1.44 (bs), 1.36 (bs), 0.98 (bs). **IR (neat, ATR, cm⁻¹)** 2916, 2848, 1644, 1549, 1463, 1367, 1241, 1219, 1178, 1154, 1146, 907, 720. **GPC (TCB, 140 °C):** M_n = 22 kg/mol, $Đ$ = 4.19. **TGA (°C)** parent T_d = 428, product T_d = 225 (T_{d1} = 194, T_{d2} = 318). **DSC (°C):** parent T_m = 125 with 41% crystallinity (ΔH = 122 J/g), product T_m = 95 with 21% crystallinity (ΔH = 63 J/g).

Determination of percent iodination of LLDPE: Upon purification, the percent iodination of LLDPE can be determined through integration of the ¹H NMR. Considering the composition of the polymer, the peaks between 0.8 – 2.0 ppm were set to total to 4 protons. The protons *alpha* the incorporated iodo group that appear between 4.15 – 4.3 ppm are used to determine mol % iodination per repeat unit. Only secondary C–H iodination was observed.

Trifluoromethylthiolated LLDPE (P4): DOW™ DNDA-1081 NT 7 Linear Low Density Polyethylene Resin, (1-phenylvinyloxy)amide, and *S*-(trifluoromethyl) benzenesulfonothioate were reacted according to General Polymer Procedure. LLDPE (M_n = 19 kg/mol, $Đ$ = 4.76, 19% branched, 15 mg, 0.54 mmol) reacted with (1-phenylvinyloxy)amide (23 mg, 0.05 mmol) and *S*-(trifluoromethyl) benzenesulfonothioate (26 mg, 0.11 mmol) in chlorobenzene (0.4 mL) upon heating at 130 °C for 30 min. The resultant material (10 mg) was 3 mol % trifluoromethylthiolated LLDPE. Collection of the filtrate revealed 91% conversion of the functionalized amide to the parent amide by ¹⁹F NMR.

The following was gathered using 3 mol % trifluoromethylthiolated LLDPE:

¹H NMR (500 MHz, C₂D₂Cl₄, 110 °C) δ 3.25 (bs), 1.79 (bs), 1.61 (bs), 1.55 (bs), 1.49 (bs), 1.41 (bs), 1.02 (bs). **¹⁹F NMR (400 MHz, C₂D₂Cl₄, 80 °C)** δ –41.00, –39.87, –39.85. **IR (neat, ATR, cm⁻¹)** 2917, 2849, 1648, 1549, 1464, 1367, 1280, 1277, 1148, 1107, 907, 731, 720 . **GPC (TCB, 140 °C):** M_n = 22 kg/mol, $Đ$ = 7.74. **TGA (°C)** parent T_d = 428, product T_d = 317. **DSC (°C):** parent T_m = 125 with 41% crystallinity (ΔH = 122 J/g), product T_m = 103 with 12% crystallinity (ΔH = 35.2 J/g).

Determination of percent trifluoromethylthiolation of LLDPE: Upon purification, the percent trifluoromethylation of LLDPE can be determined through integration of the ¹H NMR. Considering the composition of the polymer, the peaks between 0.8 – 2.0 ppm were set to total to 4 protons. The protons *alpha* the incorporated trifluoromethylthiol group that appear between 3.2 – 3.3 ppm are used to determine mol % trifluoromethylthiolation per repeat unit. Only secondary C–H trifluoromethylthiolation was observed.

Thiophenolated LLDPE (P5): DOW™ DNDA-1081 NT 7 Linear Low Density Polyethylene Resin, (1-phenylvinyloxy)amide, and *S*-phenyl benzenesulfonothioate were reacted according to General Procedure I. LLDPE (M_n = 19 kg/mol, $Đ$ = 4.76, 19% branched, 40 mg, 1.43 mmol) reacted with (1-phenylvinyloxy)amide (62 mg, 0.14 mmol) and *S*-phenyl benzenesulfonothioate (72 mg, 0.29 mmol) in chlorobenzene (0.7 mL) upon heating at 130 °C for 30 min. The resultant material (42 mg) was 7 mol % functionalized LLDPE. Collection of the filtrate revealed 90% conversion of the functionalized amide to the parent amide by ¹⁹F

NMR. Employing phenyl disulfide or 2-(phenyldisulfaneyl)pyridine instead of *S*-phenyl benzenesulfonothioate yielded products with similar NMR peaks and GPC traces of 3 mol % and 4 mol % materials, respectively.

The following was gathered using 7 mol % thiophenolated LLDPE:

^{1}H NMR (500 MHz, C$_2$D$_2$Cl$_4$, 110 °C) δ 7.52 (bs), 7.37 (bs), 7.30 (bs), 3.19 (bs), 1.74 (bs), 1.62 (bs), 1.61 (bs), 1.45 (bs), 1.37 (bs), 1.04 (bs). **IR (neat, ATR, cm^{-1}):** 2917, 2849, 1586, 1464, 1439, 1279, 1149, 1026, 721, 694, 691. **GPC (TCB, 140 °C):** $M_n = 22$ kg/mol, $Đ = 4.34$. **TGA (°C)** parent $T_d = 428$, product $T_d = 317$. **DSC (°C):** parent $T_m = 125$ with 42% crystallinity ($\Delta H = 122$ J/g), product $T_m = 55$ with 10% crystallinity ($\Delta H = 28$ J/g).

Determination of percent thiophenolation of LLDPE: Upon purification, the percent thiophenolation of LLDPE can be determined through integration of the ^{1}H NMR. Considering the composition of the polymer, the peaks between 0.8 – 2.0 ppm were set to total to 4 protons. The protons *alpha* the incorporated thiophenol group that appear at 3.2 ppm are used to determine mol % thiophenolation per repeat unit. The aromatic region between 7.30 – 7.55 ppm were integrated and divided by 5 to confirm the percent incorporation concluded from the *alpha* protons. Only secondary C–H functionalization was observed.

Azidated LLDPE (P6): DOW™ DNDA-1081 NT 7 Linear Low Density Polyethylene Resin, (1-phenylvinyloxy)amide, and benzenesulfonyl azide were reacted according to General

Procedure I. LLDPE (M_n = 19 kg/mol, Đ = 4.76, 19% branched, 20 mg, 0.71 mmol) reacted with (1-phenylvinyloxy)amide (31 mg, 0.071 mmol) and benzenesulfonyl azide (26 mg, 0.14 mmol) in chlorobenzene (0.4 mL) upon heating at 130 °C for 30 min. The resultant material (14 mg) was 4 mol % azidated LLDPE. Collection of the filtrate revealed 86% conversion of the functionalized amide to the parent amide by ^{19}F NMR. Increasing the stoichiometry of the reagents increased the percent incorporation of the azide group.

The following was gathered using 4 mol % azidated LLDPE:

¹H NMR (500 MHz, C₂D₂Cl₄, 110 °C) δ 3.34 (bs), 1.64 (bs), 1.49 (bs), 1.40 (bs), 1.02 (bs). **IR (neat, ATR, cm⁻¹)** 2917, 2849, 2097, 1464, 1342, 1278, 1247, 1142, 720. **GPC (TCB, 140 °C)** M_n = 20 kg/mol, Đ = 3.78. **TGA (°C)** parent T_d = 428, product T_d = 377. **DSC (°C):** parent T_m = 125 with 41% crystallinity (ΔH = 122 J/g), product T_m = 98 with 10% crystallinity (ΔH = 31 J/g).

Determination of percent azidation of LLDPE: Upon purification, the percent azidation of LLDPE can be determined through integration of the ¹H NMR. Considering the composition of the polymer, the peaks between 0.8 – 2.0 ppm were set to total to 4 protons. The protons *alpha* the incorporated azide group that appear at 3.3 ppm are used to determine mol % azidation per repeat unit.

179
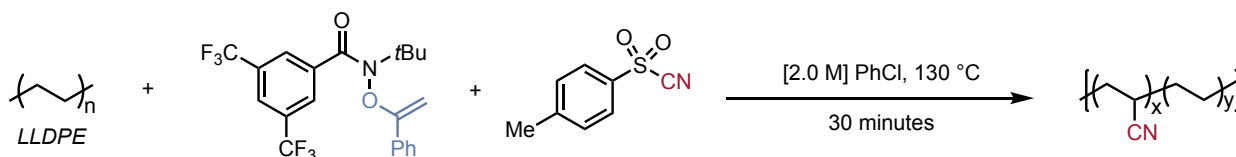
Cyanated LLDPE (P7): DOW™ DNDA-1081 NT 7 Linear Low Density Polyethylene Resin, (1-phenylvinyloxy)amide, and tosyl cyanide were reacted according to General Procedure I. LLDPE (M_n = 19 kg/mol, Đ = 4.76, 19% branched, 40 mg, 1.43 mmol) reacted with (1-phenylvinyloxy)amide (120 mg, 0.29 mmol) and tosyl cyanide (100 mg, 0.57 mmol) in chlorobenzene (0.7 mL) upon heating at 130 °C for 30 min. The resultant material was 7 mol % cyanated LLDPE (36 mg). Similar characterization data was obtained using other stoichiometric ratios of (1-phenylvinyloxy)amide and tosyl cyanide to repeat unit (see Table C.1 for exact conditions). See accompanying tables and figures for more information.

The following was gathered using 7 mol % cyanated LLDPE:

^{1}H NMR (500 MHz, C$_2$D$_2$Cl$_4$, 110 °C) δ 2.58 (bs), 1.71 (bs), 1.64 (bs), 1.56 (bs), 1.41 (bs), 1.02 (bs). **^{13}C NMR (101 MHz, C$_2$D$_2$Cl$_4$, 80 °C)** δ 122.5, 74.3, 74.1, 73.8, 32.4, 32.2, 31.8, 31.6, 29.8, 29.6, 29.2, 27.3, 27.2, 26.9, 23.1, 14.2, 14.2. **IR (neat, ATR, cm^{-1})** 2918, 2850, 2237, 1467, 1378, 720. **GPC (TCB, 140 °C)** M_n = 21 kg/mol, Đ = 3.98. **TGA (°C)** parent T_d = 428, product T_d = 339. **DSC (°C):** parent T_m = 125 with 42% crystallinity (ΔH = 122 J/g), product T_m = 96 with 2% crystallinity (ΔH = 6 J/g).

Determination of percent cyanation of LLDPE: Upon purification, the percent cyanation of LLDPE can be determined through integration of the ^{1}H NMR. Considering the composition of the polymer, the peaks between 0.8 – 2.0 ppm were set to total to 4 protons. The protons *alpha* the incorporated cyano group that appear at 2.6 ppm are used to determine mol % cyanation per repeat unit. Only secondary C–H cyanation was observed in all cases.

Reagent Loading	% conversion	% functionalization	M_n	Đ

(r.u.:amide: trap)				
10:1:2	90%	7 mol %	19	3.93
10:1:2	88%	6 mol %	20	4.78
10:1:2	--	4 mol %	20	4.50
10:1:2	--	5 mol %	20	4.38
5:1:2	85%	11 mol %	25	3.55
5:1:2	90%	7 mol %	21	3.85
5:1:2	--	7 mol %	21	3.98
2:1:2	87%	13 mol %	31	3.11
2:1:2	82%	16 mol %	42	2.63
1:1:2	82%	13 mol %	38	2.80

Table C.1 Cyanation of LLDPE at various target functionalizations dictated by the stoichiometry of the reagents. r.u. = repeat unit of the polyolefin. Percent conversion was determined by ^{19}F NMR. Percent functionalization was determined by ^{1}H NMR. Molecular weight (M_n) and dispersity ($Đ$) were determined by HT GPC.
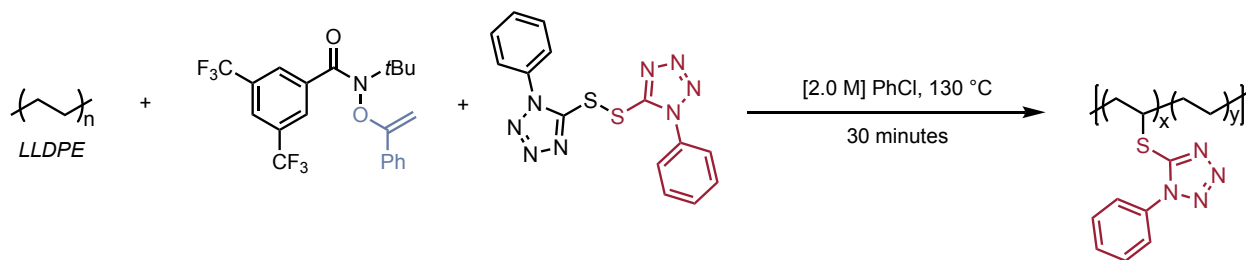
Phenyl tetrazole LLDPE (P8): DOW™ DNDA-1081 NT 7 Linear Low Density Polyethylene Resin, (1-phenylvinyloxy)amide, and phenyl tetrazole dimer were reacted according to General Polymer Procedure. LLDPE (M_n = 19 kg/mol, Đ = 4.76, 19% branched, 20 mg, 0.71 mmol) reacted with (1-phenylvinyloxy)amide (31 mg, 0.071 mmol) and phenyl tetrazole dimer (51 mg, 0.14 mmol) in chlorobenzene (0.4 mL) upon heating at 130 °C for 30 min. The resultant material (14 mg) was 2 mol % phenyl tetrazolated LLDPE. Collection of the filtrate revealed 82% conversion of the functionalized amide to the parent amide by ^{19}F NMR.

The following was gathered using 2 mol % phenyl tetrazolated LLDPE:

¹H NMR (500 MHz, C₂D₂Cl₄, 110 °C) δ 7.63 (bs), 3.96 (bs), 1.83 (bs), 1.46 (bs), 1.35 (bs), 0.96 (bs). **IR (neat, ATR, cm⁻¹)** 2916, 2849, 1599, 1500, 1462, 1394, 1386, 1245, 1238, 1074, 1073, 1017, 1015, 979, 911, 758, 719, 694. **GPC (TCB, 140 °C):** M_n = 21 kg/mol, Đ = 5.58. **TGA (°C)** parent T_d = 428, product T_d = 229 (T_{d1} = 141, T_{d2} = 373). **DSC (°C):** parent T_m = 125 with 41% crystallinity (ΔH = 122 J/g), product T_m = 91 with 6% crystallinity (ΔH = 17 J/g).

Determination of percent phenyl tetrazolation of LLDPE: Upon purification, the percent phenyl tetrazolation of LLDPE can be determined through integration of the ¹H NMR. Considering the composition of the polymer, the peaks between 0.8 – 2.0 ppm were set to total to 4 protons. The protons *alpha* the incorporated thioether group that appear between 3.9 – 4.0

ppm are used to determine mol % phenyl tetrazole per repeat unit. These protons were in agreement with the aromatic protons observed around 7.6 ppm.
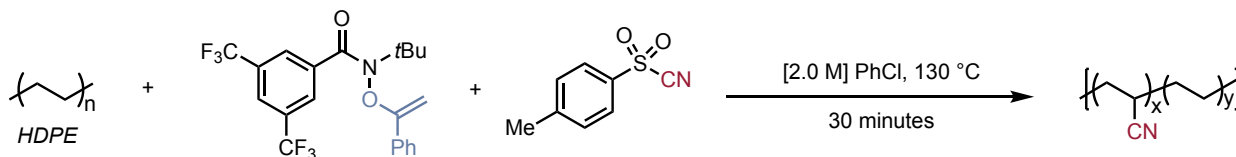
Cyanated HDPE (P9): ExxonMobil™ High Density Polyethylene, (1-phenylvinyloxy)amide, and tosyl cyanide were reacted according to General Procedure I. HDPE (M_n = 32 kg/mol, Đ = 4.27, 0% branched, 40 mg, 1.43 mmol) reacted with (1-phenylvinyloxy)amide (62 mg, 0.14 mmol) and tosyl cyanide (52 mg, 0.28 mmol) in chlorobenzene (0.7 mL) upon heating at 130 °C for 30 min. The resultant material (22 mg) was 5 mol % cyanated HDPE as whitish flakes. Collection of the filtrate revealed 84% conversion of the functionalized amide to parent amide by ^{19}F NMR.

The following was gathered using 5 mol % cyanated HDPE:

^{1}H NMR (500 MHz, C$_2$D$_2$Cl$_4$, 110 °C) δ 2.58 (bs), 1.67 (bs), 1.40 (bs), 1.01 (bs). **IR (neat, ATR, cm^{-1})** 2916, 2849, 2240, 1473, 1463, 723. **GPC (TCB, 140 °C)** M_n = 28 kg/mol, Đ = 5.24. **TGA (°C)** parent T_d = 433, product T_d = 320. **DSC (°C):** parent T_m = 129 with 62% crystallinity (ΔH = 183 J/g), product T_m = 105 with 20% crystallinity (ΔH = 59 J/g).

Determination of percent cyanation of HDPE: Upon purification, the percent cyanation of HDPE can be determined through integration of the ^{1}H NMR. Considering the composition of the polymer, the peaks between 0.8 – 2.0 ppm were set to total to 4 protons. The protons *alpha*

the incorporated cyano group that appear at 2.6 ppm are used to determine mol % cyanation per repeat unit. Only secondary C–H cyanation was observed.
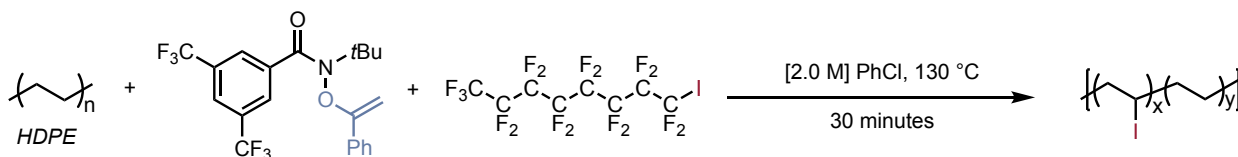

Iodinated HDPE (P10): ExxonMobil™ High Density Polyethylene, (1-phenylvinyloxy)amide, and perfluorooctyl iodide were reacted according to General Procedure I. HDPE (M_n = 38 kg/mol, $Đ$ = 8.13, 0% branched, 40 mg, 1.43 mmol) reacted with (1-phenylvinyloxy)amide (62 mg, 0.14 mmol) and perfluorooctyl iodide (81 µL, 0.28 mmol) in chlorobenzene (0.7 mL) upon heating at 130 °C for 30 min. The resultant material (44 mg) was 3 mol % iodinated HDPE as whitish flakes. Collection of the filtrate revealed 74% conversion of the functionalized amide to parent amide by ^{19}F NMR.

The following was gathered using 3 mol % iodinated HDPE:

¹H NMR (500 MHz, C₂D₂Cl₄, 110 °C) δ 4.21 (bs), 1,94 (bs), 1.78 (bs), 1.62 (bs), 1.46 (bs), 1.36 (bs), 0.97 (bs). **IR (neat, ATR, cm⁻¹)** 2916, 2849, 1473, 1463, 1281, 1143, 1063, 801, 721, 719. **GPC (TCB, 140 °C)** M_n = 41 kg/mol, $Đ$ = 7.38. **TGA (°C)** parent T_d = 433, product T_d = 251 (T_{d1} = 202, T_{d2} = 388). **DSC (°C):** parent T_m = 129 with 62% crystallinity (ΔH = 183 J/g), product T_m = 111 with 26% crystallinity (ΔH = 75 J/g).

Determination of percent iodination of HDPE: Upon purification, the percent iodination of HDPE can be determined through integration of the ¹H NMR. Considering the composition of

the polymer, the peaks between 0.8 – 2.0 ppm were set to total to 4 protons. The protons *alpha*

the incorporated iodo group that appear at 4.3 ppm are used to determine mol % iodination per

repeat unit. Only secondary C–H iodination was observed.
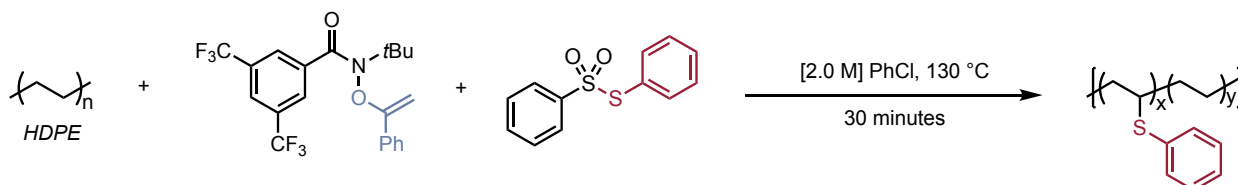
Thiophenolated HDPE (P11): ExxonMobil™ High Density Polyethylene, (1-

phenylvinyloxy)amide, and phenyl benzenesulfonate were reacted according to General

Procedure I. HDPE (M_n = 38 kg/mol, Đ = 8.13, 0% branched, 60 mg, 2.1 mmol) reacted with

(1-phenylvinyloxy)amide (92 mg, 0.21 mmol) and phenyl benzenesulfonate (110 mg, 0.43

mmol) in chlorobenzene (0.9 mL) upon heating at 130 °C for 30 min. The resultant material

(44 mg) was 8 mol % thiophenolated HDPE as whitish flakes. Collection of the filtrate revealed

85% conversion of the functionalized amide to the parent amide by ¹⁹F NMR.

The following was gathered using 8 mol % thiophenolated HDPE:

¹H NMR (500 MHz, C₂D₂Cl₄, 110 °C) δ 7.43 (bs, 2H), 7.30 (bs, 2H), 7.23 (bs, 1H), 3.10 (bs,

1H), 1.65 (bs), 1.51 (bs), 1.36 (bs), 0.97 (bs). **IR (neat, ATR, cm⁻¹)** 2915, 2849, 1585, 1473,

1463, 1438, 1093, 1027, 1026, 734, 720, 718, 692. **GPC (TCB, 140 °C)** M_n = 43 kg/mol, Đ =

7.68. **TGA (°C)** parent T_d = 433, product T_d = 398. **DSC (°C):** parent T_m = 129 with 62%

crystallinity (ΔH = 183 J/g), product T_m = 124 with 20% crystallinity (ΔH = 57 J/g).

Determination of percent thiophenolation of HDPE: Upon purification, the percent thiophenolation of HDPE can be determined through integration of the ^{1}H NMR. Considering the composition of the polymer, the peaks between 0.8 – 2.0 ppm were set to total to 4 protons. The protons *alpha* the incorporated thiophenol group that appear at 3.1 ppm are used to determine mol % thiophenolation per repeat unit. The phenyl peaks were found to be in agreement with the *alpha* protons.
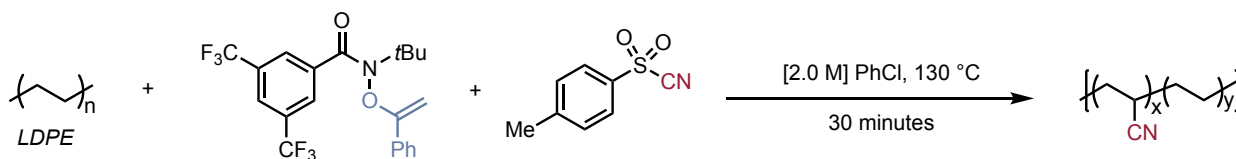
Cyanated LDPE (P12): Dow™ Polyethylene 4012 Low Density, (1-phenylvinyloxy)amide, and tosyl cyanide were reacted according to General Procedure I. LDPE (M_n = 34 kg/mol, Đ = 13.5, 49% branched, 40 mg, 1.43 mmol) reacted with (1-phenylvinyloxy)amide (62 mg, 0.14 mmol) and tosyl cyanide (52 mg, 0.28 mmol) in chlorobenzene (0.7 mL) upon heating at 130 °C for 30 min. The resultant material (28 mg) was 5 mol % cyanated LDPE as whitish flakes. Collection of the filtrate revealed 89% conversion of the functionalized amide to parent amide by ^{19}F NMR.

The following was gathered using 5 mol % cyanated LDPE:

^{1}H NMR (500 MHz, C$_2$D$_2$Cl$_4$, 110 °C) δ 2.54 (bs), 1.66 (bs), 1.50 (bs), 1.44 (bs), 1.36 (bs), 0.97 (bs). **IR (neat, ATR, cm^{-1})** 2917, 2849, 2239, 1724, 1468, 1378, 1280, 1039, 720. **GPC (TCB, 140 °C)** M_n = 40 kg/mol, Đ = 13.56. **TGA (°C)** parent T_d = 416, product T_d = 341. **DSC (°C):** parent T_m = 105 with 36% crystallinity (ΔH = 105 J/g), product T_m = 82 with 10% crystallinity (ΔH = 28 J/g).

Determination of percent cyanation of LDPE: Upon purification, the percent cyanation of LDPE can be determined through integration of the ^{1}H NMR. Considering the composition of the polymer, the peaks between 0.8 – 2.0 ppm were set to total to 4 protons. The protons *alpha* the incorporated cyano group that appear at 2.6 ppm are used to determine mol % cyanation per repeat unit. Only secondary C–H cyanation was observed.
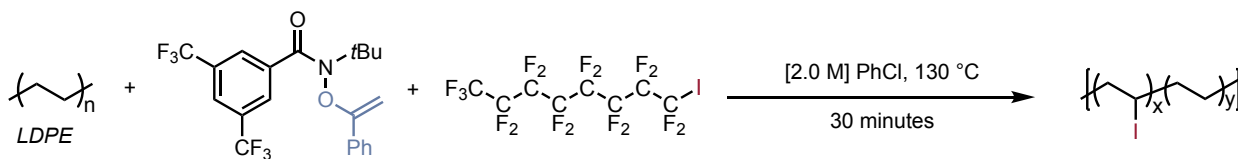

Iodinated LDPE (P13): Dow™ Polyethylene 4012 Low Density, (1-phenylvinyloxy)amide, and perfluorooctyl iodide were reacted according to General Procedure I. LDPE (M_n = 41 kg/mol, Đ = 17.10, 49% branched, 40 mg, 1.43 mmol) reacted with (1-phenylvinyloxy)amide (62 mg, 0.14 mmol) and perfluorooctyl iodide (81 µL, 0.28 mmol) in chlorobenzene (0.7 mL) upon heating at 130 °C for 30 min. The resultant material (46 mg) was 3 mol % iodinated LDPE as whitish flakes. Collection of the filtrate revealed 75% conversion of the functionalized amide to parent amide by ^{19}F NMR.

The following was gathered using 3 mol % iodinated LDPE:

^{1}H NMR (500 MHz, C$_2$D$_2$Cl$_4$, 110 °C) δ 4.21 (bs), 1.97 (bs), 1.80 (bs), 1.57 (bs), 1.46 (bs), 1.36 (bs), 0.97 (bs). **IR (neat, ATR, cm^{-1})** 2916, 2849, 1465, 1463, 1368, 1281, 1217, 1214, 1145, 719. **GPC (TCB, 140 °C)** M_n = 49 kg/mol, Đ = 15.16. **TGA (°C)** parent T_d = 416, product T_d = 245 (T_{d1} = 189, T_{d2} = 383). **DSC (°C):** parent T_m = 105 with 36% crystallinity (ΔH = 105 J/g), product T_m = 89 with 16% crystallinity (ΔH = 46 J/g).

Determination of percent iodination of LDPE: Upon purification, the percent iodination of LDPE can be determined through integration of the ^{1}H NMR. Considering the composition of the polymer, the peaks between 0.8 – 2.0 ppm were set to total to 4 protons. The protons *alpha* the incorporated iodo group that appear at 4.2 ppm are used to determine mol % iodination per repeat unit. Only secondary C–H iodination was observed.
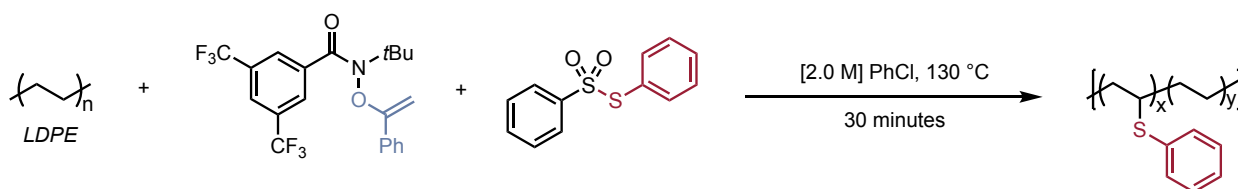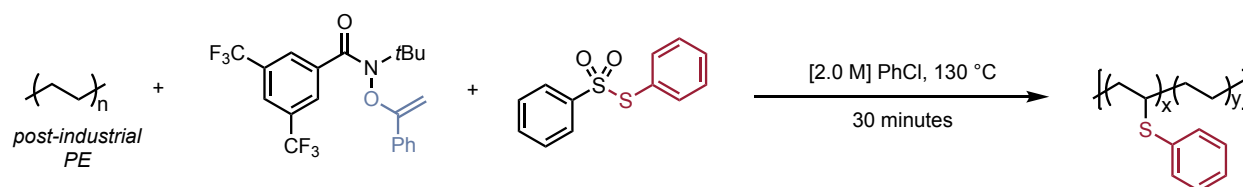

Thiophenolated LDPE (P14): Dow™ Polyethylene 4012 Low Density, (1-phenylvinyloxy)amide, and phenyl benzenesulfonate were reacted according to General Procedure I. LDPE (M_n = 34 kg/mol, Đ = 13.5, 49% branched, 40 mg, 1.43 mmol) reacted with (1-phenylvinyloxy)amide (62 mg, 0.14 mmol) and phenyl benzenesulfonate (72 mg, 0.28 mmol) in chlorobenzene (0.7 mL) upon heating at 130 °C for 30 min. The resultant material (34 mg) was 6 mol % phenyl thioether LDPE as whitish flakes. Collection of the filtrate revealed 93% conversion of the functionalized amide to parent amide by ^{19}F NMR.

The following was gathered using 6 mol % thiophenolated LDPE:

^{1}H NMR (500 MHz, C$_2$D$_2$Cl$_4$, 110 °C) δ 7.44 (bs, 2H), 7.31 (bs, 2H), 7.23 (bs, 1H), 3.11 (bs, 1H), 1.66 (bs), 1.53 (bs), 1.36 (bs), 0.98 (bs). **IR (neat, ATR, cm^{-1})** 2917, 2850, 1585, 1464, 1438, 1366, 1280, 1141, 1092, 1068, 1025, 746, 720, 691. **GPC (TCB, 140 °C)** M_n = 65 kg/mol, Đ = 13.76. **TGA (°C)** parent T$_d$ = 416, product T$_d$ = 391. **DSC (°C):** parent T_m = 105 with 36% crystallinity (ΔH = 105 J/g), product T_m = 74 with 11% crystallinity (ΔH = 32 J/g).

Determination of percent thiophenolation of LDPE: Upon purification, the percent thiophenolation of LDPE can be determined through integration of the ^{1}H NMR. Considering the composition of the polymer, the peaks between 0.8 – 2.0 ppm were set to total to 4 protons. The protons *alpha* the incorporated thiophenol group that appear at 3.1 ppm are used to determine mol % thiophenol per repeat unit. Only secondary C–H thiophenolation was observed. The phenyl peaks were found to be in agreement with the *alpha* protons.
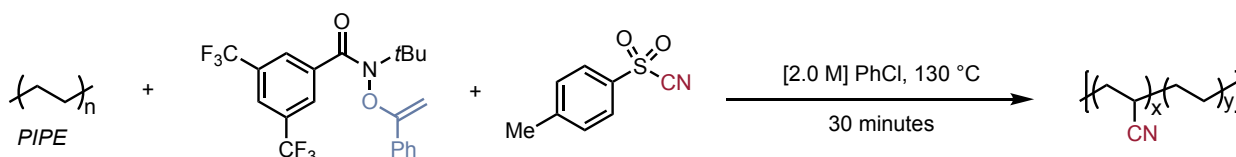
Cyanated PIPE (P15): Post-industrial PE (PIPE), (1-phenylvinyloxy)amide, and tosyl cyanide were reacted according to General Procedure I. PIPE (M_n = 45 kg/mol, Đ = 8.65, 40 mg, 1.43 mmol) reacted with (1-phenylvinyloxy)amide (62 mg, 0.14 mmol) and tosyl cyanide (52 mg, 0.28 mmol) in chlorobenzene (0.7 mL) upon heating at 130 °C for 30 min. The resultant material (30 mg) was 5 mol % cyanated PIPE as whitish flakes. Collection of the filtrate revealed 90% conversion of the functionalized amide to the parent amide by ^{19}F NMR.

The following was gathered using 5 mol % cyanated PIPE:

^{1}H NMR (500 MHz, C$_2$D$_2$Cl$_4$, 110 °C) δ 2.53 (bs), 1.66 (bs), 1.62 (bs), 1.52 (bs), 1.44 (bs), 1.36 (bs), 1.25 (bs), 0.98 (bs). **IR (neat, ATR, cm^{-1})** 2917, 2850, 2240, 1468, 1378, 1000, 720. **GPC (TCB, 140 °C)** M_n = 48 kg/mol, Đ = 8.44. **TGA (°C)** parent T$_d$ = 412, product T$_d$ = 393. **DSC (°C):** parent T_m = 109 with 24% crystallinity (ΔH = 72 J/g), product T_m = 87 with 21% crystallinity (ΔH = 60 J/g).

Determination of percent cyanation of PIPE: Upon purification, the percent cyanation of PIPE can be determined through integration of the ^{1}H NMR. Considering the composition of the polymer, the peaks between $0.8 - 2.0$ ppm were set to total to 4 protons. The protons *alpha* the incorporated cyano group that appear at 2.6 ppm are used to determine mol % cyanation per repeat unit. Only secondary C–H cyanation was observed.
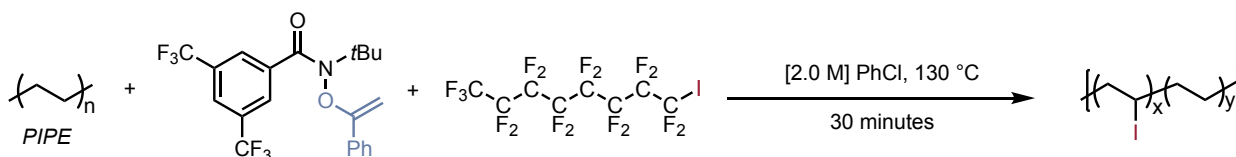
Iodinated PIPE (P16): Post-industrial PE (PIPE), (1-phenylvinyloxy)amide, and perfluorooctyl iodide were reacted according to General Procedure I. PIPE (M_n = 48 kg/mol, Đ = 14.07, 40 mg, 1.43 mmol) reacted with (1-phenylvinyloxy)amide (62 mg, 0.14 mmol) and perfluorooctyl iodide (81 μL, 0.28 mmol) in chlorobenzene (0.7 mL) upon heating at 130 °C for 30 min. The resultant material (47 mg) was 4 mol % iodinated PIPE as whitish flakes. Collection of the filtrate revealed 75% conversion of the functionalized amide to the parent amide by ^{19}F NMR.

The following was gathered using 4 mol % iodinated PIPE:

^{1}H NMR (500 MHz, C$_2$D$_2$Cl$_4$, 110 °C) δ . **IR (neat, ATR, cm^{-1})** 2916, 2849, 1473, 1464, 1366, 1281, 1241, 1216, 1146, 730, 719. **GPC (TCB, 140 °C)** M_n = 57 kg/mol, Đ = 12.60. **TGA (°C)** parent T_d = 412, product T_d = 234 (T_{d1} = 197, T_{d2} = 383). **DSC (°C):** parent T_m =

109 with 24% crystallinity (ΔH = 72 J/g), product T_m = 88 with 13% crystallinity (ΔH = 37 J/g).

Determination of percent iodination of PIPE: Upon purification, the percent iodination of PIPE can be determined through integration of the ^{1}H NMR. Considering the composition of the polymer, the peaks between 0.8 – 2.0 ppm were set to total to 4 protons. The protons *alpha* the incorporated iodo group that appear at 4.2 ppm are used to determine mol % iodination per repeat unit. Only secondary C–H iodination was observed.
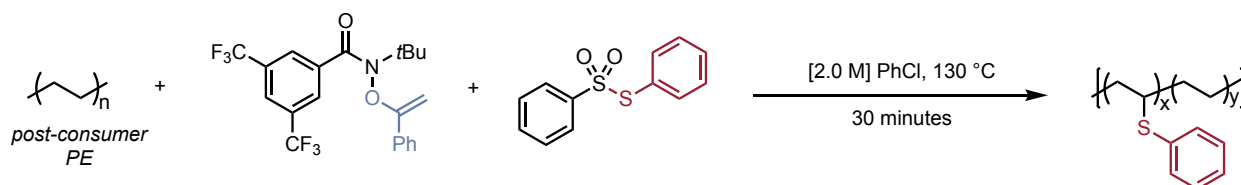

Thiophenolated PIPE (P17): Post-industrial PE (PIPE), (1-phenylvinyloxy)amide, and phenyl benzenesulfonate were reacted according to General Procedure I. PIPE (M_n = 48 kg/mol, $Đ$ = 14.07, 40 mg, 1.43 mmol) reacted with (1-phenylvinyloxy)amide (62 mg, 0.14 mmol) and phenyl benzenesulfonate (72 mg, 0.28 mmol) in chlorobenzene (0.7 mL) upon heating at 130 °C for 30 min. The resultant material (37 mg) was 6 mol % thiophenolated PIPE as whitish flakes. Collection of the filtrate revealed 91% conversion of the functionalized amide to the parent amide by ^{19}F NMR.

The following was gathered using 6 mol % thiophenolated PIPE:

^{1}H NMR (500 MHz, C$_2$D$_2$Cl$_4$, 110 °C) δ 7.44 (bs, 2H), 7.30 (bs, 2H), 7.23 (bs, 1H), 3.11 (bs, 1H), 1.66 (bs), 1.52 (bs), 1.44 (bs), 1.36 (bs), 0.97 (bs). **IR (neat, ATR, cm^{-1})** 2917, 2849, 1739, 1586, 1467, 1438, 1370, 1279, 1242, 1090, 1068, 1026, 746, 694, 692. **GPC (TCB, 140**

°C) M_n = 66 kg/mol, *Đ* = 11.73. **TGA (°C)** parent T_d = 412, product T_d = 391. **DSC (°C):**

parent T_m = 109 with 24% crystallinity (ΔH = 72 J/g), product T_m = 76 with 8% crystallinity

(ΔH = 24 J/g).

Determination of percent thiophenolation of PIPE: Upon purification, the percent

thiophenolation of PIPE can be determined through integration of the ¹H NMR. Considering

the composition of the polymer, the peaks between 0.8 – 2.0 ppm were set to total to 4 protons.

The protons *alpha* the incorporated thiophenol group that appear at 3.1 ppm are used to

determine mol % thiophenolation per repeat unit. The phenyl protons were in agreement with

the *alpha* protons.
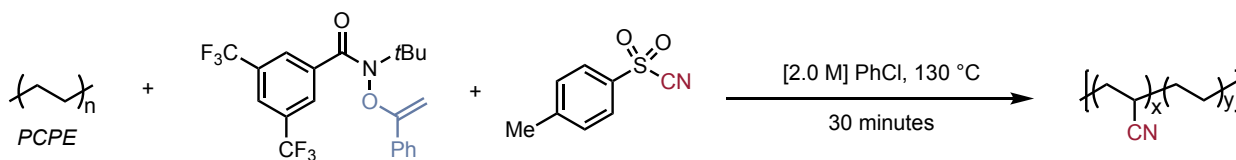
Cyanated PCPE (P18): Post-consumer PE (PCPE) gathered from PE packaging, (1-

phenylvinyloxy)amide, and tosyl cyanide were reacted according to General Procedure I.

PCPE (M_n = 34 kg/mol, *Đ* = 7.80, 40 mg, 1.43 mmol) reacted with (1-phenylvinyloxy)amide

(60 mg, 0.14 mmol) and tosyl cyanide (52 mg, 0.28 mmol) in chlorobenzene (0.7 mL) upon

heating at 130 °C for 30 min. The resultant material (36 mg) was 7 mol % cyanated PCPE as

whitish flakes. Collection of the precipitate confirmed 90% conversion of the amidyl reagent

to the parent amide by ¹⁹F NMR.

The following was gathered using 7 mol % cyanated PCPE:

¹H NMR (500 MHz, C₂D₂Cl₄, 110 °C) δ 2.60 (bs), 1.67 (bs), 1.44 (bs), 1.37 (bs), 0.99 (bs).

IR (neat, ATR, cm⁻¹): 2916, 2849, 2239, 1681, 1468, 1379, 1305, 1278, 1152, 1146, 1129,

1038, 1012, 812, 719. **GPC (TCB, 140 °C)** $M_n = 33$ kg/mol, $Đ = 7.34$. **TGA (°C)** parent T_d = 414 °C, product T_d = 370 °C. **DSC (°C):** parent $T_m = 111$ °C with 37% crystallinity ($\Delta H = 111$ J/g), product $T_m = 89$ °C with 16% crystallinity ($\Delta H = 48$ J/g).

Determination of percent cyanation of PCPE: Upon purification, the percent cyanation of PCPE can be determined through integration of the ^{1}H NMR. Considering the composition of the polymer, the peaks between 0.8 – 2.0 ppm were set to total to 4 protons. The protons *alpha* the incorporated cyano group that appear at 2.6 ppm are used to determine mol % cyanation per repeat unit. Only secondary C–H cyanation was observed.
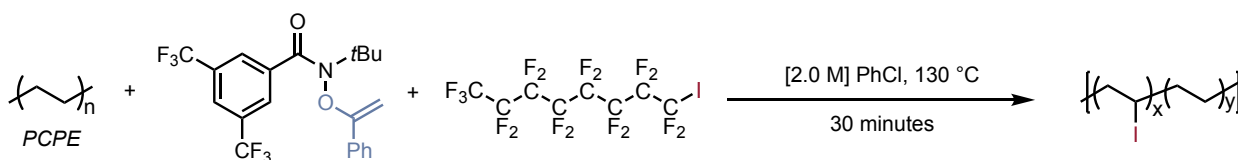
Iodinated PCPE (P19): Post-consumer PE (PCPE) gathered from PE packaging materials, (1-phenylvinyloxy)amide, and perfluorooctyl iodide were reacted according to General Procedure I. PCPE ($M_n = 40$ kg/mol, $Đ = 12.08$, 40 mg, 1.43 mmol) reacted with (1-phenylvinyloxy)amide (60 mg, 0.14 mmol) and perfluorooctyl iodide (81 μL, 0.28 mmol) in chlorobenzene (0.7 mL) upon heating at 130 °C for 30 min. The resultant material (47 mg) was 3 mol % iodinated PCPE as whitish flakes. Collection of the precipitate confirmed 74% conversion of the amidyl reagent to the parent amide by ^{19}F NMR.

The following was gathered using 3 mol % iodinated PCPE:

^{1}H NMR (500 MHz, C₂D₂Cl₄, 110 °C) δ 4.21 (bs), 1.94 (bs), 1.80 (bs), 1.61 (bs), 1.57 (bs), 1.45 (bs), 1.36 (bs), 0.97 (bs).**IR (neat, ATR, cm⁻¹)** 2916, 2849, 1473, 1462, 1367, 1281, 1238,

1216, 1146, 722, 719. **GPC (TCB, 140 °C)** M_n = 44 kg/mol, $Đ$ = 11.36. **TGA (°C)** parent T_d

= 414, product T_d = 231 (T_{d1} = 190, T_{d2} = 385)**. DSC (°C):** parent T_m = 111 °C with 37%

crystallinity (ΔH = 111 J/g), product T_m = 95 °C with 18% crystallinity (ΔH = 52 J/g).

Determination of percent iodination of PCPE: Upon purification, the percent iodination of

PCPE can be determined through integration of the ¹H NMR. Considering the composition of

the polymer, the peaks between 0.8 – 2.0 ppm were set to total to 4 protons. The protons *alpha*

the incorporated iodo group that appear at 4.2 ppm are used to determine mol % iodination per

repeat unit. Only secondary C–H iodination was observed.

Thiophenolated PCPE (P20): Post-consumer PE (PCPE) gathered from PE packaging

materials, (1-phenylvinyloxy)amide, and phenyl benzenesulfonate were reacted according to

General Procedure I. PCPE (M_n = 40 kg/mol, $Đ$ = 12.08, 40 mg, 1.43 mmol) reacted with (1-

phenylvinyloxy)amide (60 mg, 0.14 mmol) and phenyl benzenesulfonate (72 mg, 0.28 mmol)

in chlorobenzene (0.7 mL) upon heating at 130 °C for 30 min. The resultant material (35 mg)

was 6 mol % thiophenolated PCPE as whitish flakes. Collection of the precipitate confirmed

91% conversion of the amidyl reagent to the parent amide by ¹⁹F NMR.

The following was gathered using 6 mol % thiophenolated PCPE:

¹H NMR (500 MHz, C₂D₂Cl₄, 110 °C) δ 7.50 (bs, 2H), 7.36 (bs, 2H), 7.29 (bs, 1H), 3.16 (bs,

1H), 1.71 (bs), 1.58 (bs), 1.50 (bs), 1.41 (bs), 1.03 (bs). **IR (neat, ATR, cm⁻¹)** 2916, 2848,

1584, 1467, 1439, 1369, 1304, 1093, 1027, 1025, 718, 694, 692. **GPC (TCB, 140 °C)** $M_n =$ 55 kg/mol, $Đ = 10.25$. **TGA (°C)** parent $T_d = 414$, product $T_d = 392$. **DSC (°C):** parent $T_m =$ 111 °C with 37% crystallinity ($\Delta H = 111$ J/g), product $T_m = 79$ °C with 9% crystallinity ($\Delta H = 26$ J/g).

Determination of percent thiophenolation of PCPE: Upon purification, the percent thiophenolation of PCPE can be determined through integration of the ^{1}H NMR. Considering the composition of the polymer, the peaks between 0.8 – 2.0 ppm were set to total to 4 protons. The protons *alpha* the incorporated thiophenol group that appear at 3.1 ppm are used to determine mol % thiophenol per repeat unit. The phenyl protons were in agreement with the alpha protons.
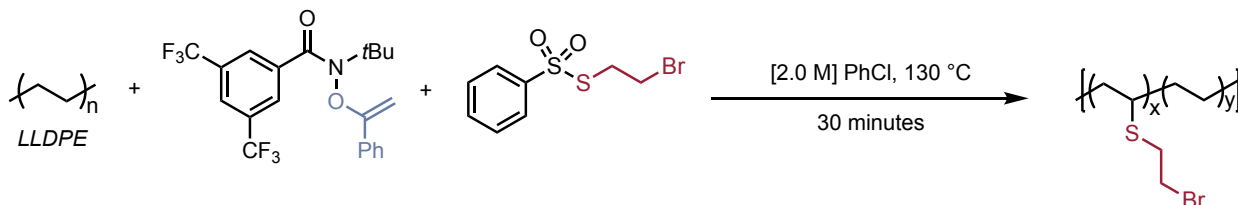
Bromoethylthiolated LLDPE (P21): DOW™ DNDA-1081 NT 7 Linear Low Density Polyethylene Resin, (1-phenylvinyloxy)amide, and *S*-(2-bromoethyl) benzenesulfonothioate were reacted according to General Polymer Procedure. LLDPE ($M_n = 18$ kg/mol, $Đ = 9.31$, 19% branched, 40 mg, 1.43 mmol) reacted with (1-phenylvinyloxy)amide (62 mg, 0.14 mmol) and *S*-(2-bromoethyl) benzenesulfonothioate (80 mg, 0.29 mmol) in chlorobenzene (0.7 mL) upon heating at 130 °C for 30 min. The resultant material (44 mg) was 5 mol % bromoethylthiolated LLDPE. Collection of the filtrate revealed 86% conversion of the functionalized amide to the parent amide by ^{19}F NMR.

The following was gathered using 5 mol % bromoethylthiolated LLDPE:

^{1}H NMR (500 MHz, C$_2$D$_2$Cl$_4$, 110 °C) δ 3.53 (bs, 2H), 3.00 (bs, 2H), 2.68 (bs, 1H), 1.63 (bs), 1.49 (bs), 1.36 (bs), 0.98 (bs). **IR (neat, ATR, cm^{-1})** 2917, 2849, 1577, 1541, 1473, 1463, 1369, 1279, 1250, 1188, 1140, 722, 720. **GPC (TCB, 140 °C):** M_n = 25 kg/mol, $Đ$ = 9.32. **TGA (°C)** parent T_d = 428, product T_d = 235 (T_{d1} = 159, T_{d2} = 380). **DSC (°C):** parent T_m = 125 with 41% crystallinity (ΔH = 122 J/g), product T_m = 100 with 11% crystallinity (ΔH = 32 J/g).

Determination of percent bromoethylthiolation of LLDPE: Upon purification, the percent bromoethylthiolation of LLDPE can be determined through integration of the ^{1}H NMR. Considering the composition of the polymer, the peaks between 0.8 – 2.0 ppm were set to total to 4 protons. The protons *alpha* the incorporated bromo group that appear around 3.5 ppm are used to determine mol % bromoethylthiolation per repeat unit. The protons *alpha* the bromide atom were in agreement with the protons *alpha* the sulfur atom. Only secondary C–H functionalization was observed.
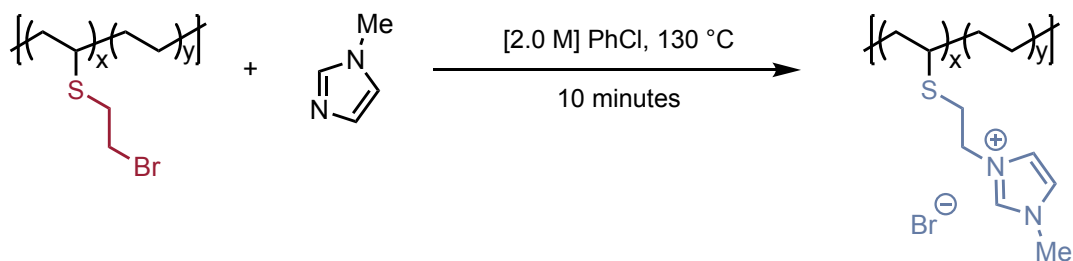
Imidazolium-functional LLDPE (P22): Bromoethylthiolated LLDPE (5 mol % funct, 590 mg, 21 mmol polyolefin, 1.1 mmol bromoethylthiol) reacted with methyl imidazole (1.7 mL, 21 mmol) in chlorobenzene (7 mL) upon heating at 130 °C for 10 min. The resultant material (582 mg) was 4 mol % imidazolium-functional LLDPE.

The following was gathered using 4 mol % imidazolium-functional LLDPE:

¹H NMR (500 MHz, C$_2$D$_2$Cl$_4$, 110 °C) δ 10.55 (bs, 1H), 7.30 (bs, 2H), 4.62 (bs, 2H), 4.14 (bs, 3H), 3.13 (bs, 2H), 2.73 (bs, 1H), 1.63 (bs), 1.46 (bs), 1.36 (bs), 0.98 (bs). **IR (neat, ATR, cm^{-1})** 3409, 3105, 3046, 2917, 2850, 1573, 1468, 1279, 1172, 732, 719. **TGA (°C)** parent T_d = 428, product T_d = 257 (T_{d1} = 200, T_{d2} = 343). **DSC (°C):** parent T_m = 125 with 41% crystallinity (ΔH = 122 J/g), product T_m = 97 with 5% crystallinity (ΔH = 14 J/g).

Determination of percent imidazolium functionalization of LLDPE: Upon purification, the percent imidazolium functionalization of LLDPE can be determined through integration of the ¹H NMR. Considering the composition of the polymer, the peaks between 0.8 – 2.0 ppm were set to total to 4 protons. The protons *alpha* the incorporated imidazolium group that appear around 4.6 ppm are used to determine mol % functionalization per repeat unit. The protons *alpha* the imidazolium moiety were in agreement with the other protons located along on the side chain. Only secondary C–H functionalization was observed.

C.3 TENSILE TESTING EXPERIMENTS

Polymer films (0.1 – 0.3 mm) suitable for dynamic mechanical analysis (DMA) were prepared by melt-pressing using a PHI Manual Compression Press. DOW™ DNDA-1081 NT 7 Linear Low Density Polyethylene Resin (LLDPE) and 4 mol % imidazolium bromide LLDPE (Im$^+$-LLDPE) samples between two Kapton films (pre-treated with Frekote 770-NC) were placed between steel electrically heated platens at force 5000 psi and 150 °C for 3 minutes. Brass shims of 4 to 12 mil thickness were used to control ultimate film thickness. Films were removed from the melt press at the indicated temperature and quenched to room temperature by rapid heat transfer to an aluminum surface.

Specimens for analysis were cut into dog-bones using an ISO 527 Type 5B cutting die to standard dimensions. Test specimens were affixed to hand-tightened rubber grips on an Instron 5566 Universal Testing Machine. Tensile stress and strain were measured at room temperature using an extension speed of 1.0 mm/s. Measurements were repeated for at least 3 specimens and the values reported are averaged from the measured data. (Table C.2).

Polymer	E (MPa)	σ_B (MPa)	ε_B	U_T (MPa)
LLDPE	25	12	275%	413
LLDPE	29	13	283%	444
LLDPE	28	13	191%	303
LLDPE average	27	13	250%	387
LLDPE st. dev.	2	1	51%	74
Im$^+$-LLDPE	1.7	14	738%	694
Im$^+$-LLDPE	1.9	16	686%	745
Im$^+$-LLDPE	2.1	14	602%	648
Im$^+$-LLDPE average	*1.9*	*15*	*675%*	*696*
Im$^+$-LLDPE st. dev.	*0.2*	*1*	*69%*	*49*

Table C.2 DMA results from thin film tensile axial pull of 0.2 mm thick LLDPE and Im$^+$-LLDPE samples at a rate of 1.0 mm/s.

C.4 PHOTOS OF IONOMERS
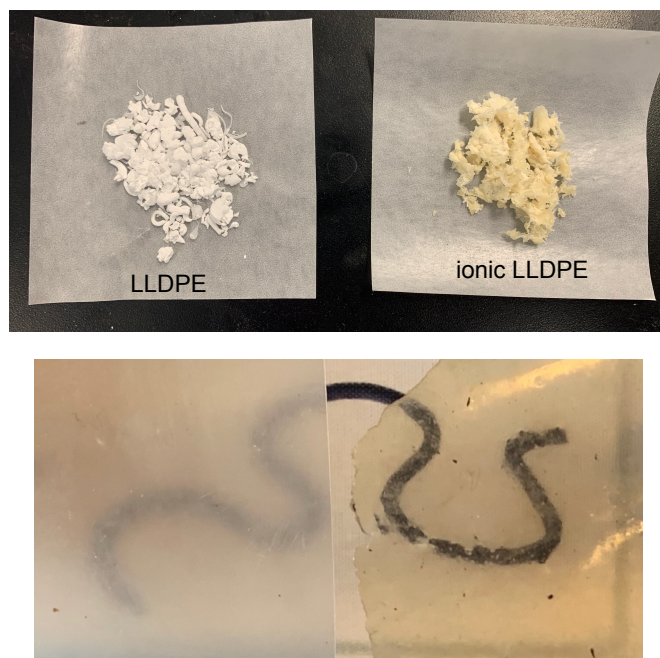
Top: Imidazolium bromide-functionalized LLDPE appears to be semi-crystalline with a slightly yellower tint than the parent LLDPE. Bottom: When trying to view an image, the film of LLDPE (left) remains translucent while the ionomer-LLDPE film (right) is more transparent.

C.5 ADDITIONAL DATA
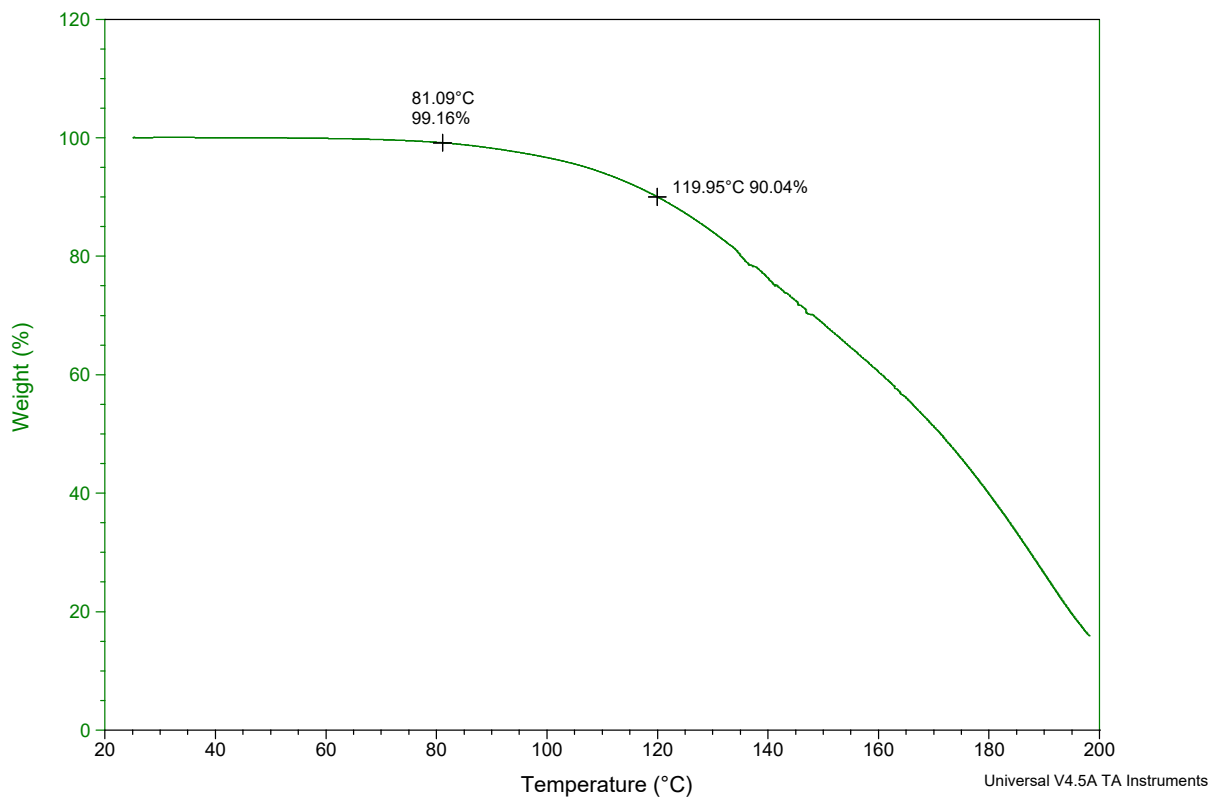
Thermal gravimetric analysis was performed on 9.5 mg of reagent **1**. At a rate of 10 °C/min, onset of decomposition was observed around 81 °C with the thermal decomposition of 10% weight loss occurring at 120 °C. We recognize the analysis of thermal decomposition via TGA is not a complete indication of how and when degradation is occurring as the material could potentially be subliming or evaporating rather than decomposing.

IR of Post-Consumer and Post-Industrial PE
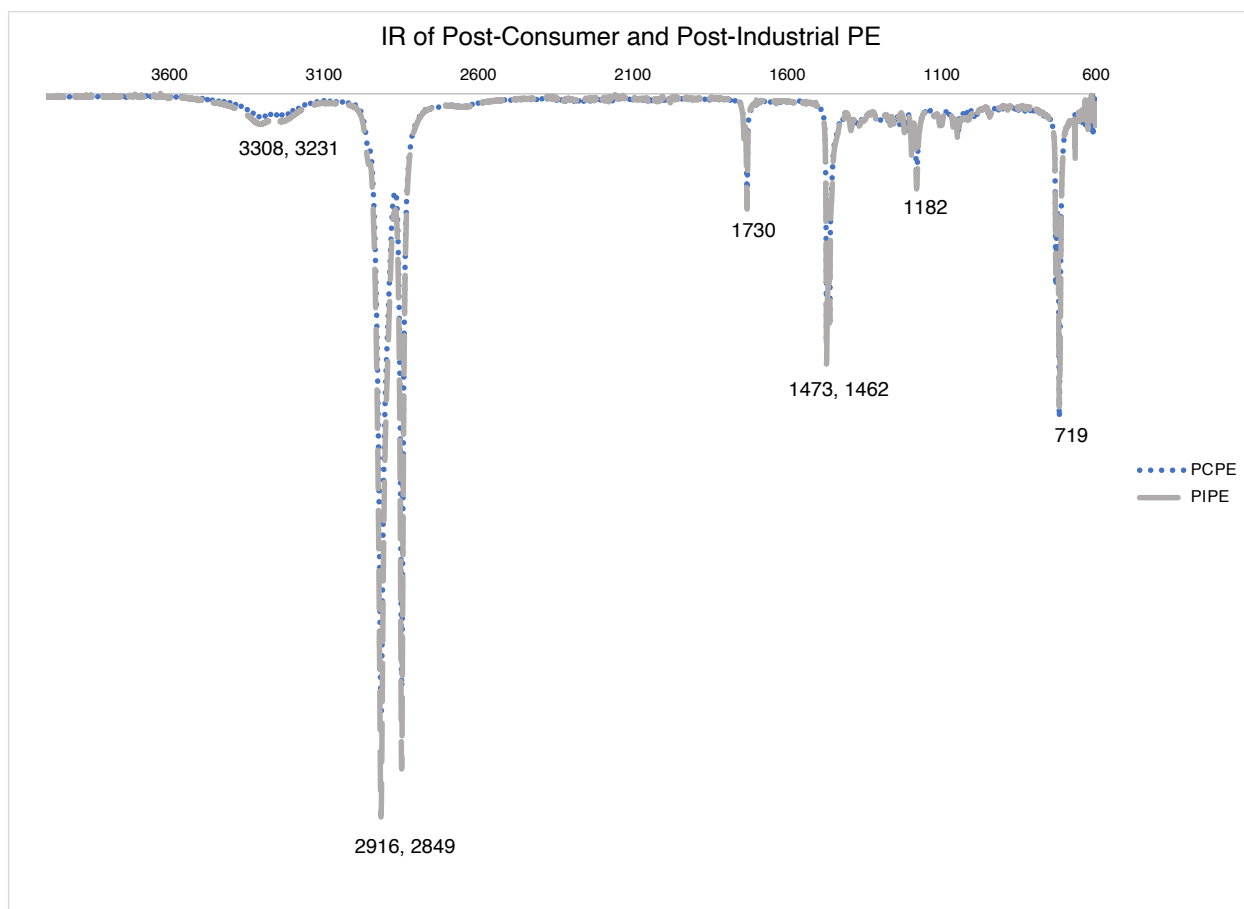
Infrared spectroscopy of post-consumer and post-industrial waste prior to functionalization. It is apparent that other structural moieties exist besides the dominant PE features at 2900, 1475, 1182, and 719 cm^{-1}.
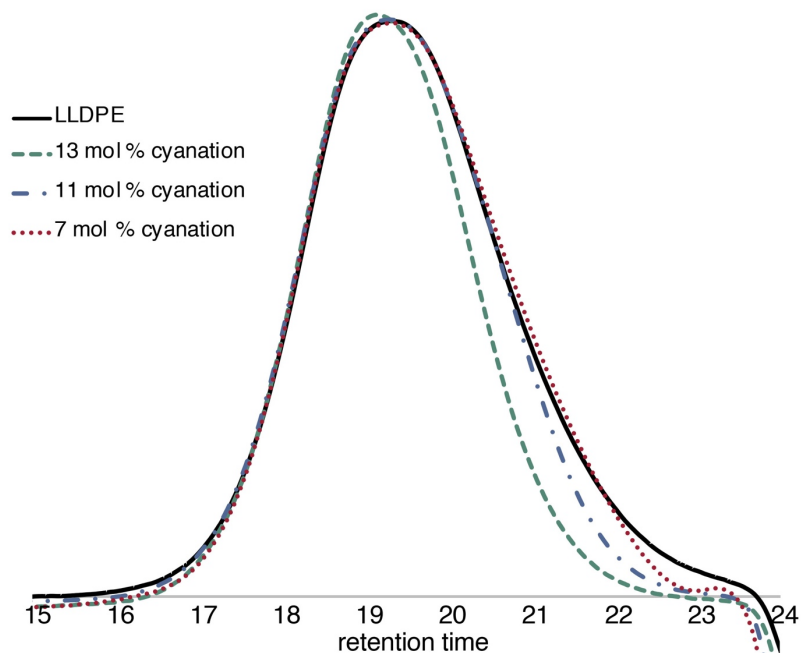
Polyolefin gel permeation chromatographs (GPC) were obtained using a Tosoh EcoSEC-HT (high temperature) GPC with refractive index detection against polystyrene standards in 1 mg/mL solutions of trichlorobenzene (TCB) at 140 °C. C–H cyanation using reagent **1** and tosyl cyanide successfully incorporated cyano groups into the polymer scaffold of LLDPE without significantly altering the molecular weight distribution according to GPC

C.6 NMRs FOR CHAPTER IV
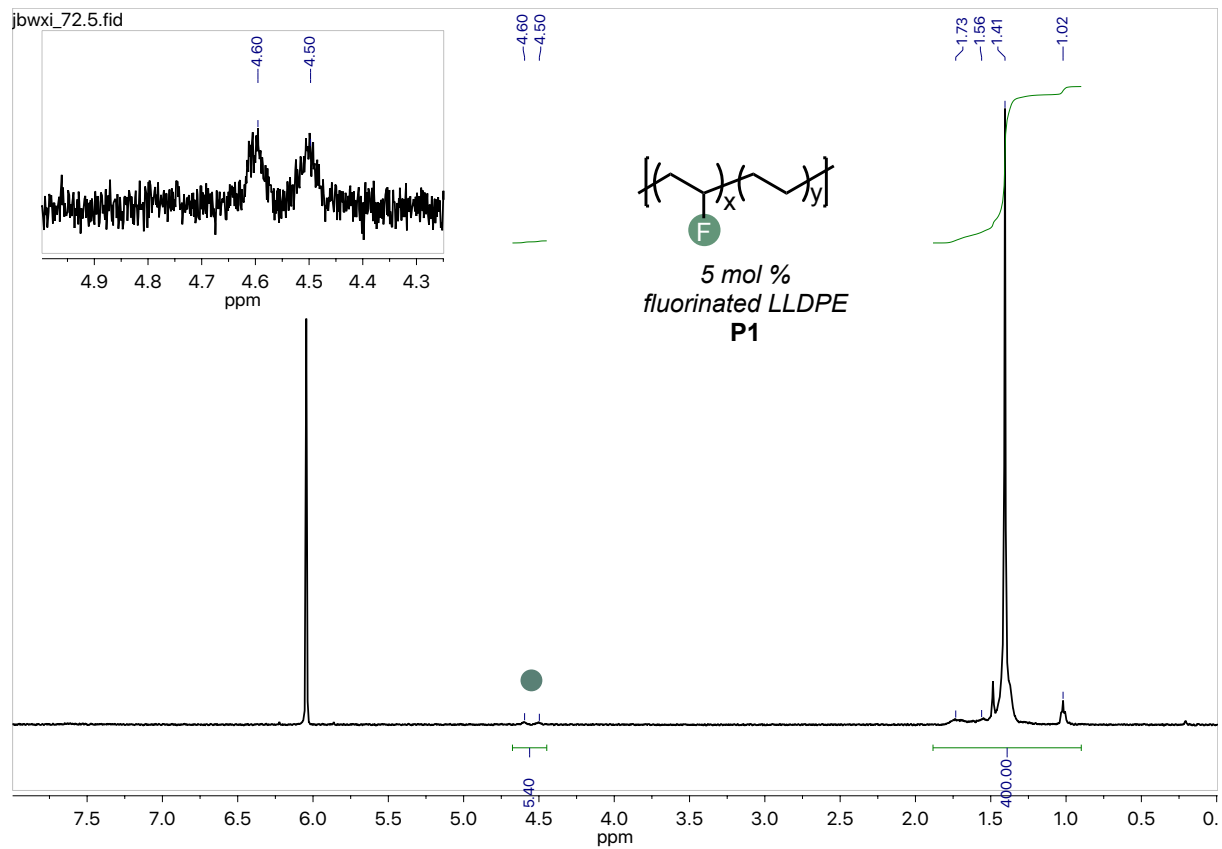
¹H NMR at 110 °C taken in C₂D₂Cl₄ of 5 mol % fluorinated LLDPE
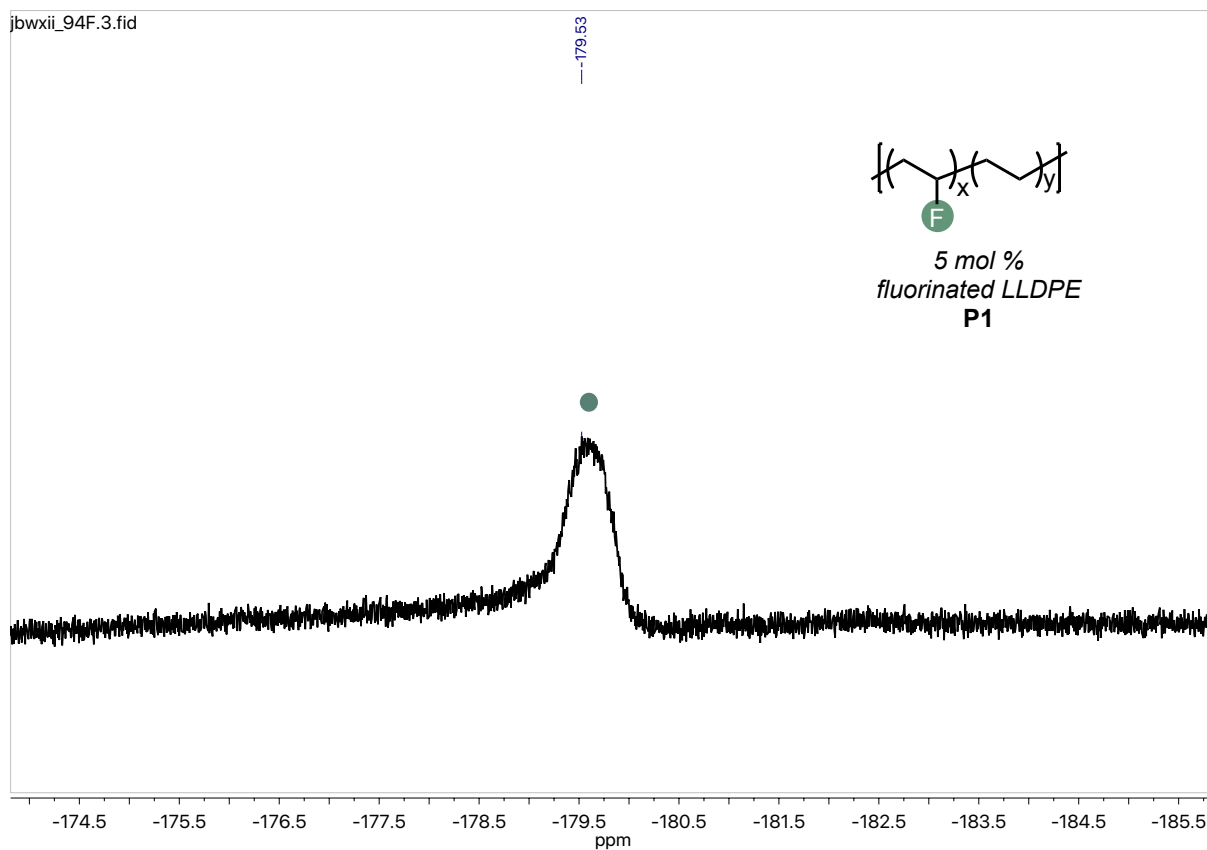
^{19}F NMR at 80 °C taken in C$_2$D$_2$Cl$_4$ of 5 mol % fluorinated LLDPE. The spectrum was referenced to trifluorotoluene at δ –63.72 ppm.
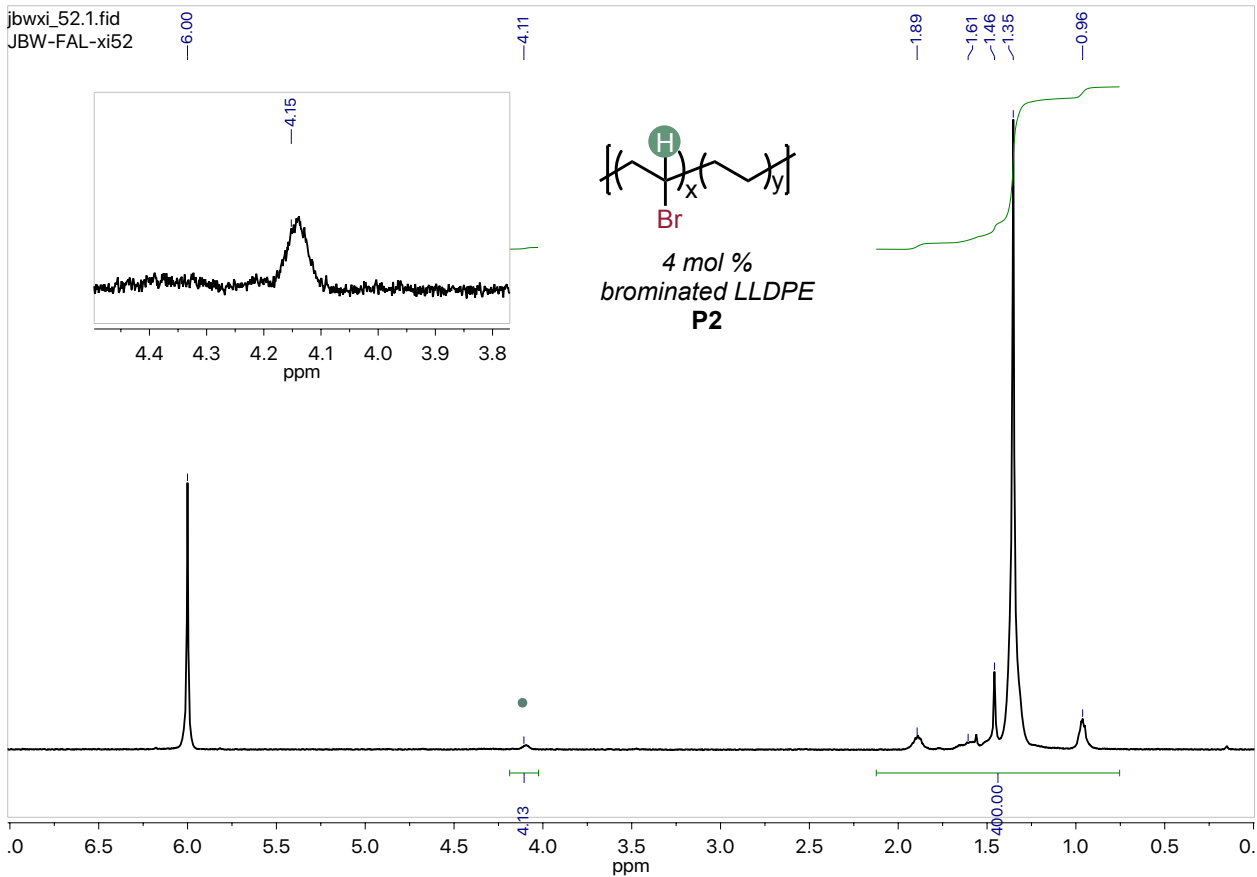
^{1}H NMR at 110 °C taken in C$_2$D$_2$Cl$_4$ of 4 mol % brominated LLDPE.
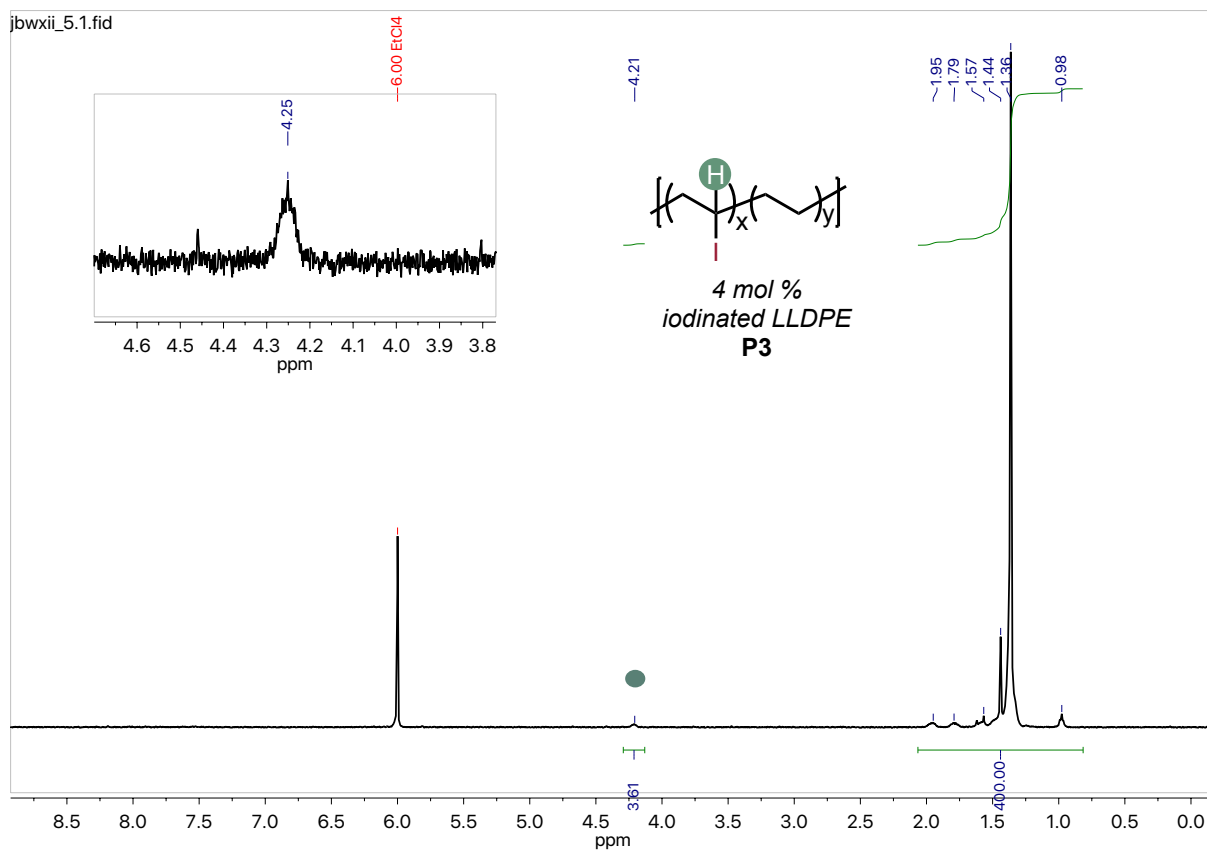
^{1}H NMR at 110 °C taken in C$_2$D$_2$Cl$_4$ of 4 mol % iodinated LLDPE
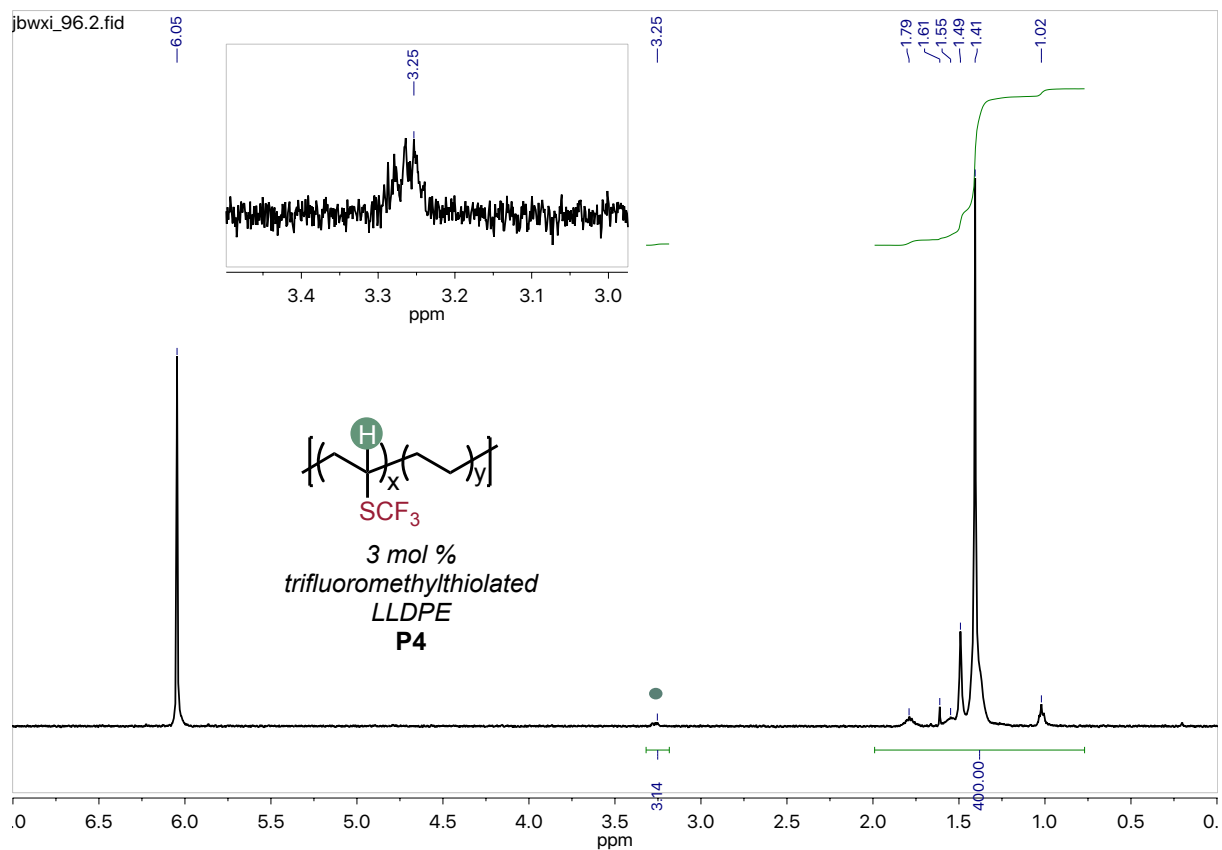
^{1}H NMR at 110 °C taken in $C_2D_2Cl_4$ of 3 mol % trifluoromethylthiolated LLDPE.
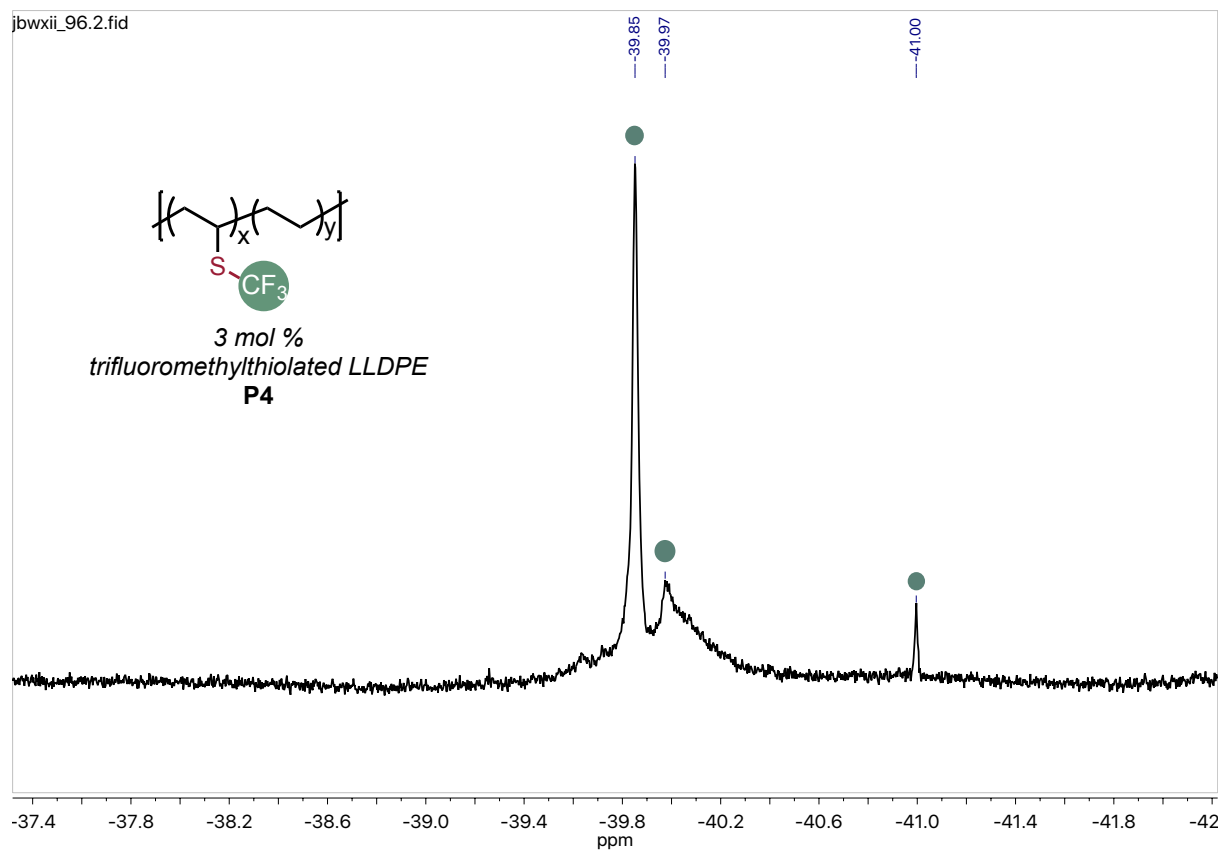
^{19}F NMR at 80 °C taken in $C_2D_2Cl_4$ of 3 mol % trifluoromethylthiolated LLDPE. The spectrum was referenced to trifluorotoluene at δ –63.72 ppm.
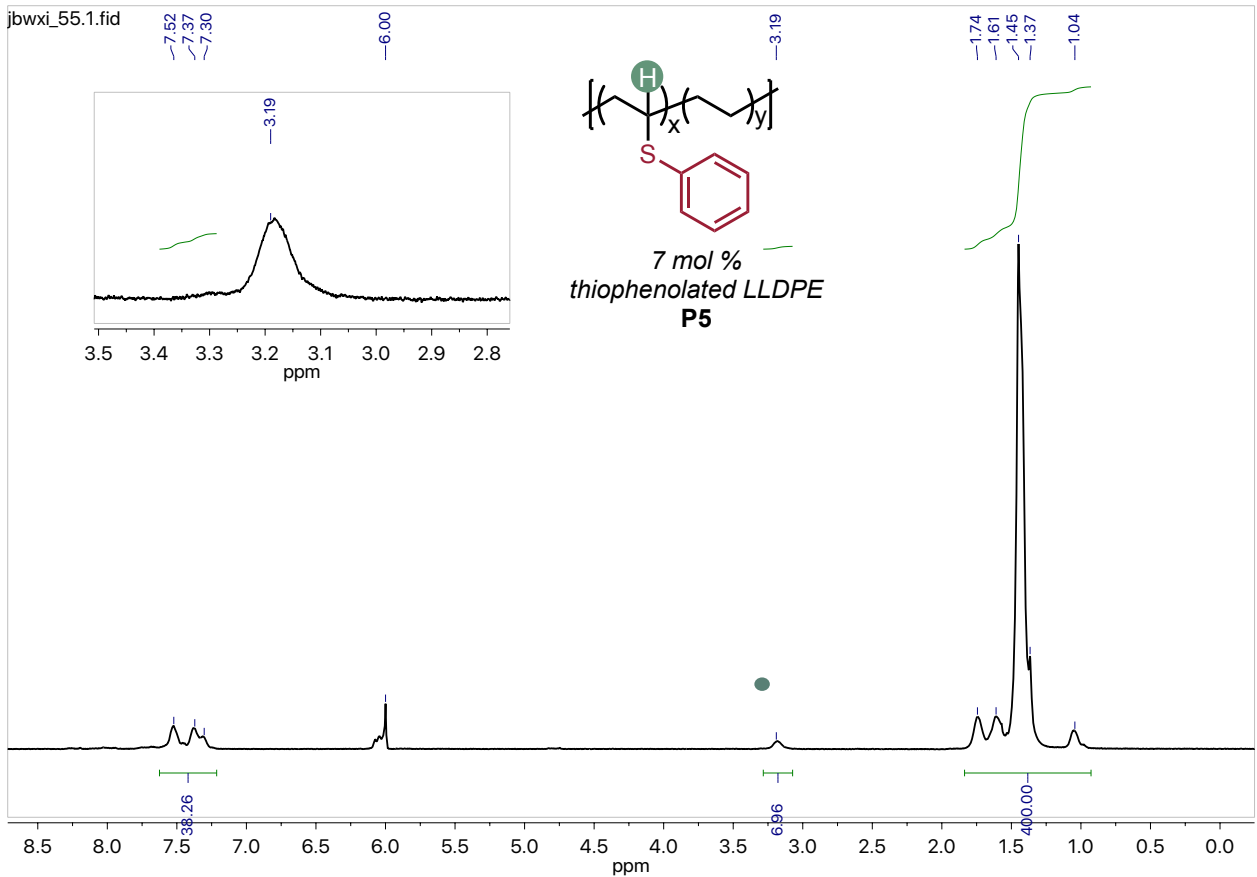
Figure C.X ^{1}H NMR at 110 °C taken in $C_2D_2Cl_4$ of 7 mol % thiophenolated LLDPE.
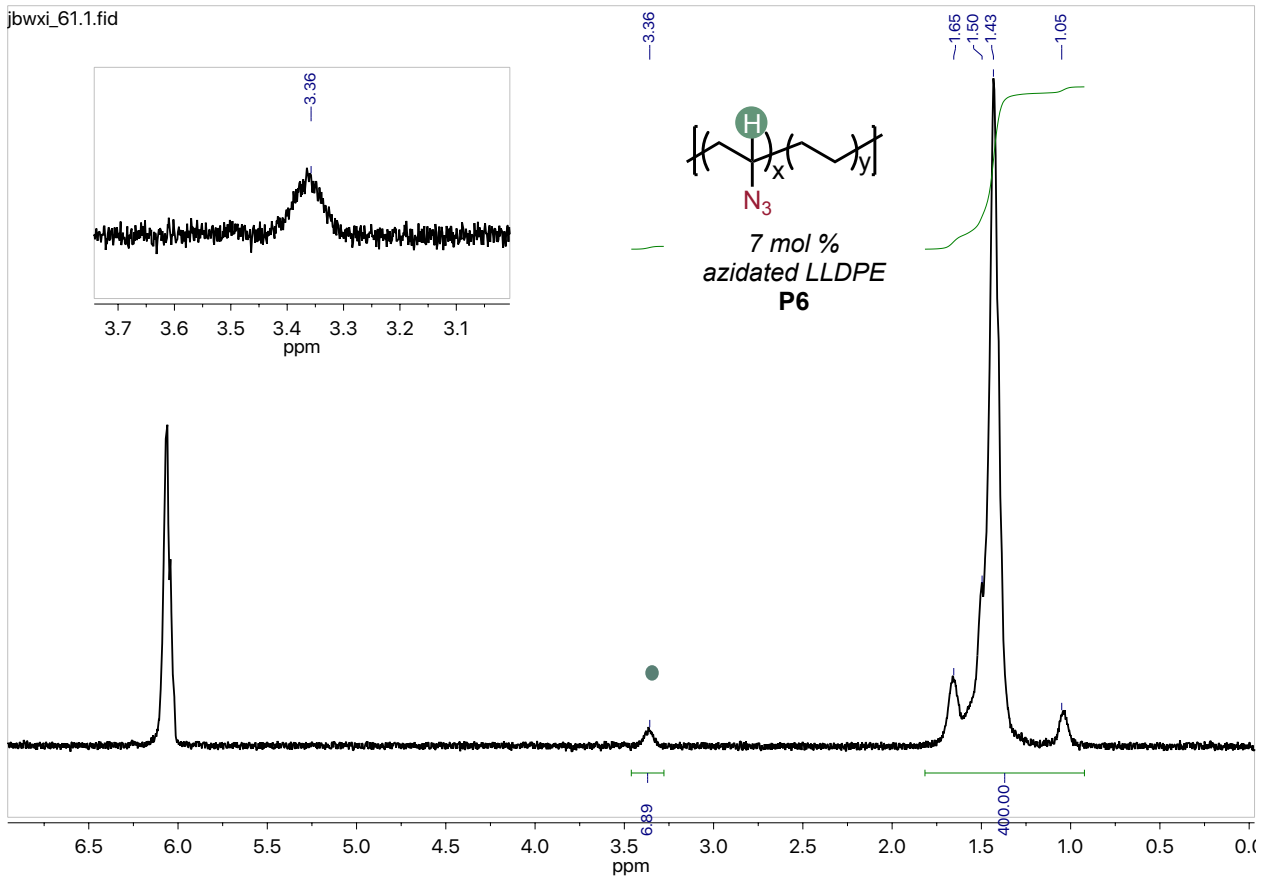
^{1}H NMR at 110 °C taken in $C_2D_2Cl_4$ of 7 mol % azidated LLDPE
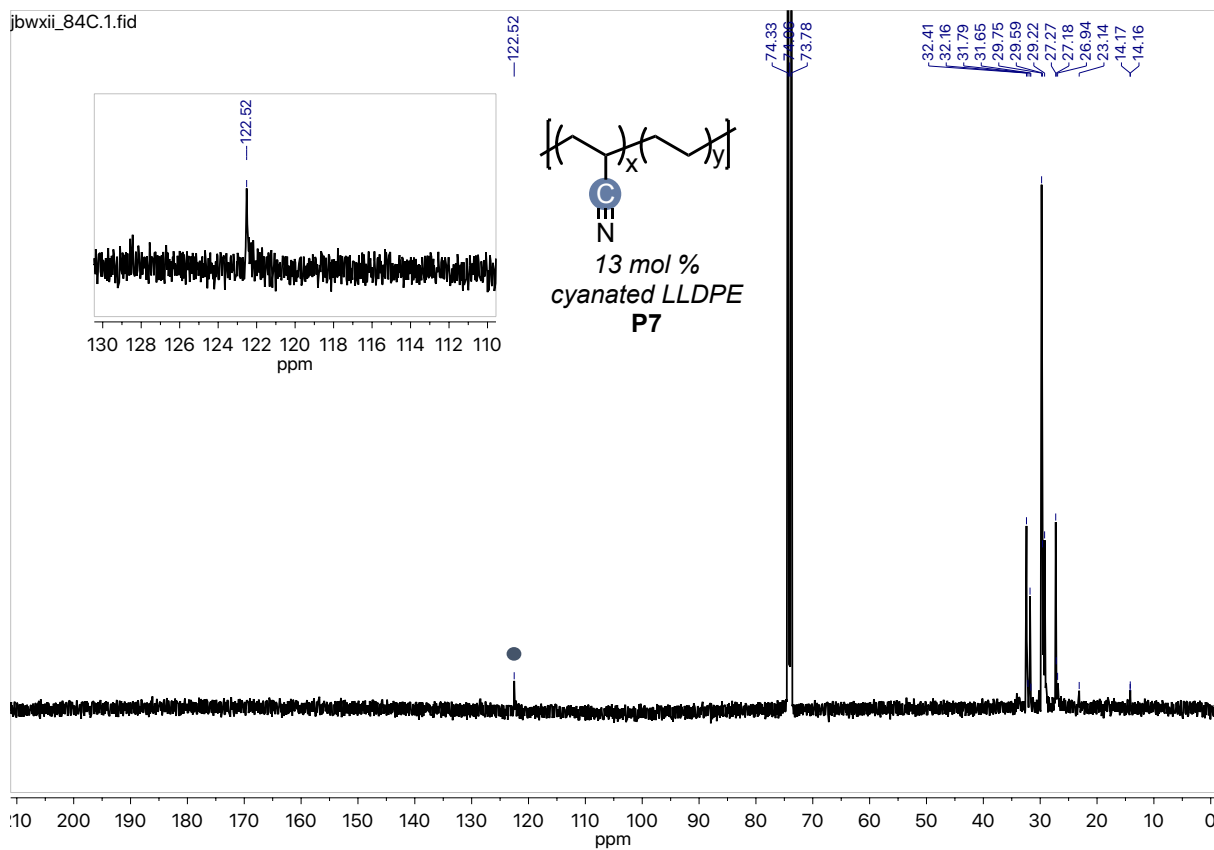
We analyzed the cyanated LLDPE via ^{13}C NMR spectroscopy at 80 °C with a 400 MHz NMR.

Analyzed with 13 mol % cyanated LLDPE, the nitrile carbon is apparent at δ –122 ppm when

referenced against $C_2D_2Cl_4$ at δ –73.78 ppm.
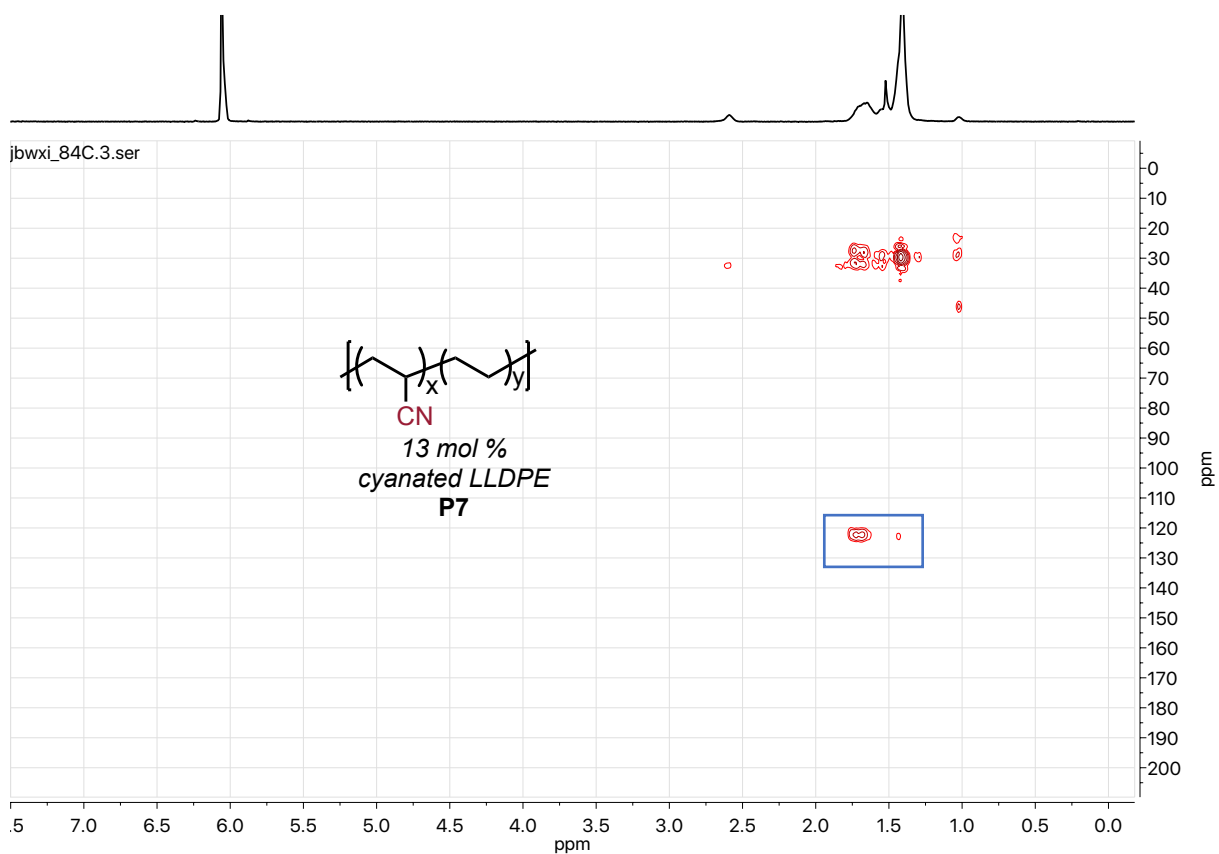
We evaluated the incorporation of a nitrile onto LLDPE by Heteronuclear Multiple Bond Correlation (HMBC) spectroscopy at 110 °C with a 500 MHz NMR. Analyzed with 13 mol % cyanated LLDPE, the y-axis shows carbons correlated in J- or W-coupling with the associated protons on the x-axis. The peaks at δ 121 ppm clearly indicate that a cyano group is present in the compound and is coupled to the polyolefin protons, likely through a W-coupling.

jbwxi_84-HSQC.1.ser

13 mol %
cyanated LLDPE
P7
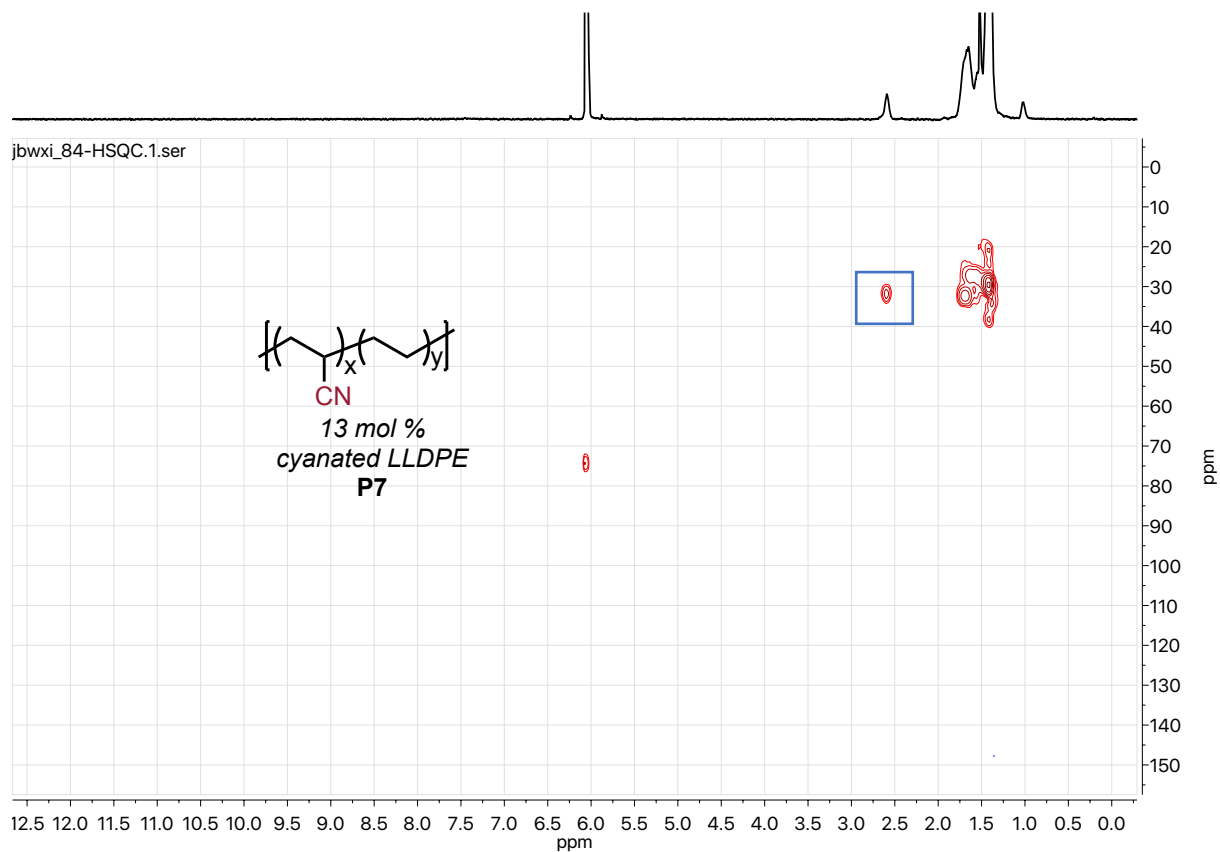
Heteronuclear Single Quantum Coherence (HSQC) spectroscopy at 110 °C with a 500 MHz

NMR was performed on 13 mol % cyanated LLDPE to confirm that the peak at d 2.54 ppm,

which we surmise is the proton *alpha* the nitrile, was within one bond of the polyolefin. The

nitrile was not observed here as the carbon atom of the nitrile does not bear a proton.
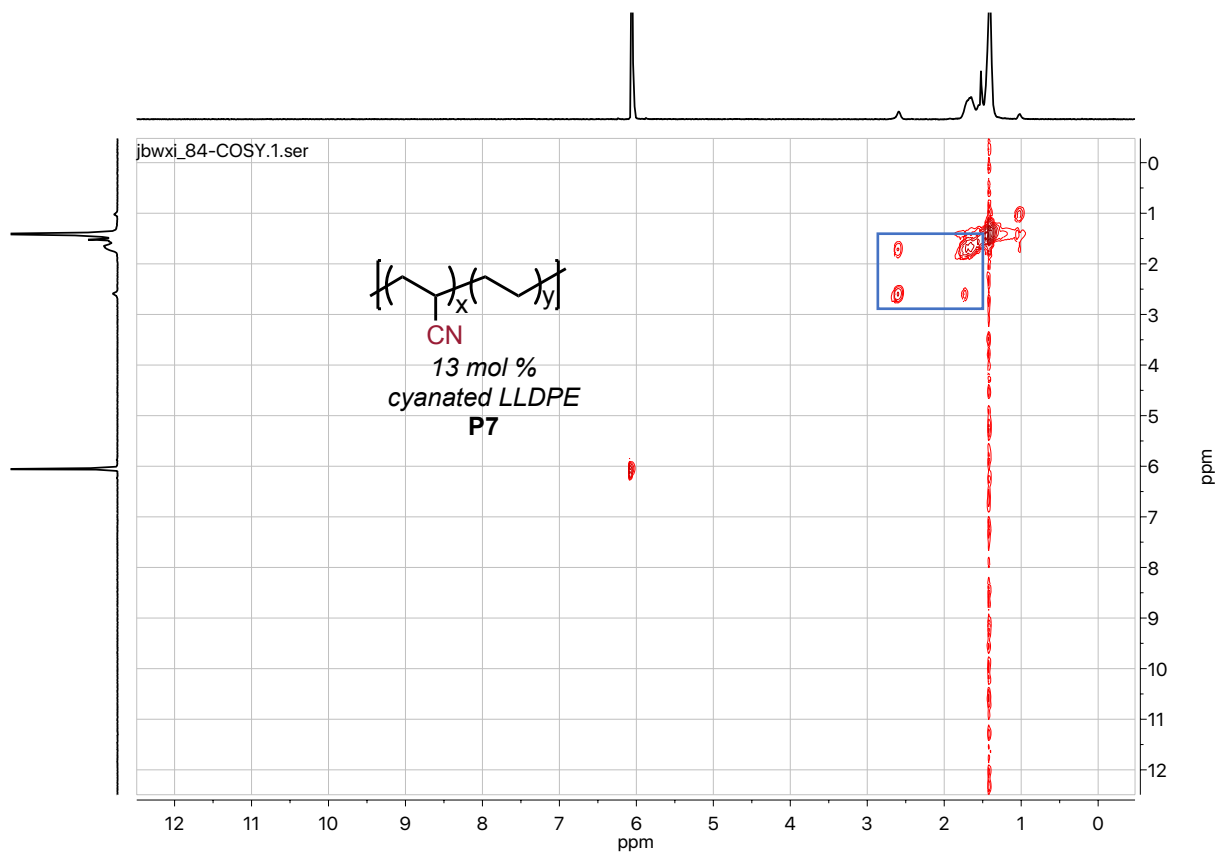
^{1}H–^{1}H Correlated Spectroscopy (COSY) was performed on 13 mol % cyanated LLDPE at 110 °C on a 500 MHz NMR. The cross peaks between the polyolefin signal at δ 1.4 ppm and the proton alpha the nitrile at δ 2.54 ppm are evident, concluding that these protons are in the same spin system.
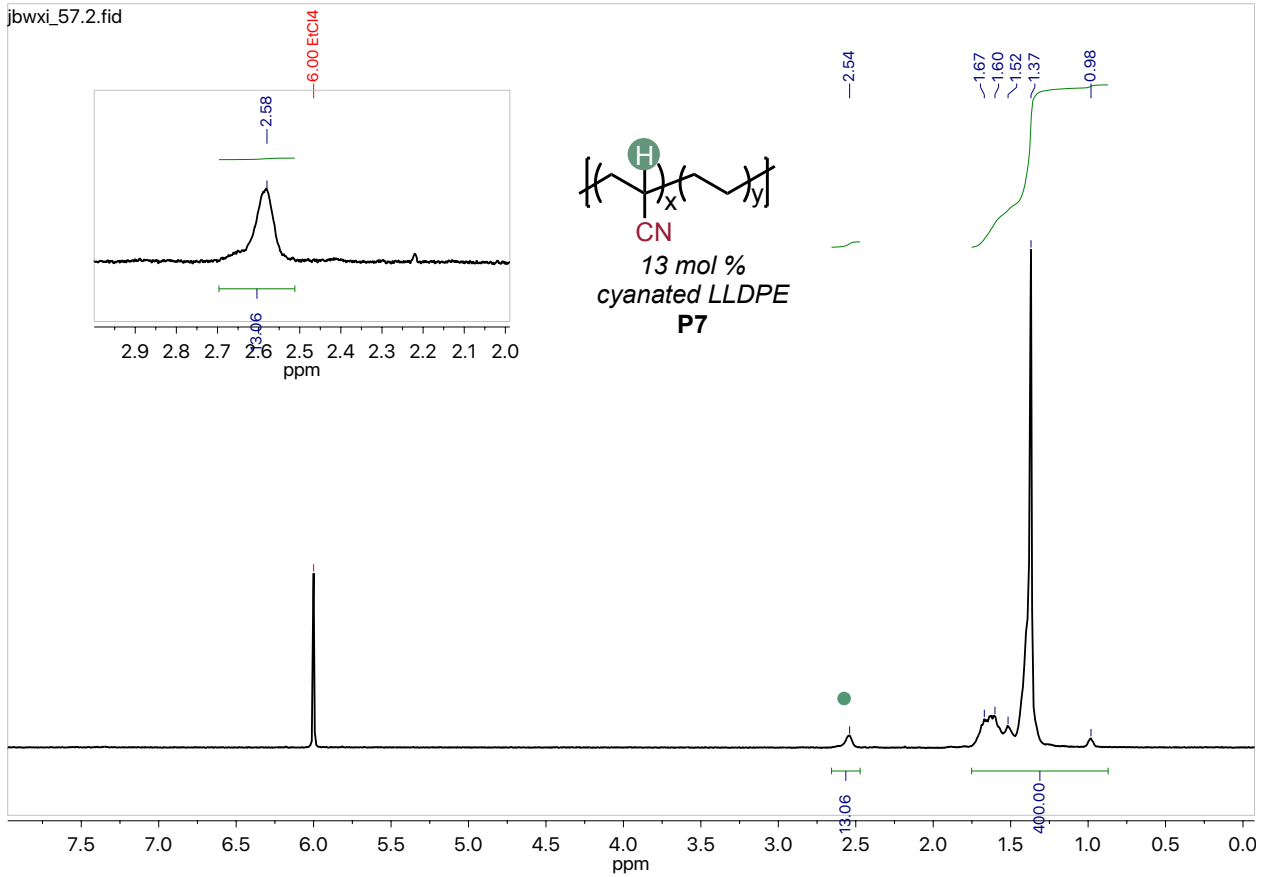
¹H NMR at 110 °C taken in C₂D₂Cl₄ of 13 mol % cyanated LLDPE
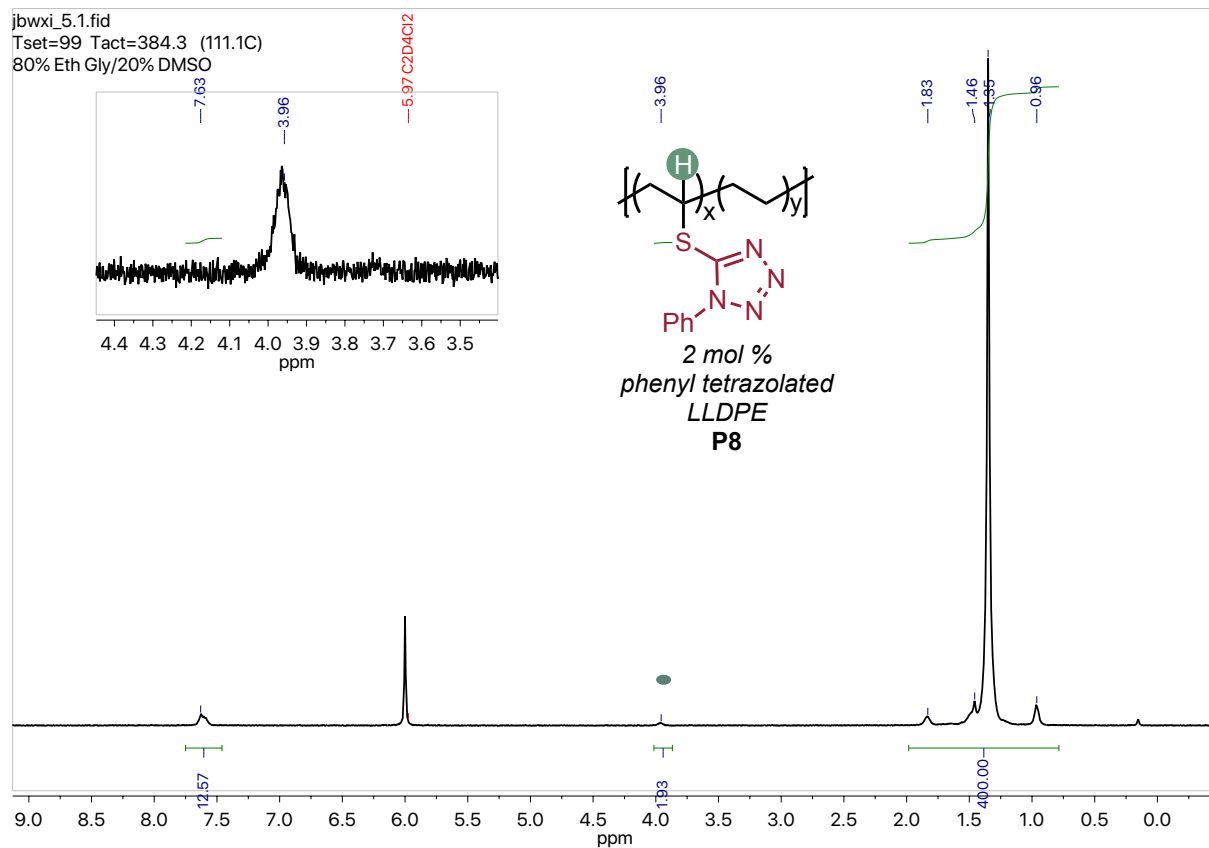
^{1}H NMR at 110 °C taken in C$_2$D$_2$Cl$_4$ of 2 mol % phenyl tetrazolated LLDPE
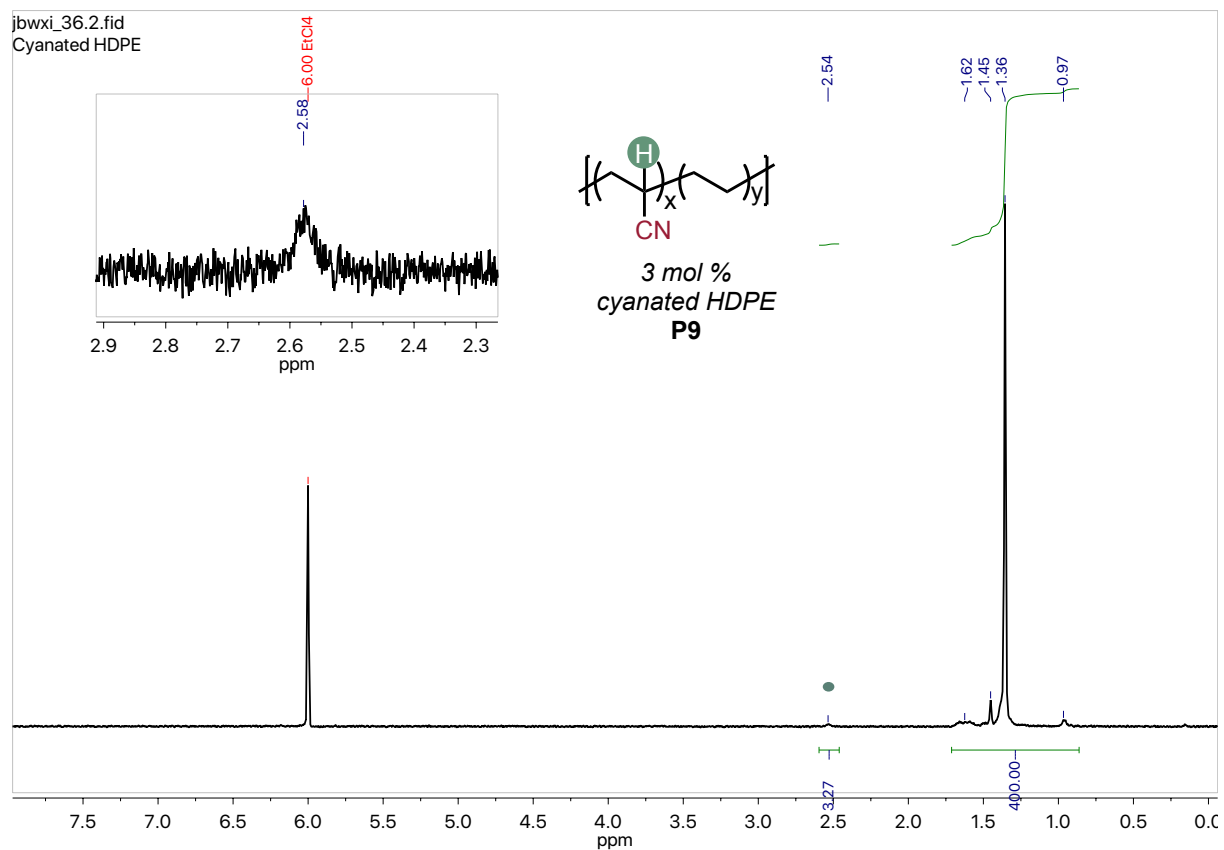
^{1}H NMR at 110 °C taken in C$_2$D$_2$Cl$_4$ of 3 mol % cyanated HDPE
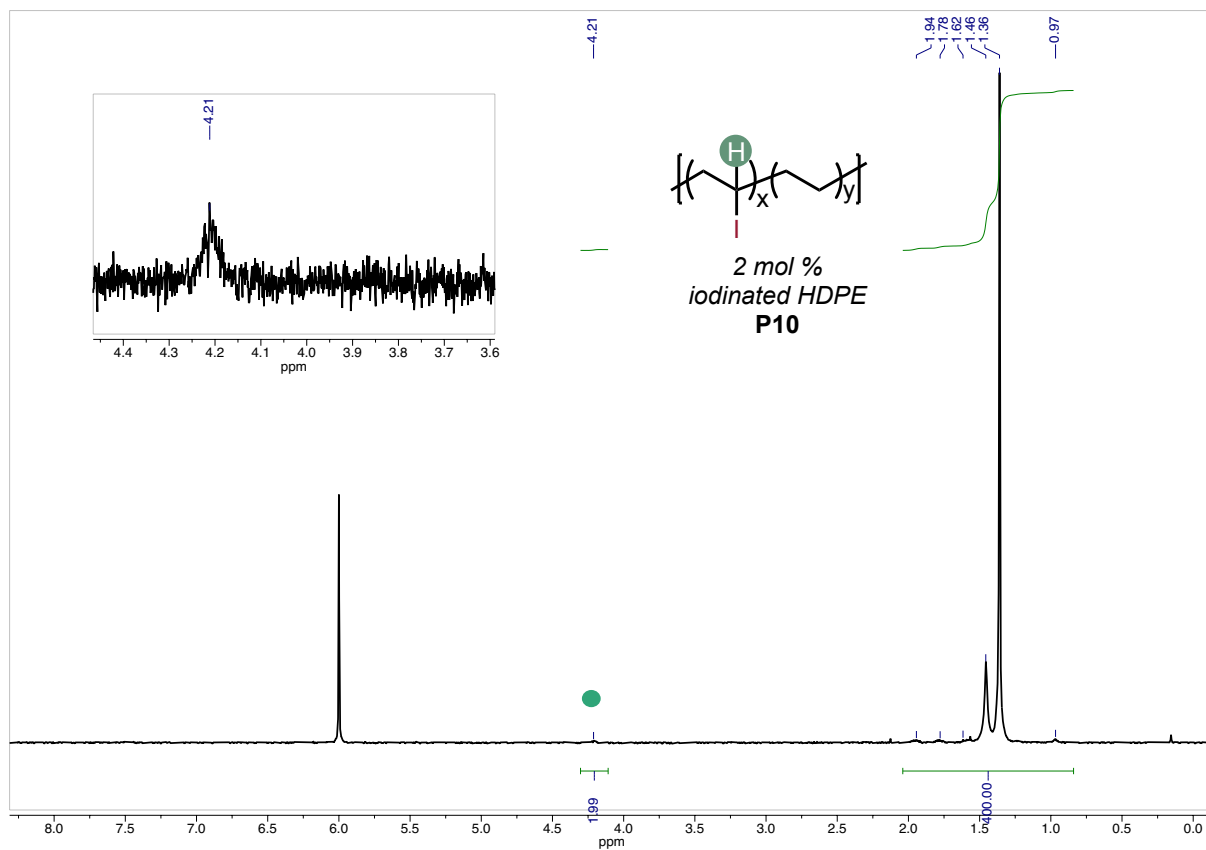
^{1}H NMR at 110 °C taken in C$_2$D$_2$Cl$_4$ of 2 mol % iodinated HDPE
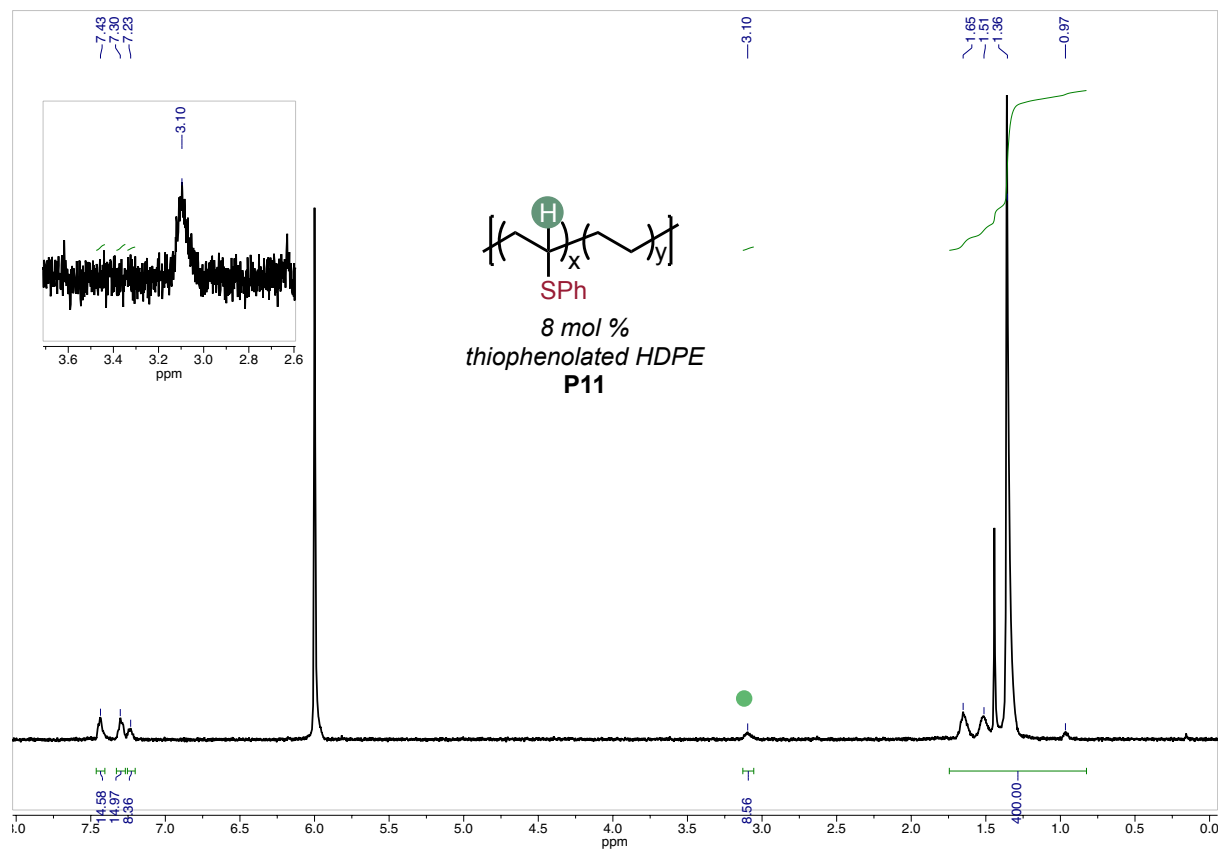
^{1}H NMR at 110 °C taken in C$_2$D$_2$Cl$_4$ of 8 mol % thiophenolated HDPE
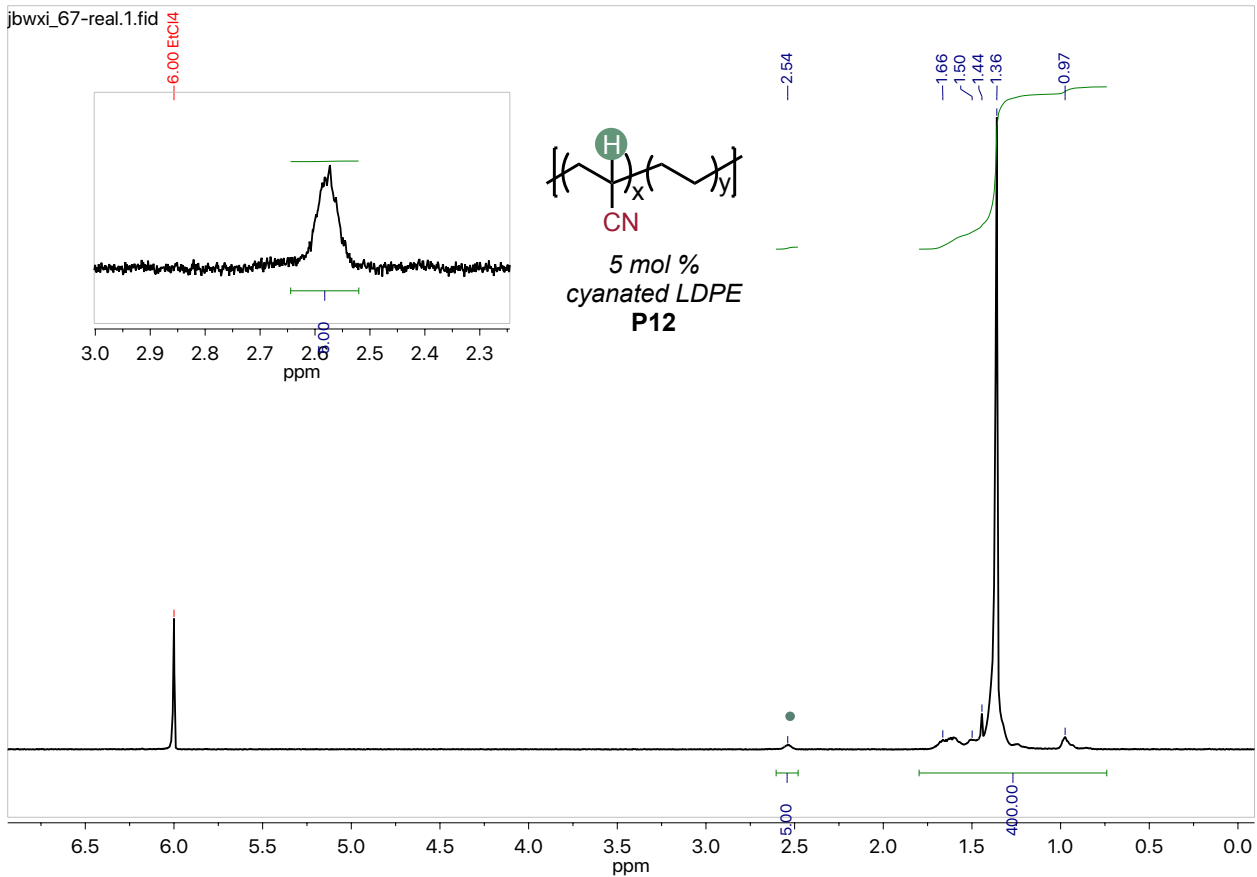
^{1}H NMR at 110 °C taken in $C_2D_2Cl_4$ of 5 mol % cyanated LDPE
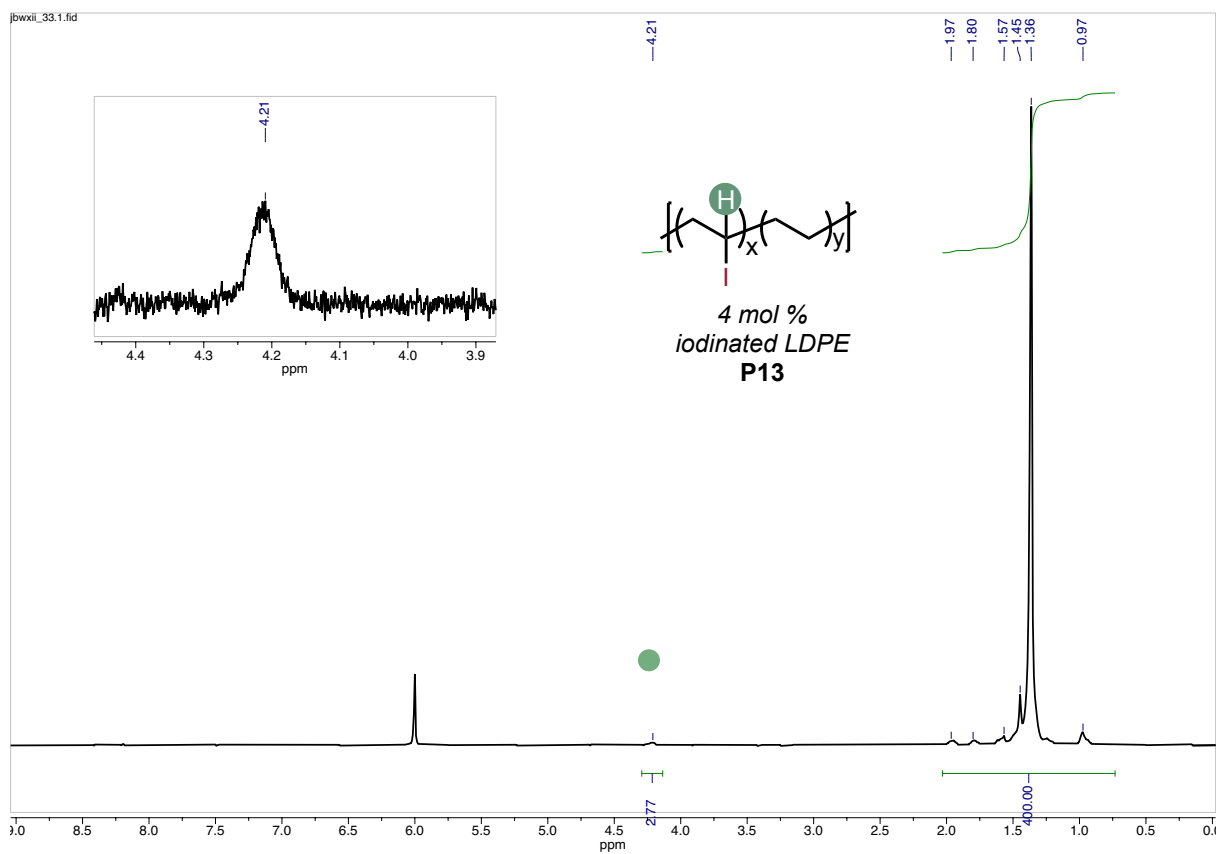
^{1}H NMR at 110 °C taken in $C_2D_2Cl_4$ of 4 mol % iodinated LDPE
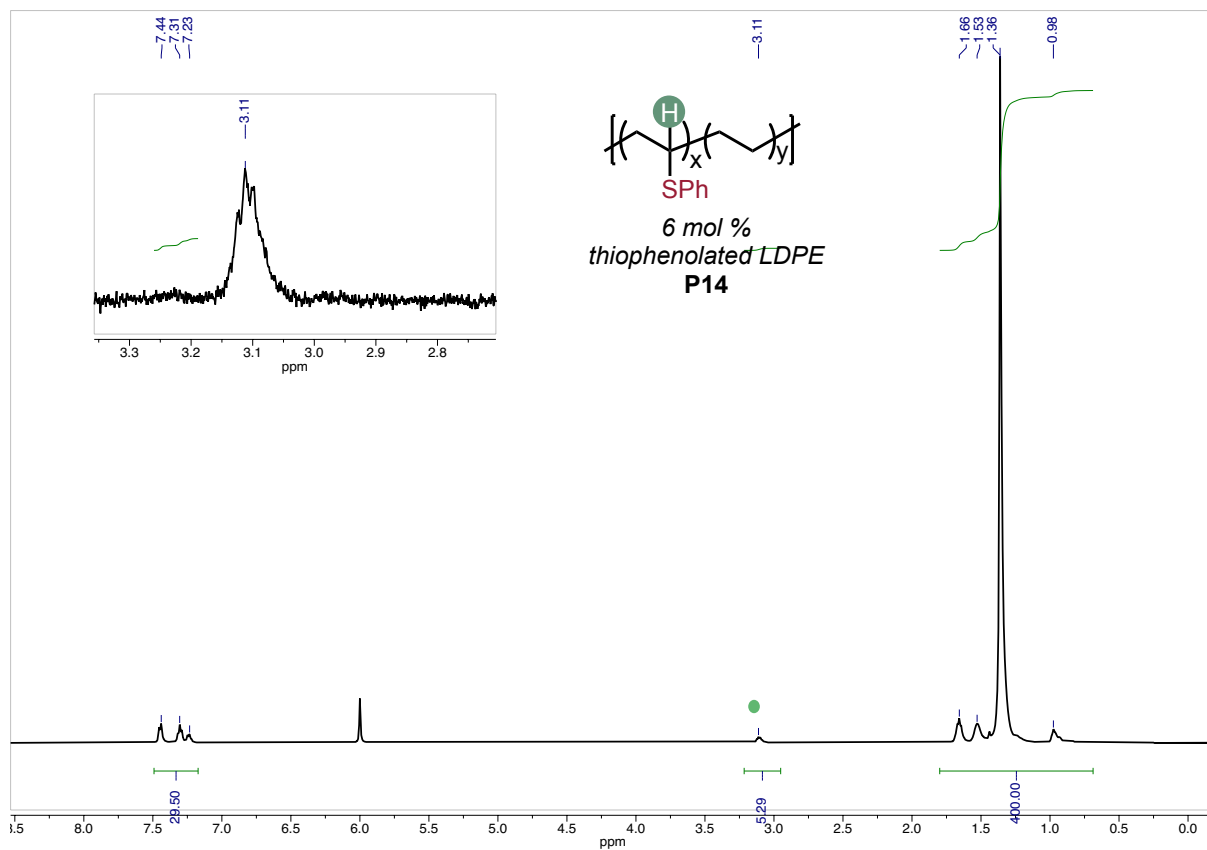
^{1}H NMR at 110 °C taken in C$_2$D$_2$Cl$_4$ of 6 mol % thiophenolated LDPE
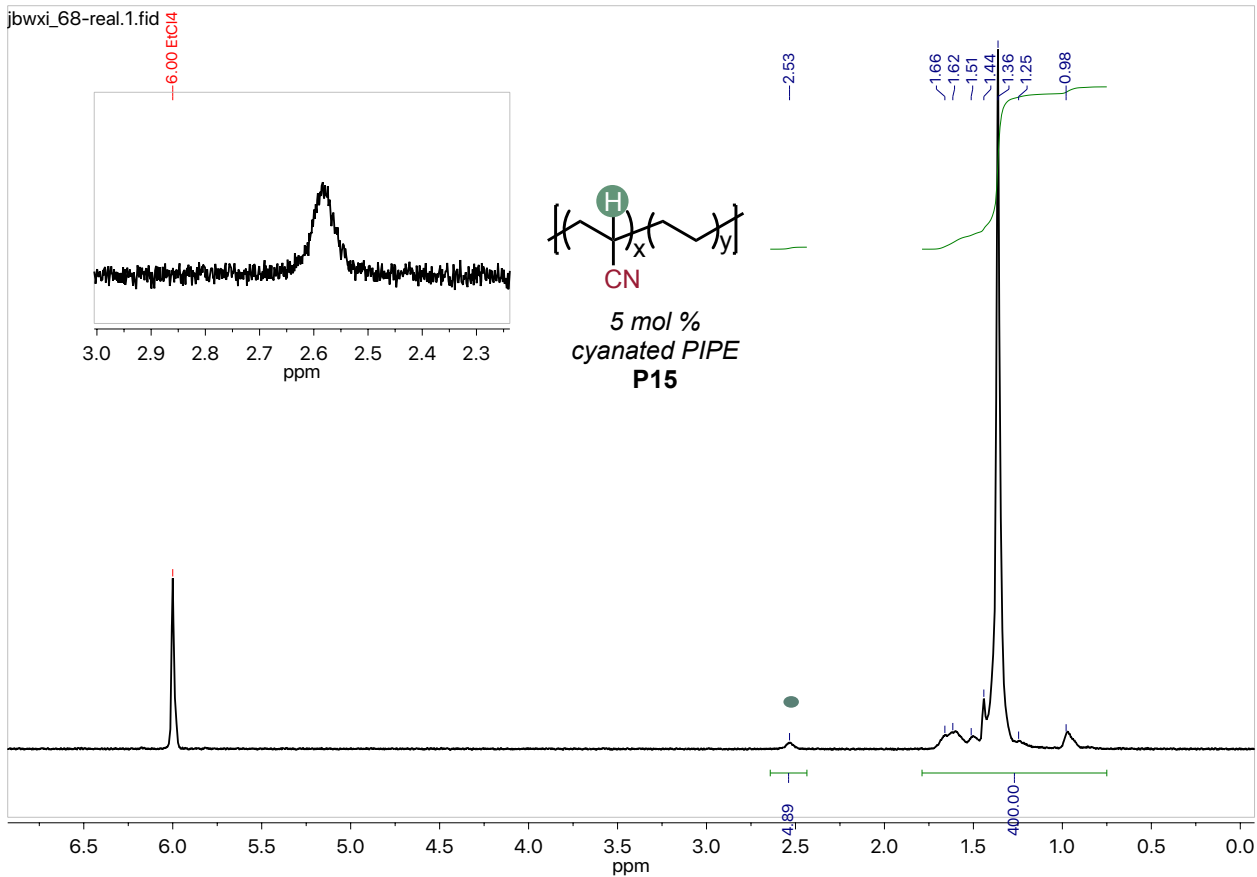
^{1}H NMR at 110 °C taken in C$_2$D$_2$Cl$_4$ of 5 mol % cyanated post-industrial PE

^{1}H NMR at 110 °C taken in C$_2$D$_2$Cl$_4$ of 4 mol % iodinated post-industrial PE
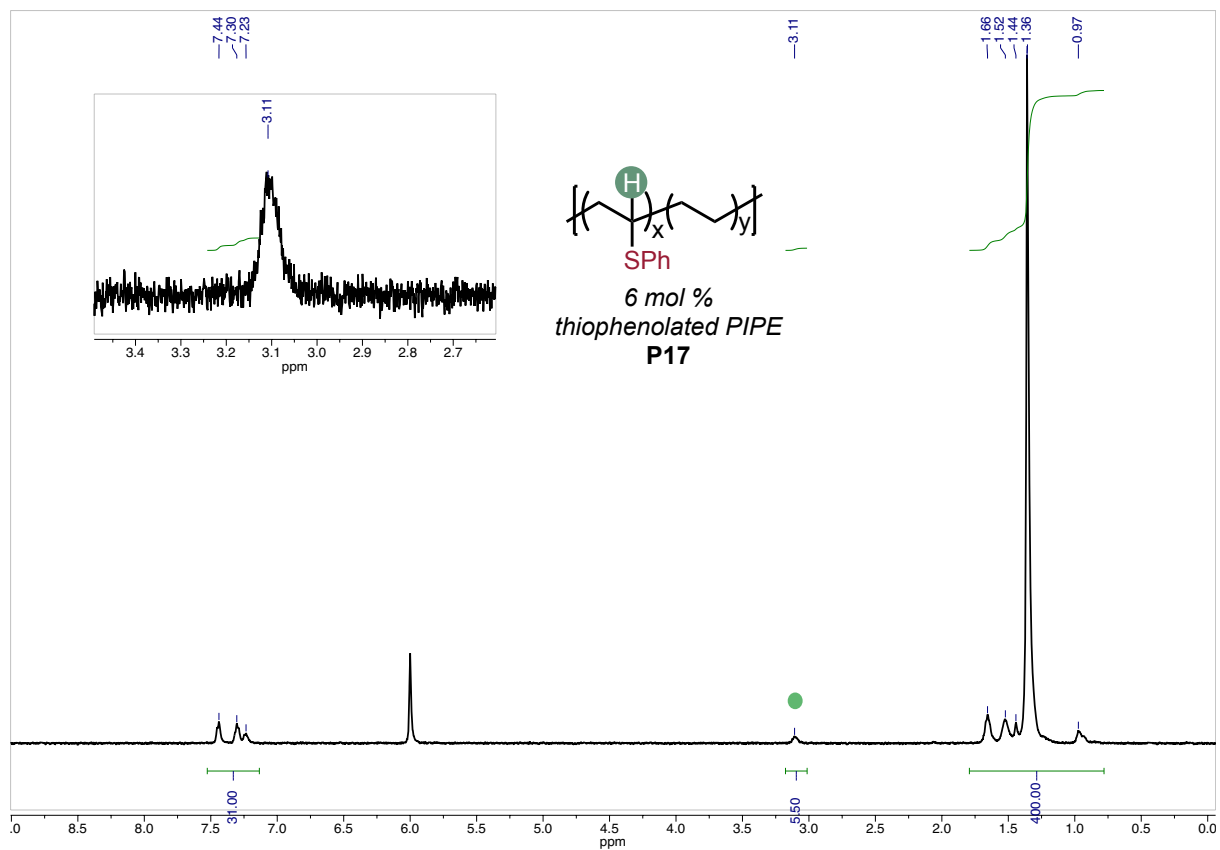
Figure C.X ^{1}H NMR at 110 °C taken in $C_2D_2Cl_4$ of 6 mol % thiophenolated post-industrial PE
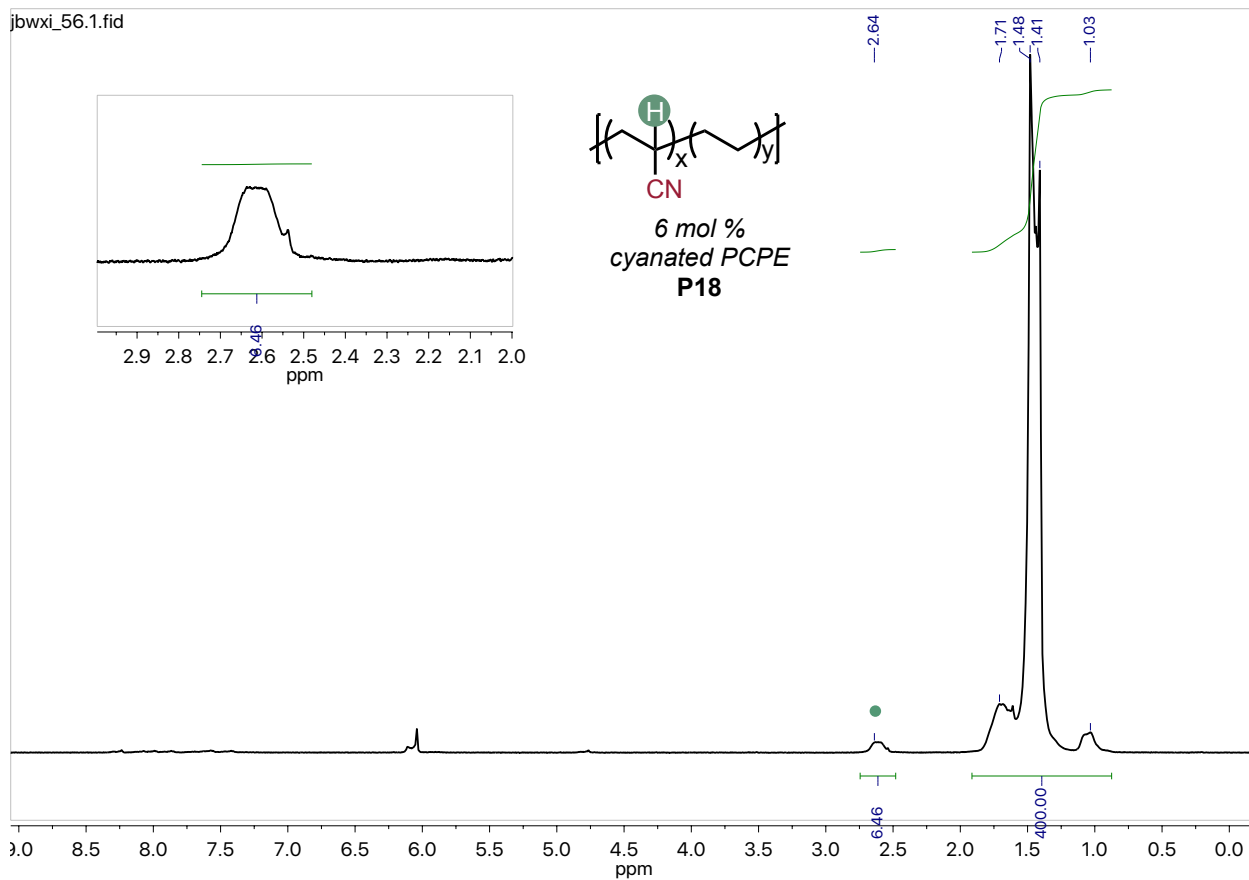
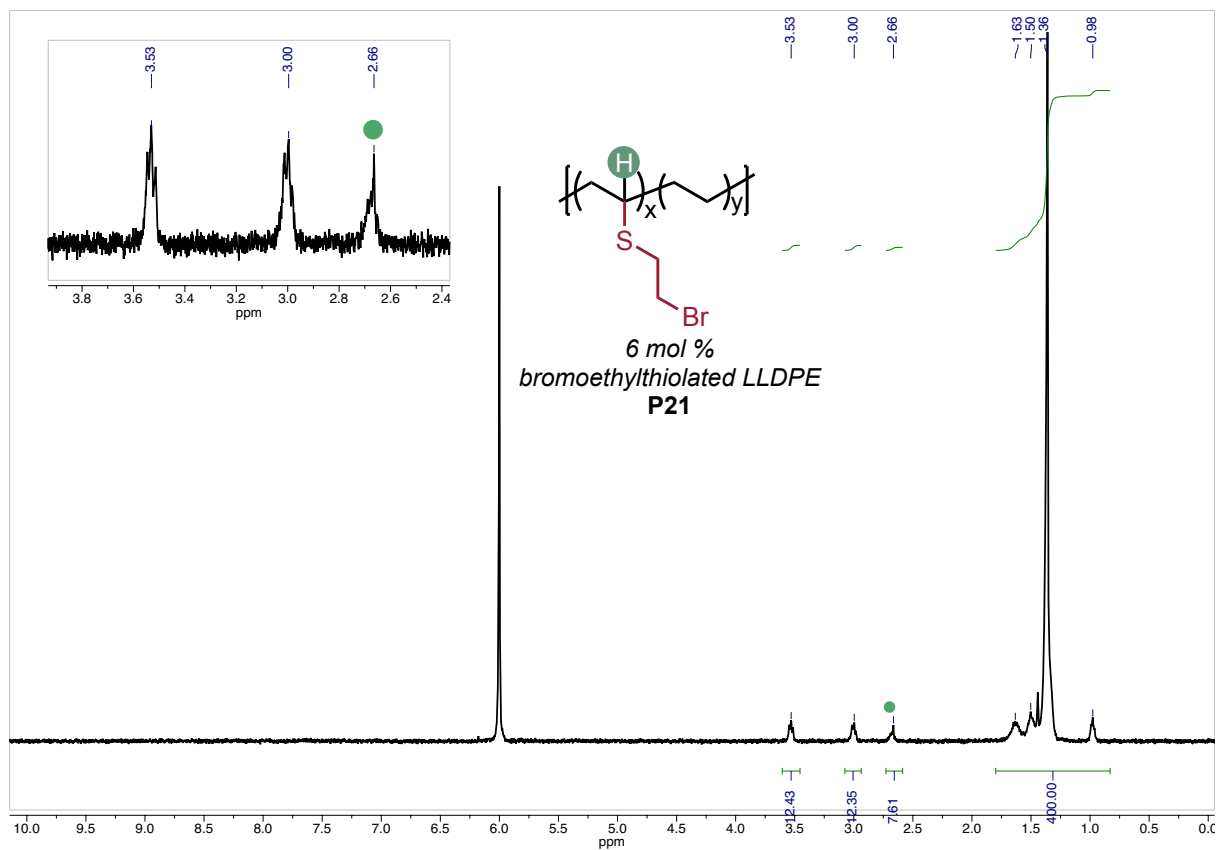^1H NMR at 110 °C taken in $C_2D_2Cl_4$ of 6 mol % cyanated post-consumer PE.
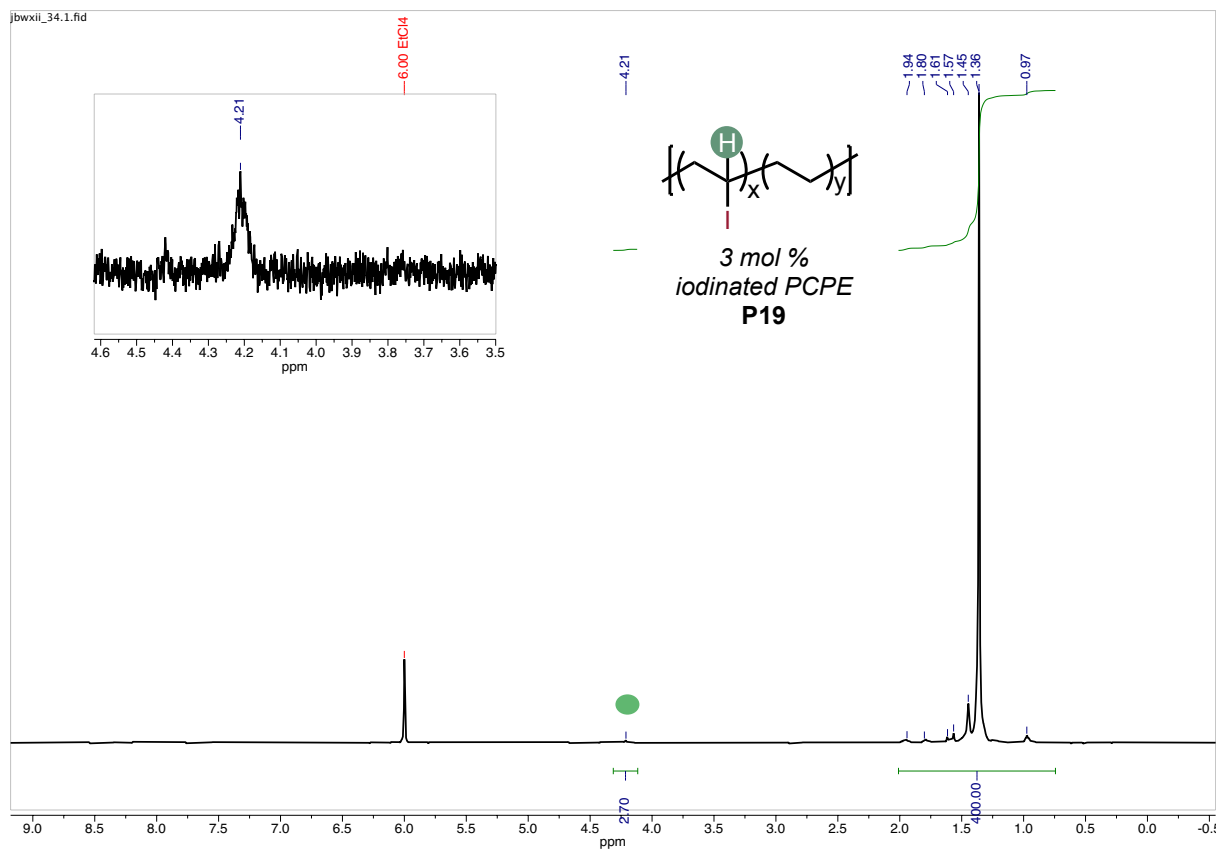
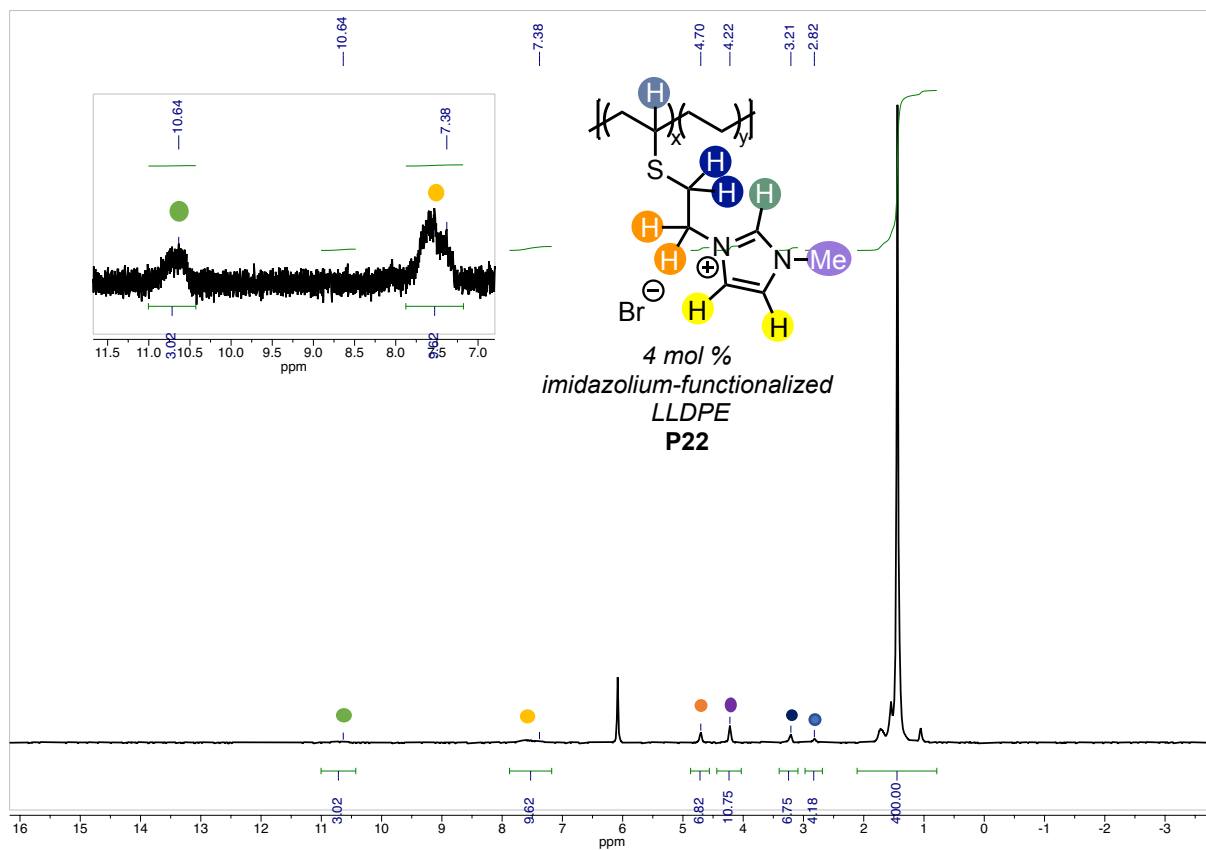^{1}H NMR at 110 °C taken in C$_2$D$_2$Cl$_4$ of 6 mol % iodinated post-consumer PE.
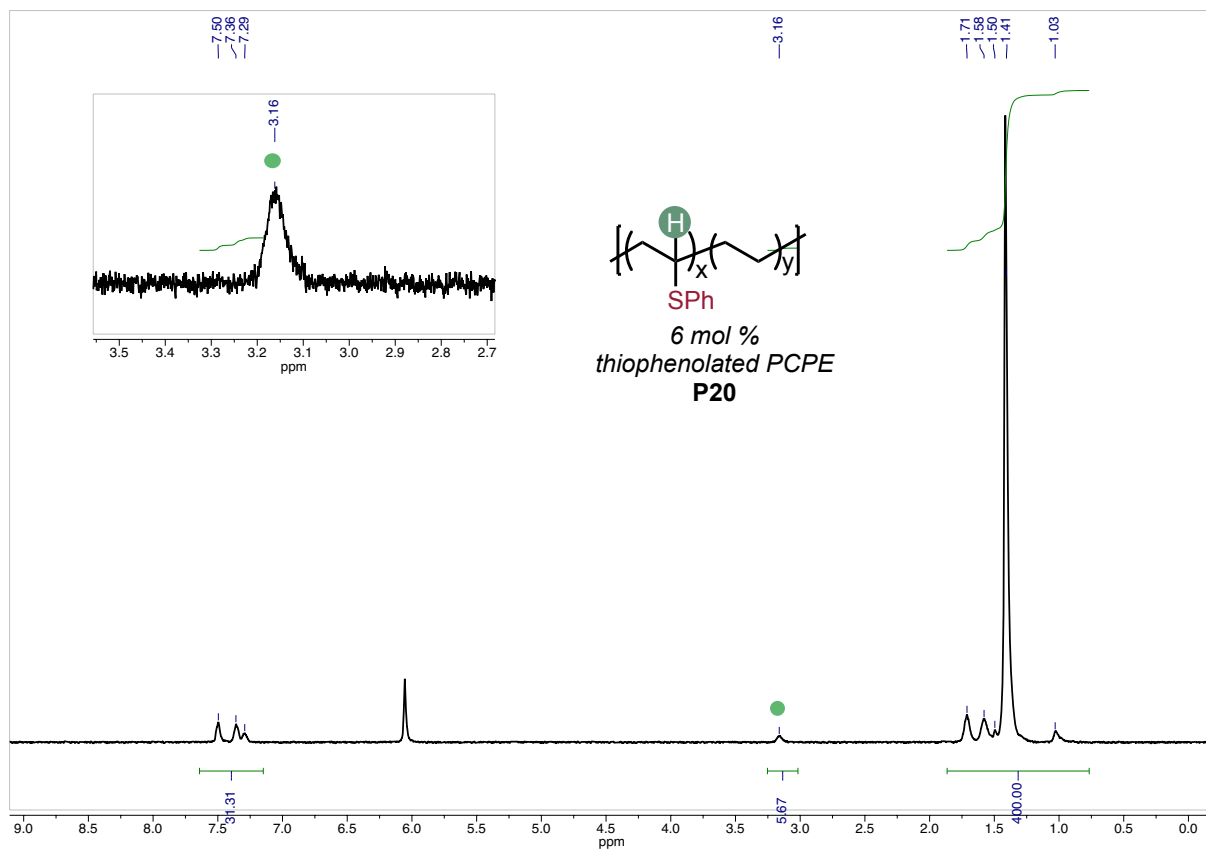
^{1}H NMR at 110 °C taken in C$_2$D$_2$Cl$_4$ of 6 mol % thiophenolated post-consumer PE

^{1}H NMR at 110 °C taken in C$_2$D$_2$Cl$_4$ of 6 mol % bromoethylthiolated LLDPE

^{1}H NMR at 110 °C taken in C$_2$D$_2$Cl$_4$ of 4 mol % imidazolium-functionalized LLDPE